KAPITAŁ LUDZKI
NARODOWA STRATEGIA SPÓJNOŚCI

Politechnika Wrocławska

UNIA EUROPEJSKA
EUROPEJSKI
FUNDUSZ SPOŁECZNY

ROZWÓJ POTENCJAŁU I OFERTY DYDAKTYCZNEJ POLITECHNIKI WROCŁAWSKIEJ

Wrocław University of Technology

Environmental Quality Management

Wojciech Adamski, Małgorzata Szlachta

WATER TREATMENT TECHNOLOGY

Principles and Modeling

Wrocław 2011

Projekt współfinansowany ze środków Unii Europejskiej w ramach
Europejskiego Funduszu Społecznego

Wrocław University of Technology

Environmental Quality Management

Wojciech Adamski, Małgorzata Szlachta

WATER TREATMENT TECHNOLOGY

Principles and Modeling

Wrocław 2011

Reviewer: Andrzej M. Dziubek

ISBN 978-83-62098-68-2

Published by PRINTPAP Łódź, www.printpap.pl

TABLE OF CONTENTS

1. INTRODUCTION

Water in the hydrosphere can be classified according to the of dissolved constituents:
- fresh water – total dissolved solids (TDS) less than 1,500 g/m^3,
- brackish water – TDS up to 5,000 g/m^3,
- saline water –greater than 5,000 g/m^3.

Seawater is usually in the 30,000 ÷ 34,000 g/m^3 TDS range.
Most of the water used by humans is derived from freshwater resources – surface water sources (rivers, lakes, reservoirs) and groundwater aquifiers.

Normally fresh water because of its composition is not ready for use without treatment. It must be treated for
- suspended solids removal,
- colloidal suspension removal; that is the reason for the color of water,
- removal of high molecular organic compounds that give water taste and color,
- elimination of bacteria, algae and viruses,
- iron and manganese compound removal,
- removal of carbon dioxide and other gasses,
- water softening and demineralization.

The composition of natural water is influenced by the conditions in the catchment area and depends on the soil and rock environment. Substances of natural origin occurring in the water are treated as admixtures, whereas anthropogenic substances are referred to as pollution.

Surface water is much more prone to contamination than groundwater and is characterized by a large variation in composition depending on the size of the flow. The quality of groundwater is mainly determined by natural factors and the risk of contamination results from the degree of contact with contaminated surface water and the potential migration of contaminants from the soil surface. Therefore, an aquifer well insulated from the possibility of contamination is characterized by a relatively stable water composition and should be the main source of water supply. In the absence of disposable groundwater resources, first-class surface water should be talen.

The study of water quality should be carried out over a sufficiently long time covering the entire range of the variability of water composition. For surface water, this may be a hydrological year. The composition of groundwater can be determined after test pumping for the acquisition time that provides stable discharge [51, 52]. The diagnosis of water composition variability allows a range of technological research to determine possible water treatment processes and their sequence parameters.

Water Treatment technologies can be established through a process investigation in a laboratory or at the pilot plant scale in addition to mathematical models of unit processes.

Mathematical modeling in the design and operation limits the research to determining kinetic and diffusive parameters of the processes.

Mathematical modeling of any unit processes of treatment ought to consist of at least four stages:

– identification of the most significant and dominant mechanisms by process investigation,

– construction of an equation or system of equations that describe the relations within the system,

– analytical or numerical solution of the equation or system of equations,

– verification of simulated values by comparison with experimental values and in the case of unsatisfactory conformity, the model should be calibrated or the procedure started again from the very beginning.

The possibility of applying sensible models and the complexity of phenomena within the system require some simplifications. However, it is important to remember that too much simplification in a model can lead to significant error in prediction.

The principle objective of this book is to provide a guide on the basics for the mathematical modeling of unit processes in surface and groundwater treatment. Six physical, four chemical and three physic-chemical unit operations are described.

Each chapter first presents the process principles and demonstrates the formulation of mathematical models while providing examples of model application.

2. PROPERTIES OF WATER

Water in the environment is never pure and always contains impurities which are natural and anthropogenic in origin.

2.1. Physical Properties of Water

The physical properties of water can be divided into standard properties such as density, specific weight, dynamic and kinematic viscosity, vapor pressure and into others that show wide variation in magnitude such as color, turbidity, odor, taste, temperature and solids concentration.
Standard temperature-dependent properties are presented in table 1.

Table 1. Standard temperature-dependent properties.

Temperature	**Density**	**Specific Weight**	**Dynamic viscosity**	**Kinematic viscosity**	**Vapor pressure**
°C	**kg/m^3**	**N/m^3**	**N·s/m^2**	**m^2/s**	**N/m^2**
0	1,000	9,810	$1.79\cdot10^{-3}$	$1.79\cdot10^{-6}$	611
5	1,000	9,810	$1.51\cdot10^{-3}$	$1.51\cdot10^{-6}$	872
10	1,000	9,810	$1.31\cdot10^{-3}$	$1.31\cdot10^{-6}$	1,230
15	999	9,800	$1.14\cdot10^{-3}$	$1.14\cdot10^{-6}$	1,700
20	998	9,790	$1.00\cdot10^{-3}$	$1.79\cdot10^{-6}$	2,340
25	997	9,781	$8.91\cdot10^{-4}$	$8.94\cdot10^{-7}$	3,170
30	996	9,771	$7.96\cdot10^{-4}$	$7.99\cdot10^{-7}$	4,250
35	994	9,751	$7.20\cdot10^{-4}$	$7.24\cdot10^{-7}$	5,630
40	992	9,732	$6.53\cdot10^{-4}$	$6.58\cdot10^{-7}$	7,380
50	988	9,693	$5.47\cdot10^{-4}$	$5.54\cdot10^{-7}$	12,300

– **Color** in water is caused by dissolved minerals, dyes or humic acids from plants.
– **Turbidity** in water is a measure of the cloudiness and is caused by the presence of suspended matter which scatters and absorbs light.
– **Odor** is caused by many organic and some inorganic chemicals as well as by algae and other organisms.
– **Taste**, like odor, may be due to decaying micro-organisms or algae.

– **Temperature**, is the most significant parameter in lake water with regard to lake stability.

– **Solids** content of water is one of the most important parameters. The amount, size and type of solids depend on the specific water. One can distinguish total solids (TS), suspended solids (SS), total dissolved solids (TDS = TS – SS), total volatile solids (TVS) and volatile suspended solids (VSS).

The classification of solid particle sizes that occur in water is presented in Figure 1.

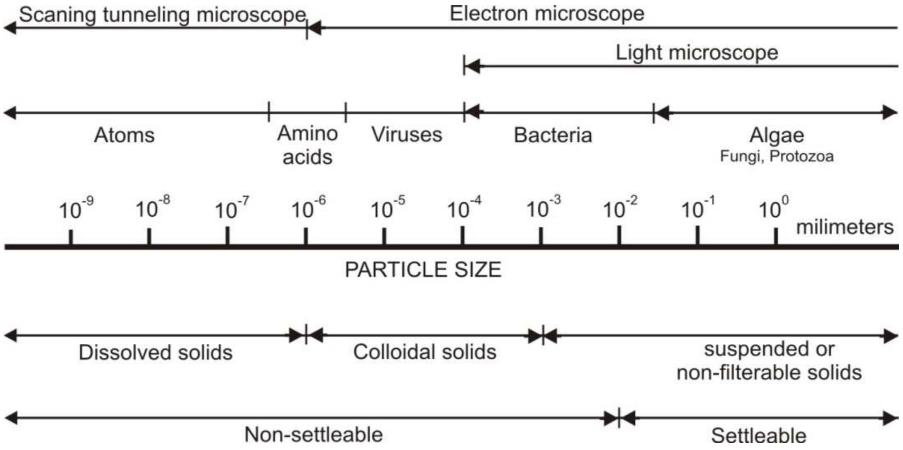

Fig. 1. Particle size classification of solids in water.

2.2. Inorganic Chemical Properties of Water

The chemical processes influencing the quality of water are

– Acid – base reactions

– Exchange processes between the atmosphere and water

– Precipitation and dissolution of substances

– Oxidation – reduction reaction

– Adsorption – desorption processes

The chemical properties of water that are in widespread use include

– **pH** value that is defined as the negative logarithm of the hydrogen ion concentration and is unitless.

Water dissociates slightly into hydrogen (H^+) and (OH^-) ions.

In the absence of foreign materials in water (distilled water) concentrations of hydrogen and hydroxyl ions are equal $[H^+] = [OH^-]$ as required by electroneutrality (Σ cations = Σ anions).

Water is neutral when the pH = pOH = 7. Natural water pH values differ from 7 and are dependent on

– the type of rock/soil from which acid/alkaline compounds can be eroded
– the carbonate system and the concentration of carbonates and carbon dioxide
– the exposure to wastewater or atmospheric pollutants
– **Alkalinity and Acidity**

Alkalinity is defined as the capacity of water to accept hydrogen ions and is often described as the buffering capacity (acid neutralizing capacity – ANC). Acidity is a measure of the base neutralizing capacity (BNC).

The carbonate species that contribute to alkalinity are
– Hydroxide ion, OH^-
– Carbonate ion, CO_3^{2-}
– Bicarbonate ion, HCO_3^{2-}
– Carbon dioxide, CO_2

Alkalinity can be defined by the equation

$$[Alk] = [OH^-] + 2[CO_3^{2-}] + [HCO_3^-] - [H^+], \quad [eq/m^3]$$

– **Hardness** is expressed principally by the sum of divalent metallic cations, Ca^{2+} and Mg^{2+}. The ions causing hardness have their origin in soil and geological formations.

Hardness is calculated in g $CaCO_3/m^3$ and is made up of
– Carbonate hardness or temporary hardness (TH) since this form is removed by prolonged boiling. Carbonate hardness is associated with bicarbonate and carbonate and with carbonate ions.
– Noncarbonate hardness is associated with other anions, particularly chloride and sulfate ions.

The balance between noncarbonate and carbonate hardness is important in water softening and in scale formation.

– **Conductivity** is a measure of the ability of an aqueous solution to carry an electric current. The electric current is conducted in the solution by the movement of ions.

A higher number of ions (the greater concentration of dissolved salts) results in a higher ionic mobility and thus higher conductivity.

Pure water does not conduct electricity so the conductivity is approximately equal to 0.05 μS/cm.

Seawater with a high concentration of salts has a conductivity of about 40,000 μS/m.

2.3. Organic Chemical Properties of Water

Organic compounds in water can be of natural origin (NOM) and anthropogenic origin – synthetic organic matter (SOM).

Natural organic matter (NOM) consists mostly of proteins, lipids, carbohydrates and humic substances.

Proteins are made up of carbon, hydrogen, oxygen, sulfur and nitrogen with the basic building blocks being amino acids ($C_5H_7NO_2$).

Lipids comprise fats, waxes, oils, hydrocarbons, which are insoluble in water but soluble in some organic chemical solvents.

Carbohydrates contain carbon, hydrogen and oxygen, include cellulose, starch, lignin, glucose ($C_6H_{12}O_6$).

Humic substances_may be divided into two basic types, both of acidic character: fulvic and humic acid.

Soil, peat, forest bed, vegetative remains can be the source of humic substances.

The main components of synthetic organic matter (SOM) are

Pesticides and agrichemicals, including chlorinated hydrocarbons, organophosphates and herbicides.

Surfactants, which are used for washing, emulsifying, wetting, foaming, have two parts:

– hydrophobic part, which is insoluble in water and soluble in oils (non-polar liquids),

– hydrophilic part, which is soluble in water and insoluble in oils.

Halogenated hydrocarbons are the final products of the reaction of halogens with hydrocarbons. The most significant halogenated hydrocarbons are trihalomethanes (THMs) such as chloroform ($CHCl_3$) and bromoform ($CHBr_3$).

The overall concentration of organic content of water (NOM + SOM) can be measured by indicators such as BOD_5, COD, PV, TOC, UV Absorbance.

BOD_5 (biochemical oxygen demand) is the amount of dissolved oxygen used from the water sample by micro-organisms as they break down organic material at 20°C over a 5-day period.

COD (chemical oxygen demand) test measures the amount of oxygen needed to chemically oxidize the organics in water. The oxidizing agent is potassium dichromate in an acid solution.

PV (permanganate value) is the same test like COD, but the oxidizing agent used is potassium permanganate.

TOC (total organic carbon) test measures all carbon as CO_2; therefore, the inorganic carbon (HCO_3^-; CO_2; CO_3^{2-}) must be removed by acidifying and aerating the sample prior to the test. The test is carried out by oxidizing the organic carbon to carbon dioxide at a temperature of about 950°C.

UV Absorbance (with the wavelength 254 nm) is the logarithm of the ratio of the intensities of the incident ultraviolet light and the transmitted light which depends on the level of pollution.

UV Absorbance enables the identification of the dissolved organic carbon fractions (DOC) that have a relatively high concentration of aromatic compounds. UV Absorbance shows the compounds with aromatic rings such as humic acid, tannins, lignins and phenols.

Information on the characteristics of water organic compounds is given by the specific absorbance of UV radiation (Specific UV Absorbance – SUVA).

SUVA is defined as the UV Absorbance to DOC ratio.

SUVA determines the reactivity of NOM and through this the risk of disinfection by – product formation.

2.4. Biological Properties of Water

The field of aquatic microbiology includes diverse organisms. The major groups of interest are bacteria, viruses, algae, fungi and protozoa. All the groups are significant in terms of their ecology, public health impact and treatment effects.

3. WATER QUALITY STANDARDS

Quality standards of water used for domestic and industrial purposes are constantly being modified and the number of standardized indicators is growing [20, 32, 75, 80]. This is due to the increased diversity of specific pollution, better analytical capabilities allowing for their accurate identification, wider knowledge about water chemistry, interaction between pollutants and natural components of water, as well as the impact of a particular water composition on consumer health [21, 74, 89]. Among the new indicators, anthropogenic contaminations prevail, as well as indicators for oxidation by-products.

Table 2. Drinking Water Quality Standards.

No	**INDICATOR, NAME OF SUBSTANCE**	**UNIT**	**THE HIGHEST ACCEPTABLE CONCENTRATION OR RANGE**
1	2	3	4
PHYSICAL INDICATORS			
1	Color	gPt/m^3	15
2	Turbidity	NTU	1
3	pH		6.5÷9.5
4	Conductivity	µS/cm	2500
5	Taste	-	acceptable
6	Odor	-	acceptable
INORGANIC SUBSTANCES			
7	Ammonia	gNH_4^+/m^3	0,5
8	Antimony	gSb/m^3	0.005
9	Arsenic	gAs/m^3	0.01
10	Nitrate	gNO_3^-/m^3	50
11	Nitrite	gNO_2^-/m^3	0.5
12	Boron	gB/m^3	1.0
13	Available chlorine	gCl_2/m^3	0.1÷0.3
14	Chloride	gCl^-/m^3	250
15	Chromium	gCr/m^3	0.05
16	Cyanide	gCN/m^3	0.05

17	Fluoride	gF/m^3	1.5
18	Aluminum	gAl/m^3	0.2
19	Cadmium	gCd/m^3	0.003
20	Magnesium	gMg/m^3	50
21	Manganese	gMn/m^3	0.05
22	Copper	gCu/m^3	2.0
23	Nickel	gNi/m^3	0.02
24	Lead	gPb/m^3	0.025
25	Mercury	gHg/m^3	0.001
26	Selenium	gSe/m^3	0.01
27	Sulfate	gSO_4^{2-}/m^3	250
28	Sodium	gNa/m^3	200
29	Hardness	$gCaCO_3/m^3$	500
30	Iron	gFe/m^3	0.2
ORGANIC SUBSTANCES			
31	Acryloamide	mg/m^3	0.1
32	Aldrin	mg/m^3	0.03
33	Benzene	mg/m^3	1.0
34	Benzo(a)pyrene	mg/m^3	0.01
35	Vinyl chloride	mg/m^3	0.50
36	1,2 dichloroethane	mg/m^3	3.0
37	Deldrine	mg/m^3	0.03
38	Epichlorohydrin	mg/m^3	0.1
39	Epoxiheptachlorine	mg/m^3	0.03
40	Heptachlorine	mg/m^3	0.03
41	Phthalate dibutyl	mg/m^3	20.0
42	Microcystine-LR	mg/m^3	1.0
43	Pesticide	mg/m^3	0.1
44	Σ Pesticides	mg/m^3	0.5
45	Surfactants (anionic)	mg/m^3	200
46	Trichloretylene	mg/m^3	10.0
47	Σ Trichlorobenzene	mg/m^3	20.0
48	Σ Trichlorethene and Tetrachlorethene	mg/m^3	10.0
49	Σ Polyaromatic hydrocarbons	mg/m^3	0.1
50	Permanganate value	mg/m^3	5.0

DISINFECTION BY-PRODUCTS			
51	Bromate (BrO_{3-})	mg/m^3	10
52	Bromodichloromethane	mg/m^3	15
53	Chloramine	mg/m^3	500
54	Chlorate(ClO_{3-})	mg/m^3	200
55	Chlorate(ClO_{2-})	mg/m^3	200
56	Formaldehyde	mg/m^3	50
57	Carbon tetrachloride	mg/m^3	2.0
58	Trichloracetaldehyde	mg/m^3	10.0
59	Trichloromethane (chloroform)	mg/m^3	30.0
60	2,4,6-Trichlorophenol	mg/m^3	200
61	Σ Trihalomethans	mg/m^3	100
RADIONUCLIDES			
62	Total acceptable dose	mSv/year	0.1
63	Tritium	Bq/l	100

4. CLASSIFICATION OF WATER TREATMENT METHODS

Contaminations are removed from intake water by physical, chemical and more recently biological methods. The treatment processes changing water composition resulting from the operation of physical forces are classified into the first group. Typical unit operations included in this category are screening, mixing, aeration and air stripping, flocculation, sedimentation, filtration, adsorption ion exchange and membrane processes.

Purification processes in which the addition of chemical compounds transforms contaminations so that they are easily released from water in physical processes are classified as chemical methods. This group includes chemical precipitation, oxidation, coagulation and disinfection. Finally, the methods in which the change in the structure of pollution is due to biochemical oxidation are classified as biological methods. In water treatment, biological processes usually accompany other unit processes such as infiltration, slow filtration and adsorption on granular activated carbon. Separate reactors for nitrification and denitrification are also used [52, 66].

5. INTEGRATED SYSTEMS OF WATER TREATMENT

For achieving proper water quality a sequence of unit processes (integrated system of methods) must very often be used.

The intake water in mountain regions in the upper reaches of rivers may require only filtration and disinfection, whereas the water from rivers in their lower reaches may require more sophisticated treatment technology. Groundwater from great depths, from the layers isolated from possible external contamination, may even require no treatment beyond stabilization. An increasing share of intake is surface water. The need for the purification of large quantities of surface water has decreased interest in slow filtration and resulted in the application of rapid filtration preceded by coagulation and sedimentation. With increasing levels of surface water pollution, the classic coagulation-rapid filtration system was successively enlarged to include sorption on powdered activated carbon and sorption on granular activated carbon in the flow system. A further increase in the level of surface water pollution requires the inclusion of initial oxidation and oxidation before sorption filters to the treatment system. Surface water can be purified with artificial infiltration, a process that may be either independent or incorporated into the technological systems described above.

The integrated system can be sometimes replaced by a hybrid reactor (multifunctional reactor in which several unit processes proceed simultaneously), for example an upflow sludge blanket, upflow direct sand filtration reactor, slow sand filter. A hybrid reactor or a system of hybrid reactors can be the element in an integrated system of water treatment.

Table 3 summarizes the major contaminants that occur in intake waters and the unit processes or the sequences of processes for their removal.

The presented technological systems of surface water treatment may be implemented in various design systems that depend on the required amount of purified water and the level of contamination.

Coagulation can be performed in separate reactors: rapid mixing chambers, and pipelines supplying water to free mixing chambers, that is reactors in which the orthokinetic flocculation process is implemented.

For sedimentation after the process of flocculation, settling tanks with vertical or horizontal flow and settling tanks with a layer of suspended sediment can be applied. Using a settling tank with suspended sediment (upflow sludge blanket clarifiex) eliminates the necessity of placing separate flocculation reactors in the construction system. Flocculation occurs in the suspended sediment zone, whereas sedimentation occurs in clarification zone.

Table 3. Unit Operations and Integrated Systems Used to Remove the Major Water Contaminants.

Contaminant	**Unit processes or integrated systems**	**Clasifications** **C - Chemical** **P - Physical**
Pathogenic organisms	Oxidation - chlorination - ozonation	C C
Turbidity and suspended matter	Screening Sedimentation Filtration Coagulation-Flocculation-Sedimentation-Filtration	P P P C-P-P-P
Color	Adsorption Ion exchange Coagulation-Flocculation-Sedimentation-Filtration	P/C C C-P-P-P
Taste and odors	Oxidation Adsorption Aeration	C P P
Organic matter	Adsorption Ion exchange Ozonation Coagulation-Flocculation-Sedimentation-Filtration	P C C C-P-P-P
Hardness ions Ca^{2+}; Mg^{2+}	Chemical precipitation Ion exchange	C C
Dissolved gases	Stripping Aeration Chlorination	P P C
Heavy metals	Chemical precipitation Ion exchange	C C
Ion and manganese	Ion exchange Oxidation-Precipitation- Filtration	C C-P-P
Dissolved solids	Adsorption Reverse osmosis Distillation	P P P

Another hybrid reactor is an upflow direct sand filter in which flocculation and filtration take place [53]. Changing the contact filter filling from sand to granular activated carbon expands the technology to include the process of adsorption [4].

Groundwater can be purified in a gravitational system when an open system of aeration is required. This is often the case when water contains manganese and a high concentration of iron which justifies the application of sedimentation after aeration and prior to filtration. The pressure system of groundwater treatment is used mainly in small plants at high water alkalinity levels and a general iron concentration below 5 g/m^3. In the case of an increased permanganate value together with intense color and when iron is bound in organic compounds, a system composed of aeration and contact filtration is used.

In very small plants, a system with a chemically binding carbon dioxide bed may be used.

6. MANAGEMENT OF SLUDGE AND SEWAGE FROM WATER TREATMENT PROCESSES

In the processes of water treatment certain amounts of sewage and sludge are formed which contain pollution removed from water and the reagents used.

These sediments are mostly post-coagulation sediments, sediments of iron hydroxide precipitated from groundwater or infiltration water, sediments from precipitation methods of treatment such as softening and sediments precipitated from sewage.

Process wastewater is backwash water from the rinsing of filtration, adsorption, ionite and microstrainer beds, concentrates extracted in membrane processes, post-regeneration solutions from ionites and backwash water after rinsing tanks and devices. The amount and qualities of sediments and sewage depend on the composition of purified water.

The average amount of sewage and sediments is up to 5% of the volume of the water treated and the main part in this amount is backwash water which is characterized by over a 99.9% hydration. Sediment hydration oscillates in the range 97 ÷ 99.6 %.

The purpose of sludge and wastewater management in water treatment plants is the maximum reduction of their volume and management of solid and liquid phase in a way that is harmless to the environment.

Volume reduction takes place in the processes of thickening, dewatering and drying, which differ in the degree of dehydration.

Backwash water and sludge thickening, as well as their dewatering, is often preceded by the process of conditioning which is the change of sediment structure by reducing adhesion force between water and solid particles.

Conditioning can be carried out with physical methods: freezing out, heating, exposure to magnetic field and ultrasound, and chemical methods: the use of inorganic and organic polymers.

Thickening can be gravitational, flotational or mechanical, e.g. in sludge centrifuges.

Dewatering is carried out under natural conditions: evaporation and filtration on the fields and in sludge lagoons, and under mechanical conditions: vacuum filters, filter presses and sludge centrifuges.

Dehydrated sludge can be deposited at sludge dumps, in natural or artificial cavities and can serve as the raw material for the recovery of the reagents.

Supernatant sludge extracted in the process of sewage water and sludge thickening are most often discharged to surface water or the sewer system and much less frequently to the water treatment circuit.

Sometimes water treatment plants discharge mixed sludge to urban drainage where they can aid the process of wastewater purification [52].

7. PHYSICAL METHODS OF WATER TREATMENT

The group of physical methods of water processing includes

– screening,
– aeration and stripping with air,
– flocculation,
– sedimentation,
– filtration,
– adsorption,
– ion exchange
– membrane processes.

Mixing, classified as a physical process, is a very important process operation accompanying the majority of unit processes in water treatment.

Screening is a process which aims to protect pumps and other devices from mechanical damage. The devices used in this process are screens and sieves located at the water intake. For algae blooms microstrainers are also used.

7.1. Mixing

Mixing is one of the most widely applied processes necessary to unify the system, maintain homogeneous temperature, remove thermal stratification, etc. A common application of mixing in water treatment is the mixing of chemical substances added to water: coagulants and disinfectants.

In most systems, the process of natural mixing of the components added to water is very slow and is due to the flow, hydrodynamic dispersion and diffusion. Therefore to accelerate the process, mechanical energy is introduced into the system mainly through the application of spinning elements. These elements generate eddy currents as a result of the velocity gradient forming inside the solution. Eddy currents and actually the relation between the size of a whirl and the size of the particles mixed decide the mixing efficiency. The particles smaller than the whirl size move in a set mutual position within the whirl and the effects of mixing are in this case, thereby, weak [45, 62].

The basic types of mixers are mechanical mixers (propeller, turbine, frame, screw, plate, anchor), hydraulic and pneumatic.

The **Solution mixing ratio** is the function of turbulence formed within the system and consequently the size of eddy currents along with the damping forces that are present in the solution that suppress liquid movements. The mixing ratio may be defined as the ratio of a driving force that creates eddy currents to the resistance from the damping forces. Liquid flow in relation to a mixer can be laminar or turbulent. The flow's character is established by the critical Reynolds number which is defined for mechanical mixers by the following equation:

$$\mathrm{Re} = \frac{u \cdot L \cdot \rho_w}{\eta_w} \tag{1}$$

where

$u = 2\pi LN$ – peripheral speed [m/s],

N – rotational speed [s^{-1}],

L – linear dimension of the mixer [m],

ρ_w – water density [kg/m^3],

η_w – water dynamic viscosity coefficient [kg/m·s].

$$\mathrm{Re} = \frac{2\pi L^2 N \rho_w}{\eta_w} \tag{2}$$

Thus, for a defined Reynolds number, laminar flow occurs for Re < 30 – 50.

A very important parameter when designing the mixing process is **power consumption**. For a differential element of the mixer shield of length dl and height h (Fig. 2), the resistance force from the liquid (dR) is described by the following equation [45]:

$$dR = k_M \frac{u^2}{2} \rho_w dF \tag{3}$$

in which

dF = h · dl – surface of the differential element of the mixer [m^2],

k_M – resistance coefficient.

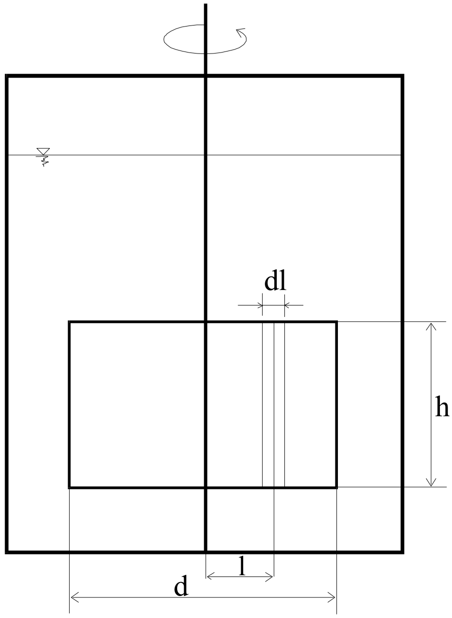

Fig. 2. Shield plate mixer design.

Taking into account the definition of peripheral speed, Equation (3) is transformed as follows:

$$dR = k_M \frac{(2\pi LN)^2}{2} \rho_w h \cdot dl \tag{4}$$

The consumed power (dP) is expressed by the product of resistance force (dR) and the path made by the element of a mixer in the unit time, namely peripheral speed (u).

$$dP = u \cdot dR = 2\pi \ LNk_M \frac{(2\pi \ LN)^2}{2} \rho_w h \cdot dl = 4\pi^3 k_M N^3 \rho_w hL^3 dl \tag{5}$$

After integrating the above equation with the limits from P = 0 to P = P and from l = 0 to l = r, where r is the mixer radius, the result is

$$P = \pi^3 k_M N^3 \rho_w h\, r^4 \qquad [W] \tag{6}$$

After introducing $d_M = 2r$ and expressing the height of the mixer as diameter multiple $h = c \cdot d_M$, the result is

$$P = \pi^3 k_M N^3 \rho_w c \cdot d_M \left(\frac{d_M}{2}\right)^4 \tag{7}$$

Including all constant constituents (π, k_M, c, 0.0625) into K_M coefficient, the power equation takes the final form

$$P = K_M \cdot \rho_w N^3 d_M^5 \tag{8}$$

The K_M resistance coefficient is often defined as the Newton number (Ne). Its value can be defined from the following correlative equation

$$K_M = Ne = \frac{a}{Re^b} \tag{9}$$

The values of a and b constant coefficients depend on the types of mixer and flow. For laminar flow ($Re < 30 \div 50$) b = 1. With the increase of turbulence $b \to 0$ and the resistance coefficient also approaches a constant quantity. The dependence of the K_M resistance coefficient on Reynolds number for various kinds of mixers is presented in Figure 3. [38, 45].

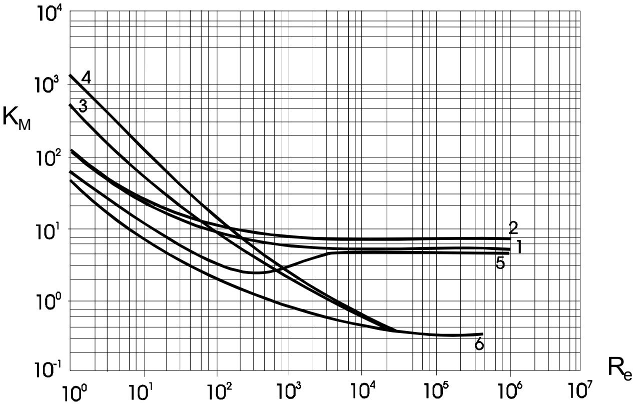

Fig. 3. Dependence of resistance coefficient on Reynolds number for selected types of mixers.

Curve No. 1 shows the dependence $K_M = f(Re)$ for s frame mixer, No. 2 for a plate mixer, No. 3 for an anchor mixer, No. 4 for a two-element helical mixer, No. 5 for

a turbine mixer with six paddles and four baffles in the tank, No. 6 for a propeller mixer.
Figure 4. presents the schemes of the above-mentioned mixers.

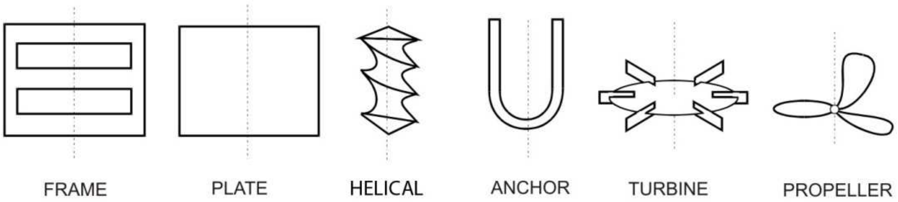

Fig. 4. Schemes of analyzed mechanical mixers.

For the purposes of the analysis of mixing power demand, a standard configuration of a tank with four vertical baffle plates and without baffles has been defined. Designs of a tank with baffles and a frame mixer, a tank with baffles and a turbine mixer, and a tank without baffles and with a propeller mixer are shown in Figure 5.

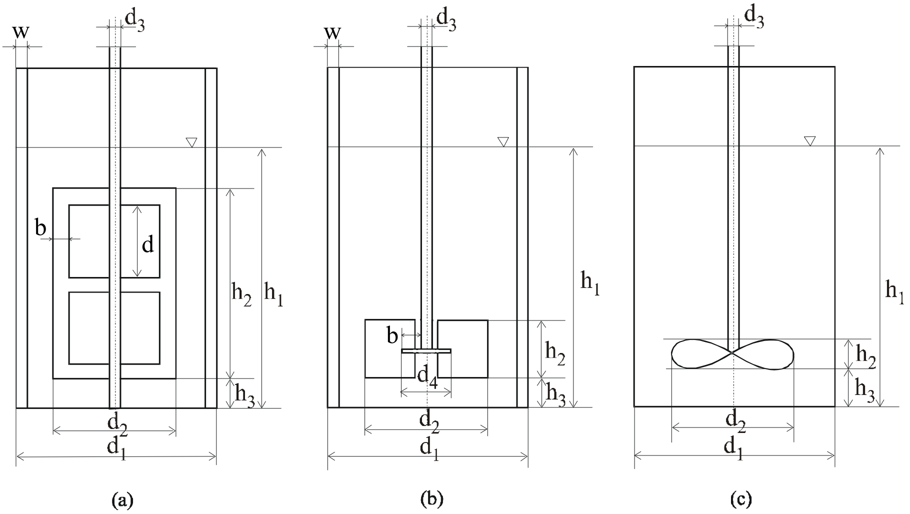

Fig. 5. Designs of a standard tank for estimating the resistance coefficient (K_M) at the application of (a) frame mixer, (b) turbine mixer, and (c) propeller mixer.

Characteristic relations between particular dimensions of tanks and mixers were compared in Table 4.

Table 4. Relations between particular dimensions of a standard tank and mixers applied [62].

Relative dimension	**(a)**	**(b)**	**(c)**
d_2/d_1	0.5	0.33	0.33
h_2/d_2	1.5	0.2	0.36
h_3/d_3	0.2	1.0	0.03
h_1/d_1	1.0	1.0	0.75
w/d_1	0.1	0.1	-
b/d_2	0.1	0.25	-
d_4/d_1	-	0.25	-
d/d_1	0.6	-	-

When determining the K_M coefficient with the use of other mixers, their linear dimensions as well as their location in the tank should be the same as in the case of the mixers presented in Figure 5.

For standard tanks without vertical baffles, mixing can be described by the correlative equation

$$\Phi = \frac{K_M}{(Fr)^y} = k(Re)^x \tag{10}$$

where

Φ – function of power,

$Fr = \frac{N^2 d_M}{g}$ – Froude number,

g - gravitational acceleration, [m/s^2],

$Re = \frac{N d_M^2 \rho_w}{\eta_w}$ – Reynolds number,

k, y, x – constants.

For the tanks with baffled plates, in which there are no whirls, constant y equals 0 and the correlative equation is as follows:

$$\Phi = K_M = k(Re)^x \tag{11}$$

In the range of laminar flow it was observed that constant x = -1, and for turbulent flow x = 0. So the power equation for laminar flow looks as follows:

$$P = kN^2 d_M^3 \eta_w \tag{12}$$

and for the turbulent flow

$$P = kN^3 d_M^5 \rho_w \qquad (13)$$

The constant k is the function of the mixer type and the character of the flow. For example, for a 3-paddle propeller mixer and a laminar flow k = 41.0, and for a turbulent flow k = 0.32. For a turbine mixer with 6 paddles these values are k = 71.0 and k = 6.30 for the laminar and turbulent ranges, respectively. Formulas (12) and (13) present approximate values of power demand.

To start a mixer, additional power is needed to overcome the forces of inertia and friction.

Power demand required to start a mixer can be determined from the empirical formula of Kasatkin [45]:

$$P_s = P(1 + 0.134 Re^{0.22}) \qquad (14)$$

Calculated driving power should be enlarged by the losses in driving gears. Depending on the construction of those gears, the efficiency of energy utilization is from 60 to 90%.

To design a mixing process, modeling studies are often used. Transferring the results of research to the full technical scale should be carried out maintaining the conditions of geometrical and hydrodynamic similarity. While transferring the scale, it should be remembered that for a demanded mixing time, the power used per unit water volume must be constant.

Mixing time is a very important process parameter, which decides both its effects and its economics.

To unify the system of components of similar densities and viscosities, the optimal process time can be determined on the basis of Zlokarnik diagrams [45], presenting the dependency N·t = f(Re) for various types of mixers (Fig. 6).

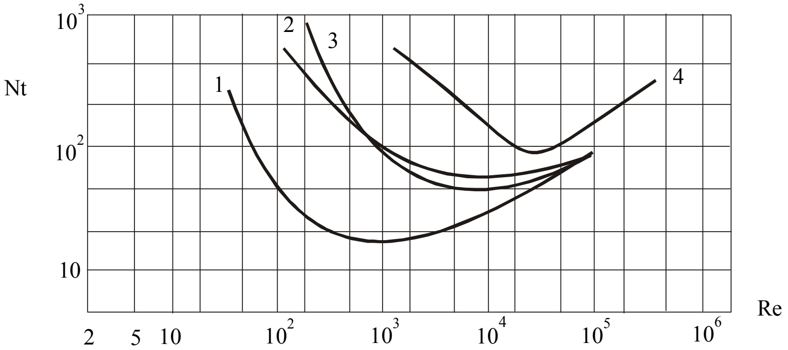

Fig. 6. Characteristics of mixing times for selected types of mixers and mixing systems.

These curves are valid for the full molecular homogenization of components in a tank. The product of rotational speed (N) and mixing time (t) is defined as dimensionless time and it changes in the range from 5 to 10^3 [45].
Curve 1 concerns a plate mixer. Curves 2 and 4 depict the dependency for a mixing system in a tank with four vertical baffles, with turbine and propeller mixers, respectively. Finally, curve 3 concerns an anchor mixer.

When choosing an optimal mixer concerning the demand for mixing energy, one can use a practical Zlokarnik diagram which presents the dependency of modified typical power value $(Pd_M^2\rho_w^2/\eta_w^3)$ on typical mixing value $(t\eta_w/d_M^2\rho_w)$ (Fig. 7).

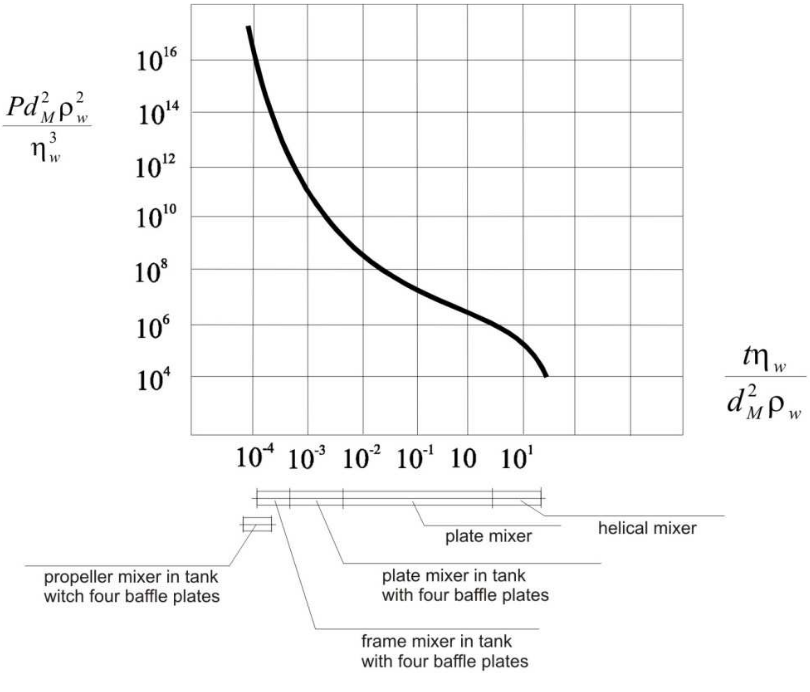

Fig. 7. Modified typical power value as a function of a typical mixing value.

The dimensionless mixing number decreases with a decreasing dynamic viscosity coefficient. To homogenize the system with water, the viscosity of which is $\eta_w \leq 2 \cdot 10^{-3}$ kg/m·s, mixing time can be estimated from an empirical formula

$$t = 10^{-4} d_M^2 \frac{\rho_w}{\eta_w} \qquad [h] \qquad (15)$$

Solution mixing conditions are often characterized by a **velocity gradient** (G[s^{-1}]). This gradient is defined as a velocity difference of two points or elementary solution volumes, disposed perpendicularly to the direction of liquid flow. It referrs to the friction forces between two elementary layers moving at different speeds and is described by the following formula:

$$G = \sqrt{\frac{P}{\eta V}} \qquad [s^{-1}] \qquad (16)$$

where P is the power introduced into the system [W], V is the volume of the solution [m^3], η is the dynamic viscosity of the solution [kg/m·s].

The notion of velocity gradient is used to describe completely mixed flow reactors in which a fixed concentration in maintained. Frequently to model the mixing process, **the product of gradient and mixing time** is used (G·t) which describes the intensity of mixing. The dimensionless G·t product is defined as the Camp number. This number is an important parameter when modeling flocculation.

The mixing process of the chemicals added to water may be realized with the use of flow hydraulics in pipelines and in open inter-object ducts. The injection of fluid reagents or the stream of sprayed liquid to the pipeline working under pressure has become a common method of rapid mixing in small water treatment plants and also often in cases when mixing of reagents added to water is a modification of an existing technological system.

The dissipation of energy in the systems of **mixing in pipelines** can be determined on the basis of the quantity of pressure loss and the size of the flow [62].

$$P = Q \cdot \rho_W \cdot g \cdot h \qquad [W] \qquad (17)$$

In the above equation, Q is the flow rate [m^3/s],
g – gravitational acceleration (9.81 m/s^2), ρ_w – specific water gravity [kg/m^3],
h – pressure loss [m].
A modified form of Equation (17) allows the determination of the so called volume of energy dissipation

$$\frac{P}{V} = \frac{\rho_W \cdot g \cdot h}{t} \qquad (18)$$

where V – volume of energy dissipation [m^3], t – retention time [s].
The loss of pressure h [m] in straight segments of pipelines and for laminar flows can be determined from the following formulas:

– for pipelines with very smooth external surfaces

$$h = 0.54 \cdot 10^{-3} L \cdot V_p^{1.75} / D^{1.25} \qquad (19)$$

– for pipelines with smooth surfaces

$$h = 0.78 \cdot 10^{-3} L \cdot V_p^{1.86} / D^{1.25} \qquad (20)$$

– for pipelines with coarse internal surfaces

$$h = 1.15 \cdot 10^{-3} L \cdot V_p^{1.95} / D^{1.25} \tag{21}$$

– for pipelines with very coarse surfaces

$$h = 1.68 \cdot 10^{-3} L \cdot V_p^{2.0} / D^{1.25} \tag{22}$$

In Equations (19) ÷ (22) D is the pipeline diameter [m], V_p is the linear flow rate [m/s], L is the length of energy dissipation zone [m].

To determine velocity gradient, an empirical formula with a relatively good approximation can be used

$$G = 564\left(\frac{\lambda}{D}\right)^{1/2} V_p^{3/2} \tag{23}$$

In the above formula, λ is the frictional resistance coefficient in the Darcy-Wiesbach equation. The friction coefficient is a function of Reynolds number and the laminar flow area $\lambda = \sim 0.25$ [62].

Mixing through the water flow corresponds with molecular diffusion and hydrodynamic dispersion. The most beneficial mixing conditions and the shortest energy dispersion zone are achieved when the injection of reagent occurs at the pipeline axis (Fig. 7a)

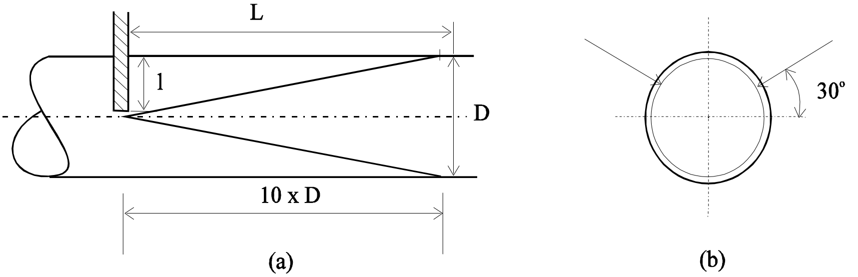

Fig. 8. Diagram of reagent mixing in a pipeline.

If l/D = 0.5, then L/D = 10. In practice, the outlet of the nozzle which delivers the reagent is located a few millimeters from the internal wall of the pipeline that transports water. In such situations, e.g. for the value l/D = 0.05, total mixing occurs at the point L/D = 60. Using two nozzles feeding the reagent considerably shortens the distance after which total mixing occurs. It is most effective to locate injections above the horizontal diameter of the pipeline intersection at the angle of 30°to the diameter (Fig. 8b). With such a configuration of the nozzles and at the ratio l/D = 0.05 the total homogenization of the system will happen at the point L/D = 20.

The volume of the water in which the introduced energy is dispersed varies from $2.5\pi D^3$ to $15\pi D^3$ depending on the method of reagent injection. To increase the efficiency of mixing, which is inversely proportional to the dispersion volume, the change of the ratio of introduced energy per unit volume is applied through curving the pipeline, reducing or enlarging its diameter. It is assumed that the mixing in the pipeline is effective if the energy dissipation zone length is equal to five times the pipeline diameter (dispersion volume is $1.25\pi D^3$).

The pressure loss due to a rapid increase of the pipeline diameter is

$$h = \frac{V_{p1}^2 - V_{p2}^2}{2g} \tag{24}$$

where V_{p1} and V_{p2} are the velocities before the widening of the pipeline and after it, respectively [m/s].

Pressure loss caused by a rapid diminution of the diameter is described by equation [62]

$$h = 0.35\,\frac{(V_{p1} + V_{p2})^2}{g} \cdot \left[1 - \left(\frac{d}{D}\right)^2\right]\left[\left(\frac{D}{d}\right)^4 - 1\right] \tag{25}$$

in which D and d are diameters of the principal pipe and the pipe with a reduced diameter, respectively [m].

As the criterion of the mixing ratio serves the value of dimensionless dispersion number (Disp), which is defined by equation

$$\mathrm{Disp} = E / V_p \cdot L \tag{26}$$

in which

$E = \frac{1}{2} \cdot \frac{V_p L \cdot \Gamma^2}{T^2} = \frac{1}{2} \cdot \frac{V_p^2}{T} \Gamma^2$ – dispersion coefficient [m^2/s],

V_p – average flow rate [m/s],

L – the length of energy dissipation zone [m],

T – average detention time [s],

Γ^2 – variance of detention time distribution [s^2] (Gaussian distribution is assumed).

When the value of the dispersion number $\mathrm{Disp} = 0$, the dispersion process does not occur and the flow can be analyzed as ideal piston flow. At $\mathrm{Disp} < 0.01$ a small dispersion occurs; in the range of $\mathrm{Disp} \in (0.01; 0.1)$ there is average dispersion and at $\mathrm{Disp} > 0.1$ the dispersion is large. With very high dispersion numbers the system is completely mixed [62].

Energy introduced to the pipeline with a stream of sprayed liquid may be estimated according to formula

$$P = \frac{0.75 f_d \cdot V_w^2 \rho_r}{2g} \tag{27}$$

where

f_d – the surface of the nozzle opening, through which the sprayed fluid is introduced [m^2],

V_w – the speed of fluid injection [m/s],

ρ_r – density of injected fluid [kg/m^3].

Mixing with compressed air is a common process both in water purification and in sewage treatment. This method is used in systems which require not only homogenization, but also oxidation.

In the process of bubble formation, the average velocity gradient is described by equation [62]

$$G^2 = 10^5 \frac{Q_p \cdot H}{\eta_w \cdot V(H/2 + 10.33)} \qquad [s^{-1}] \qquad (28)$$

where

Q_p – air flow volumetric velocity [m^3/s],

H – height of water layer above the diffusion zone [m],

η_w – water dynamic viscosity[kg/m·s],

V – solution volume [m^3].

The maximum velocity gradient is formed in the zone of bubble formation and can be approximated by the following equation:

$$G_{max} = g(\rho_w - \rho_p)\frac{d_p}{6\eta} \qquad (29)$$

where

ρ_w, ρ_p – density of water and air, respectively [kg/m^3],

d_p – representative diameter of air bubbles [m],

η – dynamic viscosity of the mixture [kg/m·s].

In the process of pressure flotation, the air fed to the flotation tank causes ~ 10% expansion of the water layer. The air bubbles formed are approximately 10^{-3} m diameter. In such a system, with the height of water layer above the diffusion zone equal to 2 m, the maximum velocity gradient is 1,500 ÷ 3,000 s^{-1}. Average gradient values are in the range of 200 ÷ 300 s^{-1}.

In the processes of aeration and oxidation, the bubbles formed are of ~ $5 \cdot 10^{-3}$ m in diameter with the ratio of volumetric rate of gas flow to water flow equal to approximately 0.1. In such a case with the water layer H = 2 m the maximum gradient is $G_{max} < 8{,}200$ s^{-1} and the average gradient is $G < 200$ s^{-1} [62].

Mixing with compressed gas is often aided by mechanical mixing.

In the process of flocculation, **hydraulic labyrinth mixers**, in a vertical and horizontal design, are also used (Fig. 9).

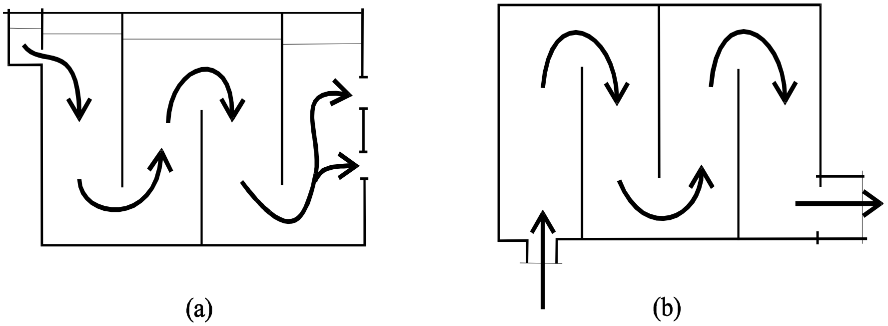

(a) (b)

Fig. 9. Designs of labyrinth chambers of free mixing with (a) vertical, (b) horizontal flow.

Average flow speed in these types of mixers should be about 0.5 m/s. Usually, chambers of four, max. six baffles are designed.

Energy dissipation in labyrinth mixers may be defined by Equation (17) as with the mixing process in pipelines. The velocity gradient corresponding with this equation is described by the following relation:

$$G = \sqrt{\frac{g \cdot h}{\mu \cdot T_H}} \qquad (30)$$

where

μ – kinematic viscosity [m^2/s],

T_H – hydraulic detention time [s].

For rapid mixing of chemicals added to water, **hydraulic jump chambers** are also used. The design of such a chamber is shown in Figure 10.

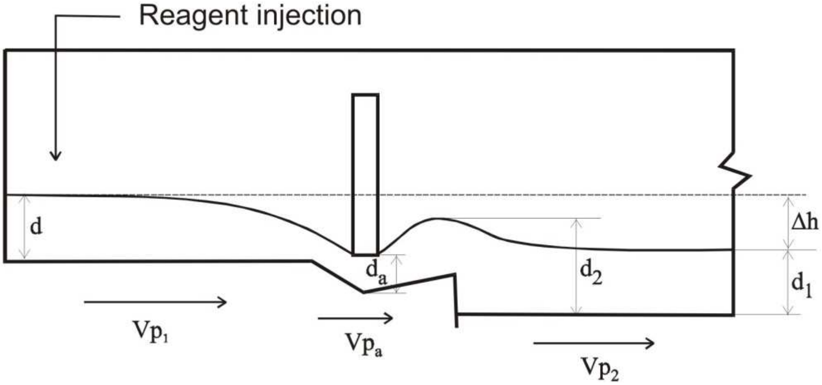

Fig. 10.The design of a hydraulic jump chamber.

The gap height and velocity of the flow coming through it is defined by the Froude number:

$$\mathrm{Fr} = \frac{V_{p\,a}^2}{g \cdot d_a} \tag{31}$$

mixers with hydraulic jumps are classified according to the value of the Froudenumber:

– mixers with pre-jump $1.7 \le \mathrm{Fr} \le 2.5$,
– mixers with transition jump $2.5 < \mathrm{Fr} \le 4.5$,
– mixers with stabilized jump $4.5 < \mathrm{Fr} \le 9$,
– mixers with choppy jump $\mathrm{Fr} > 9$.

The level of water beyond the gap (d_2) is correlated with the size of the gap by the Froude number:

$$\frac{d_2}{d_a} = \frac{1}{2}(\sqrt{1 + 8\mathrm{Fr}^2} - 1) \tag{32}$$

The length of the mixing zone (L) is estimated from Chow's equation [16], the relation $L/d_2 = f(\mathrm{Fr})$ described in Figure 11.

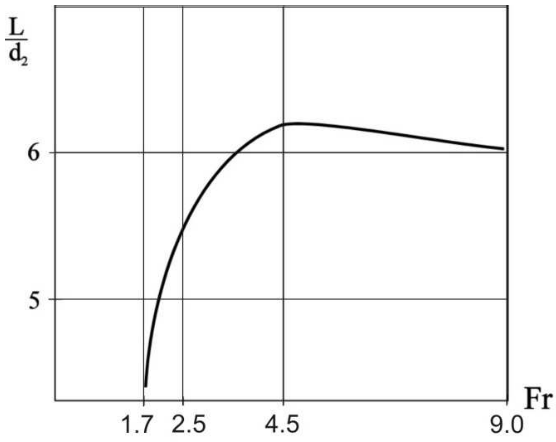

Fig. 11. Diagram for estimating mixing zone length.

Pressure loss in the gap is defined as follows:

$$\Delta h = \frac{(d_2 - d_a)^3}{4d_2d_a} \tag{33}$$

Mixing time in this type of a device is determined on the basis of an average from jump in velocity Vp_a and the velocity in the channel of water outflow immediately after the jump.

In practice, modeling a mixing process with a hydraulic jump is based on successive iterations. Usually in technological systems of water purification mixers with pre-jump are designed which are in the Froude number range of $Fr \in (1.7; 2.5)$. For this type of mixer, the velocity gradient is in the range of $G = 500 \div 1{,}000\ s^{-1}$. The volumetric rate flow Q, flowing to the jump through the channel of width s, at an assumed velocity Vp_1, has a layer height equal to

$$d = \frac{Q}{Vp_1 \cdot s} \tag{34}$$

For a selected type of hydraulic jump a Froude number is first assumed. Assuming that the water layer height in the discharge channel will be the same as in the inlet channel ($d_1 = d$), the assumed value of backwater should be $d_2 > d_1$. From Equation (32) value d_a is determined, and from diagram 11 for the assumed number Fr L/d_2 is read and the length of mixing zone is established (L). From Equation (33) the size of pressure loss (Δh) is determined. The average flow rate in a mixer (Vp_s) is defined by the following formula:

$$Vp_s = \frac{Vp_a + Vp_2}{2} = \frac{Q(d_a + d_2)}{2s \cdot d_2 \cdot d_a} \tag{35}$$

Mixing time is determined from equation

$$t = \frac{L}{Vp_s}, \tag{36}$$

and the velocity gradient is determined from Equation (30) transformed as follows:

$$G = \frac{d_2 - d_a}{2d_2 \cdot d_a}\sqrt{\frac{Q \cdot g(d_2^2 - d_a^2)}{2\mu \cdot L \cdot s}} \tag{37}$$

If the velocity gradient determined from the above equation does not fit into the range advised for the assumed mixer type, the above procedure should be repeated for different input data.

In large open-air technological systems such as settling tanks, water storage tanks, **wind-induced mixing** may occur. While it has no direct technological application, it can disturb the sedimentation process or cause secondary aeration. The design of wind induced currents is shown in Figure 12.

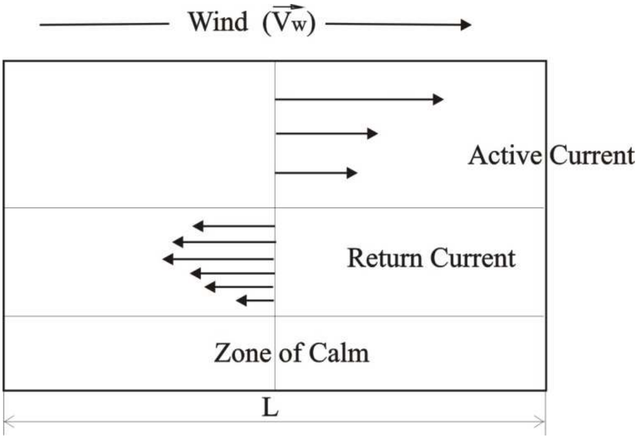

Fig. 12. Design of wind-induced mixing.

Wind of velocity V_w may induce active currents of velocity V_{act} proportional to the size of the tank surface

$$V_{act} = \alpha V_w \tag{38}$$

in which α is proportionality coefficient.
The average velocity gradient of wind-induced mixing is defined by the relation

$$G^2 = \frac{\alpha(\alpha V_w)^2}{4\mu \cdot t} \tag{39}$$

in which

t = L/pV$_w$ – wind mixing time,

L – length of the surface exposed to the wind,

therefore

$$G^2 = \frac{\alpha(\alpha V_w)^3}{4\mu \cdot L} \tag{40}$$

μ is kinematic viscosity [m^2/s]

The values of the proportionality coefficient α vary from 0.01 to 0.05.

Usually, the value of the velocity gradient of wind-induced mixing fits into the range $G = 0.1 \div 0.01$ s^{-1}. Therefore, it does not have a major influence on the mixing of tank contents. It can, however, disturb the course of technological processes. [62].

7.1.1. Example Calculations

EXAMPLE 1

Determine the velocity gradient of mixing with a propeller mixer at a rotational speed $N = 0.25$ s^{-1} of the contents of a standard tank with diameter $d_1 = 3.0$ m, filled to the height $H = 4.0$ m.

The contents of the tank is a solution with density $\rho = 1{,}000$ kg/m^3 and dynamic viscosity $\eta = 10^{-3}$ kg/m·s.

The value of the ratio of the mixer diameter to the tank diameter $d_2/d_1 = 0.33$ for a propeller mixer was obtained from Table 4.

The Reynolds number was determined (Equation 1) for the following dimensions of the mixer: $L = d_2/2 = (0.33 \cdot 3)/2 = 0.495$ m:

$$Re = \frac{2\pi L^2 N\rho}{\eta} = \frac{2 \cdot 3.14\,(0.495)^2 \cdot 0.25 \cdot 1{,}000}{10^{-3}} = 3.85 \cdot 10^5$$

From equation $K_M = f(Re)$ for a propeller mixer (line 6 in Figure 2) for a determined value Re, the value of resistance coefficient $K_M = 0.5$ was obtained.

Power demand was determined from Equation 8:

$$P = K_M \cdot \rho \cdot N^3 \cdot d_2^5 = 0.5 \cdot 1000\,(0.25)^3\,(0.33 \cdot 3)^5 = 7.43\ \text{W}$$

The mixing velocity gradient was determined from Equation (16):

$$G=\sqrt{\frac{P}{\eta V}}=\sqrt{\frac{P}{\eta\frac{\pi d_1^2}{4}H}}=\sqrt{\frac{7.43}{10^{-3}\frac{3.14\cdot 3^2}{4}\cdot 4}}=16.22\ s^{-1}$$

EXAMPLE 2

Design a hydraulic mixer with pre-jump for which the Froude number is in the range Fr $\in$ (1.7; 2.5), and the mixing velocity gradient is G $\in$ (500; 1,000) s^{-1}. The volumetric velocity of the inflow to the mixing chamber through the channel of the width s = 1.0 m is Q = 2,500 m^3/h. The water kinematic viscosity is $\mu = 10^{-6}$ m^2/s.
Assuming the flow velocity in the inlet channel equal to V_{p_1}=2.0 m/s, the height of the water layer is

$$d=\frac{Q}{V_{p_1}\cdot s}=\frac{\frac{2{,}500}{3{,}600}}{2\cdot 1}=0.35\ m$$

Assuming that the height of water layer in the outlet channel (d_1) is the same as in the inlet channel, the following backwater behind the gap is assumed: ($d_2 > d_1$) d_2 = 0.55 m.
The first step assumes Froude number Fr = 2.5.
The value of the gap width is determined from Equation (32):

$$d_a=\frac{2d_2}{\sqrt{1+8Fr^2}-1}=\frac{2\cdot 0{,}55}{\sqrt{1+50}-1}=\frac{1.1}{6{,}14}=0.18\ m$$

Diagram 11 for Fr = 2.5 gave L/d_2 = 5.25 and zone mixing length L was determined

$$L=5.25d_2=5.25\cdot 0.55=2.89\ m$$

Pressure loss (Δh) was determined from Equation (33)

$$\Delta h=\frac{(d_2-d_a)^3}{4d_2\cdot d_a}=\frac{(0.55-0.18)^3}{4\cdot 0.55\cdot 0.18}=0.128\ m$$

Average flow rate in the mixer (V_{p_s}) determined from Equation (35) is

$$V_{p_s}=\frac{V_{p_a}+V_{p_2}}{2}=\frac{Q\left(d_a+d_2\right)}{2s\cdot d_2\cdot d_a}=\frac{\frac{2{,}500}{3{,}600}\left(0.18+0.55\right)}{2\cdot 1\cdot 0.18\cdot 0.55}=2.56\ m/s$$

Mixing time determined from Equation (36) is

$$t=\frac{L}{V_{p_s}}=\frac{2.89}{2.56}=1.13\ s$$

Mixing velocity gradient was determined from Equation (37)

$$G=\frac{d_2-d_a}{2d_2\cdot d_a}\sqrt{\frac{Q\cdot g\left(d_2^2-d_a^2\right)}{2\mu\cdot L\cdot s}}=\frac{0.55-0.18}{2\cdot 0.55\cdot 0.18}\sqrt{\frac{\frac{2{,}500}{3{,}600}9.81\left(0.55^2-0.18^2\right)}{2\cdot 10^{-6}\cdot 2.89\cdot 1}}=1.87\cdot 5642=1{,}055\ s^{-1}$$

As the designated velocity gradient is greater than the maximum gradient for an mixer with pre-jump, in the second step a lower value of Froude number is assumed Fr = 2.

Gap width:

$$d_a=\frac{2d_z}{\sqrt{1+8Fr^2}-1}=\frac{2\cdot 0.55}{\sqrt{1+32}-1}=\frac{1.1}{4.74}=0.23\ m$$

From diagram 11 for Fr = 2, $L/d_2 = 5.0$ was obtained and the length of mixing zone L was determined

$$L=5.0\cdot d_2=5.0\cdot 0.55=2.75\,m$$

Pressure loss (Δh)

$$\Delta h=\frac{\left(d_2-d_a\right)^3}{4d_2\cdot d_a}=\frac{\left(0.55-0.23\right)^3}{4\cdot 0.55\cdot 0.23}=0.065\ m$$

Average flow rate $\left(V_{p_s}\right)$

$$V_{p_s}=\frac{V_{p_a}+V_{p_2}}{2}=\frac{Q\left(d_a+d_2\right)}{2s\cdot d_2\cdot d_a}=\frac{\frac{2{,}500}{3{,}600}\left(0.23+0.55\right)}{2\cdot 1\cdot 0.55\cdot 0.23}=2.14\ m/s$$

Mixing time

$$t=\frac{L}{V_{p_s}}=\frac{2.75}{2.14}=1.29\ s$$

Mixing velocity gradient

$$G=\frac{d_2-d_a}{2d_2\cdot d_a}\sqrt{\frac{Q\cdot g\left(d_2^2-d_a^2\right)}{2\mu\cdot L\cdot s}}=\frac{0.55-0.23}{2\cdot 0.55\cdot 0.23}\sqrt{\frac{\frac{2{,}500}{3{,}600}\,9.81\left(0.55^2-0.23^2\right)}{2\cdot 10^{-6}\cdot 2.75\cdot 1}}=1.265\cdot 556=703.4\,s^{-1}$$

The mixing velocity gradient determined in the second step is in the range of gradients for mixing with pre-jump so the mixing parameters are set correctly.

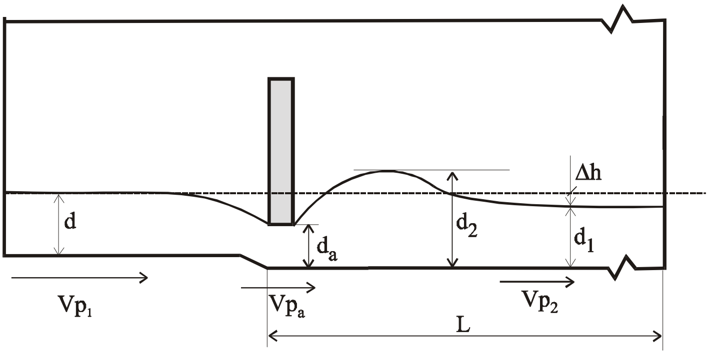

$d = d_1 = 0.35$ m,
$d_a = 0.23$ m,
$\Delta h = 0.065$ m,
$L = 2.75$ m.

7.2. Aeration and Stripping

Modeling of aeration process is based on Henry's law, which specifies the influence of pressure on solutions of gases in liquids. According to this law, at a given temperature, the ratio of gas pressure in the air at the water-air interface to the concentration of this gas in a solution is constant and does not depend on pressure. This law also applies to the process of air stripping of volatile contaminants.

The main aeration methods used in water technology are cascade aeration through crash jets on draining beds and pipe beds, and by means of compressed air. The purpose of aeration is primarily the oxidation of highly reduced compounds and their transformation so that they can be removed from water. In wastewater technology, oxygen supplied with the air is used by the heterotrophic microorganisms to degrade organic pollutants. During aeration, the mixing of reactor contents is also performed.

Predicting the rate of oxygen transport to the system is always based on the model described by Equation (41). The volumetric oxygen mass transfer coefficient $k_L \cdot a$ is the function of temperature, intensity and mixing type, tank geometry and the composition of aerated water.

The rate of oxygen mass transport in the process of re-aeration is described by

$$r_R = k_L \cdot a\left(C_{O_2}^s - C_{O_2}\right) \tag{41}$$

where other parameters are

$C^s_{O_2}$ – oxygen saturation concentration of water mass at a given temperature [gO_2/m^3],

C_{O_2} – oxygen concentration in the water [gO_2/m^3].

The effect of temperature on the volumetric mass transfer coefficient is described by the following equation:

$$k_L \cdot a_{(T)} = k_L \cdot a_{(20)} \theta^{T-20} \tag{42}$$

where

$k_L \cdot a_{(T)}$ – transfer coefficient at temperature T (s^{-1}),

$k_L \cdot a_{(20)}$ – transfer coefficient at temperature 20°C (s^{-1}).

The temperature coefficient θ varies depending on the conditions under which the test is carried out and generally falls in the range 1.015 ÷ 1.04. A typical value θ for both the aeration with compressed air and mechanical aeration is 1.024. The effect of mixing intensity and system geometry is difficult to determine by theoretical means. It is, therefore, necessary to conduct tests at least at a laboratory scale [19]

Air stripping is increasingly used to remove gases such as CO_2 and H_2S and volatile organic contaminants of anthropogenic origin such as TCE and DBCP.

In technological systems for heavily contaminated groundwater, filtration and adsorption processes are used next to air stripping. Adsorption in this system is used to remove non-volatile organic pollutants.

The efficiency of air stripping depends on the size of the interface surface, the surface tension of the solution and the driving module of mass transfer of pollutants between the solution and the air [19, 37].

An increase of interface surface is obtained by the fragmentation of the stream at the tower entry point. In the process of flow through the filling, a continuous division of water drops is achieved providing a significant reduction in surface tension, which is the smallest at the time of drop re-formation of. In order to increase the mass transfer driving module, air passed in the counter-current cannot contain volatile contaminants stripped from water.

The kinetics of mass transfer at the solution-air interface are based on Henry's law and the mass balance of the stripped contamination in the system.

The computational scheme of a counter-current stripping tower is shown in Figure 13.

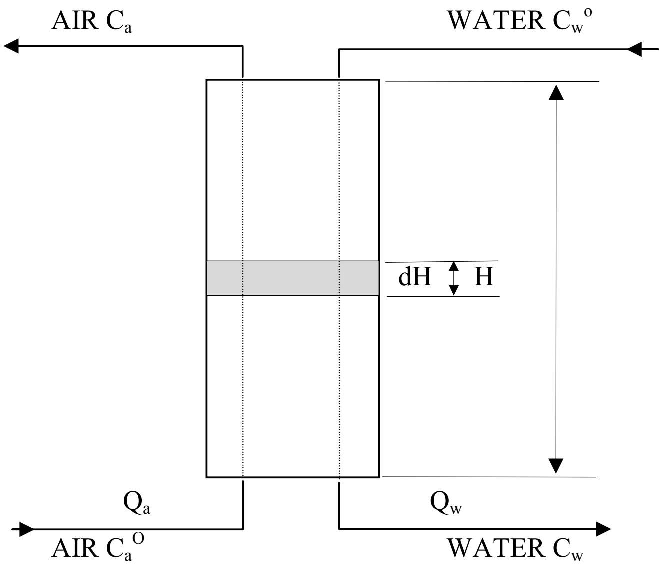

Fig. 13. Computational scheme of counter-current stripping tower.

The mass balance of volatile contaminants in the system is

$$Q_a \cdot dc_a = Q_w dc_w \tag{43}$$

That is, an increase in air pollution load is equal to the decrease in water pollution load. In Equation (43) Q_a and Q_w are the rates of the flow through the tower of the air and water, respectively and C_a and C_w are the concentrations of pollutants in the air and water, respectively. After integration from C_a^o to C_a, and from C_w to C_w^o the following is obtained

$$Q_a\left(C_a - C_a^o\right) = Q_w\left(C_w^o - C_w\right) \tag{44}$$

Assuming that $C_a^o = 0$ and $C_w = 0$ and that, according to Henry's law, the concentration of contaminants at the tower outlet is in balance with the concentration of contaminants in the inflow, a theoretical amount of air necessary for 100% water purification from volatile contaminants can be determined:

$$Q_a \cdot C_a = Q_w \cdot C_w^o \tag{45}$$

$$\frac{Q_a}{Q_w} = \frac{C_w^o}{C_a} = \frac{1}{m} \tag{46}$$

In the above equation, m is Henry's constant, which is dependent on temperature (T[°C]) according to equation

$$m = 0.117 \exp[0.02612(32 + 1.8T)] \quad (47)$$

Analyzing the mass transfer process related to the driving module in the air, the following equation can be written:

$$Q_a \cdot dC_a = k_a \left(C_a^* - C_a\right) ds \quad (48)$$

in which

C_a^* – equilibrium concentration in the air [g/m^3],

k_a – constant rate of pollutants diffusion in the air [m/h],

ds – the boundary surface of interface, through which diffusion occurs [m^2].

$$ds = z \cdot F \cdot dH \quad (49)$$

where

F – cross-sectional area of the tower [m^2],

z – the boundary surface of interface tallied for m^3 of tower volume [m^2/m^3],

dH – differential element of tower height [m].

When analyzing the process in relation to the driving module in the solution, the following equation can be written:

$$Q_w \cdot dC_w = k_w \left(C_w - C_w^*\right) ds \quad (50)$$

in which

C_w^* – equilibrium concentration in the water [g/m^3],

k_w – constant rate of pollutants diffusion in the solution [m/h].

The height of the tower necessary to reduce the concentrations of volatile impurities from the value of C_w^o to C_w is calculated after integrating Equation (50)

$$H = \frac{Q_w}{k_w \cdot z \cdot F} \int_{c_w}^{c_w^o} \frac{dC_w}{C_w - C_w^*} \quad (51)$$

In Equation (51), the expression before the integral is defined as the mass transfer unit height, and is often marked as $(HTU)_w$.
The value of $(HTU)_w$ depends on the type of tower filling and on the volume of delivered air per volume unit purified water and should be determined through experiments [37].
The integral in Equation (51) is often marked as N_w and is the amount of mass transfer unit heights.
Similarly, analyzing the process in relation to the driving module in the air phase, the equation of tower height takes the following form:

$$H = \frac{Q_a}{k_a \cdot z \cdot F} \int_{c_a^o}^{c_a} \frac{dC_a}{C_a^* - C_a} \quad (52)$$

Similarly, the value before the integral is marked as $(HTU)_a$ and the integral as N_p. Solving this integral requires defining the equilibrium concentration, which is the function of concentration C_a $[C_a^* = f(C_a)]$.

Assuming the balance equation (44) as the basis for considerations and assuming that $C_a^o = 0$, $C_w^o = C_w$ the result is

$$Q_a \cdot C_a = Q_w C_w - Q_w C_w^z \qquad (53)$$

in which

C_w^z – the assumed concentration of contaminants in the column outflow [g/m^3].

Solving Equation (53) with regard to C_w the following is obtained:

$$C_w = \frac{Qa}{Q_w} C_a + C_w^z \qquad (54)$$

Assuming that the temperature along the tower is constant (T = const)

$$C_a^* = mC_w^o = \frac{mQ_a}{Q_w} C_a + mC_w^z \qquad (55)$$

The number of mass transfer unit heights in relation to the air is, therefore

$$N_a = \int_{C_a^o=0}^{C_a} \frac{dC_a}{\frac{mQ_w}{Q_a} C_a + mC_w^z - C_a} \qquad (56)$$

and

$$N_a = \frac{1}{\frac{mQ_a}{Q_w} - 1} \ln\left[C_p \left(\frac{mQ_p}{Q_w} - 1 \right) + mC_w^z \right] \Bigg|_{C_a^o=O}^{C_a} \qquad (57)$$

$$N_a = \frac{1}{\frac{mQ_a}{Q_w} - 1} \ln \frac{C_a \left(\frac{mQ_w}{Q_a} - 1 \right) + mC_w^z}{mC_w^z} \qquad (58)$$

The value of C_a determined from Equation (55)

$$C_a = \left(C_w^o - C_w^z \right) \frac{Q_w}{Q_a} \qquad (59)$$

is inserted to Equation (58) and after transforming it, the final N_p value is achieved

$$N_a = \frac{\frac{Q_w}{mQ_a}}{1-\frac{Q_w}{mQ_a}} \ln\left[\frac{C_w^o}{C_w^z}\left(1-\frac{Q_w}{mQ_a}\right)+\frac{Q_w}{mQ_a}\right] \qquad (60)$$

In the above equation Q_w/Q_a is the number of moles of water per mole of air = $(m^3 water/m^3 air)\cdot 1.25\cdot 10^3$.

As mentioned before, the mass transfer unit height is a function of the tower package and the Q_a/Q_w ratio. In professional literature, a large volume of experimental data for specific cases can be found presented in charts. An example course of the relation: $(HTU)_a = f\left(\frac{Q_a}{Q_w}\right)$ for a tower packed with pine slats of $(3.5 \cdot 5.0)\cdot 10^{-2}$ m diameter is shown in Figure 14.

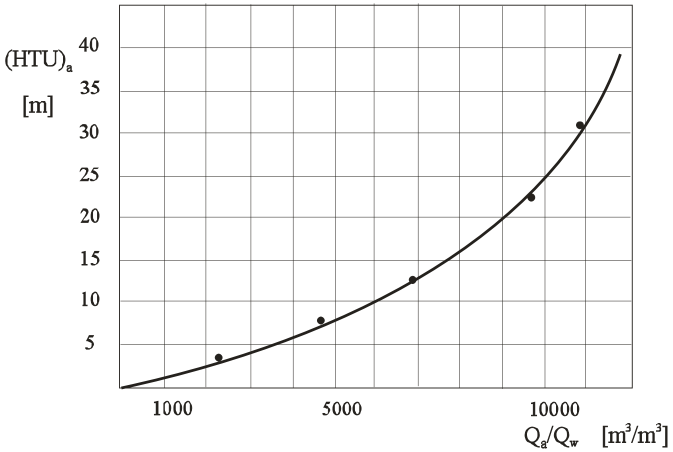

Fig. 14. Dependence of mass transfer unit height on the amount of air per unit water volume.

An analytical determination of the mass transfer unit height requires that for the assumed efficiency of the process (Q_a) and the tower intersection (F), the coefficient of the diffusion rate of pollutants in the air (k_a) and the border surface of the interface (z) should be determined. To estimate the value of k_a, the model of mass transfer with unforced flow and falling drops of liquid was suggested. The phenomena occurring in such a system are truly approximated by the Frössling correlation equation [37]:

$$Sh = 2 + 0.552\,Re^{0.5}\cdot Sc^{0.33} \qquad (61)$$

in which

$Sh = \frac{k_a \cdot d}{D_m}$ – Sherwood number,

d – diameter of a formed drop [m],

D_m – molecular diffusion coefficient of water pollution particles in the air $[m^2/h]$,

$Re = \frac{V_w \cdot d \cdot \rho_w}{\eta_w}$ – Reynolds number,

V_w – relative flow rate between water and air [m/h],

η_w – water dynamic viscosity coefficient [kg/m·h],

ρ_w – water density $[kg/m^3]$,

$Sc = \frac{\eta_a}{\rho_a \cdot D_m}$ – Schmidt number,

η_a – air dynamic viscosity coefficient [kg/m·h],

ρ_p – air density $[kg/m^3]$.

For spraying water, when the diameters of the drops are very small and their consequent settling velocity is also small, Reynolds number can be omitted and then $Sh \rightarrow 2$.

The approximate values of settling velocity of water drops in atmospheric air are presented in Table 5. This table also contains critical velocities at which the drops of a certain diameter break up.

Because the settling velocity of the drops with a diameter of $6 \cdot 10^{-3}$ m is close to the velocity at which they are broken up, in principle, it is not possible to produce freely settling drops with a larger diameter.

Table 5. Settling velocities of water drops and critical velocities in relation to drop diameters [37].

Drop diameter [10^{-3} m]	**Settling velocity [m/s]**	**Break-up velocity [m/s]**
0.05	0.0548	-
0.2	0.71	224.6
0.5	2.13	89.9
1.0	3.87	46.3
2.0	5.85	24.7
3.0	7.26	18.0
4.0	7.92	14.32
5.0	8.17	12.19
6.0	8.23	10.17

Determining a representative water drop diameter is difficult. Drop size is affected by physical properties of water. At a greater water density the drops are smaller. The drop size increases slightly with an increase of solution viscosity.

When estimating drop size, the size is assumed to be constant, as is the settling velocity of the drops and the rate of pollutant mass transfer coefficient.
The average diameter of water drops forming in the process of water spraying can be estimated from the Nukiyama and Tanasawa formula [37]:

$$d = \frac{585\sqrt{\delta}}{V_w\sqrt{\rho_w}} + 597\left(\frac{\eta_w}{\sqrt{\delta\rho_w}}\right)^{0.45}\left(\frac{1000Q_w}{Q_a}\right)^{1.5} \tag{62}$$

in which

d – average diameter of the drop [10^{-6}m],
δ – surface tension of fluid [10^{-1}Pa],
ρ_w – water density [10^{-3}kg/m^3],
η_w – fluid viscosity [Pa·s],
Q_w, Q_a – volumetric velocity of water and air, respectively [m^3/s].

The diffusion coefficient D_m [m^3/h] can be determined from the Stokes-Einstein equation [83]:

$$D_m = \frac{K_B T}{3\pi\eta d_z} \tag{63}$$

in which

$K_B = 1.38 \cdot 10^{-23}$ [J/K] – Boltzman constant,
T – temperature [K],
η – dynamic viscosity coefficient of a medium in which diffusion takes place [Ns/m^2],
d_z – diameter of a pollutant particle [m].

The values of diffusion coefficients in the air (D_m) for selected contaminants are summarized in Table 6 [37].

Table 6. Diffusion coefficients of selected pollutants in air.

Compound	**Formula**	**D_m [m^2/h]**
Ammonia	NH_3	0.0731
Carbon dioxide	CO_2	0.0497
Benzene	C_6H_6	0.0277
Naphthalene	$C_{10}H_8$	0.0185
Anthracene	$C_{14}H_{10}$	0.0152
Toluene	C_7H_8	0.0255
p - Xylene	C_8H_{10}	0.0202
Diphenyl	$C_{19}H_{10}$	0.022
Benzidine	$C_{12}H_{12}N_2$	0.0107
n - Octane	C_8H_{18}	0.0182

The size of the interface surface (z) depends on the type of filling, its size and the method of filling. The value of the parameter for typical fillings is summarized in Table 7. [37].

Table 7.The value of the unit surface “z” for typical fillings of stripping towers.

Filling Type	**Dimensions**			**Filling Porosity**	**Bulk density**	**Unit surface “z”**
	Diameter	**Length**	**Width**			
	10^{-3}m			**-**	**kg/m^3**	**m^2/m^3**
Ceramic rings	16	16	2	0.73	730	410
	25	25	2,4	0.81	505	215
	38	38	4,4	0.76	577	151
	50	50	4,4	0.79	457	120
	75	75	9,5	0.71	714	97
	100	100	12,7	0.62	930	87
	125	125	14,3	0.66	825	79
	150	150	16	0.67	802	70
Ceramic saddles	12.5			0.68	720	460
	25			0.69	670	260
	38			0.70	670	165
Coke	25			0.53	600	120
	40			0.55	590	85
	75			0.58	550	42
Quartz	25			0.37	1,600	120
	40			0.43	1,450	85
	75			0.46	1,380	42

7.2.1. Example Calculations

EXAMPLE 1

Determine the efficiency of ammonia removal (C/C_0) in the air stripping process in the counter-current tower of a height H = 5.0 m, cross-sectional area F = 100 m^2 and filled with ceramic rings with a unit surface z = 87 m^2/m^3. The volumetric velocity of water inflow to the tower is Q_w = 500 m^3/h and the adopted ratio Q_a/Q_w = 3,000.
The temperature of the water-air mixture is T = 15°C so Henry's constant is

$$m = 0.117 \exp\left[0.02612(32 + 1.8T)\right] = 0.55$$

The ammonia molecular diffusion coefficient in air D_m = 0.0731 m^2/h (Table 6).
At an assumed size of formed drops d = 10^{-3} m, the value of constant diffusion velocity of ammonia in the air is described by the following relation:

$$k_a = \frac{2D_m}{d} = \frac{2 \cdot 0.0731}{10^{-3}} = 146.2 \text{ m/h}$$

Estimation of the value of mass transfer unit height

$$(HTU)_a = \frac{Q_p}{k_p \cdot z \cdot F} = \frac{3{,}000 \cdot 500}{146.2 \cdot 87 \cdot 100} = 1.18 \text{ m}$$

The efficiency of ammonia removal was determined from a transformed equation

$$H = (HTU)_a \cdot N_a$$

$$\frac{C}{C_0} = \frac{1-a}{\exp\dfrac{H(1-a)}{(HTU)_a \cdot a} - a}$$

$$a = \frac{Q_w}{m\,Q_a} = \frac{1.25 \cdot 10^3}{0.55 \cdot 3000} = 0.757$$

$$\frac{C}{C_0} = \frac{1-0.757}{\exp\dfrac{5(1-0{,}757)}{1.18 \cdot 0.757} - 0.757} = \frac{0.243}{3.14} = 0.077$$

EXAMPLE 2

From the data in Example 1, determine the tower height required to achieve 90% efficiency of the ammonia stripping process.

$$H = (HTU)_a \cdot \frac{a}{1-a} \ln\left[\frac{C_0}{C}(1-a)+a\right]$$

$$H = 1.18 \cdot \frac{0.757}{1-0.757} \ln[10(1-0.757)+0.757] = 4.26\,\mathrm{m}$$

EXAMPLE 3

For the data in Example 1 (15°C), determine the change in the efficiency of the ammonia stripping process when the system temperature drops to 10°C and increases to 20°C; Identify the necessary changes in the Q_a/Q_w ratio in order to maintain the same level of process efficiency $C/C_0 = 0.077$.
Henry's constant at temperature T = 10°C is:

$$m = 0.117 \exp[0.02612(32+1.8 \cdot 10)] = 0.432$$

Process efficiency in temperature T = 10°C

$$a = \frac{1.25 \cdot 10^3}{0.432 \cdot 3{,}000} = 0.964$$

$$\frac{C}{C_0} = \frac{1-0.964}{\exp\frac{5(1-0.964)}{1.18 \cdot 0.964} - 0.964} = \frac{0.036}{0.207} = 0.17$$

The necessary change in the Q_p/Q_w ratio to maintain the temperature T = 10°C and the process efficiency for temperature T = 15°C equals $C/C_0 = 0.077$.
The value Q_a/Q_w is determined using the method of successive approximations taking in the first step that

$$a < a \text{ (temp. 15°C)}$$

It was assumed that $a_1 = 0.7$

$$\frac{Q_a}{Q_w} = \frac{1.25 \cdot 10^3}{m \cdot a_1} = \frac{1.25 \cdot 10^3}{0.432 \cdot 0.7} = 4{,}133$$

$$Q_a = 4{,}133 \cdot Q_w = 4{,}133 \cdot 500 = 2{,}066{,}500\ \mathrm{m^3/h}$$

$$(\mathrm{HTU})_{a\,(10^\circ C)} = \frac{2{,}066{,}500}{146.2 \cdot 87 \cdot 100} = 1.625\ \mathrm{m}$$

$$\frac{C}{C_0} = \frac{1-0.7}{\exp\frac{5(1-0.7)}{1.625\cdot 0.7} - 0.7} = \frac{0.3}{3.04} = 0.098$$

In the second step it was assumed that
$a_2 = 0.6$

$$\frac{Q_a}{Q_w} = \frac{1.25\cdot 10^3}{0.432\cdot 0.6} = 4{,}822.5$$

$$Q_a = 4{,}822.5 \cdot 500 = 2{,}411{,}265\ \mathrm{m^3/h}$$

$$(\mathrm{HTU})_{a\,(10^\circ C)} = \frac{2{,}411{,}265}{146.2 \cdot 87 \cdot 100} = 1.896\ \mathrm{m}$$

$$\frac{C}{C_0} = \frac{1-0.6}{\exp\frac{5(1-0.6)}{1.896\cdot 0.6} - 0.6} = \frac{0.4}{5.20} = 0.077$$

The system temperature drop from 15 to 10°C causes a drop in process efficiency from $C/C_0 = 0.077$ to $C/C_0 = 0.17$. Maintaining process efficiency at the same level requires nearly a 40% increase in the Q_a/Q_w ratio from 3,000 to 4,822.5.

Henry's constant at temperature T = 20°C is

$$m = 0.117\exp[0.02612(32 + 1.8\cdot 20)] = 0.691$$

The process efficiency at temperature T = 20°C is

$$a = \frac{1.25\cdot 10^3}{0.691\cdot 3{,}000} = 0.603$$

$$\frac{C}{C_0} = \frac{1-0.603}{\exp\frac{5(1-0.603)}{1.18\cdot 0.603} - 0.603} = \frac{0.397}{15.67} = 0.025$$

The necessary change of the Q_a/Q_w ratio to maintain the temperature of 20°C, the process efficiency at temperature 15°C is equal to $C/C_0 = 0.077$:
In the first step

$$a > a\ (\text{temp. } 15^\circ C)$$

It was assumed that $a_1 = 0.8$

$$\frac{Q_a}{Q_w}=\frac{1.25\cdot 10^3}{m\cdot a_1}=\frac{1.25\cdot 10^3}{0.691\cdot 0.8}=2{,}261$$

$$Q_a=2{,}261\cdot Q_w=2{,}261\cdot 500=1{,}130{,}500\ m^3/h$$

$$(HTU)_{a\,(20^\circ C)}=\frac{1{,}130{,}500}{146.2\cdot 87\cdot 100}=0.888\ m$$

$$\frac{C}{C_0}=\frac{1-0.8}{\exp\frac{5(1-0.8)}{0.888\cdot 0.8}-0.8}=\frac{0.2}{3.286}=0.061$$

In the second step
$a_2 = 0.9$

$$\frac{Q_a}{Q_w}=\frac{1.25\cdot 10^3}{0.691\cdot 0.9}=2{,}010$$

$$Q_a=2{,}010\cdot 500=1{,}005{,}000\ m^3/h$$

$$(HTU)_{a\,(20^\circ C)}=\frac{1{,}005{,}000}{146.2\cdot 87\cdot 100}=0.79\ m$$

$$\frac{C}{C_0}=\frac{1-0.9}{\exp\frac{5(1-0.9)}{0.79\cdot 0.9}-0.9}=\frac{0.1}{1.12}=0.089$$

In the third step
$a_3 = 0.86$

$$\frac{Q_a}{Q_w}=\frac{1.25\cdot 10^3}{0.691\cdot 0.86}=2{,}103.5$$

$$Q_a=2{,}103.5\cdot 500=1{,}051{,}750\ m^3/h$$

$$(HTU)_{a\,(20^\circ C)}=\frac{1{,}051{,}750}{146.2\cdot 87\cdot 100}=0.827\ m$$

$$\frac{C}{C_0}=\frac{1-0.86}{\exp\frac{5(1-0.86)}{0.827\cdot 0.86}-0.86}=\frac{0.14}{1.815}=0.077$$

The increase in system temperature from 15 to 20°C causes the increase of process efficiency from $C/C_0 = 0.077$ to $C/C_0 = 0.025$. Maintaining process efficiency at the same level requires diminishing the Q_a/Q_w ratio from 3,000 to 2,103.5.

7.3. Flocculation

Flocculation is defined as a process in which, through a collision of destabilized colloidal or pseudo-colloidal particles, larger particles are formed and subsequently removed in sedimentation and / or filtration processes.

Processes which destabilize dispersion systems are coagulation, chemical or biological oxidation causing destruction of protective colloids, changes in the system conditions such as pH, temperature, addition of adjuvants. Coagulation still remains the most important process preparing the system for flocculation.

The most important factor limiting the flocculation process is the energy of mutual repulsion of particles in the system. This energy is described by the van der Waals equation. It shows that the energy of repulsion increases rapidly with decreasing distance between particles.

The first stage of the process, the so called **perikinetic flocculation**, is the result of random collisions which are the effects of Brownian motion and the motion of the liquid [29, 60].

According to Fick's First Law for transient diffusion, in a system of homogenic dispersion, that is for the particles of equal size and chemical composition, the number of collisions resulting from Brownian motions equals

$$I = 8\pi D R_o n_0^2 \left(\frac{1 + R_o}{\sqrt{2\pi D t}} \right) \tag{64}$$

In practice, after a short time from initiating the process, the expression in brackets equals unity and the above equation is simplified to the form

$$I = 8\pi D R_o n_0^2 \tag{65}$$

in which

I – number of collisions in unit time and in the unit volume,

$D = \frac{K_B \cdot T}{6\pi\eta r}$ - mutual diffusion coefficient [m^2/s],

$K_B = 1.38 \cdot 10^{-23}$ J/K – Boltzman constant,

T – temperature [K],

r – radius of dispersed particles [m],

η – dynamic viscosity coefficient [kg/m·s],

R_o – radius of particles interaction [m],

n_o – initial number of particles.

Since the probability of particles binding is equal or proportional to the probability of collision, the change in the number of particles due to perikinetic flocculation is expressed by the following equation:

$$\frac{dn}{dt} = -8\pi \cdot DR_o n^2 = \alpha \cdot n^2 \tag{66}$$

The above formula is the basic equation of second-order kinetics. A generalized model for polydispersion solutions according to Hahn is as follows [62]:

$$n_k = \frac{n_0}{(1 + t / T_f)^{\alpha+1}} \left(\frac{t}{T_f} \right)^{1-\alpha} \tag{67}$$

In the above equation:

$T_f \approx \frac{1}{\alpha} \approx \frac{1}{4\pi DR_o n_0}$ – the time for half of flocculation

Based on this generalization

$$I_{ij} = 4\pi D_{ij} n_i n_j \tag{68}$$

where

I_{ij} – the number of collisions in the unit time and in the unit volume between the particles of “i” and “j” size,

D_{ij} – mutual diffusion coefficient for “i” and “j” particles, equal approximately $D_i + D_j$,

R_{ij} – the radius of interaction between two particles – distance between the centers of two binding particles (commonly assumed is the sum of those particles' radii)

n_i, n_j – the concentrations of “i” and “j” particles.

The rate of concentration change of 'k' particles (n_k), where k = i + , can be written as

$$\frac{dn_k}{dt} = \frac{1}{2} \sum_{\substack{i=1,\\ j=k-1}}^{k-1} 4\pi D_{ij} R_{ij} n_i n_j - n_k \sum_{i=1}^{\infty} 4\pi D_{ik} R_{ik} n_i \tag{69}$$

In the above equation the first sum describes particle binding to dimension “k”, the second sum – to a dimension greater than “k”.

The coefficient of mutual diffusion, or Brownian diffusion, is inversely proportional to particle size and when all the particles are approximately the same size, the product of $D_{ij} R_{ij}$ may be replaced by the expression $2DR_g$, where the D and R_g values are characterized by a replacement particle. Using this approximation enables an analytical solution of the velocity equation to determine the quantity of particles in a given volume, regardless of their size, as a function of time

$$\frac{n_t}{n_0} = \frac{1}{1 + \frac{t}{T_f}} \qquad (70)$$

where n_t – is the total number of particles in time t from the beginning of the process and n_0 is the initial number of particles.

In the process of flocculation, initial homogeneous dispersion of the system changes into polydispersion. Moreover, due to the increase in particle size, the effect of Brownian motion on particle transfer decreases progressively. Also, the size of the energy barrier of particle interaction increases proportionally to the cross section of the particles. Consequently, with increasing particle size, the probability of their perikinetic contact decreases.

When the solution in which the particles are suspended is in motion, it causes particle transfer and thus the interaction between particles may then take place.

Flocculation in which the contact between the particles is forced by local velocity gradients is known as **orthokinetic flocculation.**

The model for this type of particle aggregation, proposed by Smoluchowski, assumes that the particles of "i" and "j" type are in contact with each other due to the existence of a local velocity gradient dV/dz of a fixed value and constant direction (Figure 15) [34, 60].

The contact takes place when the center of “i” particle enters the interaction zone of the “j” particle. At this point, the radius of an active collision is R_{ij} (Figure 14b). The movement of one particle in relation to the second particle is associated with the movement of the water stream. The field through which the effective transfer occurs is described by the following equation (Figure 14c)

$$dF = 2\sqrt{R_{ij}^2 - z^2}\, dz \qquad (71)$$

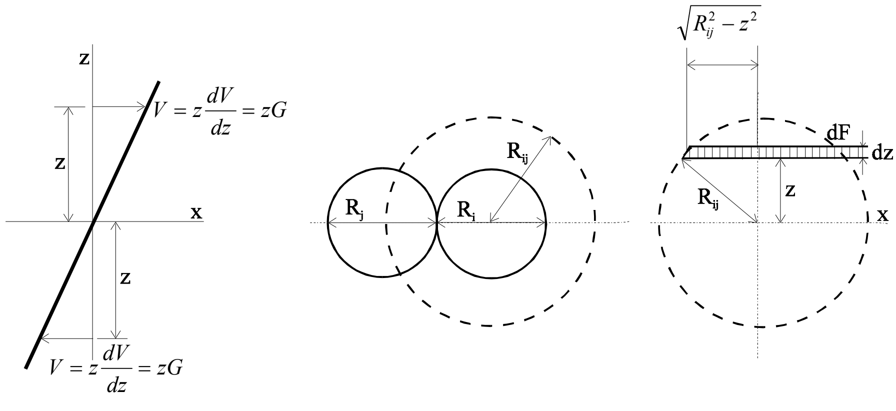

(a) (b) (c)

Fig. 15. Distribution of collision fields in orthokinetic flocculation.

The flow through this surface is

$$dQ = z\frac{dV}{dz}2\sqrt{R_{ij}^2 - z^2}\,dz \tag{72}$$

and the flow through the whole sphere surrounding the particle is

$$Q = 2\int_0^{R_{ij}} G\sqrt{R_{ij}^2 - z^2}\,z\,dz = \frac{4}{3}GR_{ij}^2 \tag{73}$$

According to this theory, if the mixing forces the laminar movement of water, the probability of particle collisions is expressed as follows:

$$J = \frac{4}{3}\left(R_{ij}\right)^3 n_i n_j G \tag{74}$$

G is the velocity gradient with laminar flow, R_{ij} is the radius of the sphere of influence.

The velocity gradient of flocculation systems in water treatment systems is produced through mixing: mechanical, hydraulic, in the suspended sediment layer and during flow through a filter layer. In such systems, mixing conditions are not known; Camp and Stein have therefore proposed the application in system analysis of the overall velocity gradient [13]. The relationship between the probability of particle collisions and the probability of their agglomeration can be a parameter to determine the velocity gradient required to achieve the greatest efficiency of the flocculation process

$$\frac{J}{I} = \frac{R_{ij}^2 \cdot G}{3\pi D_{ij}} = 1 \tag{75}$$

Thus, the velocity gradient is defined by the relation

$$G = \frac{3\pi D_{ij}}{R_{ij}^2} \qquad (76)$$

Analytical determination of the velocity gradient requires the knowledge of diffusion coefficient values (D_{ij}) and the radius of interaction (R_{ij}). Assuming the average size of colloidal particles $r = 5 \cdot 10^{-8}$ m, the radius of mutual interaction $R_{ij} = 10^{-6}$ m, the system temperature of T = 293 K and the viscosity of water at that temperature at $\eta_w = 0.001$ kg/m·s and Boltzmann constant, then the average mixing velocity gradient in the flocculation process is $G = 4.3\ s^{-1}$.
In practice, the gradient value is not less than $G = 10\ s^{-1}$.
When there is no possibility to evaluate the geometry of the system, the value of the velocity gradient can be determined from the equation of the energy dissipation rate given by Camp in the form (16) [13].
An increase in a single particle size during flocculation happens very quickly, and within 10 ÷ 60 seconds from the end of coagulation, one can assume macroscopic flocculation. This phase of the process, according to Hudson, can be modeled by a system made up of single particles and larger flocs of an equivalent radius R_F and the number of n_F. Flocculation occurs through the contact between particles and flocs at a speed described by the relationship:

$$\frac{dn}{dt} = -\frac{4}{3}\pi\ n\ n_F R_F^3 G \qquad (77)$$

This equation derived by Camp and Stein is adequate for laminar flow and does not take into account the phenomenon of disintegrating flocs, which always takes place in the flocculation system. For the turbulent regime, Argaman and Kaufman proposed an equation of general reduction of the initial number of particles, which is a superposition of aggregation and fragmentation resulting from erosion, mixing or flow [24]:

$$\frac{dn_1}{dt} = -4\pi\alpha k R_F^3 n_1 n_F \bar{u}^2 + \beta \frac{R_F^2}{R_1^2} n_F \bar{u}^2 \qquad (78)$$

and

$$\frac{n_o}{n_1} = \frac{1 + 4\pi\alpha k R_F^3 n_F \bar{u}^2 t}{1 + \left(\dfrac{\beta R_F^2 n_F \bar{u}^2 t}{n_o R_1^2} \right)} \qquad (79)$$

in the above equations

n_o, n_1 – the number of single particles at the beginning of the process and after time t, respectively,

$\bar{u}^2$ – the average of the squares of the flocculation rate $[m^2/s^2]$,

n_o/n_1 – the factor of agglomeration speed,
α – coefficient of effective collisions between particles n_1 and n_F,
β – disintegration coefficient.

The average of the squares of the flocculation rate is defined by the equation

$$\overline{u}^{2} = P \cdot G \tag{80}$$

in which P is a mixing parameter and according to Argaman and Kaufman is ~ $4.6 \cdot 10^{-6}$ m^2/s for a frame mixer and ~ $2.3 \cdot 10^{-6}$ m^2/s for a turbine mixer. Average floc size is inversely proportional to $\overline{u}^{2}$:

$$R_F = K/\overline{u}^{2} = K/PG \tag{81}$$

By simplifying and expressing all constant parameters globally in a constant agglomeration k_a and a disintegration constant k_b, the equation of the agglomeration rate for a particular flocculation system (78) takes the following form:

$$\frac{dn_1}{dt} = -k_a n_1 G + k_b n_o G^2 \tag{82}$$

Separation of variables and integration with the limits from t = 0 to t = t and from $n_1 = n_o$ to $n_1 = n_1$ leads to the following forms

$$\int_{n_1}^{n_o} \frac{dn_1}{(k_b n_o G^2 - k_a n_1 G)} = \int_0^t dt \tag{83}$$

$$\frac{1}{k_a G} \ln \frac{k_b n_o G^2 - k_a n_o G}{k_b n_o G^2 - k_a n_1 G} = t \tag{84}$$

$$\frac{n_o (k_b G - k_a)}{k_b n_o G - k_a n_1} = \exp(k_a G t) \tag{85}$$

$$n_1 = \frac{k_b}{k_a} n_o G + n_o \left(1 - \frac{k_b}{k_a} G\right) \exp(-k_a G t) \tag{86}$$

and

$$\frac{n_1}{n_o} = \frac{k_b}{k_a} G + \left(1 - \frac{k_b}{k_a} G\right) \exp(-k_a G t) \tag{87}$$

or

$$k_a = (Gt)^{-1} \ln \frac{1 - \frac{k_b}{k_a} G}{\left(\frac{n_1}{n_o} - \frac{k_b}{k_a} G \right)} \tag{88}$$

At equilibrium, i.e. in a situation where the quantity of generated flocs equals the number of the disintegrated ones, the second term on the right side of Equation (87) can be neglected and then

$$\left(\frac{n_1}{n_o} \right)_E = \frac{k_b}{k_a} G \tag{89}$$

The methodology of determining the parameters k_a and k_b was developed by Bratby [62]. It uses the Te Kippe equation for the value of the velocity gradient:

$$G = \sqrt{\frac{2\pi\ NT}{V \cdot \eta}} \tag{90}$$

in the above equation

N – rotating speed [s^{-1}],
T – the introduced turning moment [kgm^2/s^2],
V – solution volume [m^3],
η – dynamic viscosity coefficient [kg/ms].

The average values of k_a coefficients determined in the tests of turbidity and color removal are as follows:

– for turbidity removal $k_a = 2.5 \cdot 10^{-4}$,
– for color removal $k_a = 3.09 \cdot 10^{-4}$.

The value of the disintegration coefficient k_b is constant only for a defined gradient (G) and the relation $k_b = f(G)$ determined through experiments is

$$k_b = k_1 \ln G + k_2 \tag{91}$$

For example, for a system of flocculation after the process of coagulation with aluminum sulfate, parameters k_1 and k_2 determined in laboratory tests have the following values:

– for turbidity removal $k_1 = -\ 0.87 \cdot 10^{-7}$, $k_2 = 7.7 \cdot 10^{-7}$,
– for color removal $k_1 = -\ 3.04 \cdot 10^{-6}$, $k_2 = 15.2 \cdot 10^{-6}$

Thus, the values of k_b for the removal of turbidity and color are respectively:

$$k_b = (7.7 - 0.87 \ln G) \cdot 10^{-7} \quad [s] \tag{92}$$

$$k_b = (15.2 - 3.04 \ln G) \cdot 10^{-6} \quad [s] \tag{93}$$

According to most literature data, the average velocity gradient in flocculation is in the range G = 40 ÷ 80 s^{-1}.The best results are obtained for the product of Gt equal to about 10^5 and no less than $6 \cdot 10^4$, in the case of using a completely mixed flow reactor and in the range (5 ÷ 6) 10^4 for hydraulic mixers.

In the case of using mechanical mixers in the process of flocculation, the peripheral speed of external elements of a mixer should not exceed 0.8 m/s. The surface of mixer blades must not exceed 20% of the cross section of the tank in which the flocculation process is performed.

Flocculation time is generally 15 ÷ 30 minutes, 60 minutes are rarely required [62].

7.3.1. Example Calculations

EXAMPLE 1

Determine the necessary mixing velocity gradient (G) in the flocculation process realized in a reactor at a hydraulic retention time of $T_H = 600$ s to achieve an agglomeration efficiency of destabilized colloidal particles that cause color equal to $n_l/n_0 = 0.4$.

The solution of the problem was carried out using Equation (87), assuming the value of parameter $k_a = 3.09 \cdot 10^{-4}$ and parameter k_b described by Equation (93)

$$k_b = (15.2 - 3.04 \ln G) \cdot 10^{-6}$$

The solution was carried out by the method of subsequent approximations, assuming in the first step the values G = 20 s^{-1}

$$\frac{n_1}{n_0} = \frac{(15.2 - 3.04 \ln 20)10^{-6}}{3.09 \cdot 10^{-4}} 20 + \left(1 - \frac{(15.2 - 3.04 \ln 20)10^{-6}}{3.09 \cdot 10^{-4}} 20\right) \cdot$$

$$\cdot \exp\left(-3.09 \cdot 10^{-4} \cdot 20 \cdot 600\right) = 0.394 + 0.606 \exp\left(-3.708\right) = 0.41$$

In the second step G = 10 s^{-1}

$$\frac{n_1}{n_0} = \frac{(15.2 - 3.04 \ln 10)10^{-6}}{3.09 \cdot 10^{-4}} 10 + \left(1 - \frac{(15.2 - 3.04 \ln 10)10^{-6}}{3.09 \cdot 10^{-4}} 10\right) \cdot$$

$$\cdot \exp\left(-3.09 \cdot 10^{-4} \cdot 10 \cdot 600\right) = 0.265 + 0.735 \exp\left(-1.85\right) = 0.38$$

In the third step G = 15 s^{-1}

$$\frac{n_1}{n_0} = \frac{(15.2 - 3.04 \ln 15)10^{-6}}{3.09 \cdot 10^{-4}} 15 + \left(1 - \frac{(15.2 - 3.04 \ln 15)10^{-6}}{3.09 \cdot 10^{-4}} 15\right) \cdot$$

$$\cdot \exp\left(-3.09\cdot 10^{-4}\cdot 15\cdot 600\right)=0.338+0.662\ \exp\left(-2.78\right)=0.38$$

In the fourth step G = 18 s^{-1}

$$\frac{n_1}{n_0}=\frac{\left(15.2-3.04\ \ln 18\right)10^{-6}}{3.09\cdot 10^{-4}}18+\left(1-\frac{\left(15.2-3.04\ \ln 18\right)10^{-6}}{3.09\cdot 10^{-4}}18\right)\cdot$$

$$\cdot \exp\left(-3.09\cdot 10^{-4}\cdot 18\cdot 600\right)=0.374+0.626\ \exp\left(-3.34\right)=0.396$$

In the fifth step G = 18.5 s^{-1}:

$$\frac{n_1}{n_0}=\frac{\left(15.2-3.04\ \ln 18.5\right)10^{-6}}{3.09\cdot 10^{-4}}18.5+\left(1-\frac{\left(15.2-3.04\ \ln 18.5\right)10^{-6}}{3.09\cdot 10^{-4}}18.5\right)\cdot$$

$$\cdot \exp\left(-3.09\cdot 10^{-4}\cdot 18.5\cdot 600\right)=0.379+0.621\ \exp\left(-3.43\right)=0.4$$

The analysis of agglomeration efficiency at mixing velocity gradients lower than G = 10 s^{-1} showed that the efficiency at these gradients decreases (G = 8 s^{-1} → $\frac{n_1}{n_0}$ = 0.405; G = 5 s^{-1} → $\frac{n_1}{n_0}$ = 0.496). Therefore, the only efficiency possible to achieve for the analyzed system is $\frac{n_1}{n_0}$ = 0.38.

EXAMPLE 2

Determine the conditions of performing the process of flocculation – G and T_H, at which for the data as in Example 1, maximum agglomeration efficiency of destabilized colloidal particles causing color will be achieved.

The problem was solved by adopting different hydraulic retention times for the assumed mixing velocity gradient. The results of calculations are summarized in the table:

G $[s^{-1}]$	T_H [s]	Camp number GT_H	$\frac{n_1}{n_0}$
1	2	3	4
5	150	750	0.827
	300	1,500	0.691
	600	3,000	0.496
	1,200	6,000	0.297
	1,800	9,000	0.218
	3,600	18,000	0.170
	5,400	27,000	0.167
	7,200	36,000	0.167
10	150	1,500	0.727
	300	3,000	0.556
	600	6,000	0.380
	1,200	12,000	0.283
	1,800	18,000	0.268
	3,600	36,000	0.265
	5,400	54,000	0.265
	7,200	72,000	0,265
15	150	2,250	0.668
	300	4,500	0.503
	600	9,000	0.379
	1,200	18,000	0.340
	1,800	27,000	0.338
	3,600	54,000	0.338
	5,400	81,000	0.338
20	150	3,000	0.634
	300	6,000	0.489
	600	12,000	0.409
	1,200	24,000	0.394
	1,800	36,000	0.394
	3,600	72,000	0.394

The highest process efficiency is achieved at a minimum value of mixing velocity gradient ($G = 5\ s^{-1}$) and the value of Camp number > $1.8\cdot10^4$ ($T_H > 1.0$ h). At higher gradients, maximum achievable efficiencies are also obtained for Camp numbers > $1.8\cdot10^4$.

7.4. Sedimentation

Gravity separation of suspended matter in water is the oldest and most widely used method for removing it. The particles whose density is greater than the density of water tend to settle on the bottom of a reactor. The particles with a smaller density float to the water surface.

In water technology, sedimentation is applied to pre-treatment before conventional systems, to the removal of post-coagulation suspended solid and in the process of chemical precipitation for the removal of iron compounds.

Sedimentation is a simple operation. In an ideal system, the particulates move horizontally as a result of advective transfer and vertically under the force of gravity (Figure 16).

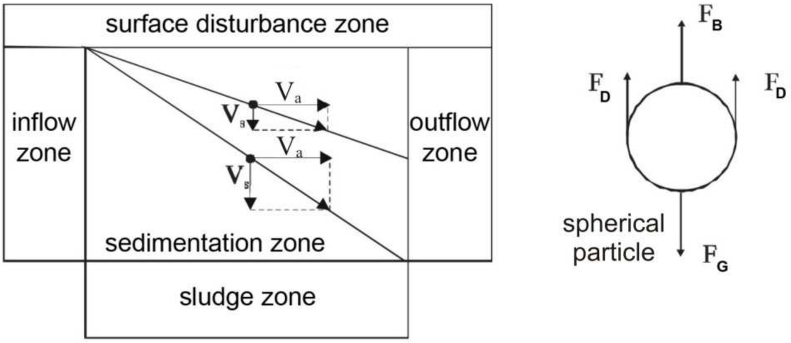

Fig. 16. Diagram of particle movement in the process of sedimentation.

In the analysis of the sedimentation of granular particles, they are assumed not to interact. Referring to Figure 16, the following balance of forces acting on a sedimenting particle can be written

$$m_p \cdot \frac{dV_s}{dt} = F_G - F_B - F_D \tag{94}$$

where

m_p – mass of sedimenting particle [kg],

V_s – sedimentation velocity [m/s],

F_G – gravitational force [N],

F_B – buoyant force [N],

F_D – drag force [N].

The net gravitational force is the difference F_G - F_W, which amounts to

$$F_G - F_B = (\rho_p - \rho_w) g V_p \tag{95}$$

where

ρ_p i ρ_w – density of the sedimenting particle and water, respectively [kg/m^3],
g – gravitational acceleration [m/s^2],
$V_p = \pi d_p^3 / 6$ – the volume of the particle [m^3],
d_p – the diameter of the particle [m].

The resisting force is the function of cross-section area of the particle, sedimentation velocity, solution density and resistance coefficient [24, 47]

$$F_D = \lambda \cdot A_p \cdot \rho_w \cdot \frac{V_s^2}{2} \tag{96}$$

$A_p = \frac{\pi d_p^2}{4}$ – cross-section area of a particle [m^2],
λ –drag coefficient.

For a spherical particle, the drag coefficient may be estimated by means of the following equation:

$$\lambda = \frac{24}{Re} + \frac{3}{\sqrt{Re}} + 0.34 \tag{97}$$

in which Re is Reynolds number defined by the equation

$$Re = \frac{V_s \cdot d_p \cdot \rho_w}{\eta_w} \tag{98}$$

in which η_w is water dynamic viscosity [kg/m·s].

In an ideal system **final sedimentation velocity** is achieved relatively fast; therefore, the expression of acceleration may be omitted. The equation of the balance of forces for a granular particle (94) may then be simplified:

$$F_G - F_B = F_D \tag{99}$$

Substituting in the above equation formulas (95) and (96) produces

$$(\rho_p - \rho_w) \cdot g \cdot V_p = \lambda \cdot A_p \cdot \rho_w \frac{V_s^2}{2} \tag{100}$$

and solving the previous equation with respect to V_s

$$V_s = \sqrt{\frac{2(\rho_p - \rho_w) g \cdot V_p}{\lambda \cdot A_p \cdot \rho_w}} = \sqrt{\frac{2(\rho_p - \rho_w) g \cdot \frac{\pi d_p^3}{6}}{\lambda \cdot \frac{\pi d_p^2}{4} \cdot \rho_w}} \tag{101}$$

and

$$V_s = \sqrt{\frac{4}{3} \frac{(\rho_c - \rho_w) g \cdot d_c}{\lambda \cdot \rho_w}} \tag{102}$$

For laminar flow (Re < 0.3), the first term of Equation (97) dominates; it can therefore be assumed that

$$\lambda = \frac{24}{\mathrm{Re}} \tag{103}$$

and then the speed of a granular particle settling is described by Stokes equation [24, 47]

$$V_s = \frac{g(\rho_p - \rho_w) d_p^2}{18\eta_w} \tag{104}$$

In the range of turbulent flow ($10^3 < \mathrm{Re} < 2 \cdot 10^5$), where λ has a constant value $\lambda = 0.44$, the Newton formula for settling velocity is effective in the following form:

$$V_s = \sqrt{\frac{3.03 g d_p (\rho_p - \rho_w)}{\rho_w}} \tag{105}$$

For a transitional movement between laminar and turbulent flows ($0.3 < \mathrm{Re} < 10^3$), the Allen equation is effective [47]:

$$V_s = 0.2\left[\left(\frac{\rho_p - \rho_w}{\rho_w}\right)\right]^{0.72} \frac{d_p^{1.18}}{\left(\frac{\eta_w}{\rho_w}\right)^{0.45}} \tag{106}$$

The terminal sedimentation velocity of a particle with defined diameter (d_p) and density (ρ_p) in water with a defined viscosity (η_w) is determined by iteration, assuming in the first step that the velocity is described by Stokes equation (104). After determining the sedimentation velocity, the value of Reynolds number is checked from a modified form of Equation (98) which takes into account the shape factor of a grain ϕ whose value for irregular shapes shall be equal to 0.85.

When the calculated value of Re is greater than 0.3, then in the next step the final velocity is determined from Equation (102) in which the resistance coefficient λ is defined from formula (97). To determine the value of the resistance coefficient, the value of Re determined in step one is assumed.

The above procedure of determining V_s from Equation (102) at the value of λ determined from Equation (97) which is in a function of Reynolds number determined in the previous step is repeated until the difference in the determined terminal sedimentation velocity V_s and the velocity determined in the previous step is not more than a few percent, similar as the difference in the numeral quantity of the Reynolds numbers. At such differences in the velocities it is believed that the estimation of a terminal sedimentation velocity is sufficiently accurate.

The values of water density and viscosity as a function of temperature are presented in Table 1. The algorithm of estimating final sedimentation velocity is presented in Figure 17.

Another parameter determining sedimentation efficiency is advective particle transfer rate in a reactor. All suspended substances are a mixture of particles of different sizes, which settle at different speeds. If one assumes that there is a homogeneous sphere of inflow to the settling tank, then the distribution of particle size at the entrance to the settler is the same for the whole depth. All particles with a sedimentation rate (V_s) greater than the advective transfer rate (V_a) will be removed regardless of the height at which they will enter the settler. The particles with a sedimentation rate lower than the flow rate ($V_s < V_a$) will be removed in the amount proportional to the V_s / V_a ratio.

Therefore, the most important parameter in the modeling of sedimentation is the **critical sedimentation velocity** (V_{st}), which expressed in relation to other variables, is as follows [88]:

$$V_{st} = \frac{H}{T_H} = \frac{H}{V/Q} = \frac{Q \cdot H}{V} = \frac{Q}{V/H} = \frac{Q}{b \cdot L} = \frac{Q}{F_s} \tag{107}$$

where

H – active depth of a settling tank [m],
V – volume of a settling tank [m^3],
T_H – hydraulic detention time [h],
Q – flow rate [m^3/s],
b – width of a settling tank [m],
L – length of a settling tank [m],
F_s – projection area of a settling tank [m^2].

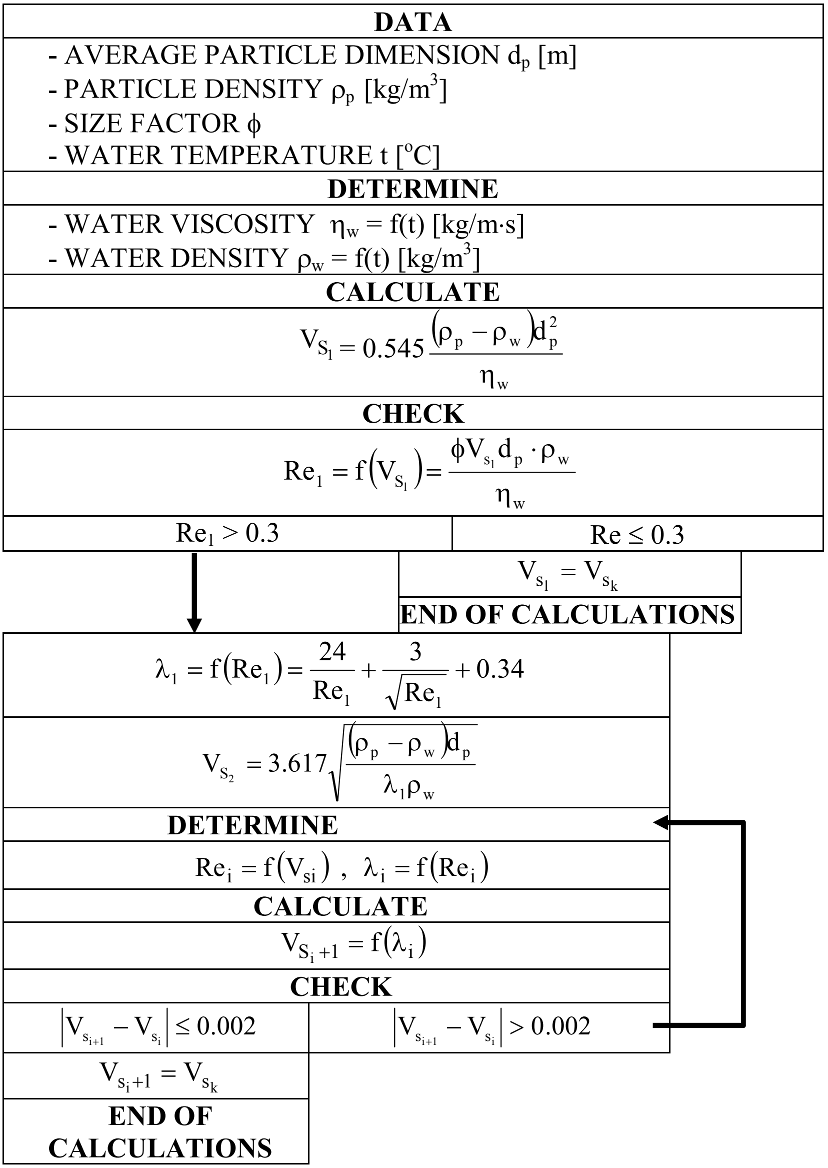

Fig. 17. Algorithm of the estimation of the terminal sedimentation rate.

The interpretation of relation (107) for three basic types of settling tanks is presented below.

From the diagram of a settling tank with a horizontal flow (Fig. 18) and the distribution of particle transport rates, the critical sedimentation rate is $V_{st} = H/T_H = Q/F_s$.

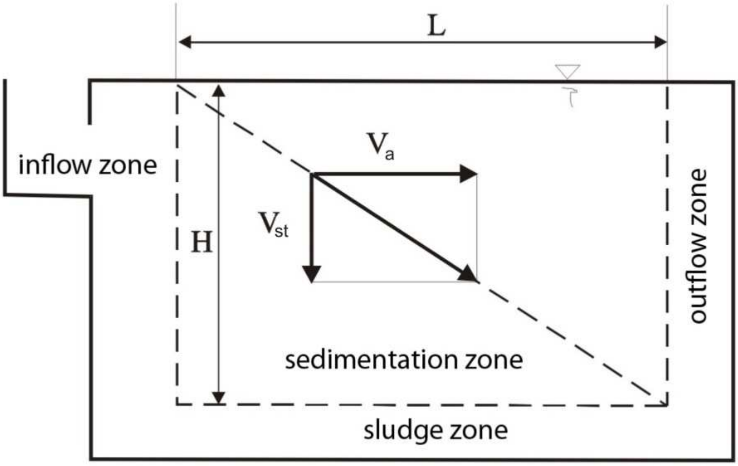

Fig. 18. Diagram of a horizontal settling tank.

In the case of a vertical settling tank, the flow rate is $V_a = Q/F_s$ (Figure 19).

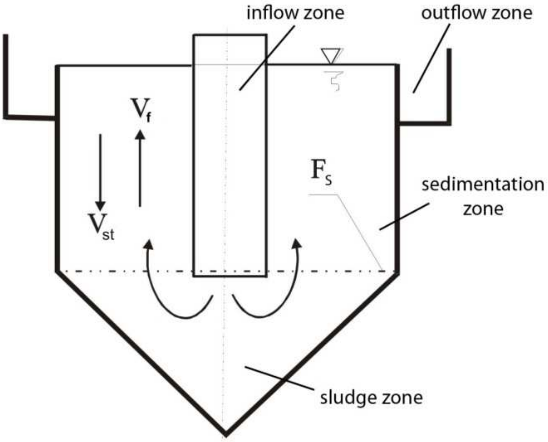

Fig. 19. Diagram of a vertical settling tank.

The limiting condition for particle removal applies when the critical sedimentation velocity (V_{st}) is equal to the ascending velocity (V_a).
Therefore: $V_{st} = V_a = Q/F_s$.
In the case of a radial settling tank, the diagram of which is shown in Figure 20, the hydraulic detention time is described by equation

$$T_H = \int_{R_1}^{R_2} \frac{dR}{V_a} \tag{108}$$

in which

$$V_a = \frac{Q}{2\pi RH}$$ – velocity of advective particle transfer [m/s],

that is

$$T_H = \frac{2\pi H}{Q} \int_{R_1}^{R_2} RdR = \frac{\pi\left(R_2^2 - R_1^2\right)H}{Q} = \frac{F_{os} \cdot H}{Q} \tag{109}$$

And so

$$V_{st} = \frac{H}{T_H} = \frac{H}{F_s \cdot \frac{H}{Q}} = \frac{Q}{F_s} \tag{110}$$

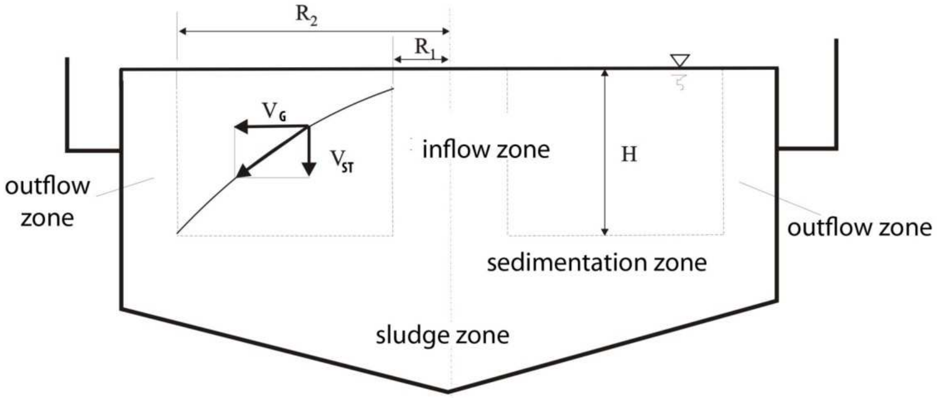

Fig. 20. Diagram of a radial settling tank.

The above analysis of the work of vertical, horizontal and radial settling tanks shows that sedimentation depends on the hydraulic load of the settling tanks and does not depend on the tank depth [90].

Real sedimentation systems differ considerably from ideal systems. Above all, the assumption that there is no interaction between settling particles is flawed. Moreover, flow formulas in actual settling tanks show deviation from ideal conditions [81].

In the event of a significant concentration of particles in the water, there are three types of interactions between sedimenting particles:

– perikinetic flocculation, in which the particles collide and as a result the particle size increases,

– fluidization of the system, in which the particles are so close to each other that the flow is limited and the particles move as one homogeneous block,

– thickening, in which the particles though colliding squeeze water from the flocs, thereby decreasing their size.

Hindered settling occurs at a volumetric concentration of suspended matter $> 0.22\%$ which corresponds to $6.0\ g/dm^3$ mass concentration of inorganic suspended matter in surface water or calcium carbonate suspended solid, but only $2.5\ g/dm^3$ of organic suspended matter [51]. During the hindered settling of granular particles, their velocity may be determined from Stokes equation (104) modified by a factor allowing for the changing porosity in time of the suspended matter system [47]

$$V_s = \frac{g(\rho_p - \rho_w) d_p^2}{18\eta_w} \varepsilon^2 \cdot f(\varepsilon) \tag{111}$$

The function f(ε) depends on the size of intermolecular space and the shape of settling particles and its value is determined empirically. For spherical particles the function f(ε) may be determined from the empirical equation

$$f(\varepsilon) = 10^{-1,82\,(1-\varepsilon)} \tag{112}$$

For the porosity of a spherical suspended matter system in the range 0.3 ÷ 0.7, the equation determining the particle settling rate takes the form

$$V_s = 6.83 \cdot 10^{-3}\ \frac{g(\rho_p - \rho_w) d_p^2 \cdot \varepsilon^3}{\eta_w\ (1-\varepsilon)} \tag{113}$$

Water technology most often deals with flocs which are formed in the processes of coagulation and flocculation and with granular suspended matter in primary sedimentation.

The **settling of floc suspended solids** is a more complicated process than settling of granular suspended solids. This results from the fact that flocs are strongly fluidized and that the size and shape of settling particles are changing. As a result of particle agglomeration, the settling velocity of a single floc particle is greater than the settling velocity of a particle set; so it is greater than mass sedimentation. This results from taking some part of the water by flocculating particles.

According to Smoluchowski's theory, the process of particles joining in bigger agglomerates is described by the following relation:

$$\frac{1}{n_2} - \frac{1}{n_1} = k(t_2 - t_1) \tag{114}$$

where

n_2 and n_1 are the number of particles suspended after time t_2 and t_1, respectively,

k is a parameter dependent on the number of mutual collisions in a unit time.

The increase of particle size is limited and after achieving critical size, the particles disintegrate into smaller particles.

The floc structure contains large quantities of water and the specific gravity of flocs may be calculated from formula [52]

$$\rho_k = \frac{100}{\dfrac{100-u}{\rho_p} + \dfrac{w}{\rho_w}} \tag{115}$$

in which

w – floc hydration [%],

ρ_p – particle density [kg/m^3],

ρ_w – water density [kg/m^3].

Whereas the volume of hydrated flocs is determined by equation

$$V_k = \frac{\rho_c}{\rho_k}\left(\frac{100}{100-w}\right)\sum V_{sm} \tag{116}$$

in which V_{sm} – volume of dry floc mass [m^3].

The density of suspended matter of flocs formed in the processes of coagulation and chemical precipitation are summarized in Table 8 [51].

Table 8. Density of particles precipitated from water.

Floc composition	**Floc density [kg/m^3]**
$Al(OH)_3$	1,002
$Fe(OH)_4$	1,009.2
$Fe(OH)_2$	1,008.7
50% $Al(OH)_3$ + 50% $Fe(OH)_3$	1,004.3
$Al(OH)_3$ + 25 g/m^3 of suspended solid in water	1,004
$Al(OH)_3$ + 1000 g/m^3 of suspended solid in water	1,070
$Al(OH)_3$ + color 50 gPt/m^3	1,002.9
$Al(OH)_3$ + color 100 gPt/m^3	1,004.1
$Mg(OH)_2$	1,004.5
$CaCO_3$	1,430
15% $Mg(OH)_2$ + 85% $CaCO_3$	1,120
25% $Mg(OH)_2$ + 75% $CaCO_3$	1,045

Typical ranges of flow rate used in water treatment practice are represented as follows:

- sedimentation after turbidity coagulation with aluminum salts – 1.8 ÷ 2 m/h,
- sedimentation after colour coagulation with aluminum salts – 1.5 ÷ 1.8 m/h,
- sedimentation after decarbonization with calcium, with a low quantity of magnesium salts – 2.5 ÷ 4.6 m/h,
- sedimentation after decarbonization with calcium, with a high quantity of magnesium salts – 2.1 ÷ 3.8 m/h [90].

7.4.1. Example Calculations

EXAMPLE 1

Determine the terminal sedimentation rate of calcium carbonate particles of an average particle size $d_p = 5\cdot10^{-4}$ m and density $\rho_p = 1{,}430$ kg/m^3. The water temperature is 20°C, hence the dynamic viscosity $\eta_w = 1.002\cdot10^{-3}$ kg/m·s, and water density $\rho_w = 998.2$ kg/m^3. The shape factor of sedimenting particles is $\phi = 0.9$.
In the first step, estimate the sedimentation rate assuming that it is described by the Stokes equation (104)

$$V_{s_1} = 0.545\frac{(\rho_c-\rho_w)\,d_c^2}{\eta_w} = 0.545\frac{(1{,}430-998.2)\cdot(5\cdot10^{-4})^2}{1.002\cdot10^{-3}} = 0.0587\ \mathrm{m/s}$$

Check the value of Reynolds number

$$\mathrm{Re}_1 = \frac{\phi V_{s_1}\cdot d_c\cdot\rho_w}{\eta_w} = \frac{0.9\cdot0.0587\cdot5\cdot10^{-4}\cdot998.2}{1.002\cdot10^{-3}} = 26.31$$

Because $\mathrm{Re}_1 > 0.3$, in the second step the sedimentation rate was determined from Equation (102) at coefficient λ determined from Equation (97), in which Re equals 26.31:

$$\lambda_1 = \frac{24}{\mathrm{Re}_1} + \frac{3}{\sqrt{\mathrm{Re}_1}} + 0.34 = \frac{24}{26.31} + \frac{3}{\sqrt{26.31}} + 0.34 = 1.84$$

$$V_{s_2} = 3.617\sqrt{\frac{(\rho_c-\rho_w)\,d_c}{\lambda_1\cdot\rho_w}} = 3.617\sqrt{\frac{(1{,}430-998.2)\cdot5\cdot10^{-4}}{1.84\cdot998.2}} = 0.0392\ \mathrm{m/s}$$

Because $\left|V_{s_1} - V_{s_2}\right| = 0.0195 > 0.002$ the procedure of determining V_{st} is repeated and in the third step it is assumed that $\mathrm{Re}_2 = f(V_{s_2})$ and $\lambda_2 = f(\mathrm{Re}_2)$:

$$\mathrm{Re}_2 = \frac{0.9\cdot0.0392\cdot5\cdot10^{-4}\cdot998.2}{1.002\cdot10^{-3}} = 17.57$$

$$\lambda_2 = \frac{24}{17.57} + \frac{3}{\sqrt{17.57}} + 0.34 = 2.42$$

$$V_{s_3} = 3.617\sqrt{\frac{(1{,}430-998.2)\cdot5\cdot10^{-4}}{2.42\cdot998.2}} = 0.0342\ \mathrm{m/s}$$

$\left|V_{s_2} - V_{s_3}\right| = 0.005 > 0.002$ so in the fourth step:

$$\mathrm{Re}_3 = \frac{0.9 \cdot 0.0342 \cdot 5 \cdot 10^{-4} \cdot 998.2}{1.002 \cdot 10^{-3}} = 15.33$$

$$\lambda_3 = \frac{24}{15.33} + \frac{3}{\sqrt{15.33}} + 0.34 = 2.67$$

$$V_{s_4} = 3.617\sqrt{\frac{(1{,}430 - 998.2) \cdot 5 \cdot 10^{-4}}{2.67 \cdot 998.2}} = 0.0325\ \mathrm{m/s}$$

Because $\left|V_{s_3} - V_{s_4}\right|$ = 0.0017 < 0.002 then the velocity determined in the fourth step is the terminal sedimentation rate.

EXAMPLE 2

Determine the removal efficiency of calcium carbonate for particles given in Example 1 and a concentration $C_0 = 150\ \mathrm{g/m^3}$, from a stream of a volumetric velocity of flow $Q = 500\ \mathrm{m^3/h}$, in a horizontal settling tank of an area $F = 200\ \mathrm{m^2}$. The final sedimentation rate determined in Example 1 is $V_{st} = 0.0325$ m/s.
The mass balance of suspended matter in the settling tank for steady state

$$Q \cdot C_0 = QC + V_{st} \cdot F \cdot C$$

Concentration in the tank outlet

$$C = \frac{Q\,C_0}{Q + V_{st} \cdot F} = \frac{\frac{500}{3{,}600} \cdot 150}{\frac{500}{3{,}600} + 0.0325 \cdot 200} = 3.14\ \mathrm{g/m^3}$$

Tank efficiency

$$\eta = \frac{C_0 - C}{C_0} \cdot 100\% = \frac{150 - 3.14}{150} \cdot 100\% = 97.9\ \%$$

7.5. Filtration

Filtration is one of the most important processes in water treatment technology. The removal of solid phase particles from water during filtering is done as a result of many unit processes occurring on the surface and in the filter bed such as screening, flocculation, sedimentation, adsorption, adhesion and cohesion.

Screening is the process occurring on the bed surface. Particles larger than the diameter of intergranular capillaries are retained. The removal of particles with a smaller diameter is the result of flocculation and sedimentation. The increase of particle size in the bed favors their retention. As a result of adsorption forces operating between contaminant particles and the surface of material filling the filter, intergranular porosity is reduced. As the time of filter work passes, the amount of material accumulated in the internal structure increases and a rise in pressure loss above the filter's initial value occurs. At some point, the pressure loss reaches the value at which the filter must be cut out of service and cleaned. The final pressure loss is a controllable variable as is the outlet quality. When approaching the end of filtration cycle, the intergranular space of the bed becomes fuller and suspended matter removal efficiency decreases, namely the amount of suspended substances in the outflow begins to increase. When the water quality exceeds acceptable concentration limits or acceptable filter pressure loss limits, the filtration layer must be rinsed.

In an ideal system, the time of achieving the final acceptable pressure loss should correspond with the time of achieving the acceptable value of concentration in the outflow (Figure 21).

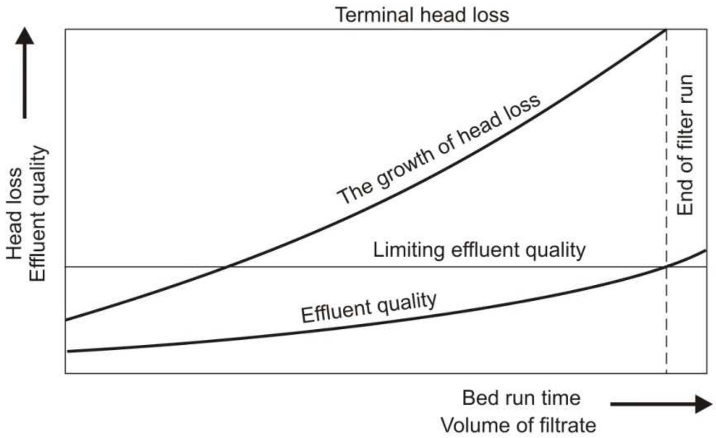

Fig. 21. Head loss and outflow quality as a function of bed run time and filtrate volume.

Most filters with granular medium are cleaned by counter-current rinsing of accumulated suspended matter. Rinsing intensity must provide for bed expansion. Suspended matter retained in the bed is removed by shearing forces produced by rinsing water. Additionally, purifying is achieved as a result of mutual abrasion of individual bed grains.

Suspended matter removed from the bed is transported to settling tanks together with rinsing water. Designing the process of filter rinsing is an integral element of designing the whole filtration system.

In water treatment technology, apart from standard rapid single-layer filters, e.g. sand filters with a supporting gravel layer, in use are filters with a deep bed, filters with a pulsatory bed, multi-layer filters and slow sand filters.

Among many systems of filtration hydraulics, the most widely used are systems that can be classified into two categories:

– methods based on a constant filtration rate,
– methods with a decreasing flow rate.

In both groups there are methods with constant pressure loss and methods with increasing pressure loss.

In the modeling of filtration process, two classes of models are distinguished:

– forecasting models of pressure loss with clean water flow through the filtration layer,
– simulation models of filtration cycle time.

Mathematical models of clean water filtration through a porous medium are similar to those models which have been formulated for water flows in a soil layer. Basic formulas describing pressure loss with clean water flow through the layer are:

- Carman-Kozeny formula[14]

$$h = \frac{f}{\phi}\frac{1-\varepsilon}{\varepsilon}\frac{H}{d}\frac{V_f^2}{g} \tag{117}$$

for a homogeneous layer and for a non-homogeneous bed

$$h = \frac{1}{\phi}\frac{1-\varepsilon}{\varepsilon}\frac{HV_f^2}{g}\sum f\frac{P}{d_g} \tag{118}$$

where

h – head loss [m],

f – fraction factor,

$$f = 150\frac{1-\varepsilon}{\mathrm{Re}} + 1.75 \tag{119}$$

$$Re = \frac{\phi\ d \cdot V_f \cdot \rho_w}{\eta_w} \tag{120}$$

d – representative grain diameter [m],

$d_g = \sqrt{d_1 \cdot d_2}$ – geometric diameter [m],

d_1, d_2 – representative diameters of bottom and top fraction range, respectively,

ε – layer porosity,

H – depth of filtration bed [m],

V_f – filtration rate [m/s],

ϕ = ~0.85 – shape factor,

g = 9.81 m/s^2 – gravitational acceleration

P – percentage participation of grains from a given fraction,

ρ_w – water density [kg/m^3],

η_w – water dynamic viscosity [kg/m·s].

- Fair–Hatch formula [35] for a homogeneous bed

$$h = k\mu\ s^2 \frac{(1-\varepsilon)^2}{\varepsilon^3} \frac{H}{d^2} \frac{V_f}{g} \tag{121}$$

and for non-homogeneous bed

$$h = k\mu \frac{(1-\varepsilon)^2}{\varepsilon^3} (H \cdot V_f) \left(\frac{s}{\phi}\right)^2 \sum \frac{P}{d_g^2} \tag{122}$$

in which

k = ~ 6 – filtration constant,

μ – water kinematic viscosity [m^2/s],

s = 6 ÷ 7.7 – shape factor.

- Rose formula [77] for a homogeneous bed:

$$h = \frac{1{,}067}{\phi} \lambda \frac{H\ V_f^2}{\varepsilon^4 \cdot d \cdot g} \tag{123}$$

and for a non-homogeneous bed

$$h = \frac{1{,}067}{\phi} \frac{HV_f^2}{\varepsilon^4 g} \sum \lambda \frac{P}{d_g} \tag{124}$$

where λ is the drag coefficient defined by Equation (97)

- Hazen formula [36]:

$$h = \frac{1}{c} \cdot \frac{60}{1.8T + 42} \cdot \frac{H}{d_{10}^2} \cdot V_f \tag{125}$$

in which

c = 600 ÷ 1,200 – consolidation coefficient,
T – temperature [^{o}C],
V_f – filtration rate [m/d],
d_{10} – effective diameter of grains [mm].

A Mathematical model of the time – spatial distribution of contaminants in a filtration bed originates from the mass balance equation in the element of a layer volume [41]

$$\frac{\delta q}{\delta t} \Delta V + \varepsilon\ (t) \frac{\delta C}{\delta t} \Delta V = QC\big|_{H} - QC\big|_{H+\Delta H} \tag{126}$$

In the above balance

$\frac{\delta q}{\delta t}$ – rate of solids deposited inside the filter [g/m^3·s],
ε(t) – average porosity variable in time,
$\frac{\delta C}{\delta t}$ – change in average concentration of solids in pore space in time [g/m^3·s],
ΔV – element of bed volume [m^3],
Q – volumetric filtration velocity [m^3/s],
C – concentration of suspended solids [g/m^3],
H – depth of bed [m].

Introducing to the balance equation (126) relation ΔV = F · ΔH, in which F is the cross-section of bed, and allowing for Q = F · V_f and assuming that ΔH → 0 the result is

$$-V_f \frac{\delta C}{\delta H} = \frac{\delta q}{\delta t} + \varepsilon\ (t) \frac{\delta C}{\delta t} \tag{127}$$

The left side of the equation defines the difference between the mass of suspended matter flowing in the filter section and the mass that flows out of the section. The first expression on the right side of the equation represents the accumulation rate of suspended matter inside the bed. The second expression is the mass change rate of the suspended matter in the solution filling the intergranular space. In the flow process, the solution quantity in the bed is small when compared with the whole volume flowing through the bed; therefore, the balance equation (127) may be transformed into the following form

$$-V_f \frac{\delta C}{\delta H} = \frac{\delta q}{\delta t} \tag{128}$$

This form of the equation is the most common form encountered in literature [40, 91]. Solving it requires the knowledge of the function of the changes in suspended matter concentration with the depth of the bed:

$$\frac{\delta C}{\delta H} = f(z_1, z_2, z_3, ..., z_n) \tag{129}$$

$z_1 \div z_n$ are parameters limiting suspended matter removal from the solution. An exemplary course of changes in the suspended matter concentration depending on depth for water filtration system after coagulation with flocculation and sedimentation with a representative particle diameter $d_{10} = 0.5 \cdot 10^{-3}$ m and velocity $V_f = 5.0$ m/h are shown in Figure 22 [90, 91].

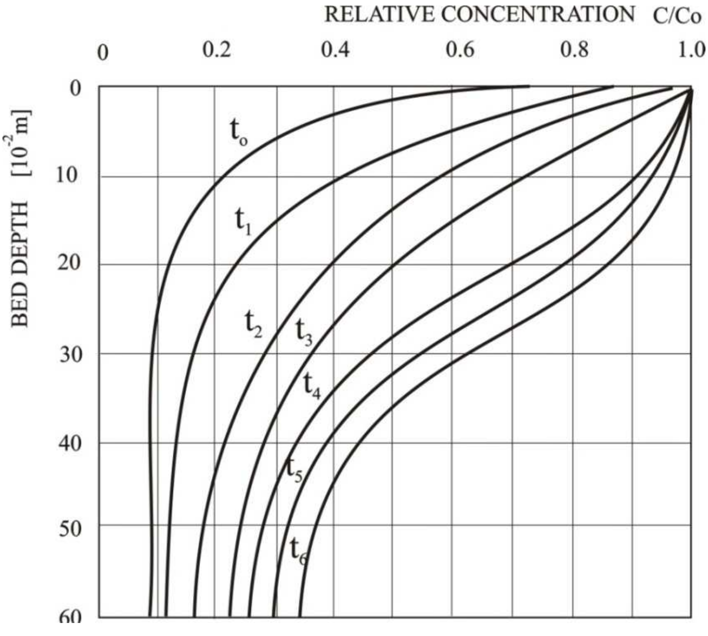

Fig. 22. Distribution of the suspended matter concentration with the bed depth for various duration times of filtration.

Likewise, the knowledge of the factors limiting the change of suspended matter with time retained in the filter is required:

$$\frac{\delta q}{\delta t} = f(z_1, z_2, z_3, \ldots, z_n) \tag{130}$$

Both functions are extensively discussed in literature [91]. Despite numerous attempts, an experimental determination of general physical equations to simulate the distribution in the outflow concentration from various depths of the bed at every moment of the cycle and rate of change in the amount accumulated in the layer have failed.

However, for the specific surface water purification systems in the processes of coagulation, flocculation and sedimentation a general equation describing the results of the experiment can be formulated

$$(C)_{t_n;H_i} = C_o \exp\{-[(\alpha t_n + \beta)\ln H_i + 2{,}3(\gamma - \delta t_n)]\} \tag{131}$$

in which

$(C)_{t_n;H_i}$ – suspended matter concentration in the outflow from a layer of height H_i [10^{-2} m] after time t_n [h] from the beginning of filtration cycle,

C_o – suspended matter concentration in the filter inflow,

α, β, γ, δ – experimental coefficients dependent on filtration velocity, layer characteristics, suspended matter type.

The experimental coefficients for a filtration system of post-coagulation suspended matter after sedimentation through a bed depth 0.6 ÷ 1.0 m and effective diameter $0.5 \cdot 10^{-3}$ m with velocity $V_f = 5 \div 10$ m/h are as follows: 0.12; 0.4; 0.3; 0.24.

The real increase in pressure loss in the filtration process was determined based on modified forms of equations of pressure loss with clean water flow. The key difficulty in obtaining an accurate simulation of the growth in pressure loss is the necessity of taking into account the porosity as a function of the degree of fulfillment with the suspended solid and its compressibility. The complexity of this issue makes the application of most of the suggested formulas difficult or even impossible.

An alternative approach is to simplify the problem and make the increase of pressure loss dependent solely on the amount of material retained in the bed. The loss of pressure is then calculated from the expression:

$$h_t = h_o + \sum_{i=1}^{n} (h_i)_t \tag{132}$$

in which

h_t – total head loss in time t [m],

h_o – total initial head loss at clean water flow [m],

$(h_i)_t$ – the loss in the i-th layer of the filter in time t [m].

The form of the equation for defining pressure loss in the i-th layer is as follows:

$$\left(h_i\right)_t = a\left(q_i\right)_t^b \tag{133}$$

where

$(q_i)_t$ – the quantity of material retained in the i-th layer in time t [g/m^3],
a, b – constants.

For a system with Equation (131), parameters a and b are $1.42 \cdot 10^{-2}$ and 2.41, respectively.

The dependence of the increase of pressure loss on the amount of suspended matter retained in the filtration bed at various representative diameters of bed grains is presented in Figure 23.

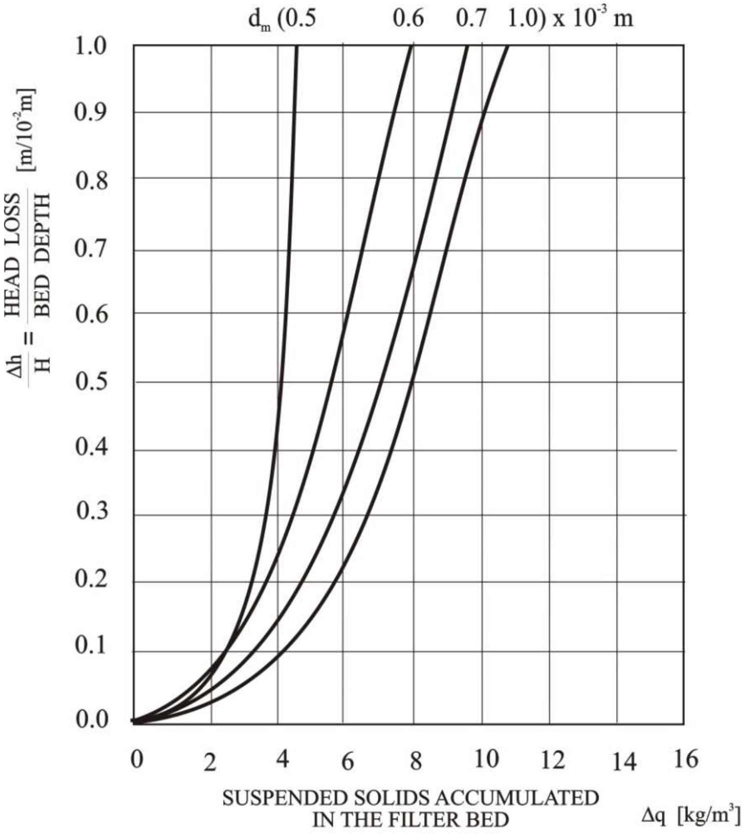

Fig. 23. Increase of pressure loss as a function of the amount of suspended matter retained in the layers of various representative diameters of grains.

An algorithm for determining the filter bed run time to achieve the assumed value of pressure loss is presented in Figure 24.

DATA

- SUSPENDED SOLIDS CONCENTRATION IN THE INFLOW Co [g/m^3]
- FILTRATION VELOCITY V_f [m/h]
- ACCEPTABLE ASSUMED PRESSURE LOSS h_t [m]
- MODEL PARAMETERS α, β, γ, δ, a, b

ASSUME

- TIME OF PROCESS ANALYSIS FROM THE BEGINNING OF THE CYCLE; $t_1; t_2; t_3; \ldots\ldots t_n$ [h]
- ANALYSED BED DEPTHS $H_1; H_2; H_3; \ldots\ldots H_i$ [10^{-2} m]

CALCULATE

$$\left(C_1\right)_{t_1} = C_0 \cdot \exp\left\{-\left[\left(\alpha t_1 + \beta\right)\ln H_1 + 2{,}3\left(\gamma - \delta t_1\right)\right]\right\}$$
$$\left(C_2\right)_{t_1} = C_0 \cdot \exp\left\{-\left[\left(\alpha t_1 + \beta\right)\ln H_2 + 2{,}3\left(\gamma - \delta t_1\right)\right]\right\}$$
$$\left(C_3\right)_{t_1} = C_0 \cdot \exp\left\{-\left[\left(\alpha t_1 + \beta\right)\ln H_3 + 2{,}3\left(\gamma - \delta t_1\right)\right]\right\}$$
$$\vdots$$
$$\left(C_i\right)_{t_1} = C_0 \cdot \exp\left\{-\left[\left(\alpha t_1 + \beta\right)\ln H_i + 2{,}3\left(\gamma - \delta t_1\right)\right]\right\}$$

$$\left(C_1\right)_{t_2} = C_0 \cdot \exp\left\{-\left[\left(\alpha t_2 + \beta\right)\ln H_1 + 2{,}3\left(\gamma - \delta t_2\right)\right]\right\}$$
$$\left(C_2\right)_{t_2} = C_0 \cdot \exp\left\{-\left[\left(\alpha t_2 + \beta\right)\ln H_2 + 2{,}3\left(\gamma - \delta t_2\right)\right]\right\}$$
$$\left(C_3\right)_{t_2} = C_0 \cdot \exp\left\{-\left[\left(\alpha t_2 + \beta\right)\ln H_3 + 2{,}3\left(\gamma - \delta t_2\right)\right]\right\}$$
$$\vdots$$
$$\left(C_i\right)_{t_2} = C_0 \cdot \exp\left\{-\left[\left(\alpha t_2 + \beta\right)\ln H_i + 2{,}3\left(\gamma - \delta t_2\right)\right]\right\}$$

$$\left(C_1\right)_{t_3} = C_0 \cdot \exp\left\{-\left[\left(\alpha t_3 + \beta\right)\ln H_1 + 2{,}3\left(\gamma - \delta t_3\right)\right]\right\}$$
$$\left(C_2\right)_{t_3} = C_0 \cdot \exp\left\{-\left[\left(\alpha t_3 + \beta\right)\ln H_2 + 2{,}3\left(\gamma - \delta t_3\right)\right]\right\}$$
$$\left(C_3\right)_{t_3} = C_0 \cdot \exp\left\{-\left[\left(\alpha t_3 + \beta\right)\ln H_3 + 2{,}3\left(\gamma - \delta t_3\right)\right]\right\}$$
$$\vdots$$
$$\left(C_i\right)_{t_3} = C_0 \cdot \exp\left\{-\left[\left(\alpha t_3 + \beta\right)\ln H_i + 2{,}3\left(\gamma - \delta t_3\right)\right]\right\}$$

$$\vdots$$

$$\left(C_1\right)_{t_n} = C_0 \cdot \exp\left\{-\left[\left(\alpha t_n + \beta\right)\ln H_1 + 2{,}3\left(\gamma - \delta t_n\right)\right]\right\}$$
$$\left(C_2\right)_{t_n} = C_0 \cdot \exp\left\{-\left[\left(\alpha t_n + \beta\right)\ln H_2 + 2{,}3\left(\gamma - \delta t_n\right)\right]\right\}$$
$$\left(C_3\right)_{t_n} = C_0 \cdot \exp\left\{-\left[\left(\alpha t_n + \beta\right)\ln H_3 + 2{,}3\left(\gamma - \delta t_n\right)\right]\right\}$$
$$\vdots$$
$$\left(C_i\right)_{t_n} = C_0 \cdot \exp\left\{-\left[\left(\alpha t_n + \beta\right)\ln H_i + 2{,}3\left(\gamma - \delta t_n\right)\right]\right\}$$

$$\begin{aligned}
&(\Delta C_1)_{t_1} = C_0 - (C_1)_{t_1}\\
&(\Delta C_2)_{t_1} = (C_1)_{t_1} - (C_2)_{t_1}\\
&(\Delta C_3)_{t_1} = (C_2)_{t_1} - (C_3)_{t_1}\\
&\vdots\\
&(\Delta C_i)_{t_1} = (C_{i-1})_{t_1} - (C_i)_{t_1}
\end{aligned}$$

$$\begin{aligned}
&(\Delta C_1)_{t_2} = C_0 - (C_1)_{t_2}\\
&(\Delta C_2)_{t_2} = (C_1)_{t_2} - (C_2)_{t_2}\\
&(\Delta C_3)_{t_2} = (C_2)_{t_2} - (C_3)_{t_2}\\
&\vdots\\
&(\Delta C_i)_{t_2} = (C_{i-1})_{t_2} - (C_i)_{t_2}
\end{aligned}$$

$$\begin{aligned}
&(\Delta C_1)_{t_3} = C_0 - (C_1)_{t_3}\\
&(\Delta C_2)_{t_3} = (C_1)_{t_3} - (C_2)_{t_3}\\
&(\Delta C_3)_{t_3} = (C_2)_{t_3} - (C_3)_{t_3}\\
&\vdots\\
&(\Delta C_i)_{t_3} = (C_{i-1})_{t_3} - (C_i)_{t_3}
\end{aligned}$$

$$\vdots$$

$$\begin{aligned}
&(\Delta C_1)_{t_n} = C_o - (C_1)_{t_n}\\
&(\Delta C_2)_{t_n} = (C_1)_{t_n} - (C_2)_{t_n}\\
&(\Delta C_3)_{t_n} = (C_2)_{t_n} - (C_3)_{t_n}\\
&\vdots\\
&(\Delta C_i)_{t_n} = (C_{i-1})_{t_n} - (C_i)_{t_n}
\end{aligned}$$

$$\begin{aligned}
&(\Delta q_1)_{t_1} = -V_f \frac{(\Delta C_1)_{t_1}}{0 - H_1} t_1 \cdot 10^{-3}\\
&(\Delta q_2)_{t_1} = -V_f \frac{(\Delta C_2)_{t_1}}{H_1 - H_2} t_1 \cdot 10^{-3}\\
&(\Delta q_3)_{t_1} = -V_f \frac{(\Delta C_3)_{t_1}}{H_2 - H_3} t_1 \cdot 10^{-3}\\
&\vdots\\
&(\Delta q_i)_{t_1} = -V_f \frac{(\Delta C_i)_{t_1}}{H_{i-1} - H_i} t_1 \cdot 10^{-3}
\end{aligned}$$

$$\left(\Delta q_1\right)_{t_2} = -V_f \frac{\left(\Delta C_1\right) t_2}{0 - H_1}\left(t_2 - t_1\right)\cdot 10^{-3}$$

$$\left(\Delta q_2\right)_{t_2} = -V_f \frac{\left(\Delta C_2\right) t_2}{H_1 - H_2}\left(t_2 - t_1\right)\cdot 10^{-3}$$

$$\left(\Delta q_3\right)_{t_2} = -V_f \frac{\left(\Delta C_3\right) t_2}{H_2 - H_3}\left(t_2 - t_1\right)\cdot 10^{-3}$$

$$\vdots$$

$$\left(\Delta q_i\right)_{t_2} = -V_f \frac{\left(\Delta C_i\right) t_2}{H_{i-1} - H_i}\left(t_2 - t_1\right)\cdot 10^{-3}$$

$$\left(\Delta q_1\right)_{t_3} = -V_f \frac{\left(\Delta C_1\right) t_3}{0 - H_1}\left(t_3 - t_2\right)\cdot 10^{-3}$$

$$\left(\Delta q_2\right)_{t_3} = -V_f \frac{\left(\Delta C_2\right) t_3}{H_1 - H_2}\left(t_3 - t_2\right)\cdot 10^{-3}$$

$$\left(\Delta q_3\right)_{t_3} = -V_f \frac{\left(\Delta C_3\right) t_3}{H_2 - H_3}\left(t_3 - t_2\right)\cdot 10^{-3}$$

$$\vdots$$

$$\left(\Delta q_i\right)_{t_3} = -V_f \frac{\left(\Delta C_i\right) t_3}{H_{i-1} - H_i}\left(t_3 - t_2\right)\cdot 10^{-3}$$

$$\vdots$$

$$\left(\Delta q_1\right)_{t_n} = -V_f \frac{\left(\Delta C_1\right) t_n}{0 - H_1}\left(t_n - t_{n-1}\right)\cdot 10^{-3}$$

$$\left(\Delta q_2\right)_{t_n} = -V_f \frac{\left(\Delta C_2\right) t_n}{H_1 - H_2}\left(t_n - t_{n-1}\right)\cdot 10^{-3}$$

$$\left(\Delta q_3\right)_{t_n} = -V_f \frac{\left(\Delta C_3\right) t_n}{H_2 - H_3}\left(t_n - t_{n-1}\right)\cdot 10^{-3}$$

$$\vdots$$

$$\left(\Delta q_i\right)_{t_n} = -V_f \frac{\left(\Delta C_i\right) t_n}{H_{i-1} - H_i}\left(t_n - t_{n-1}\right)\cdot 10^{-3}$$

$$\left(\Delta h_1\right)_{t_1} = a\left(\Delta q_1\right)_{t_1}^{b} \cdot H_1$$

$$\left(\Delta h_2\right)_{t_1} = a\left(\Delta q_2\right)_{t_1}^{b} \cdot \left(H_2 - H_1\right)$$

$$\left(\Delta h_3\right)_{t_1} = a\left(\Delta q_3\right)_{t_1}^{b} \cdot \left(H_3 - H_2\right)$$

$$\vdots$$

$$\left(\Delta h_i\right)_{t_1} = a\left(\Delta q_i\right)_{t_1}^{b} \cdot \left(H_i - H_{i-1}\right)$$

$$\begin{aligned}
\left(\Delta h_1\right)_{t_2} &= a\left(\Delta q_1\right)_{t_2}^{b} \cdot H_1 \\
\left(\Delta h_2\right)_{t_2} &= a\left(\Delta q_2\right)_{t_2}^{b} \cdot \left(H_2 - H_1\right) \\
\left(\Delta h_3\right)_{t_2} &= a\left(\Delta q_3\right)_{t_2}^{b} \cdot \left(H_3 - H_2\right) \\
&\vdots \\
\left(\Delta h_i\right)_{t_2} &= a\left(\Delta q_i\right)_{t_2}^{b} \cdot \left(H_i - H_{i-1}\right)
\end{aligned}$$

$$\begin{aligned}
\left(\Delta h_1\right)_{t_3} &= a\left(\Delta q_1\right)_{t_3}^{b} \cdot H_1 \\
\left(\Delta h_2\right)_{t_3} &= a\left(\Delta q_2\right)_{t_3}^{b} \cdot \left(H_2 - H_1\right) \\
\left(\Delta h_3\right)_{t_3} &= a\left(\Delta q_3\right)_{t_3}^{b} \cdot \left(H_3 - H_2\right) \\
&\vdots \\
\left(\Delta h_i\right)_{t_3} &= a\left(\Delta q_i\right)_{t_3}^{b} \cdot \left(H_i - H_{i-1}\right)
\end{aligned}$$

$$\vdots$$

$$\begin{aligned}
\left(\Delta h_1\right)_{t_n} &= a\left(\Delta q_1\right)_{t_n}^{b} \cdot H_1 \\
\left(\Delta h_2\right)_{t_n} &= a\left(\Delta q_2\right)_{t_n}^{b} \cdot \left(H_2 - H_1\right) \\
\left(\Delta h_3\right)_{t_n} &= a\left(\Delta q_3\right)_{t_n}^{b} \cdot \left(H_3 - H_2\right) \\
&\vdots \\
\left(\Delta h_i\right)_{t_n} &= a\left(\Delta q_i\right)_{t_n}^{b} \cdot \left(H_i - H_{i-1}\right)
\end{aligned}$$

$$\begin{aligned}
\left(\sum \Delta h\right)_{t_1} &= \left(\Delta h_1\right)_{t_1} + \left(\Delta h_2\right)_{t_1} + \left(\Delta h_3\right)_{t_1} + \cdots + \left(\Delta h_i\right)_{t_1} \\
\left(\sum \Delta h\right)_{t_2} &= \left(\Delta h_1\right)_{t_2} + \left(\Delta h_2\right)_{t_2} + \left(\Delta h_3\right)_{t_2} + \cdots + \left(\Delta h_i\right)_{t_2} \\
\left(\sum \Delta h\right)_{t_3} &= \left(\Delta h_1\right)_{t_3} + \left(\Delta h_2\right)_{t_3} + \left(\Delta h_3\right)_{t_3} + \cdots + \left(\Delta h_i\right)_{t_3} \vdots \\
\left(\sum \Delta h\right)_{t_n} &= \left(\Delta h_1\right)_{t_n} + \left(\Delta h_2\right)_{t_n} + \left(\Delta h_3\right)_{t_n} + \cdots + \left(\Delta h_i\right)_{t_n}
\end{aligned}$$

$h_0 = f\left(H_i\right)$ – loss at clean water flow

PRINTING THE RESULTS OF CALCULATIONS

$$h_0 + \left(\sum \Delta h\right)_n = f\left(t_n\right)$$

Fig. 24. Algorithm of calculations of head loss growth with bed run time.

Project parameters of the filtration process are

- filtering material type, representative size of material particles, grain uniformity, layer depth,
- filtration velocity,
- method of running the process,
- the method and intensity of backwashing.

Exploitation parameters, especially the duration of the filtration cycle and rinsing time, are determined experimentally on a pilot scale or through a comparison with the parameters of a working installation at a full technological scale.

The ranges of basic project and exploitation parameters of filtration process are summarized in Table 9.

Table 9.Parameters of used filtration layers and exploitation parameters of the filtration process.

Filter type	**UC** **d_{60}/d_{10}**	**d_{10}** **$[10^{-3}m]$**	**H** **[m]**	**V_f/V_w** **[m/h]**
Slow sand	1.8 ÷ 3.0	0.25 ÷ 0.35	0.7 ÷ 1.2	0.1
Rapid sand after coagulation cleaned with water	1.25 ÷ 1.75	0.35 ÷ 0.5	0.5 ÷ 0.9	(4.8 ÷ 15)/(20 ÷ 60)
Rapid sand after coagulation cleaned with water and air	1.25 ÷ 1.75	0.5 ÷ 0.75	0.5 ÷ 1.0	(4.8 ÷ 15)/(20 ÷60)
Rapid for Fe and Mn removal cleaned with water and air	1.25 ÷ 1.75	0.75 ÷ 1.0	1.0 ÷ 1.5	(4.8 ÷ 15)/(20 ÷60)
Upflow direct filter	2.5	0.55 ÷ 0.65	2.0	(4.8 ÷ 15)/(20 ÷60)
Rapid anthracite	1.2 ÷ 1.7	1.0 ÷ 1.2	0.9 ÷ 1.8	(4.8 ÷ 15)/(20 ÷60)
Rapid 2-layer sand-anthracite	1.25 ÷ 1.75	sand 0.6 ÷ 1.0 anthracite 1.0 ÷ 2.0	$H_a = 1/3H_s$ $H_a \geq 0.3$	(10 ÷ 20)/(30 ÷80)
Rapid 2-layer sand-activated carbon	1.25 ÷ 1.75	sand 0.6 ÷ 1.0 carbon 2.0 ÷ 4.0	$H_s = 0.7$ $H_c = 0.5$	(10 ÷ 20)/(30 ÷80)

Filter backwashing is a very important process that when conducted properly allows for the proper accumulation of suspended solids in the filter layer during the filtration cycle.

The methods used for cleaning the bed include rinsing with water in a counter-current direction, rinsing with air, surface cleaning, chemical cleaning and various combinations of the above-mentioned methods.

The most common method of filter layer cleaning is rinsing in counter-current with pre-filtered water. Based on the results of experiments it was found that the rinsing of conventional filters is optimal when the bed expansion during rinsing is about 50%. Under such conditions, most beneficial is the effect of mutual abrasion of bed particles causing the detachment of accumulated suspended solids from the particle surface and the removal of the suspended solids to the settling tanks.

Surface cleaning is preceded by an essential rinsing cycle. Water is supplied through orifices in pipelines, which are rotating or fixed arms located ~ 5 cm above the surface of the filter layer. Surface washing begins ~ 2 minutes before the main rinsing step. Air can be applied before or simultaneously with rinsing using water. When the air flows through the layer, contaminants deposited in the layer are disintegrated. Rinsing with air reduces the amount of rinsing water needed. In case of accidental contamination of the layer with grease and fats, chemical cleaning with detergents and bleach compounds is applied. A specified portion of the cleaning solution is passed pulsating through the layer for about 30 minutes and then the bed is rinsed with water in counter-current.

The hydraulics of backwashing are based on the principle stating that to expand the filter layer, the pressure loss must be equal to the mass of granular medium in the water. The mathematical representation of this relation takes the following form:

$$h = H_e(1-\varepsilon_e)\frac{\rho_p - \rho_w}{\rho_w} \tag{134}$$

in which

h – pressure loss required to enter the bed into expansion [m],

H_e – height of filtration layer in expansion [m],

ε_e – layer porosity in expansion,

ρ_p – filter material density [kg/m^3],

ρ_w – water density [kg/m^3].

As individual particles of the filtration layer are maintained in suspended solid by the forces of liquid resistance, based on the theory of sedimentation it can be proved that

$$\lambda A_p \cdot \rho_w \frac{V_w^2}{2}\Phi(\varepsilon_e) = (\rho_p - \rho_w)gV_p \tag{135}$$

where

λ – drag coefficient,

A_p – cross-section area of filtrating material particle [m^2],

V_p – volume of filtrating material particle [m^3],

V_w – rinsing water flow rate [m/s],

$\Phi(\varepsilon_e)$ – correction coefficient as V_w is the velocity of rinsing water, not the velocity of layer particle sedimentation.

The following definition of the correction coefficient was experimentally determined:

$$\Phi(\varepsilon_e) = \left(\frac{V_s}{V_w}\right)^2 = \left(\frac{1}{\varepsilon_e}\right)^9 \tag{136}$$

and

$$\varepsilon_e = \left(\frac{V_w}{V_s}\right)^{0.22} \tag{137}$$

or

$$V_w = V_s \cdot \varepsilon_e^{4.54} \tag{138}$$

As the volume of filtration medium per surface unit remains constant

$$(1-\varepsilon)H = (1-\varepsilon_e)H_e \tag{139}$$

Therefore

$$\frac{H_e}{H} = \frac{1-\varepsilon}{1-\varepsilon_e} = \frac{1-\varepsilon}{1-\left(\frac{V_w}{V_s}\right)^{0.22}} \tag{140}$$

Knowledge of the height of a layer in expansion (H_e) is needed to determine the minimum height of the level of the backwash water trough above the level of filtration layer. For the assumed parameters of the layer (H, ε, d_p, ρ_p) and the assumed porosity of the bed in expansion (ε_e), the terminal sedimentation velocity V_{st} (algorithm in Figure 17) is first determined through iteration, and then the rinsing velocity is determined from Equation (138). From Equation (140) the height of the layer in expansion (H_e) is determined [24, 47].

7.5.1. Example Calculations

EXAMPLE 1

Determine the head loss growth in the process of water filtration with a suspended solid concentration of $C_0 = 30\ \text{g/m}^3$ through a bed with a height $H = 0.8$ m, porosity $\varepsilon = 0.4$ and a representative grain diameter $d_{10} = 0.5 \cdot 10^{-3}$ m at the velocity of $V_f = 5$ m/h. Experimental parameters of the equation defining the outflow concentration as a function of bed run time and layer height (131) are

$\alpha = 0.12$; $\beta = 0.4$; $\gamma = 0.3$; $\delta = 0.24$, and the constants of the equation of head loss as a function of the quantity of retained suspended solid (133) are $a = 1.42\cdot10^{-2}$; $b = 2.41$. The assumed bed depths at which the increase of pressure loss is analyzed are $H_1 = 20$ cm; $H_2 = 40$ cm; $H_3 = 60$ cm; $H_4 = 80$ cm. The assumed times for the process analysis from the beginning of the cycle are $t_1 = 1$ h, $t_2 = 3$ h, $t_3 = 6$ h, $t_4 = 12$ h.

Calculate the concentration in the outflow from the layers after time $t_1 = 1$ h:

$$\left(C_1\right)_{t_1} = C_0 \cdot \exp\left\{-\left[\left(\alpha t_1 + \beta\right)\ln H_1 + 2.3\left(\gamma - \delta t_1\right)\right]\right\}$$

$$\left(C_1\right)_{t_1} = 30 \cdot \exp\left\{-\left[\left(0.12\cdot 1 + 0.4\right)\ln 20 + 2.3\left(0.3 - 0.24\cdot 1\right)\right]\right\} = 5.50\ \mathrm{g/m^3}$$

$$\left(C_2\right)_{t_1} = 30 \cdot \exp\left\{-\left[0.52\ln 40 + 0.138\right]\right\} = 3.84\ \mathrm{g/m^3}$$

$$\left(C_3\right)_{t_1} = 30 \cdot \exp\left\{-\left[0.52\ln 60 + 0.138\right]\right\} = 3.11\ \mathrm{g/m^3}$$

$$\left(C_4\right)_{t_1} = 30 \cdot \exp\left\{-\left[0.52\ln 80 + 0.138\right]\right\} = 2.67\ \mathrm{g/m^3}$$

Calculate the concentration in the outflow from the layers after time $t_2 = 3$ h:

$$\left(C_1\right)_{t_2} = 30 \cdot \exp\left\{-\left[\left(0.12\cdot 3 + 0.4\right)\ln 20 + 2.3\left(0.3 - 0.24\cdot 3\right)\right]\right\} = 8.09\ \mathrm{g/m^3}$$

$$\left(C_2\right)_{t_2} = 30 \cdot \exp\left\{-\left[0.76\ln 40 - 0.966\right]\right\} = 4.78\ \mathrm{g/m^3}$$

$$\left(C_3\right)_{t_2} = 30 \cdot \exp\left\{-\left[0.76\ln 60 - 0.966\right]\right\} = 3.51\ \mathrm{g/m^3}$$

$$\left(C_4\right)_{t_2} = 30 \cdot \exp\left\{-\left[0.76\ln 80 - 0.966\right]\right\} = 2.82\ \mathrm{g/m^3}$$

Calculate the concentration in the outflow from the layers after time $t_3 = 6$ h:

$$\left(C_1\right)_{t_3} = 30 \cdot \exp\left\{-\left[\left(0.12\cdot 6 + 0.4\right)\ln 20 + 2.3\left(0.3 - 0.24\cdot 6\right)\right]\right\} = 14.38\ \mathrm{g/m^3}$$

$$\left(C_2\right)_{t_3} = 30 \cdot \exp\left\{-\left[1.12\ln 40 - 2.62\right]\right\} = 6.62\ \mathrm{g/m^3}$$

$$\left(C_3\right)_{t_3} = 30 \cdot \exp\left\{-\left[1.12\ln 60 - 2.62\right]\right\} = 4.20\ \mathrm{g/m^3}$$

$$\left(C_4\right)_{t_3} = 30 \cdot \exp\left\{-\left[1.12\ln 80 - 2.62\right]\right\} = 3.04\ \mathrm{g/m^3}$$

Calculate the concentration in the outflow from the layers after time $t_4 = 12$ h:

$$\left(C_1\right)_{t_4} = 30 \cdot \exp\left\{-\left[\left(0.12\cdot 12 + 0.4\right)\ln 20 + 2.3\left(0.3 - 0.24\cdot 12\right)\right]\right\} = 30\ \mathrm{g/m^3}$$

$$\left(C_2\right)_{t_4} = 30 \cdot \exp\left\{-\left[1.84\ln 40 - 5.934\right]\right\} = 12.78\ \mathrm{g/m^3}$$

$$\left(C_3\right)_{t_4} = 30 \cdot \exp\left\{-\left[1.84\ln 60 - 5.934\right]\right\} = 6.06\ \mathrm{g/m^3}$$

$$\left(C_4\right)_{t_4} = 30 \cdot \exp\{-[1.84 \ln 80 - 5.934]\} = 3.57\ \mathrm{g/m^3}$$

Calculate $\Delta C = C_{H_{i-1}} - C_{H_i}$ after time $t_1 = 1$ h:

$$\left(\Delta C_1\right)_{t_1} = 30 - 5.50 = 24.5\ \mathrm{g/m^3}$$

$$\left(\Delta C_2\right)_{t_1} = 5.50 - 3.84 = 1.66\ \mathrm{g/m^3}$$

$$\left(\Delta C_3\right)_{t_1} = 3.84 - 3.11 = 0.73\ \mathrm{g/m^3}$$

$$\left(\Delta C_4\right)_{t_1} = 3.11 - 2.67 = 0.44\ \mathrm{g/m^3}$$

Calculate ΔC after time $t_2 = 3$ h:

$$\left(\Delta C_1\right)_{t_2} = 30 - 8.09 = 21.91\ \mathrm{g/m^3}$$

$$\left(\Delta C_2\right)_{t_2} = 8.09 - 4.78 = 3.31\ \mathrm{g/m^3}$$

$$\left(\Delta C_3\right)_{t_2} = 4.78 - 3.51 = 1.27\ \mathrm{g/m^3}$$

$$\left(\Delta C_4\right)_{t_2} = 3.51 - 2.82 = 0.69\ \mathrm{g/m^3}$$

Calculate ΔC after time $t_3 = 6$ h:

$$\left(\Delta C_1\right)_{t_3} = 30 - 14.38 = 15.62\ \mathrm{g/m^3}$$

$$\left(\Delta C_2\right)_{t_3} = 14.38 - 6.62 = 7.76\ \mathrm{g/m^3}$$

$$\left(\Delta C_3\right)_{t_3} = 6.62 - 4.20 = 2.42\ \mathrm{g/m^3}$$

$$\left(\Delta C_4\right)_{t_3} = 4.20 - 3.04 = 1.16\ \mathrm{g/m^3}$$

Calculate ΔC after time $t_4 = 12$ h:

$$\left(\Delta C_1\right)_{t_4} = 30 - 30 = 0\ \mathrm{g/m^3}$$

$$\left(\Delta C_2\right)_{t_4} = 30 - 12.78 = 17.22\ \mathrm{g/m^3}$$

$$\left(\Delta C_3\right)_{t_4} = 12.78 - 6.06 = 6.72\ \mathrm{g/m^3}$$

$$\left(\Delta C_4\right)_{t_4} = 6.06 - 3.57 = 2.49\ \mathrm{g/m^3}$$

Calculate the mass of suspended solid retained in the layers after time $t_1 = 1$ h:

$$\left(\Delta q_1\right)_{t_1} = -V_f \frac{\left(\Delta C_1\right) t_1}{0 - H_1} t_1 \cdot 10^{-3} = 5.0 \frac{24.5}{0.2} \cdot 1 \cdot 10^{-3} = 0.6125\ \mathrm{kg/m^3}$$

$$\left(\Delta q_2\right)_{t_1} = -V_f \frac{\left(\Delta C_2\right)t_1}{H_1 - H_2} t_1 \cdot 10^{-3} = 5.0\frac{1.66}{0.2}\cdot 1\cdot 10^{-3} = 0.0415\ \mathrm{kg/m^3}$$

$$\left(\Delta q_3\right)_{t_1} = -V_f \frac{\left(\Delta C_3\right)t_1}{H_2 - H_3} t_1 \cdot 10^{-3} = 5.0\frac{0.73}{0.2}\cdot 1\cdot 10^{-3} = 0.01825\ \mathrm{kg/m^3}$$

$$\left(\Delta q_4\right)_{t_1} = -V_f \frac{\left(\Delta C_4\right)t_1}{H_3 - H_4} t_1 \cdot 10^{-3} = 5.0\frac{0.44}{0.2}\cdot 1\cdot 10^{-3} = 0.011\ \mathrm{kg/m^3}$$

Calculate the mass of suspended solid retained in the layers after time t_2 - t_1 = 2 h:

$$\left(\Delta q_1\right)_{t_2} = -V_f \frac{\left(\Delta C_1\right)t_2}{0 - H_1}\left(t_2 - t_1\right)\cdot 10^{-3} = 5.0\frac{21.91}{0.2}\cdot 2\cdot 10^{-3} = 1.096\ \mathrm{kg/m^3}$$

$$\left(\Delta q_2\right)_{t_2} = -V_f \frac{\left(\Delta C_2\right)t_2}{H_2 - H_1}\left(t_2 - t_1\right)\cdot 10^{-3} = 5.0\frac{3.31}{0.2}\cdot 2\cdot 10^{-3} = 0.166\ \mathrm{kg/m^3}$$

$$\left(\Delta q_3\right)_{t_2} = -V_f \frac{\left(\Delta C_3\right)t_2}{H_3 - H_2}\left(t_2 - t_1\right)\cdot 10^{-3} = 5.0\frac{1.27}{0.2}\cdot 2\cdot 10^{-3} = 0.0635\ \mathrm{kg/m^3}$$

$$\left(\Delta q_4\right)_{t_2} = -V_f \frac{\left(\Delta C_4\right)t_2}{H_4 - H_3}\left(t_2 - t_1\right)\cdot 10^{-3} = 5.0\frac{0.69}{0.2}\cdot 2\cdot 10^{-3} = 0.0345\ \mathrm{kg/m^3}$$

Calculate the mass of suspended solid retained in the layers after time $t_3 - t_2$ = 3 h:

$$\left(\Delta q_1\right)_{t_3} = -V_f \frac{\left(\Delta C_1\right)t_3}{0 - H_1}\left(t_3 - t_2\right)\cdot 10^{-3} = 5.0\frac{15.62}{0.2}\cdot 3\cdot 10^{-3} = 1.171\ \mathrm{kg/m^3}$$

$$\left(\Delta q_2\right)_{t_3} = -V_f \frac{\left(\Delta C_2\right)t_3}{H_2 - H_1}\left(t_3 - t_2\right)\cdot 10^{-3} = 5.0\frac{7.76}{0.2}\cdot 3\cdot 10^{-3} = 0.582\ \mathrm{kg/m^3}$$

$$\left(\Delta q_3\right)_{t_3} = -V_f \frac{\left(\Delta C_3\right)t_3}{H_3 - H_2}\left(t_3 - t_2\right)\cdot 10^{-3} = 5.0\frac{2.42}{0.2}\cdot 3\cdot 10^{-3} = 0.181\ \mathrm{kg/m^3}$$

$$\left(\Delta q_4\right)_{t_3} = -V_f \frac{\left(\Delta C_4\right)t_3}{H_4 - H_3}\left(t_3 - t_2\right)\cdot 10^{-3} = 5.0\frac{1.16}{0.2}\cdot 3\cdot 10^{-3} = 0.087\ \mathrm{kg/m^3}$$

Calculate the mass of suspended solid retained in the layers after time $t_4 - t_3$ = 6 h:

$$\left(\Delta q_1\right)_{t_4} = -V_f \frac{\left(\Delta C_1\right)t_4}{0 - H_1}\left(t_4 - t_3\right)\cdot 10^{-3} = 5.0\frac{0}{0.2}\cdot 6\cdot 10^{-3} = 0\ \mathrm{kg/m^3}$$

$$\left(\Delta q_2\right)_{t_4} = -V_f \frac{\left(\Delta C_2\right)t_4}{H_2 - H_1}\left(t_4 - t_3\right)\cdot 10^{-3} = 5.0\frac{17.22}{0.2}\cdot 6\cdot 10^{-3} = 2.583\ \mathrm{kg/m^3}$$

$$\left(\Delta q_3\right)_{t_4} = -V_f \frac{\left(\Delta C_3\right)t_4}{H_3 - H_2}\left(t_4 - t_3\right)\cdot 10^{-3} = 5.0\frac{6.72}{0.2}\cdot 6\cdot 10^{-3} = 1.008\ \mathrm{kg/m^3}$$

$$\left(\Delta q_4\right)_{t_4} = -V_f \frac{\left(\Delta C_4\right)t_4}{H_4 - H_3}\left(t_4 - t_3\right)\cdot 10^{-3} = 5.0\frac{2.49}{0.2}\cdot 6\cdot 10^{-3} = 0.374\ \mathrm{kg/m^3}$$

Calculate the increase of pressure loss in the layers after time t_1 = 1 h:

$$\left(\Delta h_1\right)_{t_1} = a\left(\Delta q_1\right)_{t_1}^{b}\cdot H_1 = 1.42\cdot 10^{-2}\left(0.6125\right)^{2.41}\cdot 20 = 0.087\ \mathrm{m}$$

$$(\Delta h_2)_{t_1} = a(\Delta q_2)_{t_1}^{b} \cdot (H_2 - H_1) = 1.42\cdot 10^{-2}(0.0415)^{2.41}\cdot 20 = 1.33\cdot 10^{-4}\ \text{m}$$

$$(\Delta h_3)_{t_1} = a(\Delta q_3)_{t_1}^{b} \cdot (H_3 - H_2) = 1.42\cdot 10^{-2}(0.01825)^{2.41}\cdot 20 = 1.83\cdot 10^{-5}\ \text{m}$$

$$(\Delta h_4)_{t_1} = a(\Delta q_4)_{t_1}^{b} \cdot (H_4 - H_3) = 1.42\cdot 10^{-2}(0.011)^{2.41}\cdot 20 = 5.41\cdot 10^{-6}\ \text{m}$$

Calculate the increase of pressure loss in the layers after time $t_2 = 3$ h:

$$(\Delta h_1)_{t_2} = a(\Delta q_1)_{t_2}^{b} \cdot H_1 = 1.42\cdot 10^{-2}(1.096)^{2.41}\cdot 20 = 0.354\ \text{m}$$

$$(\Delta h_2)_{t_2} = a(\Delta q_2)_{t_2}^{b} \cdot (H_2 - H_1) = 1.42\cdot 10^{-2}(0.166)^{2.41}\cdot 20 = 3.75\cdot 10^{-3}\ \text{m}$$

$$(\Delta h_3)_{t_2} = a(\Delta q_3)_{t_2}^{b} \cdot (H_3 - H_2) = 1.42\cdot 10^{-2}(0.0635)^{2.41}\cdot 20 = 3.70\cdot 10^{-4}\ \text{m}$$

$$(\Delta h_4)_{t_2} = a(\Delta q_4)_{t_2}^{b} \cdot (H_4 - H_3) = 1.42\cdot 10^{-2}(0.0345)^{2.41}\cdot 20 = 8.5\cdot 10^{-5}\ \text{m}$$

Calculate the increase of pressure loss in the layers after time $t_3 = 6$ h:

$$(\Delta h_1)_{t_3} = a(\Delta q_1)_{t_3}^{b} \cdot H_1 = 1.42\cdot 10^{-2}(1.171)^{2.41}\cdot 20 = 0.416\ \text{m}$$

$$(\Delta h_2)_{t_3} = a(\Delta q_2)_{t_3}^{b} \cdot (H_2 - H_1) = 1.42\cdot 10^{-2}(0.582)^{2.41}\cdot 20 = 0.077\ \text{m}$$

$$(\Delta h_3)_{t_3} = a(\Delta q_3)_{t_3}^{b} \cdot (H_3 - H_2) = 1.42\cdot 10^{-2}(0.181)^{2.41}\cdot 20 = 4.62\cdot 10^{-3}\ \text{m}$$

$$(\Delta h_4)_{t_3} = a(\Delta q_4)_{t_3}^{b} \cdot (H_4 - H_3) = 1.42\cdot 10^{-2}(0.087)^{2.41}\cdot 20 = 7.90\cdot 10^{-4}\ \text{m}$$

Calculate the increase of pressure loss in the layers after time $t_4 = 12$ h:

$$(\Delta h_1)_{t_4} = a(\Delta q_1)_{t_4}^{b} \cdot H_1 = 1.42\cdot 10^{-2}(0)^{2.41}\cdot 20 = 0\ \text{m}$$

$$(\Delta h_2)_{t_4} = a(\Delta q_2)_{t_4}^{b} \cdot (H_2 - H_1) = 1.42\cdot 10^{-2}(2.583)^{2.41}\cdot 20 = 2.796\ \text{m}$$

$$(\Delta h_3)_{t_4} = a(\Delta q_3)_{t_4}^{b} \cdot (H_3 - H_2) = 1.42\cdot 10^{-2}(1.008)^{2.41}\cdot 20 = 0.289\ \text{m}$$

$$(\Delta h_4)_{t_4} = a(\Delta q_4)_{t_4}^{b} \cdot (H_4 - H_3) = 1.42\cdot 10^{-2}(0.374)^{2.41}\cdot 20 = 0.0265\ \text{m}$$

Calculate total pressure loss in the layers after time $t_1 = 1$ h, $t_2 = 3$ h, $t_3 = 6$ h and $t_4 = 12$ h:

$$(\Sigma\Delta h)_{t_1} = 0.087 + 1.33\cdot 10^{-4} + 1.83\cdot 10^{-5} + 5.41\cdot 10^{-6} = 0.087\ \text{m}$$

$$(\Sigma\Delta h)_{t_2} = 0.354 + 3.75\cdot 10^{-3} + 3.70\cdot 10^{-4} + 8.5\cdot 10^{-5} = 0.358\ \text{m}$$

$$(\Sigma\Delta h)_{t_3} = 0.416 + 0.077 + 4.62\cdot 10^{-3} + 7.9\cdot 10^{-4} = 0.498\ \text{m}$$

$$(\Sigma\Delta h)_{t_4} = 0 + 2.796 + 0.289 + 0.0265 = 3.112\ \text{m}$$

Calculate the pressure loss with clean water flow from Equation (121):

$$h = k\mu S^2 \frac{(1-\varepsilon)^2}{\varepsilon^3}\frac{H}{d^2}\frac{V_f}{g}$$

$$h = 6 \cdot 10^{-6} \cdot 7^2 \frac{(1-0.4)^2}{0.4^3} \cdot \frac{0.8}{(0.5 \cdot 10^{-3})^2} \cdot \frac{1.39 \cdot 10^{-3}}{9.81} = 0.75 \text{ m}$$

Calculate the total pressure loss in the layers after time $t_1 = 1$ h, $t_2 = 3$ h, $t_3 = 6$ h, $t_4 = 12$ h with consideration of the pressure loss with clean water flow:

$$h_{(t_1=1\,h)} = 0.75 + 0.087 = 0.837 \text{ m}$$

$$h_{(t_2=3\,h)} = 0.75 + 0.358 = 1.108 \text{ m}$$

$$h_{(t_3=6\,h)} = 0.75 + 0.498 = 1.248 \text{ m}$$

$$h_{(t_4=12\,h)} = 0.75 + 3.112 = 3.862 \text{ m}$$

The increase of head loss in the analyzed filtration process is presented in the figure below.

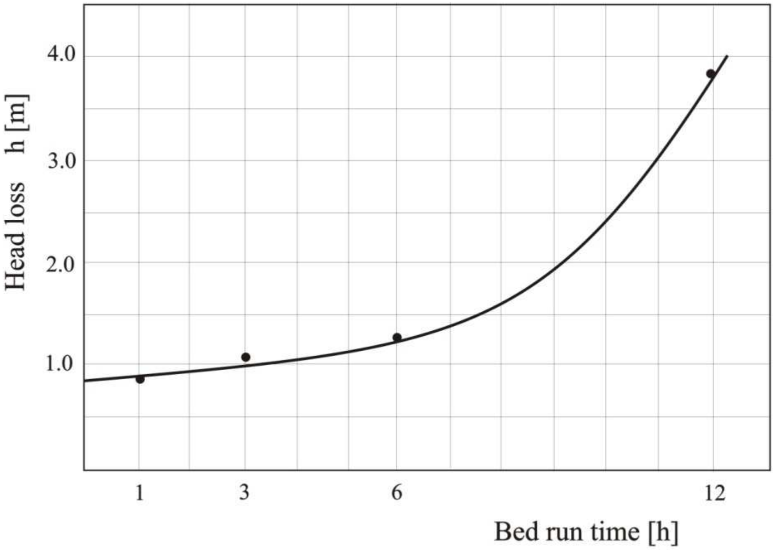

EXAMPLE 2

For the data as in Example 1, determine the required flow rate of water for rinsing the filtration bed to achieve 50% expansion ($H_e = 1.5H$).

$$\frac{H_e}{H} = \frac{1-\varepsilon}{1-\left(\frac{V_w}{V_{sk}}\right)^{0.22}}$$

$$V_w = V_{st}\left[1-\frac{H}{H_e}(1-\varepsilon)\right]^{4.54}$$

For bed grains of a representative diameter $d_c = 0.5\cdot10^{-4}$ m, shape factor $\phi = 0.85$, density $\rho_c = 2{,}600$ kg/m^3, by iteration, final the sedimentation rate was determined:

$$V_{s_1} = 0.545\frac{(\rho_p-\rho_w)d_c^2}{\eta_w} = 0.545\frac{(2{,}600-998.2)(5\cdot10^{-4})^2}{1.002\cdot10^{-3}} = 0.2178 \;\; \mathrm{m/s}$$

$$\mathrm{Re}_1 = \frac{\phi V_{s_1}\cdot d_p\cdot\rho_w}{\eta_w} = \frac{0.85\cdot0.2178\cdot5\cdot10^{-4}\cdot2{,}600}{1.002\cdot10^{-3}} = 240.19$$

$$\lambda_1 = \frac{24}{\mathrm{Re}_1}+\frac{3}{\sqrt{\mathrm{Re}_1}}+0.34 = \frac{24}{240.19}+\frac{3}{\sqrt{240.19}}+0.34 = 0.633$$

$$V_{s_2} = 3.617\sqrt{\frac{(\rho_p-\rho_w)d_c}{\lambda_1\cdot\rho_w}} = 3.617\sqrt{\frac{(2{,}600-998.2)5\cdot10^{-4}}{0.633\cdot998.2}} = 0.1287 \;\; \mathrm{m/s}$$

$$\left|V_{s_1}-V_{s_2}\right| = 0.2178-0.1287 = 0.089 > 0.002$$

$$\mathrm{Re}_2 = \frac{0.85\cdot0.1287\cdot5\cdot10^{-4}\cdot2{,}600}{1.002\cdot10^{-3}} = 141.9$$

$$\lambda_2 = \frac{24}{141.9}+\frac{3}{\sqrt{141.9}}+0.34 = 0.761$$

$$V_{s_3} = 3.617\sqrt{\frac{(2{,}600-998.2)5\cdot10^{-4}}{0.761\cdot998.2}} = 0.1174 \;\; \mathrm{m/s}$$

$$\left|V_{s_2} - V_{s_3}\right| = 0.1287 - 0.1174 = 0.0113 > 0.002$$

$$Re_3 = \frac{0.85 \cdot 0.1174 \cdot 5 \cdot 10^{-4} \cdot 2{,}600}{1.002 \cdot 10^{-3}} = 129.5$$

$$\lambda_3 = \frac{24}{129.5} + \frac{3}{\sqrt{129.5}} + 0.34 = 0.788$$

$$V_{s_4} = 3.617\sqrt{\frac{(2{,}600 - 998.2)\,5 \cdot 10^{-4}}{0.788 \cdot 998.2}} = 0.1154 \ \ \mathrm{m/s}$$

$$\left|V_{s_3} - V_{s_4}\right| = 0.1174 - 0.1154 = 0.002\ \mathrm{m/s}$$

$$V_{s_4} = V_{st} = 0.1154 \ \ \mathrm{m/s}$$

The value of the rinsing water flow rate is, therefore

$$V_w = 0.1154\left[1 - \frac{1}{1.5}(1 - 0.4)\right]^{4.54} = 0.01135 \ \ \mathrm{m/s}$$

7.6. Adsorption

Adsorption is an integral phenomenon in many natural processes in the ecosystem and in unit processes for water and wastewater treatment such as coagulation, chemical decarbonization, filtration and biochemical oxidation by activated sludge. Adsorption as a separate process is carried out in water purification systems on activated carbon. Adsorption on activated carbon is used to remove specific, dissolved organic compounds which even in trace amounts are harmful to the water consumer. The presence of these compounds in natural waters, which used to result primarily from the metabolism of aquatic organisms, is now magnified by the discharge of treated and untreated domestic and industrial wastewater and by surface run-off from agricultural land.

Since a complete identification of the particles removed in the process of adsorption (adsorbate) is not possible and it is also not possible to take into account the various interactions in water treatment systems, physical adsorption is analyzed only using a summary indication of the adsorbate concentration, especially the concentrations of total organic carbon (TOC) or dissolved organic carbon (DOC).
The **theoretical basics of the adsorption process** are examined in three planes. The first plane includes an analysis of the impact of

kinetic factors. The mathematical description is provided by the equations of adsorbate flow rate kinetics outside the adsorbent particle and the equations of the kinetics of saturation of the adsorbent particles, such as activated carbon.

The second plane includes an analysis of static factors influencing equilibrium, which is expressed by an adsorption isotherm.

The third plane covers adsorption dynamics, which in mathematical notation uses both the equations of adsorption kinetics and adsorption equilibrium as well as the adsorbate mass balance equations.

Adsorption kinetics analyzes particular phases of adsorbate mass transfer. Adsorption from aqueous solutions on porous adsorbents such as activated carbon is essentially a diffusion process and it can be divided into several stages.

The first stage is the transport of adsorbed particles in the solution mass near the active surface of the adsorbent. Adsorbate mass transfer in this stage takes place through diffusion, hydrodynamic dispersion and advection. Hydrodynamic dispersion and advection result either from the conditions of flow through the layer of adsorbent when the process is carried out in adsorption beds, or from the mixing conditions for conducting the process in a batch system.

The second stage is diffusion in the boundary layer (border film) directly near the external surface of a solid.

The third stage is the diffusion in the capillaries of sorbent grains.

Stage four is surface diffusion: particles sliding on the inner surface of the adsorbent grains.

Finally, the fifth stage is the specific adsorption, which is the fixing of sorbed particles to the active sites of the sorbent surface.

Diffusion, a unidirectional transport of adsorbate from higher to lower concentrations, results from the osmotic forces acting on dissolved particles in the direction of reducing their osmotic pressure [10, 11].

Molecular diffusion in the first stage of the adsorption process is described by the equation of Fick's First Law of Diffusion in the steady state

$$\frac{dm}{dt} = -D_m \cdot F \cdot \frac{dC}{dr} \qquad (141)$$

in which

m – adsorbate mass [g],
t – diffusion time [s],
C – adsorbate concentration [g/m^3],
r – diffusion route [m],
F – the surface of the section of diffusion stream [m^2],
D_m – molecular diffusion coefficient [m^2/h] (determined from Equation (63)).

The equation of molecular diffusion in vector notation takes the following form:

$$\overrightarrow{m_d} = -\overrightarrow{D_m} \cdot F \cdot \mathrm{grad}C \qquad (142)$$

in which

m_d – adsorbate load transferred in the diffusion process [g/h].

The second transfer mechanism in the first stage of adsorption is advection. In this process, the amount of adsorbate mass transfered is proportional to the flow rate

$$\overrightarrow{m_a} = \pi r^2 C \cdot \overrightarrow{V_f} \tag{143}$$

in which

m_a – adsorbate load transferred in the advection process [g/h],

r –integranular capillary radius [m],

V_f – flow rate [m/h].

An additional mechanism of adsorbate transfer in the first stage, hydrodynamic dispersion, is considered through increasing the molecular diffusion coefficient by the turbulent dispersion constituent ($\overrightarrow{V}_f \cdot k_x^n$)

$$D_h = D_m + \overrightarrow{V}_f \cdot k_x^n \tag{144}$$

where

k_x – system dispersiveness [m],

n – empirical constant, for the flow through porous media, is generally equal to 1.

Assuming the constancy of adsorbate concentration gradient, the summary adsorbate mass transfer in the first stage of adsorption is described by the relation

$$\overrightarrow{m} = -D_h F \,\mathrm{grad} C + \pi r^2 C \overrightarrow{V}_f \tag{145}$$

The second stage of adsorption is diffusion in the border film. Taking into account the small thickness of the border film (δ_D), assuming that the advection velocity components in the direction perpendicular to carbon surface are equal and assuming the constancy of the adsorbate concentration at every point ($\delta C/\delta t = 0$), the following equation can be written [10, 76]:

$$\pi\ r^2 \left(V_{f_H} \cdot \frac{\delta C}{\delta H} + V_{f_r} \frac{\delta C}{\delta r} \right) = D_h F \frac{\delta^2 C}{\delta r^2} \tag{146}$$

in which V_{fH}, V_{fr} are constituent velocities in the direction of flow (H) and diffusion (r).

For adsorption systems from aqueous solutions for which the Schmidt number, defined by equation

$$Sc = \frac{\mu}{D_m} \tag{147}$$

in which μ is kinematic viscosity [m^2/s], is greater than unity by several orders, the flow character is defined by the forces of viscous friction; the values of the velocity constituents may by estimated from the equation of the flow rate profile along a flat surface in the hydrodynamic border layer area (δ_H):

$$V_{f_H} = \sim V_p \frac{r}{\delta_H} \tag{148}$$

$$V_{f_r} = \sim \mu \frac{r^2}{\delta_H^3} \tag{149}$$

Assuming that the maximum flow rate is in the axis of the intergranular capillary, the thickness of the hydrodynamic border layer equals the capillary radius. Therefore, Equation (146) takes the following form:

$$\pi\ r\left(rV_f \frac{\delta C}{\delta H} + \mu \frac{\delta C}{\delta r}\right) = D_h F \frac{\delta^2 C}{\delta r^2} \tag{150}$$

For the Peclet number, defined by the equation

$$Pe = \frac{V_p \cdot d_a}{D_m} \tag{151}$$

in which d_a – adsorbate particle diameter, smaller than the unity, it may be assumed that diffusion takes place in an immovable volume of the solution and then the transfer in the second stage of adsorption is described by the equation of Fick's First Law (Equation 141).

The third stage of the adsorption process begins when the route of the free movement of adsorbate particles is smaller than the sorbent grain capillary radius.

For the analysis of adsorbate mass transfer mechanisms, activated carbon grains are modeled by rectilinear cylindrical capillaries of a constant radius. For large capillaries with a diameter of about 10^{-4} m the continuity of the stream can be assumed and then the motion of adsorbate in these capillaries is the result of diffusion described by Fick's law. In the case of capillaries with smaller diameters, the number of adsorbate particle collisions with the inner grain surface exceeds the number of collisions between particles. Then the prerequisite for the continuity of the solution filling the capillary is reduced and the adsorbate flow takes place due to effusion described by equation

$$\overrightarrow{m_e} = -D_e \frac{\pi d^2}{4} \varepsilon_z \cdot \frac{\delta C}{\delta L} \tag{152}$$

in which

m_e – adsorbate load transferred by effusion [g/h],

$D_e = \frac{D_m \varepsilon_z}{I}$ – internal diffusion (effusion) coefficient [m^2/h],

$I = 1 \div 3$ – tortuosity coefficient of grain capillaries,
ε_z – adsorbent grain porosity,
d – diameter of adsorbent particle [m],
L – penetration depth [m].

The fourth stage of the process is surface diffusion. The stream of adsorbate in surface diffusion is described by equation

$$\overrightarrow{m_s} = -D_s \frac{2V_k d_a}{L \cdot r_k \cdot \rho_a} \frac{\delta x}{\delta L} \tag{153}$$

in which
V_k – adsorbent grain capillary volume [m^3],
r_k –adsorbent grain capillary radius [m],
x – concentration in the adsorbent phase [g/kg],
ρ_a – adsorbent density [kg/m^3].

The surface diffusion coefficient D_p depends on the adsorbate concentration and for adsorption systems in water treatment it can be described by the following equation [67]:

$$D_s = D_m \frac{\exp\left(-0.2\frac{x}{x_o}\right)}{\exp k_1 - 1} C \tag{154}$$

in which
$k_1 = \sim 5.1$ – adsorption energy constant,
$x_o = f(C_o)$ – maximum adsorbed quantity per unit adsorbent weight [g/kg].

Summary adsorbate mass transfer in the internal adsorbent structure (the third and fourth step) can be described by the following equation [1].

$$\overrightarrow{m_{pr}} = \overrightarrow{m_e} + \overrightarrow{m_s} = -D_e\left(\frac{\pi\, d^2}{4}\varepsilon_z + \frac{D_s}{D_e}\frac{2V_k d_a}{Lr_k \cdot \rho_a}\right)\frac{\delta c}{\delta L} \tag{155}$$

The approximate equations of adsorption kinetics determine the rate of saturation of sorption capacity (x) as a function of the driving module of adsorption [76]. If this rate applies to a module present in the solution phase, the equation has the following form:

$$\frac{dx}{dt} = k_e\left(C - C^*\right) \tag{156}$$

where:
C^* – equilibrium adsorbate concentration [g/m^3],
k_e – external adsorbate mass transfer coefficient [s^{-1}],

As a result of the solving the above equation, one obtains the time at which the points of the initial concentration (C_o), moving down the column at a speed u will reach concentration C. At that time, these points will move for a distance equal to the mass transfer zone (h)

$$\Delta t = t_2 - t_1 = \frac{h}{u} \tag{157}$$

Transforming Equation (156) taking into account dependence (157) leads to the formula determining the size of the mass transfer zone - sorption front [h]

$$h = -V_f \int_{c}^{c_o} \frac{dC}{k_e\,(C - C^*)} \tag{158}$$

For the case when the adsorption rate is limited by internal diffusion (pore and surface diffusion), non-stationary diffusion kinetics can be described by Glückauf equation [31], in which the rate of adsorption is referred to as the module present in the adsorbent phase:

$$\frac{dx}{dt} = k_i\left(x^* - x\right) \tag{159}$$

in which:

x^* – equilibrium concentration in constant phase – in the adsorbent [g/kg],
k_i – internal adsorbate mass transfer coefficient [s^{-1}].

Because in real adsorption systems present in water treatment technology the process usually is limited by both diffusion mechanisms, the kinetic equation is frequently used in the following form

$$\frac{dx}{dt} = k_g\left(C - C^*\right) \tag{160}$$

where k_g is a general mass transfer coefficient [s^{-1}].

The general mass transfer coefficient is the function of coefficients k_e, k_i, flow rate V_f and longitudinal diffusion (dispersion) coefficient D_h. The effect of longitudinal diffusion is the result of mixing of the flow caused by the heterogeneity of the bed filling and, moreover, it depends on the effect of wall, convection mixing, molecular diffusion and the flow rate. The coefficient D_h may be determined from Equation (144).

The **adsorption static** analyzes the last stage of the process. Adsorption occurs in the system until the concentration of dissolved substance remaining in the solution is in dynamic equilibrium with the concentration of this substance on the inner surface of sorbent particles. In equilibrium there is a defined division of the adsorbate between the solution phase and adsorbent phase. A recognized and widely used form to describe this division is to present the amount of dissolved substance adsorbed per unit adsorbent weight as a function of the dissolved substance concentration remaining in the solution at a constant temperature. An expression of this type is referred to as an adsorption isotherm.

$$x = f(C)_T \tag{161}$$

Among many theories of adsorption proposed so far, the most notable because of the possibility of application in water treatment systems are Langmuir theory of single layer adsorption [54], BET theory of multilayer adsorption [12], Dubinin-Raduszkiewicz theory of micropore volume filling [22, 42] and the Freundlich theory [42].

Langmuir theory is based on a basic assumption that at a total covering of the inner adsorbent surface, the number of adsorbed particles can be no greater than the number of active sites. The adsorption layer formed isolates the actions of adsorption forces making the formation of next layers impossible. Langmuir theory was confirmed in many cases, especially in adsorption systems with a slight initial concentration of adsorbate, such systems as are used in water treatment. Mathematical description of this theory is based on an assumption that the adsorbed layer remains in dynamic equilibrium with the concentration in the solution. Only some out of the many particles in contact with the adsorbent layer are retained on the layer. The rest of the particles rebound elastically to the fluid phase. In unit time, "n" number of particles collide with the surface of a unit field, whereas, according to the kinetic theory

$$n = C(2\pi M_a K_B T)^{1/2} \tag{162}$$

where

C – adsorbate concentration [g/m^3],
M_a – adsorbate particle mass [g],
$K_B = 1.38 \cdot 10^{-23}$ J/K – Boltzman constant,
T – temperature [K].

Because in the process of adsorption a part of the surface (θ) is already covered with adsorbate particles, only the free part of the surface ($1-\theta$) is active. Adsorption velocity referred to the unit surface is therefore described by the following equation:

$$S_a = a_o(1-\theta)n \tag{163}$$

The condensation coefficient a_o is defined as a participation of inelastic collisions in a total number of collisions

$$a_o = \frac{n - n_d}{n} \tag{164}$$

n_d – number of desorbed particles.

During desorption only those parts can re-enter the solution which have sufficient energy, higher than adsorption heat (q_a). The number of particles desorbing from the unit surface in unit time is defined by equation

$$n_d = K_o \exp\left(\frac{q_a}{K_B T}\right) \tag{165}$$

where K_o – entropy coefficient.

Desorption velocity from the unit surface is described by the following relation:

$$S_d = n_d \theta \tag{166}$$

In dynamic equilibrium, the adsorption rate is equal to the desorption rate:

$$\frac{a_o \cdot n}{n_d} = \frac{\theta}{1-\theta} \tag{167}$$

The degree of surface filling is described by the relation

$$\theta = \frac{a_o \cdot n \cdot n_d^{-1}}{1 + a_o \cdot n \cdot n_d^{-1}} = \frac{bC}{1+bC} \tag{168}$$

while

$$b = \frac{a_o \exp\left(\frac{q_a}{K_B T}\right)}{K_o (2\pi M_a K_B T)^{1/2}} \tag{169}$$

The degree of surface filling may be also expressed by the ratio of adsorption capacity x at equilibrium concentration C to the adsorption capacity at a single-layer filling of surface x_m, that is:

$$\theta = \frac{x}{x_m} = \frac{bC}{1+bC} \tag{159}$$

The final form of Langmuir isotherm equation is as follows:

$$x = \frac{x_m bC}{1+bC} \tag{171}$$

BET theory, more widely applied than Langmuir theory, is restricted to the Langmuir model when the adsorption border is a single layer. According to BET theory, particles hitting the occupied sites in the inner surface of adsorbent do not leave those sites, but form adsorption complexes. With the increase of solute concentration, the number of unoccupied active sites and of active sites occupied by one adsorbate particle decreases because double, triple etc. adsorption complexes are formed.

The total amount of adsorbed substance per unit adsorbent weight is expressed by the equation

$$x = x_m(\theta_1 + 2\theta_2 + 3\theta_3 + ...) \tag{172}$$

in which θ_1, θ_2, θ_3 – is a fraction of adsorbent surface covered with a single, double and triple layer of adsorbate, respectively.

Constant equilibrium: adsorbate + free surface = single adsorption complex; adsorbate + single adsorption complex = double adsorption complex etc. are described as follows:

$$k_a^* = \frac{\theta_1}{C\theta_o}, \quad k_a^{**} = \frac{\theta_2}{C\theta_1}, \quad k_a^{***} = \frac{\theta_3}{C\theta_2}, \quad ....., \tag{173}$$

where θ_o – the part of the surface not covered with adsorbate.

The quantity of constant equilibrium of the first layer is much larger than the constants of separate layers.

To simplify the considerations it is assumed, which is slightly flawed, that the constants of equilibrium of the other layers are equal. Therefore, it can be written that

$$\theta_1 = k_a^* C\theta_o; \quad \theta_2 = k_a C\theta_1; \quad \theta_3 = k_a C\theta_2; \quad ...., \tag{174}$$

Because

$$k_a \cdot C_o = 1 \tag{175}$$

then

$$\theta_2 = \frac{C}{C_o}\theta_1, \quad \theta_3 = \frac{C}{C_o}\theta_2 = \left(\frac{C}{C_o}\right)^2 \theta_1 \tag{176}$$

After substituting the above relation to Equation (172) the result is

$$x = x_m\left(k_a^* C\theta_o + 2\frac{C}{C_o}\theta_1 + 3\left(\frac{C}{C_o}\right)^2 \theta_1 + ...\right) \tag{177}$$

and

$$x = x_m k_a^* C\theta_o\left(1 + 2\frac{C}{C_o} + 3\left(\frac{C}{C_o}\right)^2 + ...\right) \tag{178}$$

It is known that

$$\theta_o + \theta_1 + \theta_2 + \theta_3 + ... = \theta_o + k_a^* C\theta_o + k_a^* C\theta_o \frac{C}{C_o} + k_a^* C\theta_o \left(\frac{C}{C_o}\right)^2 + ... =$$

$$= \theta_o \left\{ 1 + k_a^* C \left[1 + \frac{C}{C_o} + \left(\frac{C}{C_o}\right)^2 + ... \right] \right\} = 1 \qquad (179)$$

Because the ratio C/C$_o$ ≤ 1, the sum of geometrical progression in the above equation is equal to

$$1 + \frac{C}{C_o} + \left(\frac{C}{C_o}\right)^2 + ... = \frac{1}{1 - \frac{C}{C_o}} \qquad (180)$$

and the sum of geometrical progression in Equation (178)

$$1 + 2\frac{C}{C_o} + 3\left(\frac{C}{C_o}\right)^2 + ... = \frac{1}{\left(1 - \frac{C}{C_o}\right)^2} \qquad (181)$$

After considering the above relation in Equation (178) the result is

$$x = x_m k_a^* C\theta_o \left(1 - \frac{C}{C_o}\right)^{-2} \qquad (182)$$

Substituting relation (180) to Equation (179) results in

$$\theta_0 = \frac{1 - \frac{C}{C_o}}{1 - \frac{C}{C_o} + k_a^* C} \qquad (183)$$

After substituting the above equation to Equation (182) the result is

$$x = \frac{x_m k_a^* C}{\left(1 - \frac{C}{C_o} + k_a^* C\right)\left(1 - \frac{C}{C_o}\right)} \qquad (184)$$

Because

$$C = C_o \frac{C}{C_o} = k_a^{-1} \frac{C}{C_o} \qquad (185)$$

Introducing substitution

$$k_a^* \cdot k_a^{-1} = a \tag{186}$$

to Equation (184) gives the final form of the equation of multilayer adsorption according to BET theory:

$$x = \frac{x_m \cdot a \dfrac{C}{C_o}}{\left(1 - \dfrac{C}{C_o}\right)\left[1 + (a-1)\dfrac{C}{C_o}\right]} \tag{187}$$

Characteristic courses of isotherms approximated by Langmuir and BET models are presented in Figure 25.

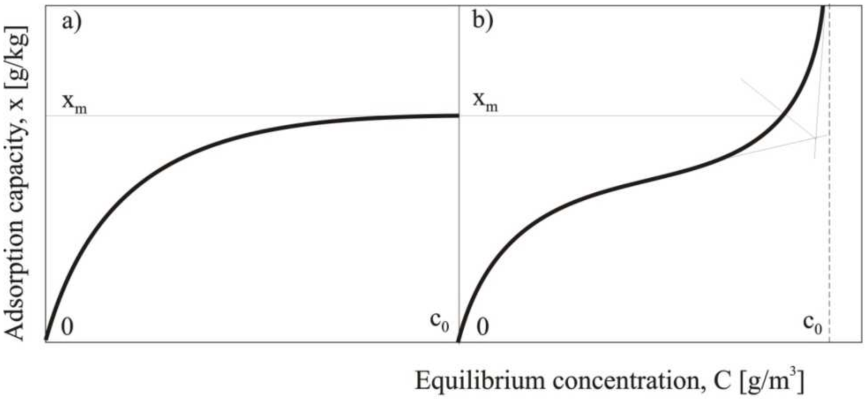

Fig. 25.Typical isotherm courses according to a) Langmuir, b) BET theories.

The **dynamics of adsorption** investigates the time-space distribution of adsorbate in the adsorption bed. Laws of adsorption dynamics indicate the degree of reduction in adsorption capacity at any section of the bed at any time during the process and the adsorbate concentration in the solution in the intergranular space depending on the hydrodynamic conditions of the process. A general mathematical model of the dynamics includes the equations of adsorbate mass balance, adsorption isotherm and kinetics.

Solving mass balance equations taking into account the longitudinal diffusion (D_h) and a convex adsorption isotherm, such as Langmuir's, assuming appropriate initial and boundary conditions leads to a steady concentration profile equation and the equation of the profile migration rate down the column [44]:

$$\frac{C - C^*}{C_o - C^*} = \exp\left(-\frac{2k_g h}{V_f + \sqrt{V_f^2 + 4D_h k_g}}\right) \tag{188}$$

$$u = \frac{V_f C_o}{C_o + x_o \rho_a} \tag{189}$$

in which:

C^* – equilibrium adsorbate concentration [g/m^3],
C_o – initial adsorbate concentration [g/m^3],
k_g – general adsorbate mass transfer coefficient [s^{-1}],
$x_o = f(C_o)$ – maximum adsorption capacity [g/kg],
D_h – dispersion coefficient [m^2/h],
ρ_a – adsorbent specific gravity [kg/m^3],
h – the height of the carbon layer, in which the concentration drops from C_o to C – adsorption front height [m],
V_f – linear velocity of the flow [m/h],
u – velocity of adsorption front migration [m/h].

For the adsorption system in which the dynamic equilibrium is described by the Langmuir isotherm equation (171) when using the operating line

$$x = \frac{x_o}{C_o} C \tag{190}$$

Equation (188) is modified to the following form

$$h = -\frac{V_f + \sqrt{V_f^2 + 4D_h k_g}}{2k_g} \ln\left|\frac{bC}{1 + bC_o}\right| \tag{191}$$

Using Equations (189) and (191) allows simulating the course of sorption column isoplans, that is to present concentration in column outflow as a function of process duration time (t).

Under specified process conditions (layer height and grain size, type and initial concentration of adsorbate, adsorption isotherm parameters and hydrodynamic conditions prevailing in the bed) from a transformed form of Equation (191) the minimum concentration that can be obtained after adsorption at the beginning of the process is determined:

$$C_{min} = \frac{1 + bC_o}{b} \exp\left(-\frac{2k_g H}{V_f + \sqrt{V_f^2 + 4D_h k_g}}\right) \tag{192}$$

In the above equation: H – sorbent layer height [m].
Then for the assumed outflow concentrations in the range $C \in (C = C_{min}; C = 0.9\ C_o)$ times are determined after which those concentrations will appear in the column outflow [1]:

$$C = C_{min}, \quad t = H \cdot V_p^{-1} \tag{193}$$

$$C = C_1, \quad t_1 = \left[H + h_1 \left(\frac{u}{V_p} - 1 \right) \right] u^{-1}, \quad h_1 = f(C_1) \tag{194}$$

$$C = C_2, \quad t_2 = \left[H + h_2 \left(\frac{u}{V_p} - 1 \right) \right] u^{-1}, \quad h_2 = f(C_2) \tag{195}$$

$$C = 0.9C_o, \quad t_c = \left[H + h_c \left(\frac{u}{V_p} - 1 \right) \right] u^{-1}, \quad h_c = f(0.9C_o) \tag{196}$$

The model taking into account all adsorbate mass transfer mechanisms in the flow system consists of the system of the following equations [1, 94]:

- equation of concentration distribution in the inner structure of adsorbent:

$$\varepsilon_z \left(\frac{\delta C_i}{\delta t} \right)_L + \rho_a \left(\frac{\delta x}{\delta t} \right)_L = \varepsilon_z D_e \frac{\delta^2 C_i}{\delta L^2} + \rho_a D_p \frac{\delta^2 x}{\delta L^2} \tag{197}$$

- initial and border conditions:

$$t = 0 \ \text{ i } \ 0 \le L < d/2, \quad C_i = x = 0 \tag{198}$$

$$t > 0 \ \text{ i } \ L = 0, \quad C_i = C_o \tag{199}$$

$$D_r \frac{\delta C_i}{\delta L} = -k_e C_i \quad \text{for} \quad L = \frac{d}{2} \tag{200}$$

- mass balance equation:

$$\frac{\Delta C_e}{\Delta t} = -\frac{24(1-\varepsilon)}{\varepsilon d^2} \left[\varepsilon_z D_e \Delta C_i + \rho_a D_s \Delta x(C_i) \right] \tag{201}$$

- equation of adsorption isotherm of the Langmuir type.

This model with formulated initial and border conditions assumes that the factors limiting the course of adsorption are all diffusion mechanisms: porous, surface, external diffusions [1, 94].

In the system of equations:

C_i – adsorbate concentration in the inner adsorbent structure [g/m^3],
C_e – adsorbate concentration in the solution after contact time t [g/m^3],
ε_z – porosity of adsorbent grains,
L – depth of adsorbent penetration [m],
D_e – porous diffusion coefficient [m^2/s],
D_s – surface diffusion coefficient [m^2/s],
x – the amount adsorbed per unit adsorbent weight [g/kg],

ρ_a – adsorbent specific gravity [kg/m^3],
d – representative diameter of adsorbent grains [m],
D_r – equivalent coefficient of diffusion [m^2/s] defined by equation:

$$D_r = \varepsilon_z D_e + \rho_a D_s \frac{dx}{dC_i} \tag{202}$$

Adoption of concentration independence of the equilibrium diffusion coefficient for the adsorption system described by non-linear adsorption isotherm implies the concentration dependence of the surface diffusion coefficient (D_s). If one accepts as reliable the equation proposed by Neretnieks defining the surface diffusion coefficient [67]

$$D_s = f\left(D_m ;\ \frac{x}{x_o} \right) \tag{203}$$

then it can be observed that increasing the value of x causes the increase in the value of the surface diffusion coefficient with a simultaneous decrease of dx/dC_i derivative for a system described by a convex adsorption isotherm. In the reverse case, a decreasing value of x causes a decrease of D_s and a simultaneous increase in the dx/dC_i derivative. In optimal conditions, it is possible that with reverse changes of the D_s parameter and dx/dC_i derivative values, their product will be a constant value [94].
Since

$$D_s \frac{dx}{dC_i} \neq f(x) \tag{204}$$

then also the equilibrium diffusion coefficient (D_r) will not depend on x and C_i.
The following notation is therefore possible

$$\rho_a D_s \left(\frac{\delta x}{\delta L} \right)_t = \rho_a D_s \frac{dx}{dC_i} \left(\frac{\delta C_i}{\delta L} \right)_t \tag{205}$$

then

$$\varepsilon_z D_e \left(\frac{\delta C_i}{\delta L} \right)_t + \rho_a D_s \left(\frac{\delta x}{\delta L} \right)_t = \left(\varepsilon_z D_e + \rho_a D_s \frac{\delta x}{\delta C_i} \right) \left(\frac{\delta C_i}{\delta L} \right)_t \tag{206}$$

Since D_r is independent from C_i and x, it is also independent from the position within the adsorbent particle (L) and from the time of process duration (t). The equation of the concentration field (197) therefore takes the following form:

$$\varepsilon_z \left(\frac{\delta C_i}{\delta t} \right)_L + \rho_a \left(\frac{\delta x}{\delta t} \right)_L = D_r \frac{\delta^2 C_i}{\delta L^2} \tag{207}$$

Also the mass balance equation is changed (201)

$$\frac{\Delta C_e}{\Delta t} = -\frac{24(1-\varepsilon)}{\varepsilon\, d^2} D_r \Delta C_i \qquad (208)$$

For the requirements of process analysis, the linearization of the adsorption isotherm equation is performed. The course of the isotherm is analyzed in four ranges in which it is described by a straight line equation [1]. For small adsorption values, the first approximation of the Langmuir adsorption isotherm is assumed:

$$x = x_m b C_i \qquad (209)$$

The equation is valid for equilibrium concentrations in the range from 0 to C_p^*, while the concentration C_p^* is determined by the relation

$$C_p^* = \frac{C_o}{4 + 3bC_o} \qquad (210)$$

In the second stage, the Langmuir equation is modified to the form

$$x = \frac{x_m b(2 + bC_o)^2}{4(1 + bC_o)^2} C_i + \frac{x_m b C_o^2}{4(1 + bC_o)^2} \qquad (211)$$

This equation is valid in the range $C_i \in \left(C_p^*; C_p^{**}\right)$ and concentration C_p^{**} is defined by the formula:

$$C_p^{**} = \frac{C_o(12 + 13bC_o)}{16 + 24bC_o + 7b^2C_o^2} \qquad (212)$$

In the third range from C_p^{**} to C_p^{***} the following equation is valid

$$x = \frac{x_m b(4 + bC_o)^2}{(4 + 5bC_o)^2} C_i + \frac{16 x_m b^2 C_o^2}{(4 + 5bC_o)^2} \qquad (213)$$

while C_p^{***} is described by the equation:

$$C_p^{***} = \frac{C_o(8 + 9bC_o)}{8 + 10bC_o + b^2C_o^2} \qquad (214)$$

The fourth analyzed range of the adsorption isotherm course is valid in the following concentration range $C_i \in \left(C_p^{***}; C_o\right)$ and the isotherm is described by the following equation:

$$x = \frac{x_m b}{(1 + bC_o)^2} C_i + \frac{x_m b^2 C_o^2}{(1 + bC_o)^2} \qquad (215)$$

So, for the particular ranges the equation of the concentration field takes the following form:

$$\frac{\delta C_i}{\delta t} = \Omega_n \ D_r \frac{\delta^2 C_i}{\delta L^2} \tag{216}$$

where n – number of the range of concentrations analyzed.
Parameters Ω_1, ... , Ω_4 are defined by the following equations:

$$\Omega_1 = \left(\varepsilon_z + \rho_w x_m b\right)^{-1} \tag{217}$$

$$\Omega_2 = 4\left(1 + bC_o\right)^2 \left[4\varepsilon_z\left(1 + bC_o\right)^2 + \rho_w x_m b\left(2 + bC_o\right)^2\right]^{-1} \tag{218}$$

$$\Omega_3 = \left(4 + 5bC_o\right)^2 \left[\varepsilon_z\left(4 + 5bC_o\right)^2 + \rho_w x_m b\left(4 + bC_o\right)^2\right]^{-1} \tag{219}$$

$$\Omega_4 = \left(1 + bC_o\right)^2 \left[\varepsilon_z\left(1 + bC_o\right)^2 + \rho_w x_m b\right]^{-1} \tag{220}$$

Partial differential equation (216) is presented as a sum of two functions

$$C_i(L,t) = C_1(L) + C_2(L,t) \tag{221}$$

The function $C_1(L)$ does not depend on variable t and presents the concentration distribution in a steady state, that is in the range

$$\lim_{t\to\infty} C_i(L,t) = C_1(L) \tag{222}$$

which generates

$$\lim_{t\to\infty} C_2(L,t) = 0 \tag{223}$$

Condition (198) leads to

$$C_i(L,0) = C_1(L) + C_2(L,0) = 0 \tag{224}$$

Whereas condition (199) leads to

$$C_i(0,t) = C_1(0) + C_2(0,t) = 0 \tag{225}$$

and condition (200) leads to

$$D_r\left(\frac{dC_1}{dL} + \frac{\partial C_2}{\partial L}\right)_{L=\frac{d}{2}} = k_e\left[C_1\left(\frac{d}{2}\right) + C_2\left(\frac{d}{2}, t\right)\right] \tag{226}$$

Boundary conditions for function $C_1(L)$ are as follows:
- from Equation (225):

$$C_1(0) = C_o \tag{227}$$

- from Equation (226)

$$D_r\left(\frac{dC_1}{dL}\right)_{L=\frac{d}{2}}=-k_eC_1\left(\frac{d}{2}\right) \tag{228}$$

The solution of Equation (221), when $\delta C_1/\delta t = 0$ and $C_i = C_1$ for given boundary conditions is

$$D_r\frac{d^2C_1}{dL^2}=0 \tag{229}$$

$$\frac{d^2C_1}{dL^2}=0 \tag{230}$$

$$\frac{dC_1}{dL}=S \tag{231}$$

$$C_1(L)=SL+U \tag{232}$$

$$C_1(0)=U=C_o \tag{233}$$

$$D_rS=-k_e\left(S\frac{d}{2}+C_o\right) \tag{234}$$

Hence

$$S=-k_eC_o\left(D_r+k_e\frac{d}{2}\right)^{-1} \tag{235}$$

and

$$C_1(L)=-k_eC_o\left(D_r+k_e\frac{d}{2}\right)^{-1}L+C_o \tag{236}$$

$$C_1(L)=C_o\left[1-\frac{k_e\,L}{D_r+k_e\frac{d}{2}}\right] \tag{237}$$

The function $C_2(L, t)$ presents the change in adsorbate concentration at a non-steady state. Boundary conditions for this function are as follows:

- from Equation (224)

$$C_2(L,0)=-C_1(L) \tag{238}$$

- from Equation (225)

$$C_2(0,\ t)=0 \tag{239}$$

- from Equation (226)

$$D_r\left(\frac{dC_2}{dL}\right)_{L=\frac{d}{2}}=-k_eC_2(L,t) \tag{240}$$

The solution of Equation (221) for $C_1 = C_2$ with the method of variable separation is as follows:

After presenting the concentration which is the function of two variables $C_i(L, t)$ as a product of the function of position (L) and the function of time (t)

$$C_i(L,t) = \varphi(L)\psi(t) \tag{241}$$

the equation of the concentration field in a modified form (216) is

$$\varphi\psi' = \Omega_n D_r \psi\varphi'' \tag{242}$$

When the solving partial differential equation in line with normal procedure, it is assumed that both sides of the equation are equal to the constant value of $-\lambda^2$. Two ordinary differential equations are then produced:

$$\frac{1}{\Omega_n D_r}\frac{\psi'}{\psi} = -\lambda^2 \tag{243}$$

$$\frac{\varphi''}{\varphi} = -\lambda^2 \tag{244}$$

The solution for these equations can be presented as follows:

$$\psi(t) = \exp\left(-\lambda^2 \Omega_n D_r t\right) \tag{245}$$

$$\varphi(L) = A\sin\lambda t + B\cos\lambda t \tag{246}$$

Because the modified concentration field equation is linear, its solution can be presented as a sum of particular solutions:

$$C = \sum_{m=1}^{\infty} \left\{\left[A_m \sin\left(\lambda_m L\right) + B_m \cos\left(\lambda_m L\right)\right]\exp\left(-\lambda_m^2 \Omega_n D_r t\right)\right\} \tag{247}$$

From Equation (239), $B_m = 0$.

On the basis of condition (240) the result is

$$C_2\left(\frac{d}{2},\ t\right) = -\frac{\Omega_n D_r}{k_e}\sum_{m=1}^{\infty} A_m \lambda_m \cos\left(\lambda_m \frac{d}{2}\right)\exp\left(-\lambda_m^2 \Omega_n D_r t\right) \tag{248}$$

Because $C_2\left(\frac{d}{2};t\right)$ is also described by Equation (247), comparing the right sides of these equations and multiplying them by $\frac{d}{2}$ gives

$$\lambda_m \frac{d}{2}\,\mathrm{ctg}\left(\lambda_m \frac{d}{2}\right) = -\frac{k_e \frac{d}{2}}{\Omega_n D_r} \qquad (249)$$

The value of expression $\frac{\lambda_m \cdot d}{2}$ at a defined right side of Equation (249) is determined by trial-and-error. Denoting

$$\lambda_m \frac{d}{2} = \gamma \qquad (250)$$

the equation defining $C_2(L, t)$ takes the form

$$C_2(L,t) = \sum_{m=1}^{\infty} A_m \sin\left(\frac{2\gamma}{d} L\right) \exp\left(-\frac{4\gamma^2}{d^2}\Omega_n D_r t\right) \qquad (251)$$

The A_m parameter is defined on the basis of condition (238). Multiplying both sides of the above equation by $\sin\left(\frac{2\gamma}{d} L\right)$, transforming it appropriately taking account the orthogonal condition produces

$$A_m = \frac{-\int\limits_0^{d/2} C_1(L)\sin\left(\frac{2\gamma}{d}L\right)dL}{\int\limits_0^{d/2} \sin^2\left(\frac{2\gamma}{d}L\right)dL} \qquad (252)$$

and

$$A_m = \frac{C_o \frac{d}{2\gamma}(\cos\gamma - 1) + \frac{k_e C_o d^2}{4\left(\Omega_n D_r + k_e \frac{d}{2}\right)\gamma^2}\left(\frac{1}{\gamma}\sin\gamma - \cos\gamma\right)}{\frac{d}{4\gamma}(\gamma - \sin\gamma\cos\gamma)} \qquad (253)$$

$$A_m = \frac{2C_o\left[(\cos\gamma - 1) + \frac{Sh}{1+Sh}\left(\frac{1}{\gamma}\sin\gamma - \cos\gamma\right)\right]}{\gamma\left(1 - \frac{\sin 2\gamma}{2\gamma}\right)} \qquad (254)$$

Whereas Sherwood number is defined by the equation

$$\mathrm{Sh} = \frac{k_e \frac{d}{2}}{\Omega_n D_r} \tag{255}$$

Because the counter of the right side of equation (254) is actually equal to -2C$_o$, then restricting to the first equation series only, the following form of function C$_2$(L, t) is produced (Equation 251):

$$C_2(L,t) = -\frac{2C_o}{\gamma\left(1-\frac{\sin 2\gamma}{2\gamma}\right)} \sin\frac{2\gamma}{d}L \exp\left(-\frac{4\gamma^2}{d^2}\Omega_n D_r t\right) \tag{256}$$

and the final solution of Equation (197) under conditions (198) ÷ (200) is

$$C_i(L,t) = C_o\left\{1-\frac{2L}{d}-\frac{2}{\gamma\left(1-\frac{\sin 2\gamma}{2\gamma}\right)}\sin\frac{2\gamma}{d}L \exp\left(-\gamma^2 \mathrm{Fo}\right)\right\} \tag{257}$$

in which the Fourier number is defined by the equation

$$\mathrm{Fo} = \frac{\Omega_n D_r t}{\left(\frac{d}{2}\right)^2} \tag{258}$$

Assuming a linear distribution of concentration adsorbed inside the particle, for further considerations the value of concentration C$_i$ determined for $L = d/4$ is assumed. With this assumption Equation (257) is simplified to the following form:

$$C_i = C_o\left\{0{,}5-\frac{d\sin\frac{2\gamma}{d}}{2\gamma-\sin 2\gamma}\exp\left(-\gamma^2 \mathrm{Fo}\right)\right\} \tag{259}$$

The procedure for determining the required contact time t with a carbon layer of a certain geometry (H, ε, d) at defined parameters of the Langmuir adsorption isotherm (x_m, b) and determined adsorbate diffusivity (D_m) to achieve the assumed concentration C_{ez} in the outflow from the layer is as follows:

- determine equilibrium concentration ranges in which the adsorption isotherm is described by a straight line equation,
- determine Ω_n coefficients modifying the D_r coefficient in particular concentration ranges,

- determine the value of parameter γ by trial-and-error for various Ω_n coefficients,
- assume the tolerance of estimating the concentration in outflow Δ,
- assume contact time t_l with the adsorbent layer and the value of Δt by which if necessary the value of t_l is corrected:

$$t_2 = t_l \pm \Delta t \tag{260}$$

- calculate the value of the adsorbate concentration in the inner adsorbent structure after contact time t_l from Equation (2.259) assuming the value Ω_1 in the first approximation for determining the value of Fourier number (Fo) and γ parameter,
- check in what concentration range the determined value of C_i is and if it is in a different range than it was assumed; then for calculating C_i, in the second step assume the value of parameter Ω from the concentration range determined in the first step,
- carry out the verifying procedure until compatibility is achieved between the equilibrium concentration range where the determined C_i lies and the value of Ω assumed for this range,
- calculate the outflow concentration from the layer after contact time t using a modified form of the adsorbate mass transfer balance equation (208):

$$C_e = C_o - \frac{24\left(1-\varepsilon\right)}{\varepsilon \cdot d^2}\Omega_n D_r \cdot C_i \cdot t \tag{261}$$

- compare the value of C_e with an assumed concentration C_{ez} and if $\left|C_e - C_{ez}\right| > \Delta$ and $C_e > C_{ez}$ a new value of contact time $t_2 = t_l + \Delta t$ is assumed and the procedure of estimating the value of C_i and C_e is repeated,

- if $\left|C_e - C_{ez}\right| > \Delta$ and $C_e < C_{ez}$ then $t_2 = t_l - \Delta t$ are assumed and the procedure of calculating C_i and C_e is repeated,

- determine the height of adsorption front (h_a) at an assumed linear flow velocity (V_f) from equation

$$h_a = V_f \cdot t \tag{262}$$

- calculate working time (t_e) of adsorption front from the relation

$$t_e = \frac{h_a}{V_p}\frac{x_m b C_e\left(1-\varepsilon\right)\rho_a}{\left(1+bC_e\right)\left(C_o - C_e\right)\varepsilon} \tag{263}$$

- calculate the working time of the column of a height H until concentration the C_e in the outflow is achieved from the relation

$$t_e^H = t_e \frac{H}{h_a} \tag{264}$$

- calculate the minimal achievable concentration in the column outflow at the beginning of the cycle $\left(C_e^{\min}\right)$ from Equation (261) while assuming the value $t = HV_p^{-1}$ and applying the determined value $C_i = f\left(t = H \cdot V_p^{-1}\right)$ from Equation (259).

The diagram of adsorption zone movement and the isoplan of the adsorption column resulting from it are presented in Figure 26.

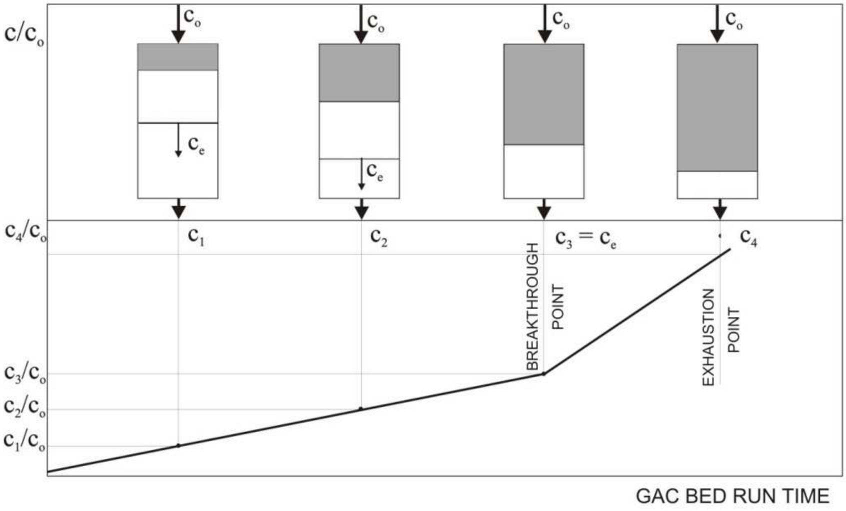

Fig. 26. The diagram of adsorption zone movement.

Applying the models presented above requires settling numerical values of Langmuir adsorption isotherm parameters (x_m, b), hydrodynamic dispersion coefficients (D_h), external adsorbate mass transfer (k_e), general transfer coefficient (k_g) and the equilibrium diffusion coefficient $D_r = f(D_e, D_p)$. It is also necessary to know the representative diameter of adsorbent particles (d), their porosity (ε_z) and layer porosity (ε).

All diffusion (D_h, D_r) and kinetic (k_e, k_g) parameters are directly or indirectly in the function of the molecular diffusion coefficient defined by Stokes-Einstein (5.63) or the Wilke – Chang equations [96]

$$D_m = 7.4 \cdot 10^{-12} \frac{(A_s \cdot M_r)^{0.5} \cdot T}{\eta\, V_m^{0.6}} \quad [m^2/s] \qquad (265)$$

in which

A_s – association parameter = 2.6 for aqueous solution,
M_r – molecular weight of dissolvent [g],
T – absolute temperature [K],
η – dynamic viscosity [kg/m×s],
V_m – molar volume of adsorbate [m^3].

The analytical determination of a coefficient based on the equations presented below requires the precise identification of adsorbate particles, their diameter and volume.

The large diversity of composition and construction of adsorbate particles present in water after various cleaning processes results in the phenomenon of competitiveness in adsorption and the effect of incomplete utilization of adsorbent sorption capacity due to the fact that smaller particles are blocked by larger ones from accessing the pore structure. Since it is not possible to fully identify adsorbate particles and take into account the superposition of various effects, only physical adsorption is analyzed in water treatment systems using a summary indication of adsorbate concentration such as total organic carbon (TOC).

Likewise, when analyzing the dynamics and kinetics of adsorption, the concept of a molecular diffusion replacement coefficient (D_{mz}) is used which on average characterizes the adsorption properties of the mixture. This coefficient can be determined from the empirical formula [1]

$$D_{mz} = \frac{7.23 \cdot 10^8\, KT}{\eta \left[\left(\gamma_z \frac{x_m}{C_o} \right)^{\delta_z} + 77 \right]^{0..5}} \quad [m^2/h] \qquad (266)$$

in which

$K = 1.38 \cdot 10^{-23}$ J/K – Boltzman constant,
T – temperature [K],
η – dynamic viscosity [kg/m×s],
x_m – the amount adsorbed in a single layer [g/kg],
C_o – initial adsorbate concentration measured by the level of TOC[gC/m^3],
γ_z, δ_z – experimental parameters dependent on the type of water treated and adsorbent used.

The values of these parameters for systems with activated carbon vary in the range: $\gamma_z = 0.9 \div 1.2$, $\delta_z = 2.5 \div 2.7$.
The equilibrium diffusion coefficient (D_r) for a multi-component system is defined by the equation [1]

$$D_r = D_{mz}\left(0.02 + 0.196\,\rho_a \frac{x_m b}{1 + bC_o}\right) \quad [\mathrm{m^2/h}] \tag{267}$$

in which ρ_a is the proper density of adsorbent – activated carbon [kg/m^3].
The dispersion coefficient (D_h) is a function of the layer geometry (ε, d), hydrodynamic conditions in the layer (V_f) and diffusiveness (Sc, j_d) and is described by the relation [2, 3]

$$D_h = 0.084\left(\frac{\varepsilon}{1-\varepsilon}\right)^2 d \cdot j_d \cdot V_p \cdot Sc^{-2/3} \quad [\mathrm{m^2/h}] \tag{268}$$

in which:

j_d – mass penetration module,
Sc – Schmidt number determined by Equation (147).

The module of mass penetration can be defined from correlating equations for various ranges of Reynolds numbers for the type and porosity of the bed.
For a steady fluidized bed and Reynolds number in the range 1 < Re < 30, the Chu equation [17] in the following form can be assumed:

$$j_d = 5.7 \cdot Re^{-0.78} \tag{269}$$

and for the range 30 < Re < 10 000

$$j_d = 1.77 \cdot Re^{-0.44} \tag{270}$$

whereas the Reynolds number is defined by equation

$$Re = \frac{V_p \cdot d \cdot \rho_a}{\eta(1-\varepsilon)} \tag{271}$$

According to Pfeffer and Happel [73], for small values of Re and all types of beds, the criterial equation in the following form can be applied:

$$j_d = Be \cdot Re^{-0.67} \tag{272}$$

The Reynolds number is defined by the equation

$$Re = \frac{V_p \cdot d \cdot \rho_a}{\eta} \tag{273}$$

And the Be parameter is defined by the formula

$$\mathrm{Be} = 1.26\ [1-(1-\varepsilon)^{5/3}]^{\ 1/3}\ [2-3(1-\varepsilon)^{1/3}+(1-\varepsilon)^{5/3}-2(1-\varepsilon)^{2}] \tag{274}$$

Evans and Gerald [43] proposed for a steady bed:

$$j_d = 2.132\,\mathrm{Re}^{-0.512} \tag{275}$$

and for a bed in expansion

$$j_d = 1.34\,\mathrm{Re}^{-0.468} \tag{276}$$

In Equations (275) and (276), Reynolds number is defined by Equation (271).

For the range of Reynolds number $1.0^{-2} < \mathrm{Re} < 3 \cdot 10^{4}$, according to Dwivedi and Upadhyay [97] the module is described by the correlation equation

$$j_d = \frac{1{,}957}{\mathrm{Re}^{0.82}} + \frac{1.685}{\mathrm{Re}^{0.444}} \tag{277}$$

in which Re is described by Equation (271).

The external adsorbate mass transfer coefficient (k_e) with the approximation of conditions in the flow system is described by the formula [8, 56]

$$k_e = 2D_{mz}\left\{d\left[\left(\frac{\varepsilon}{1-\varepsilon}\right)^{1/3}-1\right]\right\}^{-1} \quad [\mathrm{m/h}] \tag{278}$$

The above definition of the k_e coefficient states that the coefficient is important only in the layers of $\varepsilon > 0.5$ porosity and for adsorption beds in expansion. The general mass transfer coefficient (k_g) is a function of the hydrodynamic conditions prevalent in the bed (V_f, D_h) and the coefficients of external and internal mass transfer (k_e, k_i) according to the equation [76]

$$k_g = \left[k_e^{-1} + k_i^{-1} + \frac{D_h}{V_f^2}\right]^{-1} \tag{279}$$

whereas coefficient k_e is described by equation

$$k_e = \frac{2D_{mz}}{r_K \cdot \varepsilon} S(1-\varepsilon) \tag{280}$$

in which

r_K –intergranular capillary radius [m],

S – active surface per unit bed volume [m^2/m^3].
and coefficient k_i is defined by the equation

$$k_i = \frac{4D_e\varepsilon}{r_K^2(1-\varepsilon)^2} \tag{281}$$

in which D_e is the porous diffusion coefficient [m^2/h].
Considering the relation between sorbent grain porosity (ε_z) and tortuosity of grain capillaries, the assumed at level 0.1, coefficient D_e can be determined from equation

$$D_e = 0.1\,D_{mz} \tag{282}$$

Taking into account the equation of the approximated averaged value of the intergranular capillary radius [3]

$$r_K = \frac{\varepsilon\,d}{6(1-\varepsilon)} \tag{283}$$

and active surface per unit bed volume

$$S = \frac{2\varepsilon}{r_K} \tag{284}$$

relation (279) takes the following form

$$k_g = \left\{\frac{\varepsilon d\left[\varepsilon d + 10d\,(1-\varepsilon)^3\right]}{144\,D_{mz}(1-\varepsilon)^3} + \frac{D_h}{V_f^2}\right\}^{-1} \tag{285}$$

Figure 27 presents an algorithm to simulate the course of an adsorption column isoplan with a mathematical model based on Equations (197) ÷ (201) along with the equation of the Langmuir adsorption isotherm (171).

DATA

C_o – adsorbate concentration in the inflow [g/m^3]
C_{ez} – required concentration in the outflow [g/m^3]
x_m, b – Langmuir isotherm parameters [g/kg], [m^3/g]
d – representative diameter of adsorbent particles [m]
ε – porosity of adsorbent layer
ε_z – porosity of adsorbent grains
ρ_a – density of hydrated adsorbent [kg/m^3]
H – height of adsorbent layer [m]
V_p – linear flow rate [m/h]
D_m – molecular diffusion coefficient [m^2/h]
Δ – tolerance of determining outflow concentration [g/m^3]
Δt – value by which contact time is corrected [h]

CALCULATE

D_r – equilibrium diffusion coefficient [m^2/h],
from Equation (267)

k_e – external mass transfer coefficient[m/h],
from Equation (278)

modifying coefficients D_r - Ω_1; ... ; Ω_4
from Equations (217) (218) (219) (220), respectively

C_p – equilibrium concentrations defining the ranges of analyzed
concentrations from Equations (210) (212) (214)

$Sh = f(k_e, \Omega_n D_r)$ from Equation (255)

γ – parameter of Equation (251)
determined by trial-and-error method from Equation (249)

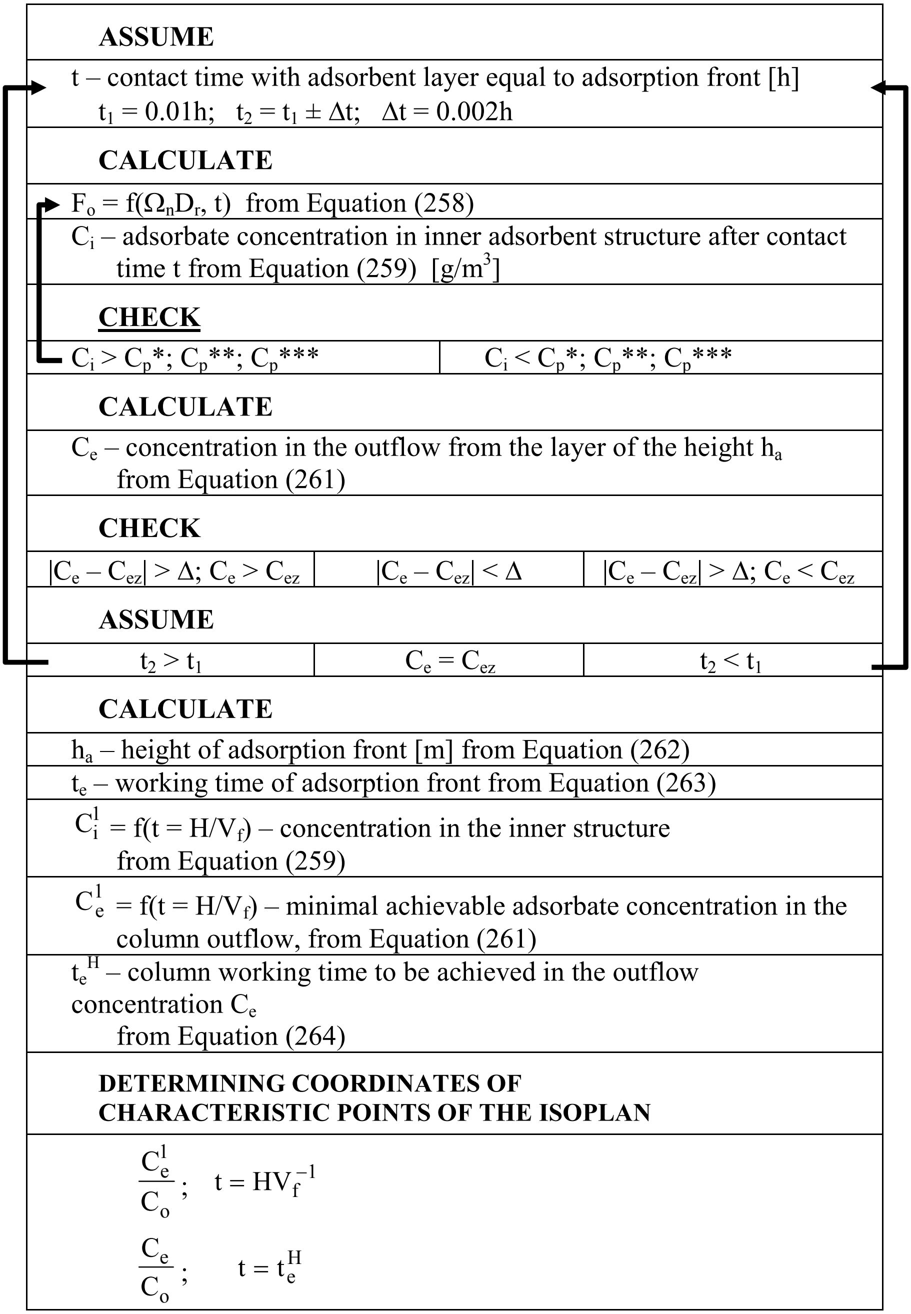

ASSUME

t – contact time with adsorbent layer equal to adsorption front [h]

$t_1 = 0.01h$; $t_2 = t_1 \pm \Delta t$; $\Delta t = 0.002h$

CALCULATE

$F_o = f(\Omega_n D_r, t)$ from Equation (258)

C_i – adsorbate concentration in inner adsorbent structure after contact time t from Equation (259) [g/m^3]

CHECK

$C_i > C_p^*; C_p^{**}; C_p^{***}$	$C_i < C_p^*; C_p^{**}; C_p^{***}$

CALCULATE

C_e – concentration in the outflow from the layer of the height h_a from Equation (261)

CHECK

$\lvert C_e - C_{ez}\rvert > \Delta; C_e > C_{ez}$	$\lvert C_e - C_{ez}\rvert < \Delta$	$\lvert C_e - C_{ez}\rvert > \Delta; C_e < C_{ez}$

ASSUME

$t_2 > t_1$	$C_e = C_{ez}$	$t_2 < t_1$

CALCULATE

h_a – height of adsorption front [m] from Equation (262)

t_e – working time of adsorption front from Equation (263)

$C_i^1 = f(t = H/V_f)$ – concentration in the inner structure from Equation (259)

$C_e^1 = f(t = H/V_f)$ – minimal achievable adsorbate concentration in the column outflow, from Equation (261)

t_e^H – column working time to be achieved in the outflow concentration C_e from Equation (264)

DETERMINING COORDINATES OF CHARACTERISTIC POINTS OF THE ISOPLAN

$$\frac{C_e^1}{C_o}; \quad t = HV_f^{-1}$$

$$\frac{C_e}{C_o}; \quad t = t_e^H$$

Fig. 27. Algorithm of adsorption column isoplan simulation.

The characteristics of the capillary system and the granulometry of selected species of activated carbon commonly used in water treatment technology are summarized in Table 10.

Table 10. Characteristics of selected species of granular activated carbon [42].

Type of activated carbon	**Apparent density**	**Effective dimension of particles**	**UC**	**ε_z**	**Pore volume**	**Specific surface**
	kg/m^3	$10^{-3}m$			cm^3/g	m^2/g
IC, America Hydrodarco 3000	430	0.8 – 0.9	1.7	0.22	0.95	600 – 650
Calgon Filtrasorb 3000	480	0.8 – 0.9	1.9	0.20	0.85	950 – 1,050
Westvaco Nuchar WU - L	480	0.85 – 1.05	1.8	0.20	0.85	1,000
Eitco 517	480	0.89	1.4	0.20	0.60	1,050
Norit SA1	460	1.0 – 2.0	1.5	0.18	0.60	900
Norit SK1	460	1.0 – 2.0	1.5	0.18	0.65	900 – 925
Norit SCM	460	1,0 – 2.0	1.5	0.1784	0.70	1,200
Sorbonit B4 (A3545)	431	0.9 – 1.5	1.75	0.25	0.87	1,030
Sorbonit B4 (A4131)	423	0.9 – 1.5	1.75	0.22	0.88	1,130
Sorbonit B4 (A4135)	412	0.9 – 1.5	1.75	0.22	0.96	1,230
ARZ - 1	530	0.8 – 1.2	1.2 – 1.5	0.2	0.75	700
AHD	430	1.0 – 1.5	1.2 – 1.5	0.2	1.12	1,000
AG	520	1.0 – 1.5	1.2 – 1.5	0.2	1.0	700
WD - Extra	520	1.8 – 2.0	1.2 – 1.5	0.18	1.3	900

7.6.1. Example Calculations

EXAMPLE 1

Determine the working time of an activated carbon column of a layer height $H = 3.0$ m, porosity $\varepsilon = 0.4$, representative grain diameter $d = 0.002$ m and density of hydrated carbon particles $\rho_a = 1{,}900$ kg/m^3, operating in a technological system of surface water treatment after coagulation with aluminum sulfate, flocculation, sedimentation and filtration. The concentration of dissolved organic carbon (DOC) in the stream flowing into the column $C_o = 5$ g/m^3 and acceptable the concentration in the outflow $C = 2$ g/m^3. The adopted linear flow rate $V_f = 5$ m/h $= 0.00139$ m/s. Parameters of Langmuir adsorption isotherm equation were determined in laboratory testing

(Equation 171) are $x_m = 60$ g/kg, $b = 1.0$ m^3/g. Specific molecular diffusion coefficient for compounds measured by DOC level in the purified water is $D_{mz} = 5.9 \cdot 10^{-10}$ m^2/s. Water dynamic viscosity is $\eta = 0.001$ kg/m·s, and its density $\rho = 1{,}000$ kg/m^3.

Solve the problem using the model of adsorption dynamics described by Equations (188) ÷ (192).

Determine height of adsorption front necessary to decrease concentration from value $C_o = 5$ g/m^3 to $C = 2$ g/m^3 (Equation 191):

$$h = -\frac{V_f + \sqrt{V_f^2 + 4D_h k_g}}{2k_g} \ln\left|\frac{bC}{1 + bC_o}\right|$$

- hydrodynamic dispersion coefficient determined from Equation (268)

$$D_h = 0.084\left(\frac{\varepsilon}{1-\varepsilon}\right)^2 d \cdot j_d \cdot V_f \cdot Sc^{-2/3}$$

- Schmidt number is

$$Sc = \frac{\eta}{\rho \cdot D_{mz}} = \frac{0.001}{1{,}000 \cdot 5.9 \cdot 10^{-10}} = 1{,}695$$

- module of mass penetration for Reynolds number

$$Re = \frac{V_f \cdot d \cdot \rho_a}{\eta(1-\varepsilon)} = \frac{0.00139 \cdot 0.002 \cdot 1{,}900}{0.001(1-0.4)} = 8.8$$

is (Equation 277):

$$j_d = \frac{1.957}{Re^{0.82}} + \frac{1.685}{Re^{0.444}} = \frac{1.957}{5.95} + \frac{1.685}{2.626} = 0.971$$

So D_h equals

$$D_h = 0.084\left(\frac{0.4}{1-0.4}\right)^2 0.002\cdot 0.971\cdot 0.00139\cdot (1{,}695)^{-2/3} = 5.53\cdot 10^{-10}\ \ \mathrm{m^2/s}$$

- general mass transfer coefficient was determined from Equation (285):

$$k_g = \left\{\frac{\varepsilon d\left[\varepsilon d + 10d\,(1-\varepsilon)^3\right]}{144\ D_{mz}(1-\varepsilon)^3} + \frac{D_h}{V_p^2}\right\}^{-1} =$$

$$= \left\{\frac{0.4\cdot 0.002\left[0.4\cdot 0.002 + 10\cdot 0.002\,(1-0.4)^3\right]}{144\cdot 5.9\cdot 10^{-10}(1-0.4)^3} + \frac{5.9\cdot 10^{-10}}{(0.00139)^2}\right\}^{-1} = 4.47\cdot 10^{-3}\ \mathrm{s^{-1}}$$

So h equals

$$h = -\frac{0.00139 + \sqrt{(0.00139)^2 + 4\cdot 5.53\cdot 10^{-10}\cdot 4.47\cdot 10^{-3}}}{2\cdot 4.47\cdot 10^{-3}}\ \ln\left|\frac{1\cdot 2}{1+1.5}\right| =$$

$$-0.311\cdot \ln\left(\frac{2}{6}\right) = 0.341\,\mathrm{m}$$

Determine migration velocity of sorption front (Equation 189)

$$u = \frac{V_p C_o}{C_o + x_o\rho_a} = \frac{V_p C_o}{C_o + \frac{x_m b C_o}{1+bC_o}\rho_a} = \frac{0.00139\cdot 5}{5 + \frac{60\cdot 1\cdot 5}{1+1\cdot 5}\cdot 1{,}900} = 7.3\cdot 10^{-8}\ \ \mathrm{m/s}$$

Determine the working time of the adsorption column until the concentration $C = 2\ \mathrm{g/m^3}$ appears in the outflow (Equation 194):

$$t = \left[H + h\left(\frac{u}{V_p} - 1\right)\right]u^{-1} = \left[3 + 0.311\left(\frac{7.3\cdot 10^{-8}}{1.39\cdot 10^{-3}} - 1\right)\right]\left(7.3\cdot 10^{-8}\right)^{-1} =$$

$$= 36{,}835{,}616\,\mathrm{s} = 426.34\ \mathrm{days}$$

EXAMPLE 2

The process of adsorption on powdered activated carbon, DOC from surface water purified in coagulation, flocculation, sedimentation and filtration is carried out in a complete – mix reactor of volume $V_r = 100\ m^3$. The intensity of the water supply is $Q = 50\ m^3/h$. Determine the necessary dose of activated carbon (D_{PAC} [g/m^3]) to decrease concentration of DOC from the value of $C_o = 5\ g/m^3$ to $C = 2\ g/m^3$. Parameters of Langmuir adsorption isotherm established in the laboratory test are $x_m = 60$ g/kg, $b = 1.0\ m^3/g$.

The mass balance for the analyzed completely mixed flow reactor takes the following form

$$\frac{dC}{dt}V_r = QC_o - QC + \left(-\frac{dx}{dt}\cdot D_{PAC}\right)V_r$$

for the conditions of a steady state, the balance equation is simplified to the form

$$QC_o = QC + \frac{dx}{dt}D_{PAC}\cdot V_r$$

After separating variables

$$Q(C_o - C)dt = D_{PAC}\cdot V_r\cdot dx$$

and differentiating in the ranges from $t = 0$ to $t = T_H$ and from $x = 0$ to $x = f(C)$:

$$Q(C_o - C)\int_0^{T_H} dt = D_{PAC}\cdot V_r \int_0^{x=f(C)} dx$$

the following relation was achieved

$$Q(C_o - C)T_H = D_{PAC}\cdot V_r\cdot x$$

in which

$$x = \frac{x_m bc}{1 + bc}$$

So the dose of activated carbon necessary to decrease the concentration from the value $C_o = 5\ g/m^3$ to $C = 2\ g/m^3$ is

$$D_{PAC} = \frac{Q(C_o - C)T_H}{V_r\cdot x} = \frac{Q(C_o - C)}{\frac{V_r}{T_H}\cdot x} = \frac{C_o - C}{x} = \frac{C_o - C}{\frac{x_m bc}{1+bc}} =$$

$$= \frac{C_o - C}{x_m bc}(1 + bc) = \frac{5-2}{60\cdot 1\cdot 2}(1 + 1\cdot 2) = 0.075\ kg/m^3 = 75\ g/m^3$$

8. CHEMICAL METHODS OF WATER TREATMENT

The group of chemical methods for water purification includes:

- oxidation,
- coagulation,
- chemical precipitation,
- disinfection.

The implementation of chemical processes is integrally connected with physical operations: oxidation and disinfection are connected with the mixing, coagulation is connected with perikinetic flocculation and through orthokinetic flocculation with mixing, and then with sedimentation, chemical precipitation is connected with sedimentation.

8.1. Oxidation

Chemical oxidation performs several important functions in water purification and can be used in many places over the process series.

Oxidation is often used at the beginning of treatment system primarily to eliminate algae and other biological forms which can multiply in the raw water storage tanks or in the pipelines supplying water to the purification station. Oxidation before coagulation can serve as an initial destabilization of colloidal systems; it can lead to the reduction of color and odor.

Up to the present, a commonly used oxidant has been chlorine. Other reagents such as potassium permanganate, chlorine dioxide, ozone and hydrogen peroxide, though useful in specific situations, have previously never been regarded as serious substitutes for chlorine. The situation changed when it was found that chlorine together with natural organic compounds forms products with potential carcinogenic properties [66, 74] such as

- trihalomethanes (chloroform, bromodichloromethane, dibromochloromethane, bromoform)
- haloacetonitriles (bromochloroacetonitrile, dibromoacetonitrile, dichloroacetonitrile, trichloroacetonitrile),
- haloorganic acids (chloroacetone, dichloroacetone, trichloroacetone),
- haloaldehydes (dichloroacetone aldehyde, trichloroacetone aldehyde),
- haloketones (1,1-dichloropropanone, 1,1,1-trichloropropanone 1,1-dichloro-2-butanone, 1,1,1-trichloro-2-butanone),
- chlorophenols (2-chlorophenol, 2,4-dichlorophenol, 2,4,6-trichlorophenol).

These compounds are now standardized forcing a thorough analysis of the concentration of their precursors or the use of chlorine substitutes.

Oxidation is integrally linked to reduction. Every redox system can be described by a summary reaction or by half-reactions of oxidation and reduction.

The measure of oxidizing or reducing substances present in the water or added to water is the oxidation-reduction potential. The potential is measured using the platinum electrode which mediates the reception of charges exchanged in oxidation and reduction processes.

For the clarity of analysis, the electrode potential is given for half-reactions. Potential values of oxidants used in water technology are summarized in Table 11 and for the reduced substances present in water in Table 12 [30, 83].

Table 11. The values of electrode potential for oxidants used [30, 83].

No.	**Oxidant**	**Reduction reaction**	**Potential E^o [V]**
1.	Gaseous chlorine	$Cl_2 + 2e^- \rightarrow 2Cl^-$	1.36
2.	Hypochlorous acid	$HOCl + H^+ + 2e^- \rightarrow Cl^- + H_2O$	1.49
3.	Hypochlorite	$ClO^- + H_2O + 2e^- \rightarrow Cl^- + 2OH^-$	0.90
4. 5.	Chloramines Monochloramine	$NH_2Cl + H_2O + 2e^- \rightarrow Cl^- + NH_3 + OH^-$ $NH_3Cl^+ + H^+ + 2e^- \rightarrow Cl^- + NH_4^+$	0.75 1.40
6. 7.	Dichloramine	$NHCl_2 + 2H_2O + 4e^- \rightarrow 2Cl^- + NH_3 + 2OH^-$ $NHCl_2 + 3H^+ + 4e^- \rightarrow 2Cl^- + NH_4^+$	0.79 1.34
8. 9.	Ozone	$O_3 + 2H^+ + 2e^- \rightarrow O_2 + H_2O$ $O_3 + H_2O \rightarrow O_2 + 2OH^-$	2.07 1.24
10. 11.	Hydrogen peroxide	$H_2O_2 + 2H^+ + 2e^- \rightarrow 2H_2O$ $HO_2^- + H_2O + 2e^- \rightarrow 3HO^-$	1.78 0.85
12.	Chlorine dioxide	$ClO_2 + 2H_2O + 5e^- \rightarrow Cl^- + 4OH^-$	1.71
13. 14. 15.	Permanganate	$MnO_4^- + 4H^+ + 3e^- \rightarrow MnO_2 + 2H_2O$ $MnO_4^- + 8H^+ + 5e^- \rightarrow Mn^{2+} + 4H_2O$ $MnO_4^- + 2H_2O + 3e^- \rightarrow MnO_2 + 4HO^-$	1.68 1.49 0.58
16. 17.	Oxygen	$O_2 + 4H^+ + 4e^- \rightarrow 2H_2O$ $O_2 + 2H_2O + 4e^- \rightarrow 4HO^-$	1.23 0.40

Table 12. The values of electrode potential for reduced compounds present in water [30, 83].

No.	**Oxidation reaction**	**Potential E^0 [V]**
1.	$Br^- + H_2O \rightarrow HBrO + H^+ + 2e^-$	-1.33
2.	$Mn^{2+} + 2H_2O \rightarrow MnO_2 + 4H^+ + 2e^-$	-1.21
3.	$ClO_2^- \rightarrow ClO_2 + e^-$	-1.15
4.	$Fe^{2+} + 3H_2O \rightarrow Fe(OH)_3 + 3H^+ + e^-$	-1.01
5.	$Fe^{2+} \rightarrow Fe^{3+} + e^-$	-0.77
6.	$Cl^- + 4OH^- \rightarrow ClO_2^- + 2H_2O + 4e^-$	-0.76
7.	$ClO2^- + 2OH^- \rightarrow ClO_3^- + H_2O + 2e^-$	-0.35
8.	$H_2S \rightarrow S + 2H^+ + 2e^-$	-0.14
9.	$NO_2^- + 2OH^- \rightarrow NO_3^- + H_2O + e^-$	-0.01
10.	$C_6H_{12}O_6 + 6H_2O \rightarrow 6CO_2 + 24H^+ + 24e^-$	-0.20

Potential values contrasted in Tables 11 and 12, so called normal potentials, are determined for the systems in which there are single-mole concentrations of oxidizing and reducing agents, [ox] = [red] = 1. This is so the thermodynamic activity of the substance equals unity.

The potential of the oxidation-reduction reaction is determined in relation to the sum of the value E° for the reaction of reduction (Table 11) and oxidation (Table 12).

The potential depends on the free energy change ΔG° and the equilibrium constant K according to equation

$$\Delta G^\circ = -nFE^\circ = -RT\ln K \tag{286}$$

in which

n – number of electrons transferred in reduction-oxidation reaction,

$F = 96.3$ kJ/(V)(e^-) – Faraday constant,

$R = 8,29 \cdot 10^{-3}$ kJ/K – gas constant,

T – absolute temperature [K].

In case of e.g. oxidizing nitrites with hypochlorite, two half-reactions can be written (No. 3 in Table 13, and No. 9 in Table 14). The potentials of these reactions are 0.9 and -0.01, respectively:

$$ClO^- + H_2O + 2e^- \rightarrow Cl^- + 2OH^-; \quad E_1^o = 0.9V \tag{287}$$

$$NO_2^- + 2OH^- \rightarrow NO_3^- + H_2O + 2e^-; \quad E_2^o = -0.01V \tag{288}$$

The summary reaction, therefore, is

$$ClO^- + NO_2{}^- \rightarrow Cl^- + NO_3^- \tag{289}$$

and the standard potential for this reaction is

$$E° = E_1^\circ + E_2^\circ = 0.9 - 0.01 = 0.89V \tag{290}$$

According to Equation (286) the free energy change is

$$\Delta G^\circ = -2 \cdot 96.3 \cdot 0.89 = -171.4 \text{ kJ} \tag{291}$$

And the equilibrium constant (K) determined also from Equation (286) at temperature 288K is

$$K = \exp\left(-\frac{\Delta G^\circ}{RT}\right) = \exp\left(\frac{171.4 \cdot 10^3}{8.29 \cdot 288}\right) = 1.5 \cdot 10^{31} \tag{292}$$

Oxidation of manganese from the second level of oxidation (Mn^{2+}) to the fourth level of oxidation (MnO_2) using hypochlorous acid is described by half-reactions (No. 2 in Table 11, and No. 2 in Table 12) and a summary reaction

$$HOCl + H^+ + 2e^- \rightarrow Cl^- + H_2O; \quad E_1^o = 1.49V \tag{293}$$

$$Mn^{2+} + 2H_2O \rightarrow MnO_2 + 4H^+ + 2e^-; \quad E_2^o = -1.21V \tag{294}$$

$$HOCl + Mn^{2+} + H_2O \rightarrow Cl^- + MnO_2 + 3H^+ \tag{295}$$

The standard potential for this reaction is

$$E° = E_1^\circ + E_2^\circ = 1.49 - 1.21 = 0.28V \tag{296}$$

Free energy change

$$\Delta G^\circ = -2 \cdot 96.3 \cdot 0.28 = -53.93 \text{ kJ} \tag{297}$$

Equilibrium constant at temperature 288K

$$K = \exp\left(\frac{53.93 \cdot 10^3}{8.29 \cdot 288}\right) = 6.46 \cdot 10^9 \tag{298}$$

The same process when using chlorine dioxide as an oxidant (No. 12 in Table 13) is described by the following half-reactions and a summary reaction

$$2\,[ClO_2 + H_2O + 5e^- \rightarrow Cl^- + 4OH^-]; \quad E_1^o = -1.71V \tag{299}$$

$$5\,[Mn^{2+} + 2H_2O \rightarrow MnO_2 + 4H^+ + 2e^-]; \quad E_2^o = -1.21V \tag{300}$$

$$2ClO_2 + 5Mn^{2+} + 6H_2O \rightarrow 2Cl^- + 5MnO_2 + 12H^+ \tag{301}$$

The standard reaction potential (301) is

$$E° = E_1^\circ + E_2^\circ = 1.71 - 1.21 = 0.50V \tag{302}$$

It is important to notice in this case the fact that the values of standard potential for half-reactions (299) and (300) are not multiplied by 2 and 5 respectively because potentials are independent of the quantity of material in the system.
The free energy change is

$$\Delta G^\circ = -10 \cdot 96.3 \cdot 0.5 = -481.5 \text{ kJ} \qquad (303)$$

and the equilibrium constant at the temperature 288K

$$K = \exp\left(\frac{481.5 \cdot 10^3}{8.29 \cdot 288}\right) = 3.87 \cdot 10^{87} \qquad (304)$$

A comparison of constants shows that the equilibrium of reaction (301) is shifted much more to the right than the equilibrium of reaction (295) which means that the use of chlorine dioxide for oxidation of $Mn^{2+} \rightarrow Mn^{4+}$ is more effective than the use of hypochlorous acid.
For non-standard conditions (temperature $\neq$ 288K; pressure $\neq 0.98 \cdot 10^{-1}$MPa) the real potential of a reaction of the type aA + bB → cC + dD is determined from the Nernst equation

$$E = E^\circ - \frac{2.3\,RT}{nF} \log \frac{[C]^c\,[D]^d}{[A]^a\,[B]^b} \qquad (305)$$

The presented method of choosing an oxidant for a specific reduced system can be regarded as preliminary. In practice, there are often deviations from theoretical dependencies. The redox process can be characterized with a high value of equilibrium constant, but with such small velocity that using it in real systems may be unfounded. Therefore, the second factor deciding oxidant application is the kinetics of oxidation.

The organic compounds present in the purified water often have a low redox potential, but the usefulness of their oxidation can be determined by kinetic parameters and is also based on the low cost of the oxidant, e.g. oxygen inserted with the air.

Kinetics of chemical oxidation is exemplified by oxidizing iron with oxygen.

The oxidation velocity of iron from the plus two oxidation state to the plus three oxidation state with oxygen is dependent on pH. With the increase of pH, the time to achieve a particular process efficiency decreases.
The stoichiometry of oxidation Fe^{2+} to Fe^{3+} can be presented by the following equation:

$$4Fe^{2+} + O_2 + 10H_2O \rightarrow 4Fe(OH)_3 + 8H^+ \qquad (306)$$

The above reaction shows that the oxidation of one gram of Fe^{2+} requires the use of 0.14 g of dissolved oxygen. The kinetics of this process at pH ≥ 5.5 is described by the following equation [86]:

$$\frac{d[Fe^{2+}]}{dt} = -k\left[P_{O_2}\right]\left[OH^-\right]^{-2}\left[Fe^{2+}\right] \qquad (307)$$

in which

k – velocity constant,

$\left[P_{O_2}\right]$ – partial pressure of oxygen in the air in equilibrium with the oxygen dissolved in water.

At temperature 293K velocity constant is $k = 4.9 \cdot 10^{10} \dfrac{m^6}{MPa\ mol^2\ h}$, and partial pressure of oxygen is $\left[P_{O_2}\right] = 2.06 \cdot 10^{-2}$ MPa.

Equation (307) shows that the reaction of oxidation is (306) of the fourth state, but of the first state in relation to concentration of ferrous ion. Therefore, this reaction can be written as a pseudo-first state reaction [55]:

$$\frac{d[Fe^{2+}]}{dt} = -k^* \left[Fe^{2+}\right] \tag{308}$$

in which

$$k^* = k \left[P_{O_2}\right]\left[OH^-\right]^2 \tag{309}$$

Using Equation (308) to design a reactor, one must assume the constancy of reaction and concentration of oxygen dissolved in the whole contents of the reactor. From Equation (307) results the lack of catalytic or inhibiting action of substances present in water. In some cases this assumption is justified. However, it is known that the presence of Cu^{2+} ions accelerates reactions and some dissolved organic substances may slow them down or even inhibit them.

Assuming oxidation in a complete – mix reactor, process efficiency is described by the relation [57]

$$E = \frac{[Fe^{2+}] - [Fe^{3+}]}{[Fe^{2+}]} = \frac{1}{1 + k^* T_H} \tag{310}$$

in which

T_H – retention time [h].

Substituting equation (309) to the above relation produces the form defining oxidation efficiency as a function of retention time and the hydroxide ion concentration. It is therefore important to define the concentration of these ions as a function of the size of the dose correcting the pH. For a pH below 8.3, the relation between $[OH^-]$, the size of lime dose (D_{CaO}), initial alkalinity [alk] and initial concentration $[CO_2]$ is defined by the equation:

$$\left[OH^-\right] = 2 \cdot 10^{-8} \left\{ \frac{[alk] + 2D_{CaO}}{[CO_2] - 2D_{CaO}} \right\} \tag{311}$$

in which

[alk] – [val/m^3],

$[CO_2]$ – [mol/m^3],

$[OH^-]$ – [mol/m^3].

The above equation is based on the conceptual definition of alkalinity [87]:

$$\text{alk} = [\text{HCO}_3^-] + 2[\text{CO}_3^{2-}] + [\text{OH}^-] - [\text{H}^+] \tag{312}$$

The above analysis assumes a lack of formation of calcium and iron carbonates.
After taking into account numerical values of constants and Equation (311), the efficiency of oxidation in the function of retention time (T_H) and the size of calcium dose (D_{CaO}) is defined by the formula

$$E = \frac{[\text{Fe}^{2+}] - [\text{Fe}^{3+}]}{[\text{Fe}^{2+}]} = \left[1 + 4.04 \cdot 10^{-7}\ T_H \left\{ \frac{[\text{alk}] + 2D_{\text{CaO}}}{[\text{CO}_2] - 2D_{\text{CaO}}} \right\}^2 \right]^{-1} \tag{313}$$

In the case when the increase of water pH is achieved through CO_2 stripping, to determine oxidation efficiency coefficient k^* in Equation (310) must be substituted with an expression defining the influence of aeration on CO_2 content.
Assuming that CO_2 stripping takes place in stripping towers of height H, the relation between initial concentration, concentration after the process and concentration of saturation is described by the relation

$$\frac{[\text{CO}_2]_s - [\text{CO}_2]_k}{[\text{CO}_2]_s - [\text{CO}_2]_p} = \exp\left(k_L \cdot a \cdot \sqrt{\frac{2H}{g}} \right) \tag{314}$$

in which

$[CO_2]_s$ – concentration of water saturation with carbon dioxide in equilibrium with concentration in the air at a specified temperature [g/m^3],

$[CO_2]_p$; $[CO_2]_k$ – concentration of carbon dioxide in raw water and after stripping, respectively [g/m^3],

k_La – general mass transfer coefficient in the aeration process [s^{-1}],

g – gravitational acceleration [m/s^2],

H – height of the tower [m].

Concentration of saturation in equilibrium with the concentration in the air as a function of water temperature is presented in Table 13.

Table 13. Solubility of carbon dioxide in water as a function of temperature.

Water temperature [K]	273	278	283	288	293	298	303	308	313	318	323	333
CO_2 solubility in water [g/m^3]	3.35	2.77	2.32	1.97	1.69	1.45	1.25	1.11	0.97	0.86	0.76	0.58

Transforming Equation (314) from the value $[CO_2]_k$ and taking into consideration the numerical value of gravitational constant leads to the following form:

$$[CO_2]_k = [CO_2]_s - \left([CO_2]_s - [CO_2]_p\right)\exp\left(-0{,}45\ k_L a H^{0.5}\right) \qquad (315)$$

At a pH below 8.3 the concentration of hydroxide ions in the water after aeration is determined from the relationship:

$$[OH^-] = 2 \cdot 10^{-8}\ \frac{[alk]}{[CO_2]_k} \qquad (316)$$

The above formula is analogous to (311) with $D_{CaO} = 0$.

Substituting Equation (315) in (316) one obtains the expression which makes the concentration of hydroxide ions dependent on parameter H (decision variable), mass transfer coefficient ($k_L a$), initial concentration of CO_2 and alkalinity:

$$[OH^-] = \frac{2 \cdot 10^{-8}\ [alk]}{[CO_2]_s - \left([CO_2]_s - [CO_2]_p\right)\exp\left(-0.45 k_L a\ H^{0.5}\right)} \qquad (317)$$

On the other hand, substituting the above equation to the formula defining the reduction constant of the pseudo first state (309) taking into account numerical values of parameters k and $[P_{O_2}]$, and then substituting it to Equation (310) leads to a relation defining the oxidation efficiency of ferrous ions when using trickling beds

$$E = \frac{[Fe^{2+}] - [Fe^{3+}]}{[Fe^{2+}]} =$$

$$= \left[1 + 4.04 \cdot 10^{-7}\ T_H \left\{\frac{[alk]}{[CO_2]_s - \left([CO_2]_s - [CO_2]_p\right)\exp\left(-0{,}45 k_L a\ H^{0.5}\right)}\right\}^2\right]^{-1} \qquad (318)$$

With a parallel application of lime dosing and aeration, the hydroxide ion concentration is determined by the relation

$$[\mathrm{OH}^-] = \frac{2\cdot 10^{-8}\left([\mathrm{alk}] + 2\mathrm{D}_{\mathrm{CaO}}\right)}{[\mathrm{CO}_2]_{\mathrm{s}} - 2\mathrm{D}_{\mathrm{CaO}} - \left([\mathrm{CO}_2]_{\mathrm{s}} - 2\mathrm{D}_{\mathrm{CaO}} - [\mathrm{CO}_2]_{\mathrm{p}}\right)\exp\left(-0.45\mathrm{k}_{\mathrm{L}}\mathrm{a}\,\mathrm{H}^{0.5}\right)} \tag{319}$$

Taking into account the numerical data of constants $[\mathrm{P}_{\mathrm{O}_2}]$ and k, the formula defining oxidation efficiency takes the following form:

$$\mathrm{E} = \frac{[\mathrm{Fe}^{2+}] - [\mathrm{Fe}^{3+}]}{[\mathrm{Fe}^{2+}]} =$$

$$= \left[1 + 4.04\cdot 10^{-7}\,\mathrm{T}_{\mathrm{H}}\left\{\frac{[\mathrm{alk}] + 2\mathrm{D}_{\mathrm{CaO}}}{[\mathrm{CO}_2]_{\mathrm{s}} - 2\mathrm{D}_{\mathrm{CaO}} - \left([\mathrm{CO}_2]_{\mathrm{s}} - 2\mathrm{D}_{\mathrm{CaO}} - [\mathrm{CO}_2]_{\mathrm{p}}\right)\exp\left(-0.45\mathrm{k}_{\mathrm{L}}\mathrm{a}\,\mathrm{H}^{0.5}\right)}\right\}^2\right]^{-1} \tag{320}$$

In real oxidation systems occurring in water technology, in addition to catalyzing and inhibiting factors, there is also the effect of different speeds of oxidation of compounds and their dissociated forms. An example could be the oxidation of phenol and phenolate ions [30]. Dissociation of phenol proceeds according to the reaction

$$\mathrm{C_6H_5OH} \leftrightarrow \mathrm{C_6H_5O^-} + \mathrm{H^+} \tag{321}$$

The process of phenol ozonization can be described by the general equation

$$\mathrm{C_6H_5OH} + 14\mathrm{O_3} \rightarrow 6\mathrm{CO_2} + 3\mathrm{H_2O} + 14\mathrm{O_2} \tag{322}$$

and the ozone consumption rate in the case of the ozonization of phenol and the products of its dissociation can be described by the equation

$$\frac{d[\mathrm{O_3}]}{dt} = \mathrm{k_1}[\mathrm{C_6H_5OH}][\mathrm{O_3}] + \mathrm{k_2}[\mathrm{C_6H_5O^-}][\mathrm{O_3}] \tag{323}$$

Velocity constants for phenol and phenolate ions are respectively, $\mathrm{k_1} = 4.68\cdot 10^3$ [m^3/mol·h] and $\mathrm{k_2} = 5.04\cdot 10^9$ [m^3/mol·h].

The phenol dissociation constant described by the equation below is

$$\mathrm{K_1} = \frac{[\mathrm{C_6H_5O^-}][\mathrm{H^+}]}{[\mathrm{C_6H_5OH}]} = 1.26\cdot 10^{-10} \tag{324}$$

The rearranged form of Equation (324) to determine the phenolate ion concentration at a defined initial phenol concentration and a specified pH is

$$\frac{[\mathrm{C_6H_5O^-}][1\cdot 10^{-\mathrm{pH}}]}{[\mathrm{C_6H_5OH}]_{\mathrm{p}} - [\mathrm{C_6H_5O^-}]} = 1.26\cdot 10^{-10} \tag{325}$$

and

$$[C_6H_5O^-] = \frac{1.26 \cdot 10^{-10}\,[C_6H_5OH]_p}{10^{-pH} + 1.26 \cdot 10^{-10}} \tag{326}$$

where $[C_6H_5OH]_p$ – initial phenol concentration

Taking into account numerical values of constants k_1 and k_2 and relation (326) modified form of the equation of ozone consumption rate is as follows:

$$\frac{d[O_3]}{dt} = 4.68 \cdot 10^3 \left\{ [C_6H_5OH]_p - \frac{1.26 \cdot 10^{-10}\,[C_6H_5OH]_p}{10^{-pH} + 1.26 \cdot 10^{-10}} \right\} [O_3] +$$

$$+ 5.04 \cdot 10^9\, \frac{1.26 \cdot 10^{-10}\,[C_6H_5OH]_p}{10^{-pH} + 1.26 \cdot 10^{-10}}\,[O_3] \tag{327}$$

and

$$\frac{d[O_3]}{dt} = [O_3]\,[C_6H_5OH]_p \left\{ 4.68 \cdot 10^3 - \frac{6.35 \cdot 10^{-1}}{10^{-pH} + 1.26 \cdot 10^{-10}} \right\} \tag{328}$$

$$\frac{d[O_3]}{dt} = k^*\,[O_3]\,[C_6H_5OH]_p \tag{329}$$

The above transformations allow the notation of the reaction of pseudo first order because of $[O_3]$. Numerical values of constant k^* depending on water pH are as follows:

pH = 10;	$k^* = -2.81 \cdot 10^9$	$[m^3/mol \cdot h]$,
pH = 9;	$k^* = -5.64 \cdot 10^8$	$[m^3/mol \cdot h]$,
pH = 8;	$k^* = -6.27 \cdot 10^7$	$[m^3/mol \cdot h]$,
pH = 7;	$k^* = -6.34 \cdot 10^6$	$[m^3/mol \cdot h]$,
pH = 6;	$k^* = -6.30 \cdot 10^5$	$[m^3/mol \cdot h]$,
pH = 5;	$k^* = -5.88 \cdot 10^4$	$[m^3/mol \cdot h]$.

As mentioned, the chemical oxidation rate is often increased by the participation of catalysts, substances which are not used during reaction. Sometimes the catalyst is the product of the reaction and such reactions are called autocatalytic. An example of an autocatalytic reaction is manganese oxidation with oxygen $Mn^{2+} \rightarrow Mn^{4+}$ [87].

This process rate is described by the equation

$$\frac{d[Mn^{2+}]}{dt} = -k_1[Mn^{2+}] - k_2[Mn^{2+}][MnO_2] \qquad (330)$$

in which

$$k_2 = k_2^*[OH^-]^2[P_{O_2}] \qquad (331)$$

The second expression on the right side of Equation (330) indicates that the Mn^{2+} oxidation rate increases with the increase of the concentration of the reaction product, which is manganese dioxide. This means that MnO_2 is a catalyst for the oxidation process. One explanation for this phenomenon is that Mn^{2+} is adsorbed on the solid manganese oxide forming a surface complex in which Mn^{2+} is more easily oxidized than the free ion Mn^{2+}.

Since for a wide pH range the solubility of MnO_2 is minimal and the formation constant of hydroxy complexes of Mn^{2+} is relatively small ($k_{comp} = 2.5 \cdot 10^{3}$ mol^{-1}) [69, 70], it can be assumed that Mn^{2+} and precipitated MnO_2 are the only relevant forms of manganese in water. Under this assumption, the integrated equation (330) is

$$t = \left[\frac{1}{k_1 + k_2 Mn_T}\right] \ln\left[\frac{\left(k_1 + k_2 Mn_T - k_2[Mn^{2+}]\right)[Mn^{2+}]_o}{\left(k_1 + k_2[MnO_2]_o\right)[Mn^{2+}]}\right] \qquad (332)$$

where

t – time of achieving assumed conditions in the system [h],
Mn_T – general manganese concentration after time t [mol/m^3],
$[MnO_2]_o$; $[Mn^{2+}]_o$ – initial concentrations [mol/m^3].

Estimation of coefficients k_1 and k_2 with a partial pressure of oxygen in the air at equilibrium with oxygen dissolved in water $[P_{O_2}] = 0.98 \cdot 10^{-1}$ MPa and at pH = 9.5 are 0.252 [h^{-1}] and $1.58 \cdot 10^4$ [(mol·h)$^{-1}$], respectively [69, 70].

8.1.1. Example Calculations

EXAMPLE 1

Determine the hydraulic retention time in a completely mixed flow reactor required to oxidize iron at a plus second level of oxidation having the concentration $[Fe^{2+}] = 8{,}95 \cdot 10^{-2}$mol/m^3 with oxygen from the air in the process of diffusion across the interface with an efficiency that guarantees the outflow concentration $[Fe^{2+}] \leq 3{,}58 \cdot 10^{-3}$ mol/m^3 given by water quality standards. At the water temperature T = 293K, partial oxygen pressure $[P_{O_2}] = 2.06 \cdot 10^{-2}$ MPa, and rate constant $k = 4.9 \cdot 10^{10}$ m^3/MPa·mol^2·h.
At water pH = 7.5, the concentration of hydroxide ions is $[OH^-] = 10^{-6.5} \cdot 10^3$ mol/m^3.
The problem was solved using a rearranged form of Equation (310):

$$\frac{[Fe^{2+}] - [Fe^{3+}]}{[Fe^{2+}]} = \frac{1}{1 + k[P_{O_2}][OH^-]^2\, T_H}$$

$$\left\{1 + k\left[P_{O_2}\right]\left[OH^-\right]^2 T_H\right\}\left\{\left[Fe^{2+}\right] - \left[Fe^{3+}\right]\right\} = \left[Fe^{2+}\right]$$

$$T_H = \left\{\frac{[Fe^{2+}]}{[Fe^{2+}] - [Fe^{3+}]} - 1\right\}\left\{k\left[P_{O_2}\right]\left[OH^-\right]^2\right\}^{-1}$$

$$T_H = \left\{\frac{0.0895}{0.0895 - \left(0.0895 - 0.00358\right)} - 1\right\}\left\{\left(4.9 \cdot 10^{10}\right) \cdot \left(2.06 \cdot 10^{-2}\right) \cdot \left(10^{-3.5}\right)^2\right\}^{-1} =$$

$$= 24 \cdot 0.0099 = 0.24 \text{ h} \approx 14 \text{ min } 24 \text{ s}$$

EXAMPLE 2

Out of three oxidants to be applied in oxidation: chlorine, permanganate and oxygen, choose the one that is characterized with the highest efficiency of oxidation of iron Fe^{2+} in water at the temperature T = 288K.
Half-reactions and summary reactions of oxidation with suggested oxidants are as follows:

Chlorine

$Cl_2 + 2e^- \rightarrow 2Cl^-$ potential $E_1^o = 1.36\ \text{V}$

$2Fe^{2+} + 6H_2O \rightarrow 2Fe(OH)_3 + 6H^+ + 2e^-$ potential $E_2^o = -1.01\ \text{V}$

$2Fe^{2+}\ Cl_2 + 6H_2O \rightarrow 2Fe(OH)_3 + 2Cl^- + 6H^+$

Permanganate

$MnO_4^- + 4H^+ + 3e^- \rightarrow MnO_2 + 2H_2O$ potential $E_1^o = 1.68\ \text{V}$

$3Fe^{2+} + 9H_2O \rightarrow 3Fe(OH)_3 + 9H^+ + 3e^-$ potential $E_2^o = -1.01\ \text{V}$

$3Fe^{2+}\ MnO_4^- + 7H_2O \rightarrow 3Fe(OH)_3 + MnO_2 + 5H^+$

Oxygen

$O_2 + 4H^+ + 4e^- \rightarrow 2H_2O$ potential $E_1^o = 1.23\ \text{V}$

$4Fe^{2+} + 12H_2O \rightarrow 4Fe(OH)_3 + 12H^+ + 4e^-$ potential $E_2^o = -1.01\ \text{V}$

$4Fe^{2+} + O_2 + 10H_2O \rightarrow 4Fe(OH)_3 + 8H^+$

Standard potentials for reactions of oxidation with:
chlorine

$$E^o = 1.36 - 1.01 = 0.35\ \text{V}$$

Permanganate

$$E^o = 1.68 - 1.01 = 0.67\ \text{V}$$

Oxygen

$$E^o = 1.23 - 1.01 = 0.22\ \text{V}$$

Free energy change ΔG^o of oxidation reaction (Equation 286) with:
chlorine

$$\Delta G^o = -\ 2 \cdot 96.3 \cdot 0.35 = -\ 67.41\ \text{kJ}$$

Permanganate

$$\Delta G^o = -\ 3 \cdot 96.3 \cdot 0.67 = -\ 193.56\ \text{kJ}$$

Oxygen

$$\Delta G^o = -\ 4 \cdot 96.3 \cdot 0.22 = -\ 84.75\ \text{kJ}$$

Equilibrium constants (K) of the reaction of oxidation (Equation 292) with:

Chlorine

$$K = \exp\left(\frac{67.41 \cdot 10^3}{8.29 \cdot 288}\right) = 1.83 \cdot 10^{12}$$

Permanganate

$$K = \exp\left(\frac{193.56 \cdot 10^3}{8.29 \cdot 288}\right) = 1.618 \cdot 10^{35}$$

Oxygen

$$K = \exp\left(\frac{84.75 \cdot 10^3}{8.29 \cdot 288}\right) = 2.607 \cdot 10^{15}$$

A comparison of reaction constants shows that the reaction most shifted to the right is the reaction of oxidation with permanganate, followed by oxidation with oxygen and chlorine. This means that the most effective is the oxidation of iron Fe^{2+} with permanganate.

8.2. Coagulation

Coagulation is defined as the process of destabilizing the colloidal system in order to reduce the level of its dispersion in the process of flocculation. Agglomerated particles are then removed by sedimentation and filtration. Although flocculation is a natural consequence of coagulation, due to the fact that these processes are governed by different mechanisms, flocculation is now treated as a separate process that takes place directly after coagulation (Chapter 7.3.) [62, 90].

Coagulation is usually the first process in the technological system of water purification. Along with oxidation and sedimentation, it is the most important process in surface water treatment and is increasingly being used to purify infiltration water and groundwater.

Surface waters contain substances of natural origin (soil erosion, dissolving minerals, the presence of live and dead aquatic organisms such as bacteria and algae) and of anthropogenic origin (dissolved organic and inorganic compounds, living organisms, and suspended matter). Most of these substances are of a colloid character and they are effectively removed by coagulation.

The stability of a colloidal system in water is an important factor in determining the method of its removal. Colloidal particles have a size from about 10^{-6} to 10^{-9} m and a surface area in the range from 100 to 5,000 m^2/g. The most important division of colloids present in water is into hydrophilic and hydrophobic colloids. The differences between these types of colloidal particles are very important in the context of their removal. An arrangement of hydrophobic particles is stable only at considerable concentrations [47]. Hydrophilic particles are easily hydrated. With very large specific surfaces the number of water particles associated with colloids is estimated at $10^{15} \div 10^{18}$ per cm^3 of volume.

A stabilizing factor for a colloidal system is electric charge. For colloidal systems in natural waters, most of the particles have a negative charge containing hydroxyl groups. The stability of such systems is mainly the result of electrical characteristics of the solution particles.

In hydrophilic colloid systems, the ions are attracted to hydrated particles. Electromotive force is formed between the particles and water. Adsorbed ions are distributed in the layer rigidly connected with the particle, called the Stern layer. The consequence of attraction of compensating ions is the production of concentration gradient between the surface of particles or rather the adsorption layer and the solution phase. Hence, the two competing forces: diffusion and electrostatic attraction separate the charges of ions contained in water creating a diffusion layer surrounding the colloidal particles, the so called Gouy-Chapman layer [62, 68]. The compensatory ion concentration decreases gradually as the distance from the interface increases. The thickness of compensating ion layer depends on the ionic radii of cations present in solution. Hence, the ratio of charge density to the surface area is larger in case of multivalent ions than monovalent. The structure of the colloidal phase particle, its electrical properties and the distribution of concentrations of positive and negative ions are shown in Figure 27.

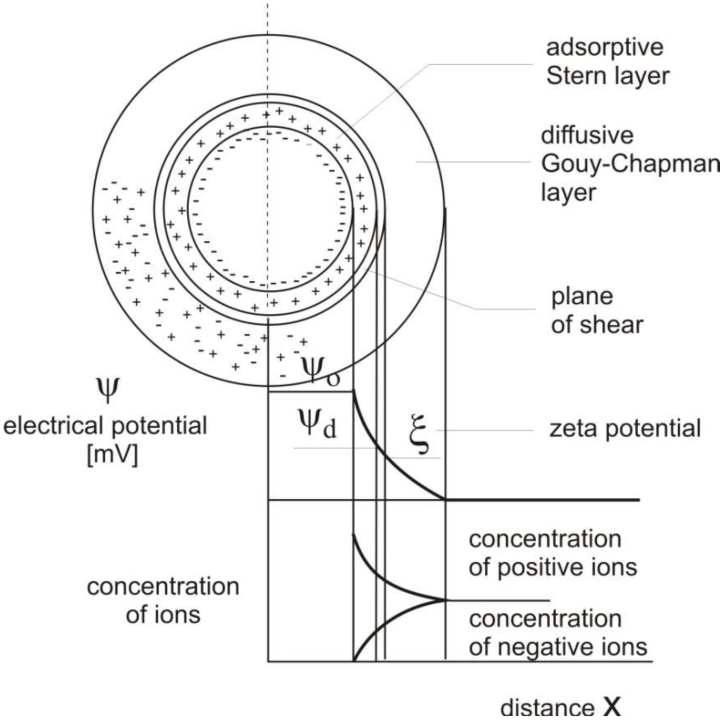

Fig. 27. Structure of colloidal particle, distribution of electric potential and ion concentrations.

In the Stern layer, the electrical potential changes from the value ψ_o to ψ_d. The thickness of this layer is approximately equal to the dimensions of the adsorbed ions. In the plane separating the layer of Stern and Gouy-Chapman a potential difference occurs. The potential drop in the diffusive part of the double layer as a function of a distance from the plane of the interface is described by the formula:

$$\psi = \psi_d \cdot \exp(-K_{D-H} \cdot x) \tag{333}$$

in which
ψ – potential energy at a distance x from the layer interface surface [mV],
ψ_d – potential of the Stern layer [mV],
$K_{D\text{-}H}$ – constant equal to the converse thickness of the double electrical layer, called the Debye-Hückel parameter.

For symmetrical electrolyte particles, the $K_{D\text{-}H}$ parameter is defined by the formula:

$$K_{D\text{-}H} = \sqrt{\frac{8\pi e^2 \Sigma n z^2}{\varepsilon K_B T}} \tag{334}$$

where:
e – electron charge [$5.4 \cdot 10^{-4}$C],
n – number of ions per unit volume [m^{-3}],
z – compensating ion valence,
ε – dielectric constant [C/V·m],
$K_B = 1.38 \cdot 10^{-23}$ J/K – Boltzman constant,
T – absolute temperature [K].

The value of the potential on the border of layers is defined as the electrokinetic zeta potential (ξ). The reduction of the electrokinetic potential to zero ($\xi = 0$) substantially alters the properties of colloidal systems and is a condition for the rapid coagulation of impurities in natural water. The beginning of the coagulation process may occur in some cases already when reducing the potential to the value of $\xi = \pm 30$ mV.

Colloid coagulation may be caused by
- electrolyte addition,
- addition of a colloid with reverse charge,
- radiochemical exposure,
- heating,
- mechanical action,
- dehydration.

In water treatment technologies the first two methods are applied. The most commonly used coagulants in water technology are salts of aluminum and iron which form positively charged hydroxides during hydrolysis and neutralize most of

the negatively charged colloidal impurities contained in water. Coagulants used most often include
– aluminum sulfate $Al_2(SO_4)_3 \cdot 18H_2O$,
– ferric sulfate $Fe_2(SO_4)_3 \cdot 9H_2O$,
– ferrous sulfate $FeSO_4 \cdot 7H_2O$,
– ferric chloride $FeCl_3 \cdot 6H_2O$,
– sodium aluminate $Na_3Al_2O_3$.

Although general relations between the size of the coagulant dose and the colloid concentration are not evaluated, carrying out the process corresponds in practice with to the following equation [62]

$$D_C = K_1\,[\mathrm{alk}] + K_2 C^n \quad [\mathrm{g/m^3}] \tag{335}$$

in which
[alk] – initial water alkalinity [val/m^3],
C – colloidal particle charge,
K_1, K_2, n – constants.

Other formulas for the proper coagulant dose mentioned in professional literature [52, 53] are

- for coagulants $Fe_2(SO_4)_3 \cdot 9H_2O$ i $FeCl_3 \cdot 6H_2O$:

$$D_C = \frac{1}{A(n-1)\,C_e^{n-1}}\left[1-\left(\frac{C_e}{C_0}\right)^{n-1}\right] \tag{336}$$

In the above formula C_0 and C_e are the initial indicator of water pollution and the indicator of a pollution after the process (e.g. color, permanganate value), respectively [g/m^3]. The values of constants A and n fall into the ranges of 0.1 ÷ 0.125 and 1.5 ÷ 2.0, respectively.

- for coagulant $Al_2(SO_4)_3 \cdot 18H_2O$:

$$D_C = \frac{1}{A}\,\ln\frac{C_0}{C_e} \tag{337}$$

The value of constant A falls in the range 0.35 ÷ 0.6. In the case of removing impurities that cause color and oxidation, lower values of the parameters A and n shall be taken. The upper ranges of the parameters of the above equations are adopted when the coagulation concerns the impurities that cause turbidity.

Usually, modeling the process of coagulation is based on stoichiometric relations between coagulants dosed into the water, natural water ingredients and pollution.

As a result of the hydrolysis of aluminum sulfate, aluminum hydroxide sparingly soluble in water is formed. Aluminum hydroxide occurs initially in the form of positively charged colloidal particles and then, together with negatively charged colloidal particles causing the turbidity and color of water, it creates neutral units. The neutral units increase their size during flocculation and then sediment under the force of gravity. Since aluminum is trivalent, hydrolysis of its salt takes place in several stages:

$$Al_2(SO_4)_3 \rightarrow 2Al^{3+} + 3SO_4^{2-} \quad \text{(dissociation)} \qquad (338)$$

$$2Al^{3+} + 2H_2O \leftrightarrow 2Al(OH)^{2+} + 2H^+ \qquad (339)$$

$$2Al(OH)^{2+} + 2H_2O \leftrightarrow 2Al(OH)_2^+ + 2H^+ \qquad (340)$$

$$2Al(OH)_2^+ + 2H_2O \leftrightarrow 2Al(OH)_3 + 2H^+ \qquad (341)$$

$$Al_2(SO_4)_3 + 6H_2O \leftrightarrow 2Al(OH)_3 + 6H^+ + 3SO_4^{2-} \qquad (342)$$

Hydrolysis is a reversible process and its degree is influenced by the concentration of hydrogen ions. Reducing the solution pH inhibits the hydrolysis of salts of weak alkaline solutions such as aluminum salt. During the hydrolysis of aluminum sulfate, the hydrogen ion concentration increases; thus hydrolysis will proceed only when these ions are removed from the solution.

Natural waters hold bicarbonate ions which during coagulation with aluminum sulfate combine with hydrogen ions to form undissociated molecules of carbonic acid:

$$6H^+ + 6HCO_3^- \rightarrow 6H_2CO_3 \qquad (343)$$

The summary reaction of aluminum sulfate dosed into water containing a large number of HCO_3^- ions and thus with higher alkalinity or carbonate hardness has the following form:

$$Al_2(SO_4)_3 \cdot 18H_2O + 3Ca(HCO_3)_2 \leftrightarrow 2Al(OH)_3 + 3CaSO_4 + 6CO_2 + 18H_2O \qquad (344)$$

According to stoichiometry, to neutralize sulfuric acid formed from 1.0 mg of $Al_2(SO_4)_3 \cdot 18H_2O$, an amount of 0.73 mg $Ca(HCO_3)_2$ is required during hydrolysis. This is the approximate value because aluminum sulfate used for water coagulation is a technical product and contains about 1% excess of H_2SO_4. In technical conditions, the calcium – carbonate equilibrium as well as the water reaction should be considered. In case the water has too low of a natural alkalinity, alkalines should be added in order to ensure aluminum sulfate hydrolysis:

$$Al_2(SO_4)_3 \cdot 18H_2O + 3Ca(OH)_2 \leftrightarrow 2Al(OH)_3 + 3CaSO_4 + 18H_2O \qquad (345)$$

It is necessary to dose $Ca(OH)_2$ when the following inequality is true:

$$[alk] < 0.009\, D_C + 0.7 \qquad (346)$$

In case of realizing this inequality to remove H^+ ions from the water, $Ca(OH)_2$ should be dosed in the following quantity:

$$D_{CaO} = 28(0.009D_C + 0.7 - [alk]) \qquad (347)$$

In the above formulas:

[alk] – water alkalinity [val/m^3],

D_C – dose of aluminum sulfate [g/m^3].

Aluminum hydroxide formed as a result of hydrolysis is of amphoteric character:

- in an acidic environment it reacts as a base:

$$Al(OH)_3 + 3H^+ \leftrightarrow Al^{3+} + 3H_2O \tag{348}$$

with the equilibrium constant defined by the equation

$$K_1 = \frac{[Al^{3+}]}{[Al(OH)_3][H^+]^3} \tag{349}$$

- in an alkaline environment, aluminum hydroxide reacts as an acid

$$H_3AlO_3 + OH^- \leftrightarrow AlO_2^- + 2H_2O \tag{350}$$

with the equilibrium constant defined by the equation

$$K_2 = \frac{[AlO_2^-]}{[Al(OH)_3][OH^-]} = \frac{[AlO_2^-][H^+]}{K_w[Al(OH)_3]} \tag{351}$$

where K_w is the constant of water dissociation.

From the modified forms of Equations (349) and (351), concentrations of the ions $[Al^{3+}]$ and $[AlO_2^-]$ can be determined:

$$[Al^{3+}] = \frac{K_1\,[Al(OH)_3]}{10^{3\,pH}} \tag{352}$$

$$[AlO_2^-] = K_2 K_w [Al(OH)_3] \cdot 10^{pH} \tag{353}$$

According to the above equations, there is a range of pH values at which aluminum hydroxide dissociation will be the smallest and almost all of the aluminum will occur as non-dissociated, hardly soluble hydroxide. For soft water this range is 5.7 ÷ 6.6; for water of average hardness it is 6.4 ÷ 7.2; and for hard water it is 7.2 ÷ 7.6 [47].

Aluminum hydroxide occurs in solution in colloidal form at a pH of the solution in the range 3.0 ÷ 9.0. The charge of precipitated colloid depends on the pH of the solution (Figure 28) [47].

In the pH range from 5.5 to 7.6 aluminum hydroxide has a positive charge. It causes, therefore, the destabilization of negatively charged colloids which are responsible for color and turbidity in natural water.

The isoelectric point, the point at which the concentrations of $[Al^{3+}]$ and $[AlO_2^-]$ are equal because the colloid nucleus is neutral, occurs when pH = 7.6 ÷ 8.2.

Iron hydroxide, which is the product of the hydrolysis of iron sulfate:

$$Fe_2(SO_4)_3 + 6H_2O \leftrightarrow 2Fe(OH)_3 + 6H^+ + 3SO_4^- \tag{354}$$

or the hydrolysis and oxidation of ferrous sulfate:

$$FeSO_4 + 2H_2O \rightarrow Fe(OH)_2 + 2H^+ + SO_4^{-} \qquad (355)$$

$$4Fe(OH)_2 + O_2 + 2H_2O \rightarrow 4Fe(OH)_3 \qquad (356)$$

has the lowest solubility when pH is in the range 5 ÷ 7. The isolelectric point occurs when pH = 7.5 ÷ 8.5. Below pH = 7.5 iron hydroxide is positively charged, and at 8.5 it is negatively charged.

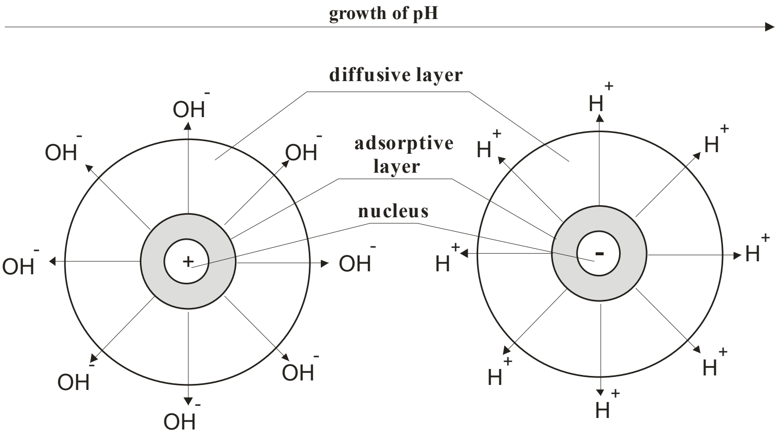

ACID ENVIRONMENT
pH = 3.0 ÷ 7.6
COLLOID NUCLEUS
$[Al(OH)_3]_m \cdot nAl^{3+}$
ADSORPTION AND DIFFUSION LAYER
OH^-, Cl^-, SO_4^{2-}, NO_2^-, NO_3^-, SO_3^{2-}, PO_4^{3-}

ALKALINE ENVIRONMENT
pH = 8.2 ÷ 9.0
COLLOID NUCLEUS
$[Al(OH)_3]_m \cdot nAlO_2^-$
ADSORPTION AND DIFFUSION LAYER
H^+, Na^+, K^+, Mg^{2+}, Ca^{2+}, Fe^{2+}, Mn^{2+}, NH_4^+

Fig. 28. Influence of water reaction on colloidal structure of aluminum hydroxide.

The efficiency of coagulation with ferrous salts (Fe^{2+}) is much smaller than the coagulation of ferric salts (Fe^{3+}). This results, among others, from a much greater solubility of ferrous hydroxide due to hydrolysis compared to ferric hydroxide. The oxidation of iron from Fe^{2+} to Fe^{3+} is necessary if ferrous salts are used for coagulation. At a pH of ~ 8.5 oxidation occurs relatively quickly with oxygen dissolved in water. The stoichiometric relations show that for the oxidation of one gram of Fe^{2+} 0.143 g of O_2 is necessary (Equation 356). At a pH less than 8.5, chlorinated ferrous sulfate should be added into the water. The following reaction then occurs:

$$6FeSO_4 \cdot 7H_2O + 3Cl_2 \rightarrow 2Fe_2(SO_4)_3 + 2FeCl_3 + 7H_2O \qquad (357)$$

According to the stoichiometry of the reaction, to oxidize one gram of $FeSO_4 \cdot 7H_2O$ one needs 0.128 gCl_2. The products of the above reaction are highly effective ferric coagulants. Fe^{2+}oxidation with potassium permanganate proceeds according to the reaction

$$FeSO_4 + KMnO_4 + 2H_2O \rightarrow Fe(OH)_3 + MnO_3 + KHSO_4 \qquad (358)$$

Oxidizing one gram of $FeSO_4 \cdot 7H_2O$ requires using 0.57 $gKMnO_4$. Resulting from the oxidation reaction (358), manganese trioxide shows good adsorption qualities increasing the effect of water purification. The formed sols of hydroxides also have adsorption qualities. On the surface of hydroxide flocs, finely dispersed suspensions, colloidal compounds and some dissolved compounds are sorbed. Adsorption in the process of coagulation applied in water technology can be approximated by the Langmuir adsorption isotherm model (Equation 171).

For each type of water there is a specified dose for a given type of coagulant to achieve process optimization. To deviate from this dose in both directions can lead to complications in the process of coagulation. A rigorous determination of coagulant dosage is particularly important for low water temperatures [47].

8.2.1. Example Calculations

EXAMPLE 1

Determine the quantity of natural alkalinity of surface water necessary for coagulation with aluminum sulfate of a dose $D_C = 50\ g/m^3$.

Reaction of aluminum sulfate with natural alkalinity:

$$Al_2(SO_4)_3 \cdot 18H_2O + 3Ca(HCO_3)_2 \leftrightarrow CaSO_4 + 2Al(OH)_3 + 6CO_2 + 18H_2O$$

According to the above reaction, one mole of aluminum sulfate reacts with three moles of lime hydroxide so the weight ratio is

$$\frac{3Ca(HCO_3)_2}{Al_2(SO_4)_3 \cdot 18H_2O} = \frac{3(162)}{666.7} = 0.73$$

For coagulant dose $D_C = 50\ g/m^3$ necessary value of natural alkalinity expressed as g HCO_3^-/m^3 is

$$\text{alk} = \frac{122}{162} \cdot 0.73 \cdot 50 = 27.49\ \text{g}\ HCO_3^- / m^3$$

The necessary value of alkalinity expressed as g $CaCO_3/m^3$ is

$$\text{alk} = \frac{100}{162} \cdot 0.73 \cdot 50 = 22.53\ \text{g}\ CaCO_3 / m^3$$

EXAMPLE 2

Determine the required amount of lime to bind to the aggressive CO_2 present in purified water in coagulation with aluminum sulfate of a dose $D_k = 50\ g/m^3$.
The alkalinity of raw water is alk= 150 g $CaCO_3/m^3$, and its pH = 7.5. Contents of various forms of CO_2 for this water read from the nomogram of carbonate-lime equilibrium are

free carbon dioxide – $CO_{2w} = 9.8\ g/m^3$,
affiliated carbon dioxide – $CO_{2p} = 7.0\ g/m^3$,
aggressive carbon dioxide – $CO_{2a} = 2.8\ g/m^3$.

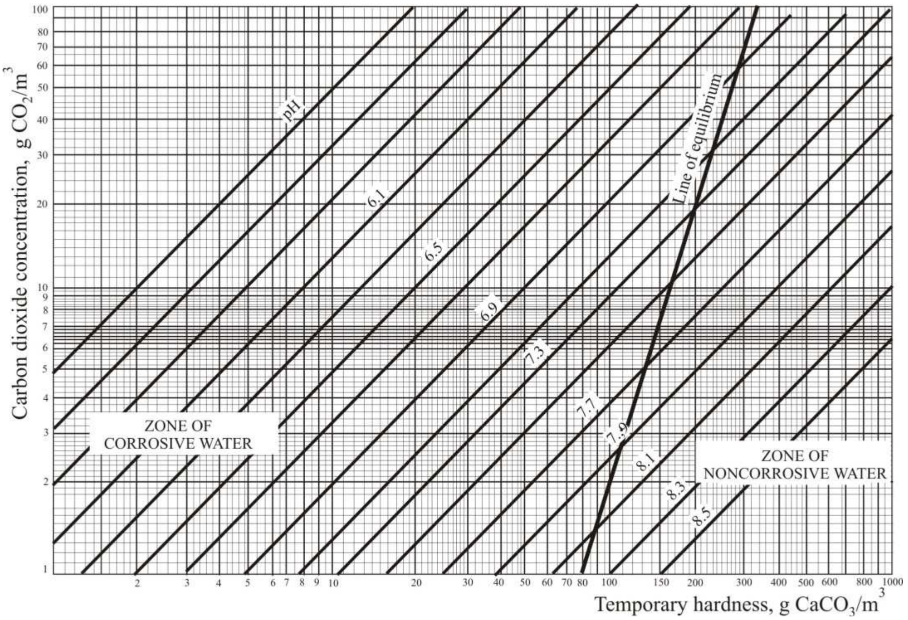

According to the stoichiometry of the reaction of aluminum sulfate with the natural alkalinity of water, one gram of added $Al_2(SO_4)_3 \cdot 18H_2O$ causes the alkalinity to drop by 0.45 $gCaCO_3/m^3$ and the free carbon dioxide to rise by 0.40 gCO_{2w}/m^3.

So the addition of 50 g $Al_2(SO_4)_3 \cdot 18H_2O$ to 1 m^3 of water causes the drop of its alkalinity by

$$\Delta alk = 50 \cdot 0.45 = 22.5 \text{ g } CaCO_3 / m^3$$

and an increase in CO_2 concentration

$$\Delta CO_2 = 50 \cdot 0.40 = 20 \text{ g } CO_2 / m^3$$

Water after coagulation includes free CO_2 in the amount of

$$CO_{2w} = 9.8 + 20 = 29.8 \text{ g} / m^3$$

and its alkalinity is

$$alk = 150 - 22.5 = 127.5 \text{ g } CaCO_3 / m^3$$

For the new water, the alkalinity concentration $CO_{2p} = 4.4$ g/m^3 was determined from the nomogram of the carbonate-lime equilibrium.

Therefore, the quantity of aggressive CO_2 in water after coagulation is

$$CO_{2a} = 29.8 - 4.4 = 25.4 \text{ g} / m^3$$

The aggressive carbon dioxide present in water should react with lime according to reaction

$$2CO_{2a} + CaO + H_2O = Ca(HCO_3)_2$$

The amount of lime required to bind to CO_{2a} is determined by the method of subsequent approximations, assuming in the first step that lime binds 20 g of CO_{2a}/m^3.

According to the above reaction, 1 mol of CaO binds 2 moles of CO_{2a} so in the analyzed case the necessary amount of lime is

$$D_{CaO} = \frac{20 \cdot 56}{88} = 12.7 \text{ gCaO} / m^3$$

Lime addition causes alkalinity to rise by

$$\Delta alk = \frac{12.7}{28} \cdot 50 = 22.7 \text{ g } CaCO_3 / m^3$$

For the new alkalinity

$$(alk)_1 = 127.5 + 22.7 = 150.2 \text{ g } CaCO_3 / m^3$$

from the nomogram of equilibrium, the value of $(CO_{2p})_1$ was read as

$$(CO_{2p})_1 = 7.0 \text{ g} / m^3$$

Contents of aggressive CO_2 after adding 12.7 g CaO/m^3:

$$(CO_{2a})_1 = 29.8 - 20 - 7.0 = 2.8 \text{ g} / m^3$$

The concentration of aggressive carbon dioxide is larger than the acceptable limits which does not give the water corrosive qualities ($CO_{2a} \leq 2$ g/m^3) so in the second step it is assumed that CaO will bind to a larger quantity of CO_{2a}. It was assumed that lime will bind 22 g CO_{2a}/m^3, so

$$\left(D_{CaO}\right)_2 = \frac{22 \cdot 56}{88} = 14.0 \text{ gCaO} / \text{m}^3$$

The above lime dosage causes alkalinity rise by

$$\Delta\text{alk} = \frac{14.0}{28} \cdot 50 = 25.0 \text{ g CaCO}_3 / \text{m}^3$$

The alkalinity after correcting the lime dosage $\left(D_{CaO}\right)_2 = 14.0 \text{ gCaO} / \text{m}^3$ is

$$\left(\text{alk}\right)_2 = 127.5 + 25.0 = 152.5 \text{ g CaCO}_3 / \text{m}^3$$

For the above alkalinity the value $\left(CO_{2p}\right)_2$ read from the nomogram of equilibrium was equal to

$$\left(CO_{2p}\right)_2 = 7.2 \text{ g} / \text{m}^3$$

Contents of aggressive CO_2 after adding 14.0 g CaO/m^3

$$\left(CO_{2a}\right)_2 = 29.8 - 22 - 7.2 = 0.6 \text{ g} / \text{m}^3$$

The rest of CO_{2a} = 0.6 g/m^3 < 2,0 g/m^3. Thus binding 22 g CO_{2a}/m^3 removes the corrosive character of water after coagulation.

8.3. Chemical Precipitation

Chemical precipitation is a process widely used for removing many contaminants. It is a part of both coagulation with aluminum and iron salts and decarbonization with lime. It is used for metal ion removal and for dephosphatation.

The models used to describe the processes of chemical precipitation can be divided into three categories: stoichiometric, equilibrium and kinetic. Categories of these models are hierarchical in relation to each other, which means that a particular system can be adequately approximated by a stoichiometric model, whereas the equilibrium model used for this purpose includes in its construction the stoichiometric model. The kinetic model contains both categories of previous models [27].

Water softening is an example of a process in which stoichiometric relations are sufficient. Similarly, the process of dephosphatation with iron and aluminum salts at the required low efficiency (~ 80%) can be described by stoichiometric relations.

Chemical equilibrium in the precipitation models is taken into account when during the process the pH changes substantially or when the reaction efficiency is controlled by the solubility of the products. The basic parameter of this category of models is the equilibrium constant. An example of this type of models is the chemical precipitation of phosphates with salts of aluminum and iron at various water pH values. Chemical equilibrium models are used to estimate phosphate removal efficiency, final pH of the system, concentrations of other compounds after the process and the size of the reagent dose.

The third category of models, in addition to the above, contains a mathematical record of the precipitation rate. Precipitation processes usually proceed rapidly. Therefore, the kinetics of e.g. dephosphatation or softening can be ignored in the considerations due to their low significance in modeling. However, depending on the conditions under which the process is carried out, the process kinetics may vary. A relatively slow reaction of calcium phosphate precipitation carried out in the portion system at pH = 8 can be significantly accelerated in the flow system through the recirculation of the precipitated sediment. In studies the reaction rate is correlated with the characteristics of reactors [65]. Models in this class may be used to forecast the residual concentration and pH of the precipitated compound as a function of the dose size and reactor type.

This chapter presents the application of equilibrium and kinetic models to describe the process of phosphate precipitation and to estimate the final pH. A set of assumptions common to all categories of models is adopted. Firstly, it is assumed that a complex water system is represented only by a few chemical compounds. Secondly, the system is isolated from the gas phase or is in equilibrium with the gas phase. This assumption is due to the fact that the mass transfer within the system or mass migration outside the system is not limited by speed. Thirdly, surface phenomena and flocculation kinetics can be eliminated from the considerations. In this respect, the models do not describe the separation of precipitated suspended solids, but only their formation.

Another simplification in constructing the models is the assumption that the solution analyzed behaves like a perfect solution and its temperature is fixed at 25°C.

The final pH is determined based on the knowledge of the initial concentrations of orthophosphates, ammonia nitrogen, alkalinity and initial pH and the dose of salts of aluminum, iron or lime. It is assumed that the system's return to the equilibrium is relatively fast.

Table 16 lists the compounds, the reactions of their changes occurring in water and the equilibrium reaction constants. This system serves as an example of a model application [27].

Table 14. Equilibrium reaction constants of the compounds present in natural waters [27].

No.	Reactions	Equilibrium constants used in the solutions	log K
1	$H_2O = H^+ + OH$	K_w	-14.0
2	$H_2CO_3 = H^+ + HCO_3$	K_1	-6.2
3	$HCO_3 = H^+ + CO_3^2$	K_2	-10.2
4	$H_3PO_4 = H^+ + H_2PO_4$	K_1	-2.2
5	$H_2PO_4 = H^+ + HPO_4^2$	K_2	-7.2
6	$H_2PO_4^2 = H^+ + PO_4^3$	K_3	-12.2
7	$NH_4OH + H^+ = NH_4^+ + H_2O$	K	9.2
8	$Al^{3+} + OH = Al(OH)^2$	$K[Al(OH)^{2+}]$	9.0
9	$Al^{3+} + 4(OH) = Al(OH)_4$	$K[Al(OH)_4^-]$	32.5
10	$Ca^{2+} + CO_3^{2-} = CaCO_3°$	$K[CaCO_3°]$	3.2
11	$Ca^{2+} + HPO_4^{2-} = CaHPO_4°$	$K[CaHPO_4°]$	2.7
12	$Ca^{2+} + PO_4^3 = CaPO_4$	$K[CaPO_4^-]$	6.5
13	$Ca_5(PO_4)_3OH = 5Ca^{2+} + 3PO_4^3 + OH$		-4.9
14	$CaCO_3 = Ca^{2+} + CO_3^2$		-8
15	$Al(OH)_3 = Al^{3+} + 3OH$		-30.4
16	$Al_{1,4}PO_4(OH)_{1,2} = 1.4Al^{3+} + 3PO_4^3 + 1.2OH^-$		-32.2

Determining the concentration of carbonates and bicarbonates on the basis of the initial alkalinity requires considering the influence of phosphates and ammonia on the value of alkalinity. For the pH range of 6 to 9, the following dependencies are true which can be used to determine the bicarbonate concentration:

$$[\text{alk}] = [\text{HCO}_3^-] + [\text{HPO}_4^{2-}] + [\text{NH}_4\text{OH}] \tag{359}$$

$$[\text{HPO}_4^{2-}] = \frac{\text{P}_\text{T}}{1 + \frac{[\text{H}^+]}{\text{K}_2}} \tag{360}$$

$$[\text{H}_4\text{OH}] = \frac{\text{N}_\text{T}}{1 + \frac{[\text{H}^+]}{\text{K}}} \tag{361}$$

In the above equations [alk], P_T, N_T denote alkalinity, general phosphorus concentration and general nitrogen concentration, respectively.

The concentration of carbonic acid and orthophophosphoric acid can be determined based on the balance of the electroneutrality of the system:

$$\text{M}_\text{i}^+ = 3[\text{PO}_4^{3-}] + 2[\text{HPO}_4^{2-}] + [\text{H}_2\text{PO}_4^-] + 2[\text{CO}_3^{2-}] + [\text{HCO}_3^-] + [\text{OH}^-] - [\text{H}^+] - [\text{NH}_4^+]$$
$$[\text{val/m}^3] \tag{362}$$

M_i^+ is the value that characterizes the initial conditions and is used in subsequent calculations of the final pH. In these calculations, the concentration of acids $[S_K]$

connected with the hydrolysis of aluminum or iron salts and the concentration of alkalines $[S_Z]$ resulting from the dissolution of lime are determined on the basis of the doses of the chemicals used:

$$Al^{3+} + 3H_2O \rightarrow Al(OH)_3 + 3H^+ \tag{363}$$

$$[S_K]_{Al} = [Al] \cdot 10^{-5} \ [val/m^3] \tag{364}$$

[Al] – aluminum dosage [g/m^3].

$$Fe^{3+} + 3H_2O \rightarrow Fe(OH)_3 + 3H^+ \tag{365}$$

$$[S_K]_{FeCl_3} = [FeCL_3] \cdot 1.86 \cdot 10^{-5} \quad [val/m^3] \tag{366}$$

[$FeCl_3$] – iron chloride dosage [g/m^3].

$$CaO + H_2O \rightarrow Ca^{2+} + 2(OH)^- \tag{367}$$

$$[S_Z]_{CaO} = [CaO] \cdot 3.57 \cdot 10^{-5} \quad [val/m^3] \tag{368}$$

[CaO] – lime dosage [g/m^3].

The increase of the concentration of acids or bases as a result of the reagent dosage shifts the dissociation of weak acids and bases in a solution. Under the new conditions

$$[S_Z] - [S_K] + M_i^+ + [H^+] + [NH_4^+] =$$

$$= 3\,[PO_4^{3-}] + 2\,[HPO_4^{2-}] + [H_2PO_4] + 2\,[CO_3^{2-}] + [HCO_3^-] + [OH^-] \tag{369}$$

In the above equation $[S_Z]$, $[S_K]$, M_i^+ are given in val/m^3. Other concentrations are mole concentrations.

For the closed system the above equation can also be written as a function of the concentration of solution components, the values of $[S_Z]$, $[S_K]$ and M_i^+, the values of equilibrium constants and $[H^+]$:

$$[S_Z] - [S_K] + M_i^+ + [H^+] + \frac{N_T[H^+]K}{1 + \frac{[H^+]}{K}} - \frac{C_T\left(1 + 2 \cdot \frac{K_2}{[H^+]}\right)}{\left(\frac{[H^+]}{K_1} + 1 + \frac{K_2}{[H^+]}\right)} +$$

$$- \frac{P_T\left(1 + 2\frac{[H^+]}{K_2} + 3\frac{[H^+]^2}{K_2 \cdot K_3}\right)}{\left(1 + \frac{K_2}{[H^+]} + \frac{K_2 \cdot K_3}{[H^+]^2}\right)} - \frac{K_w}{[H^+]} = 0 \tag{370}$$

C_T is bicarbonate alkalinity.

The above equation is a complex polynomial; the solution is carried out by means of iteration [65].

The presented procedure gives a good approximation of pH value for a closed system. In real systems, when using aluminum and iron salts for precipitation, the solution becomes saturated with CO_2 which then tends to leak into the atmosphere resulting in an increase in pH.

For precipitation with lime of carbonates or calcium phosphates in an open system, there is a tendency to absorb CO_2 from the atmosphere causing a lower pH than is apparent from Equation (370) for a closed system.

Modified **models of chemical equilibrium** were discussed on the basis of phosphate precipitation with the salts of aluminum, iron and lime [27].

According to the stoichiometry of reaction, precipitation of one mole of P requires 1.4 mol of Al. Aluminum compounds of the plus three oxidation state are substantially insoluble at a neutral pH and the stoichiometric relations adequately approximate the course of the process with its efficiency ranging up to 80 ÷ 90%. Parallel to phosphate precipitation, the pH of the solution drops as a result of the release of protons from the included hydroxides and phosphates. With a further increase of the aluminum dose, the phosphate concentration is controlled by the solubility of the reaction products. The pH changes, but there is no reduction in the concentration of the remaining phosphorus.

These models do not include the mechanisms of co-precipitation and adsorption on precipitated products in the analyzed process.

Two possible situations were analyzed. The first is when the addition of aluminum salt only causes the precipitation of aluminum phosphate. The second is when in addition to phosphorus, aluminum hydroxide is also precipitated.

In the first case, when $Al_T < 1.4P_T$ (Al_T and P_T are the general amount s of aluminum and phosphorus, respectively) precipitation is described by the equilibrium model and balance equations for the system are as follows:

$$Al_T = [1.4\ Al_{1.4}PO_4(OH)_{1.2}] + [Al^{3+}] + [AlOH^{2+}] + [Al(OH)_4^-] \qquad (371)$$

$$P_T = [Al_{1.4}PO_4(OH)_{1.2}] + [H_2PO_4^-] + [HPO_4^{2-}] \qquad (372)$$

The number of hydrogen ions $[S_K]$ formed in the system as a result of dosing aluminum can be determined from a summary reaction of precipitation in which soluble fractions of aluminum compounds are omitted:

$$1.4\ Al^{3+} + H_2PO_4^- + 1.2H_2O = Al_{1.4}PO_4(OH)_{1.2} + 3.2H^+ \qquad (373)$$

therefore

$$[S_K] = \frac{3.2}{1.4} Al_T \qquad (374)$$

The electroneutrality condition of the solution after precipitation is

$$[S_K] + [HCO_3^-] + [H_2PO_4^-] + 2[HPO_4^{2-}] + [OH^-] = [H^+] + [NH_4^+] + M_i^+ \qquad (375)$$

Equation (375) omits the concentration of soluble aluminum compounds along with $[CO_3^{2-}]$ and $[PO_4^{3-}]$ because their presence has no significant influence on the pH of the solution. These equations can be solved by substituting the concentration of the product $Al_{1.4}PO_4(OH)_{1.2}$ and using equilibrium relations from Table 16 in Equations (371) (372) and (375):

$$[Al^{3+}]^{1.4}[PO_4^{3-}][OH]^{1.2} = 10^{-32.2}[Al_{1.4}PO_4(OH)_{1.2}] \qquad (376)$$

Alternatively, when the concentration of dissolved phosphates P_S is approximately equal P_T - $Al_T/1.4$ the charge balance described by Equation (375) can be solved directly because of $[H^+]$. Concentration $[PO_4^{3-}]$ can be determined from the mass balance (371) and (372) and also from Equation (376). When the value of $Al_T/1.4$ exceeds the value of P_T, the solution will become supersaturated because of $Al(OH)_3$ and precipitative forms of aluminum can then be formed: phosphate and hydroxide. In such case balance Equation (371) is supplemented by the concentration of $Al(OH)_3$ and is as follows:

$$Al_T = [Al(OH)_3] + [1.4\ Al_{1.4}PO_4(OH)_{1.2}] + [Al^{3+}] + [AlOH^{2+}] + [Al(OH)_4^-] \qquad (377)$$

Equation (372) determining the value of P_T remains unchanged. In this case the two relations must be true:

$$[Al^{3+}][OH^-] = 10^{-30.4}\ [Al(OH)^3] \qquad (378)$$

and relation (376).

The acidity is the function of the amount of formed hydroxide and aluminum phosphate. The value $[S_K]$ changes in the range from $3Al_T$ for $Al(OH)_3$ to (3.2/1.4) Al_T for $Al_{1.4}PO_4(OH)_{1.2}$.

A similar procedure to the case presented above can be used to predict the effect of phosphate removal by using iron salts in a plus three oxidation state.

In the case of using lime for the chemical precipitation, at $pH > 9$ apart from phosphate calcium carbonate is also precipitated. At $pH < 8.5$ calcium phosphate is precipitated relatively slowly and calcium carbonate does not precipitate unless the alkalinity of the water exceeds 300 g $CaCO_3/m^3$.

Chemical precipitation carried out at a high pH is more difficult for mathematical modeling. The mass balances are much more complicated than in the previously discussed cases. This is due to the presence of ionic complexes containing CO_3, $CaHPO_4$ and $CaHPO_4^-$, which are the large fractions of calcium and phosphates present in the dissolved form [27]. Magnesium also has an impact on the process. The model of chemical precipitation should take into account the solubility of brucite, $Mg(OH)_2$ and the impact of magnesium on the concentration of magnesium carbonate and calcium phosphate. For practical purposes, given the considerable complexity of the model, these effects are not taken into account [25]. Possible mass balances to apply are as follows:

$$Ca_T = [CaCO_3] + [5Ca_5(PO_4)_3OH] + [Ca^{2+}] + [CaHPO_4] + [CaPO_4^-] \qquad (379)$$

$$P_T = [3Ca_5(PO_4)_3OH] + [HPO_4^{2-}] + [PO_4^{3-}] + [CaHPO_4] + [CaPO_4^-] \tag{380}$$

$$CO_{3T} = [CaCO_3] + [HCO_3^-] + [CO_3^{2-}] \tag{381}$$

Two equilibrium relations must be met

$$[Ca^{2+}]^5\,[PO_4^{3-}]^3[OH^-] = 10^{-49}\,[Ca_5(PO_4)_3OH] \tag{382}$$

$$[Ca^{2+}][CO_3^{2-}] = 10^{-8}\,[CaCO_3] \tag{383}$$

The dose of calcium increases the concentration of hydroxide according to the relation

$$[S_Z] = \frac{[CaO]}{56 \cdot 10^3} \cdot 2 \tag{384}$$

where [CaO] is the dose of calcium [g/m^3].

Precipitation reactions result in the release of protons:

$$5Ca^{2+} + 3HPO_4^{2-} + H_2O = Ca_5(PO_4)_3OH + 4H^+ \tag{385}$$

$$Ca^{2+} + HCO_3^- = CaCO_3 + H^+ \tag{386}$$

The condition of electroneutrality of the system is therefore as follows:

$$[S_K] + [HCO_3^-] + 2[CO_3^{2-}] + 2[HPO_4^{2-}] + 3[PO_4^{3-}] + [CaPO_4^-] + [OH^-] = \\ = [S_Z] + M_i^+ + [H^+] + [NH_4^+] \tag{387}$$

Using equilibrium relations, a set of six Equations (379) ÷ (383) and (387) may be used to determine six unknown values, that is $[CO_3^{2-}], [PO_4^{3-}], [Ca^{2+}], [H^+], [CaCO_3]$ and $[Ca_5(PO_4)_3OH]$.

The kinetics of calcium phosphate precipitation at pH = 7.5 ÷ 8.5 is described by the following formula:

$$\frac{dP}{dt} = -\frac{k[P]^{2.8}}{[C_T]} \tag{388}$$

in which [P] is the concentration of soluble orthophosphates and [C_T] is the bicarbonate alkalinity.

The reaction velocity constant k is proportional to the available surface of crystals formed. The usual assumed value is k = ~ 1.3·10^{16} h^{-1}. The above equation is the result of partial tests when the reaction was maintained at pH = 8 ± 0.1 and initial concentration Ca^{2+} equal 2 val/m^3. For these initial conditions, a good approximation of chemical precipitation kinetics produces the following equation:

$$\frac{dP}{dt} = -\frac{k^*\,[Ca^{2+}]^5[PO_4^{3-}]^3}{[H^+][C_T]} \tag{389}$$

where velocity constant k^* is equal approximately to

$$k^* = \frac{4 \cdot 10^6 \, [P]^{2.8}}{[PO_4^{3-}]^3} \tag{390}$$

The reaction kinetics with the expression $[PO_4^{3-}]$ as a function [P] in the pH range 7.6 ÷ 8.4; alkalinity 0.5 ÷ 0.7 val/m^3; calcium concentration 1 ÷ 2.5 val/m^3 may be described by the following equation:

$$\frac{dP}{dt} = -\frac{k^{**} \, [Ca^{2+}]^5 [P]^3}{[H^+]^4 \, [C_T]} \tag{391}$$

The above equation may be used to predict phosphate removal in a steady state for completely mixed flow reactors and plug flow with sediment recirculation and without recirculation.

The sediment concentration in a system with recirculation increases proportionally to the ratio of retention time of sediment in the system (T_{os}) to hydraulic retention time (T_H).

Four reactor systems are analyzed below [27]:

- completely mixed flow reactor without recirculation,
- completely mixed flow reactor with recirculation,
- series of fully mixed with recirculation at the beginning of the system,
- plug flow reactor with recirculation.

Diagrams of analyzed systems are presented in Figure 29.

Equation (391) is included to demonstrate a general model of precipitation used for determining concentrations of removed phosphates and the required calcium hydroxide dose to achieve the required pH of the solution.

A single completely mixed flow reactor without recirculation is in practice rarely used. (Fig. 29a).

The mass balance of dissolved phosphates in steady state is described by the following equation:

$$Q \cdot P_T = QP + V\frac{dP}{dt} = 0 \tag{392}$$

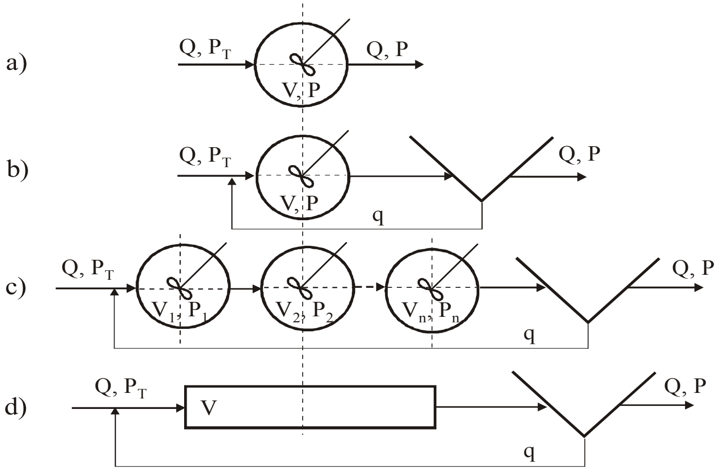

Fig. 29. Diagrams of reactor systems for chemical precipitation of phosphates with lime at low pH values.

Substituting into the equation the values of reaction rate with Equation (391) and taking into account TH = V/Q produces

$$P_T - P = \frac{k^{**} T_H [P]^3 \, [Ca^{2+}]^5}{[H^+]^4 \, [C_T]} \tag{393}$$

For a completely mixed flow reactor with sediment recirculation (Fig. 29b) the precipitation reaction velocity constant is described by the formula:

$$K_s = k^{**} \frac{T_{os}}{T_H} \tag{394}$$

Retention time for sediment in the system (T_{OS}) is defined as the general amount of sediment in the system divided by the amount of sediment removed daily from the system. In steady state, the amount of sediment removed daily from the system is equal to the amount of sediment formed during that time period. Therefore, assuming high efficiency of sediment separation, the following relation can be formed:

$$T_{os} = \frac{V \cdot C}{Q \cdot f \cdot P_T \cdot E} \tag{395}$$

where:

V – reactor volume [m^3],
C – sediment concentration in the reactor [g/m^3],
Q – volumetric velocity of flow [m^3/h],
f – coefficient of dependency of the weight of removed phosphates on the weight of sediment formed,

E – efficiency of phosphate removal.

The value of Tos can be controlled by changing the sediment concentration in the reactor (C) or by changing the hydraulic retention time ($T_H = V/Q$).

The formula defining the degree of phosphate removal with consideration of the balance Equation (392) takes the following form:

$$P_T - P = \frac{K_s T_H [P]^3 [Ca^{2+}]^5}{[H^+]^4 [C_T]} \tag{396}$$

Using the above formula requires accepting reactor characteristics and the knowledge of C_T, Ca^{2+}, pH and the initial concentration P_T.

The amount of released protons [S_K] as a result of precipitation can be determined from the reaction stoichiometry (385).

The equation defining the electroneutrality of the system allows the estimation of the value [S_Z] which is necessary to achieve the assumed pH.

Depending on the number of elements, a cascade of completely mixed flow reactors (Fig. 29c) is able to model systems with conditions between that of completely mixed flow reactors and plug flow reactors.

The degree of phosphorus removal in each reactor is determined from the balance equation. The hydraulic retention time for a particular reactor is

$$T_{H_1} = T_{H_2} = T_{H_n} = \frac{T_H}{n} \tag{397}$$

It is assumed that the reaction velocity constant K, concentration of calcium and bicarbonates and pH are approximately constant for all reactors:

$$P_T - P_1 = \frac{K T_{H_1} [P_1]^3 \ [Ca^{2+}]^5}{[H^+]^4 \ [C_T]} \tag{398}$$

$$P_1 - P_2 = \frac{K T_{H_2} \ [P_2]^3 \ [Ca^{2+}]^5}{[H^+]^4 \ [C_T]} \tag{399}$$

$$P_{n-1} - P_n = \frac{K T_{H_n} \ [P_n]^3 \ [Ca^{2+}]^5}{[H^+]^4 \ [C_T]} \tag{400}$$

The flow of recirculation (q) dilutes to some extent the water flowing into the first reactor and phosphorus concentration in the inflow is described by the formula:

$$P_T^* = \frac{QP_T + qP_n}{Q + q} \tag{401}$$

Exemplary results for the calculations of the remaining phosphorus in the systems with one, two and four completely mixed flow reactors for a typical water composition and process parameters:

($P_T = 0.3$ val/m^3, $C_T = 3.4$ val/m^3, pH = 8, $Ca^{2+} = 2$ val/m^3, T = 25°C, $Tos/T_H = 30$) are presented as a functional dependency $Pn = f(T_H)$ in Figure 30. The computer polynomial solution using the Newton-Raphson method did not take into account the change in phosphorus concentration in the inflow resulting from recirculation [65].

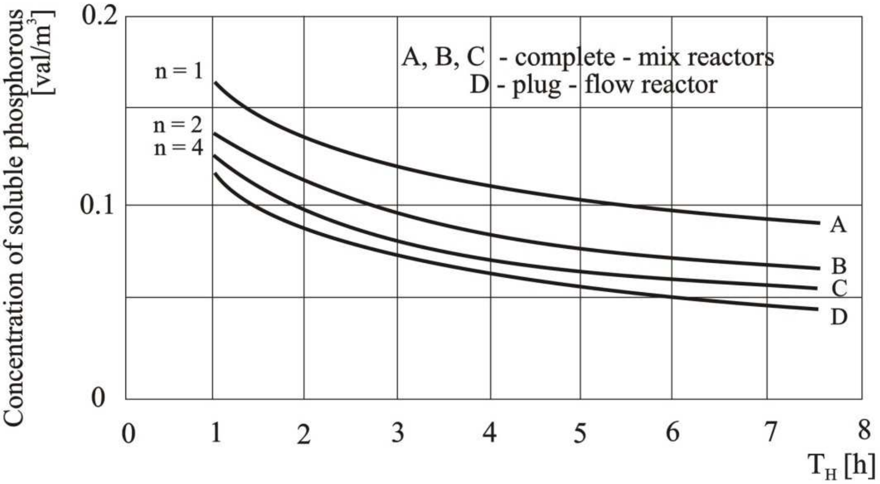

Fig. 30. Efficiency of phosphorus removal as a function of retention time for various types of reactors.

Figure 30 also presents a curve of the dependency of phosphorus removal on retention time for a plug flow reactor (Fig. 29d).

The process efficiency was determined from the velocity equation after dividing variables and integrating from 0 to T_H with the initial phosphorus concentration described by Equation (401):

$$\left(\frac{QP_T + q \cdot P}{Q+q}\right)^{-2} - P^{-2} = \frac{-2KT_H}{C_T\left(1+\frac{q}{Q}\right)} \tag{402}$$

The above equation can be also solved using the Newton-Raphson method [65].

8.3.1. Example Calculations

EXAMPLE 1

Determine the necessary quantity of reagents for softening with lime-soda for water with a temperature of 25°C and the following constituent concentrations:

Water components	Concentration [val/m^3]
Ca^{2+}	5.2
Mg^{2+}	2.8
HCO_3^-	4.8
CO_3^{2-}	0.02
Cl^-	2.1
SO_4^{2-}	1.08

The solution pH was determined from the dissociation equation of carbonic acid of the second degree:

$$HCO_3^- \leftrightarrow H^+ + CO_3^{2-}$$

$$K_2 = \frac{[H^+][CO_3^{2-}]}{[HCO_3^-]}$$

$$[H^+] = \frac{K_2\,[HCO_3^-]}{[CO_3^{2-}]}$$

The dissociation constant of carbonic acid of the second degree at a temperature of 25°C is $K_2 = 6.31 \cdot 10^{-11}$ (Table 16):

$$[H^+] = \frac{6.31 \cdot 10^{-11} \cdot 4.8}{0.02} = 1.514 \cdot 10^{-8}$$

$$pH = -\log[H^+] = 7.82$$

Determining water alkalinity

$$[alk] = [HCO_3^-] + [CO_3^{2-}] + [OH^-] + [H^+]$$

$$[OH^-] = 10^{-(14-pH)} = 10^{-6.18} = 6.61 \cdot 10^{-7}$$

$$[zas] = 4.8 + 0.02 + 6.61 \cdot 10^{-7} + 1.514 \cdot 10^{-8} = 4.82\ val/m^3$$

Determining the necessary lime dose

Lime added to water reacts with its components according to the following reactions:

$$CO_2 + Ca(OH)_2 \rightarrow CaCO_3 + H_2O$$

$$Ca(HCO_3)_2 + Ca(OH)_2 \rightarrow 2CaCO_3 + 2H_2O$$

$$Mg(HCO_3)_2 + 2Ca(OH)_2 \rightarrow 2CaCO_3 + Mg(OH)_2 + 2H_2O$$

So the necessary lime dose is

$$D_{Ca(OH)_2} = [CO_2] + [HCO_3^-] + [Mg^{2+}] =$$

$$= 0 + 4.8 + 2.8 = 7.6 \text{ val} / m^3 =$$

$$= 281.2 \text{ gCa(OH)}_2 / m^3 \text{ or } 380 \text{ gCaCO}_3 / m^3$$

Determining the necessary soda dose:
Soda added to the water reacts with its components according to the reaction

$$CaSO_4 + Na_2CO_3 \rightarrow CaCO_3 + Na_2SO_4$$

$$MgCl_2 + Na_2CO_3 \rightarrow MgCO_3 + 2NaCl$$

The necessary soda dose is

$$D_{Na_2CO_3} = [Ca^{2+}] + [Mg^{2+}] - [zas] = 5.2 + 2.8 - 4.82 = 3.18 \text{ val} / m^3$$

$$= 168.5 \text{ gNa}_2\text{CO}_3 / m^3$$

EXAMPLE 2

For water with the constituent concentrations given below determine the course of the kinetic curve of calcium phosphate precipitation:

Water components	**Concentration [val/m^3]**
Ca^{2+}	5.2
Mg^{2+}	2.8
HCO_3^-	4.8
CO_3^{2-}	0.02
Cl^-	2.1
SO_4^{2-}	1.08
PO_4^{3-}	1.2

Determination of the solution pH:

The pH was determined on the basis of the dissociation equation of carbonic acid of the second degree:

$$[H^+] = \frac{K_2[HCO_3^-]}{[CO_3^{2-}]} = \frac{6.31\cdot 10^{-11}\cdot 4.6}{0.04} = 7.256\cdot 10^{-9}$$

$$pH = 8.14$$

For water pH in the range $pH = 7.5 \div 8.5$ to determine kinetics of calcium phosphate precipitation equation (388) can be used:

$$\frac{dP}{dt} = -\frac{K[P]^{2.8}}{[C_T]}$$

$[C_T] = \sim [HCO_3^-] = 4.6$ val/m^3 – bicarbonate alkalinity,

[P] – concentration of dissolved phosphates,

$K = 1.3\cdot 10^{16}\ h^{-1}$ – velocity constant of the precipitation reaction.

Separating variables and integrating from t = 0 to t = t and from P = $[P_0]$ to P = [P] allows the determination of the kinetic curve of precipitation:

$$\int_{[P]_0}^{[P]} [P]^{-2.8} dP = -\frac{K}{[C_T]}\int_0^t dt$$

$$[P] = \left\{[P_0]^{-1.8} + \frac{1{,}8\,K}{[C_T]}t\right\}^{-0.555}$$

$$[P] = \left\{0.72 + 6.26\cdot 10^{15}\,t\right\}^{-0.555}$$

Calculated values of dissolved calcium phosphates (kinetic curve coordinates) are summarized in the following table:

Time [h]	**Concentration [val/m^3]**
0	1.2
$(3{,}600)^{-1}$	$1.61\cdot 10^{-7}$
$(60)^{-1}$	$1.66\cdot 10^{-8}$
0.25	$3.69\cdot 10^{-9}$
0.5	$2.51\cdot 10^{-9}$
1.0	$1.71\cdot 10^{-9}$
2.0	$1.16\cdot 10^{-9}$
3.0	$9.29\cdot 10^{-10}$

8.4. Disinfection

Disinfection is the last technological process before introducing water into the water distribution system. The main objective of disinfection is to destroy pathogens and protect water consumers from infection and disease. The process of disinfection involves the dosage of chemicals, mostly strong oxidants, or the application of physical agents such as ultrasound or UV rays.

Mechanisms determining disinfection efficiency are oxidation or destruction of the cell membrane with the progressive disintegration of cells and diffusion through the membrane into the cells along with the denaturation of proteins.

The efficiency of disinfectants is also determined by the chemical composition of water. Reactions of dosed compounds with specific components in water may occur that weaken their bactericidal activity. In addition, organic compounds can sorb onto the surface of microorganisms hindering the access of disinfectants to the cell membrane.

Another factor determining the efficiency of disinfection is the characteristics of the microorganisms.

Pathogenic organisms can be classified into four groups:

- bacteria in survival forms,
- protozoa in survival forms,
- viruses,
- vegetative bacteria.

Resistance of these organisms to disinfection is mainly attributed to differences in the construction of cellular structures.

The increase of the resistance of the cell membrane, cytochemical changes such as the loss of some cations and the accumulation of other essential ions, as well as partial dehydration of protoplasm may be reasons for an increased resistance to disinfection [33]. The high resistance of viruses is associated with the lack of enzymes and other sensitive systems. Disinfection of viruses is achieved primarily by denaturing proteins. The destruction of the metabolic system of vegetative bacteria occurs very fast because their respiration takes place through the cell membrane close to which other highly active systems are located.

A measure of the disinfection ability is the standard potential and electrochemical characterization. The standard potential of primary disinfectants is presented in Table 15.

A higher oxidizing potential of the compound means an easier oxidation of organic matter. If oxidation is the only mechanism deciding the course of disinfection, the disinfection force of compounds is as follows: $O_3 > ClO_2 > Cl_2 > Br_2 > I_2$.

Table 15. Standard potentials of basic disinfectants.

Compound	**Formula**	**Potential [V]**	**Approximated course of reaction**
Chlorine	Cl_2	1.36	$Cl_2 + 2e^- \lambda\ 2Cl^-$
Bromine	Br_2	1.09	$Br_2 + 2e^- \lambda\ 2Br^-$
Iodine	I_2	0.54	$J_2 + 2e^- \lambda\ 2J^-$
Ozone	O_3	2.07	$O_3 + 2e^- + 2H^+ \lambda\ O_2 + H_2O$
Chlorine dioxide	ClO_2	1.91 0.95	$ClO_2 + 5e^- + 2H_2O \lambda\ Cl^- + 4OH^-$ $ClO_2 + e^- \lambda\ ClO_2^-$

If the mechanism for determining the efficiency of disinfection is the diffusion into cells, the germicidal qualities of the compound are determined by the molecular weight and charge. Therefore, in the halogen group this series would be as follows: $I_2 > Br_2 > Cl_2$.

Thus, the choice of disinfectant must take into account the above-mentioned issues as well as possible disinfection by-products and their health effects for water consumers. In most disinfection operations, the destruction of microorganisms is a multistage process during which a wide range of physical, chemical and biological phenomena can be distinguished.

To estimate the process effects, many disinfection models are used based on experimental data.

The basic **model of disinfection kinetics** is the Chick-Watson model [15]. It defines the destruction rate of microorganisms as a chemical reaction of the first order:

$$\frac{dN}{dt} = -kN \tag{403}$$

and in an integrated form

$$\ln\frac{N}{N_o} = -kt \tag{404}$$

In the above equation

- N – number of living organisms present after time t,
- N_o – initial number of living organisms,
- k – velocity rate [s^{-1}], dependent on the type of disinfectant, type of microorganism and water quality,
- t – reaction time [s].

A modified form of the above equation taking into account the changes in the disinfectant concentration is as follows:

$$\ln\frac{N}{N_o} = -LC^n t \qquad (5.405)$$

where:

C – disinfectant concentration [g/m^3],
L – specific lethality coefficient,
n – dilution coefficient.

The coefficient n depends on the pH of the solution and disinfectant type. Its value is in approximation equal to unity.

The lethality coefficient L defines the disinfectant efficiency at its unitary concentration in unit time. A graphical interpretation of the specific lethality coefficient is presented in Figure 31 [10].

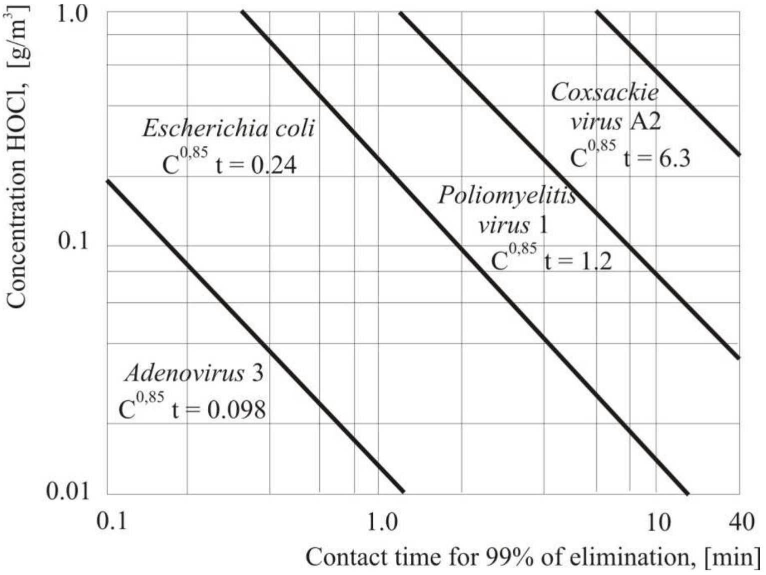

Fig. 31. Relation between time required for 99% deactivation of microorganisms and the concentration of HOCl.

Table 16 presents the values of coefficients for the specific lethality of alternative disinfectants in relation to selected bacteria, viruses and resting spores with water pH = 7 and temperature 20°C [64].

Table 16.The values of specific lethality coefficients of alternative disinfectants.

Disinfectant	***E. coli*** **Bacteria**	***Poliovirus* 1**	**Resting spores of *Entamoeba Histolytica***
O_3	2,300	920	3.1
HOCl	19.2	4.6	0.23
ClO_2	16.0	2.4	–
OCl	5.0	0.44	–
$NHCl_2$	0.84	0.00092	–
NH_2Cl	0.12	0.014	–

The coefficient values presented in Table 16 indicate that the most effective disinfectant is ozone followed by hypochlorous acid. The weakest disinfectants are chloramines.

The application of the Chick-Watson model is limited due to the fact that usually the speed of destroying organisms does not have a constant value. It is dependent on the type of organism, disinfectant form and its changing concentration.

Another model assuming that the deactivation rate is not described by a first order reaction, but instead decreases during the process is the Gard model [28]. The equation defining the deactivation drop rate is as follows:

$$-\frac{dN}{dt}=\frac{kN}{1+a(Ct)} \tag{406}$$

or in an integrated form

$$\frac{N}{N_o}=[1+a(Ct)]^{(-k/a)} \tag{407}$$

where:

N – concentration of living organisms after time t,
C – disinfectant concentration maintained at a constant level,
k – deactivation rate of the first order in time t=0,
a – velocity coefficient.

Collins and Selleck [18, 82] have observed that often at the beginning of disinfection there is stationary phase in which the population of microorganisms does not change and the deactivation rate is not constant. The velocity equation according to the Collins-Selleck model takes the same form as the equation in the Chick-Watson model (403), but to solve it the following boundary conditions are assumed:

$$k=0 \quad \text{for} \quad C\cdot t<\tau \tag{408}$$

$$k=k^{*} \quad \text{for} \quad C\cdot t=\tau \tag{409}$$

$$k = \frac{k^*}{b\left(C \cdot t\right)} \quad \text{for} \quad C \cdot t > \tau \tag{410}$$

τ is the product of the disinfectant concentration and the time that must pass until deactivation begins.
After integrating Equation (403) with the boudary conditions (408), (409) and (410), the velocity equation takes the form:

$$\frac{N}{N_o} = 1 \quad \text{for} \quad C \cdot t < \tau \tag{411}$$

$$\frac{N}{N_o} = \left(\frac{C \cdot t}{\tau}\right)^{-k^*/b} \quad \text{for} \quad C \cdot t > \tau \tag{412}$$

Parameter values of the Collins-Selleck model in relation to the *coli* bacteria present in various solutions depending on the type of disinfectant are in the following ranges:

- for chlorine: $\tau = 0.59 \div 4.06$; $-k^*/b = 2.12 \div 2.82$,
- for chlorine dioxide: $\tau = 0.03 \div 0.89$; $-k^*/b = 0.75 \div 0.81$ [95].

The empirical Horn model based on Chick-Watson equations has the following form [39]:

$$\frac{dN}{dt} = -LNt^mC^n \tag{413}$$

in which m is a parameter dependent on disinfectant and microorganism type. To deactivate *E. coli* bacteria with chlorine, the assumed value $m = 2$ [23].

Another class of models can be obtained assuming that deactivation is a reaction of a different order than the first order with respect to the concentration of surviving microorganisms. An example of this type of model is the model developed by Roy for deactivating the *poliovirus* 1 using ozone with a zero ozone-demand to oxidate water components [78, 79]:

$$\frac{dN}{dt} = -kCN^{0.69} \tag{414}$$

In the above equation k is the reaction velocity constant.

An equation with a similar form approximates well the deactivation process of *E. coli* with the use of chlorine dioxide [9].

Usually, the kinetics of microorganism deactivation is determined in partial reactors. When applying disinfection kinetics models with the use of UV rays, the chemical disinfectant concentration is replaced by the exposure rate expressed in units of energy per units of surface [33].

8.4.1. Example Calculations

EXAMPLE 1

Compare the necessary contact times for the 99% elimination of *E. coli* bacteria with ozone, hypochlorous acid, chlorine dioxide and monochloramine when using equal disinfectant doses of 2 g/m^3.

Lethality coefficients (L) taken from Table 16 are 2,300; 19.2; 16 and 0.12, respectively.

The necessary contact times were determined from a modified form of Equation (405):

$$t = -\frac{\ln\frac{N}{N_o}}{LC^n} = -\frac{\ln 0.01}{L \cdot 2^1} = \frac{4.605}{L}$$

$$t_{O_3} = \frac{4.605}{2{,}300} = 2 \cdot 10^{-3} \ \ s$$

$$t_{HOCl} = \frac{4.605}{19.2} = 0.24 \ \ s$$

$$t_{ClO_2} = \frac{4.605}{16} = 0.29 \ \ s$$

$$t_{NH_2Cl} = \frac{4.605}{0.12} = 38.37 \ \ s$$

9. PHYSICO-CHEMICAL METHODS OF WATER TREATMENT

Using hybrid reactors in which several unit processes, both physical and chemical, are conducted simultaneously is one of the methods of purifying water having a relatively good quality, that is free of suspended matter.
Among this type of simultaneously conducted processes there are

- upflow sludge blanket flocculation & coagulation,
- upflow direct sand filtration,
- upflow direct GAC filtration & adsorption.

9.1. Upflow sludge Blanket Flocculation & Sedimentation

The concept of performing coagulation in a layer of suspended sludge was developed at the beginning of the last century and the intensive use of this method and research for its optimization dates back to the 1950s [62].
Due to the mechanism of coagulation-flocculation, a suspended sediment layer can be compared with the process implemented in a volumetric system. The hydraulic phenomena are similar to the phenomena occurring in the process of coagulation-flocculation in porous media, i.e. in the processes of so-called "surface coagulation" and "contact coagulation" [60].

Flocculation in a suspended sediment layer is carried out during the flow through the layer. The process is intensified through the use of the catalytic and sorption properties of the sludge so that the dose of coagulant needed to achieve the relevant parameters of purified water is lower in comparison with the process of volumetric coagulation [49].

The principle of operation of suspended sediment is based on fluidized bed hydrodynamics which determines the phase separation, mass transport, mixing conditions and the structure of the suspended sediment depending on the flow rate. The floc surface is irregular and the sizes vary considerably affecting the sedimentation velocity. For the analysis of the process, the sedimentation velocity for a floc of medium size is assumed. In vertical flow at low turbulence the influence of irregular particle shapes on sedimentation velocity can be neglected.
The equation for a single particle sedimentation velocity (V_s) can be defined based on Allen's equation of the form [93]

$$V_s = \frac{1}{2}\left(\frac{\rho_p - \rho_w}{\rho_w} g\right)^{2/3} \frac{a - \frac{2}{5}\bar{a}}{\mu^{1/3}} \qquad (415)$$

where:

ρ_ω and ρ_p – are water density and floc density, respectively [kg/m^3],

$g = 9.81$ m/s^2 – gravitational acceleration,

μ – water kinematic viscosity [m^2/s],

a – particle radius [m],

$\bar{a}$ – upper boundary radius of a particle, at which the sedimentation rate is described by the Stokes equation [m].

Optimum flow rate (V_f) in a fluidal layer is described by the principle:

$$V_f = V_s \cdot \varepsilon^m \qquad (416)$$

in which

$\varepsilon \in (0; 1)$ – porosity,

m – parameter independent from Reynolds number and the shape of sedimenting floc, varying in the range from $m = 2.5$ for turbulent flow to $m \le 5$ for laminar flow.

Maximum flow rates through suspended sediment layer must be used while simultaneously maintaining the layer stability. Restrictions on using high speeds result from the mechanical properties of flocs which depend on raw water, coagulants and the flocculants used [93].

The optimum range of applied flow rates is

- when using aluminum sulfate $V_p = 2.2 \div 4.7$ m/h,
- when using aluminum sulfate with the addition of active silica $V_p = 4.3 \div 9.0$ m/h,
- when using chlorinated iron sulfate $V_p = 2.9 \div 7.2$ m/h.

The structure of suspended sediment should be uniform and the parameter describing this structure is the cohesion coefficient. This coefficient determines the increase of flow velocity corresponding to the increased unit expansion of the layer. The relation between flow velocity (V_f), cohesion coefficient (k) and layer expansion (E) is presented in conformity with the relation:

$$V_f = k(E-1) \qquad (417)$$

The physical interpretation of the cohesion coefficient is the flow rate at the sediment expansion E = 2.

At the flow rate 3.6 ÷ 4.5 m/h sediments are rinsed from the suspended sediment layer. At velocities in the range of 9 ÷ 10 m/h the structure of sediment is broken [50].

Suspended sediment with a proper structure is characterized by values of the cohesion coefficient in the range 1.2 ÷ 1.5 m/h.

The layer porosity is closely correlated with layer expansion and sediment hydration. Porosity or hydration of sediment is used to evaluate the hydraulic conditions in the layer [63].

Sediment porosity (ε) is defined by the relation

$$\varepsilon = \frac{V_w}{V_w + V_p} \tag{418}$$

in which V_w and V_p – are volumes of water and flocs in the layer, respectively. Assuming that the floc density is approximately equal to water density

$$\varepsilon = \frac{M_w}{M_w + M_p} \tag{419}$$

M_w and M_p are the water and floc masses, respectively.

Sediment hydration (u) is defined as

$$u = \frac{M_w + M_{wc}}{M_w + M_{wp} + M_{fs}} \tag{420}$$

M_{wp} and M_{fs} are the masses of water in the floc and sold phase, respectively. Comparing Equations (419) and (420) leads to a formula defining the relation between the porosity of the suspended sediment layer and sediment hydration

$$\varepsilon = \frac{u}{1 + \frac{M_{wp}}{M_w}} \tag{421}$$

Substituting relation (421) into (416) an equation for the optimum flow rate as a function of sediment hydration and water mass in the reactor is obtained:

$$V_f = V_s \left(\frac{u}{1 + \frac{M_{wp}}{M_w}} \right)^m \tag{422}$$

Solving the system of Equations (417) and (422) leads to a formula defining the cohesion coefficient (k) as a function of porosity and expansion of the layer

$$k = \frac{V_s\, \varepsilon^m}{E - 1} \tag{423}$$

Water temperature has a major impact on the course of the process. According to

Equation (415), the influence of temperature on flow rate is connected with the change in water viscosity and can be defined as

$$\frac{V_{f_1}}{V_{f_2}} = \left(\frac{\mu_2}{\mu_1}\right)^{1/3} \tag{424}$$

In temperature range 277 ÷ 293K the velocity ratio falls into the range 0.825 ÷ 1.0. This means that a temperature change of 16K which occurs in real technological water treatment systems causes a 17.5% decrease in the flow rate in suspended sediment. This change can be reduced by maintaining the proper floc density.
The influence of floc density on the sediment flow rate is defined by the relation:

$$\frac{V_{f_1}}{V_{f_2}} = \left(\frac{\rho_{c_1} - \rho_{w_1}}{\rho_{c_2} - \rho_{w_2}}\right)^{2/3} \tag{425}$$

Maintaining the stable operation of reactors with suspended sediment and thus maintaining a constant efficiency with a changing water temperature requires keeping the following conditions in the reactor

$$\left(\frac{\rho_{c_1} - \rho_{w_1}}{\rho_{c_2} - \rho_{w_2}}\right)^{2/3} = 1.2 \tag{426}$$

According to the above reaction, it is necessary to increase the floc density (ρ_{c_1}) by approximately 1.5% in water with a temperature of 277K in relation to the floc density in water with a temperature of 293K. This is achieved by the use of high molecular weight compounds during low temperatures, such as polyelectrolytes [62].

The conditions for creating and destroying suspended sediment flocs are characterized by velocity gradients.
The average gradient of the liquid flow rate (G) in the suspended sediment layer is defined by the formula [92]:

$$G = \sqrt{\frac{C \cdot g \cdot V_f (\rho_c - \rho)}{(1-C)\rho \cdot \mu}} \tag{427}$$

where C is the volumetric concentration of the flocs.
The designated value of the gradient for a stable system is a few s^{-1} [58]. The size and compactness of a floc depends on the size of the gradient. For large values of G, small but comprimated flocs are formed. For small values of G, large flocs with a loose structure are generated. Small gradient values guarantee a high efficiency for the simultaneous execution in one reactor of flocculation and sedimentation.

9.2. Upflow Direct Sand Filtration

Another step in the development of water treatment technologies in relation to coagulation in a suspended sediment layer is contact coagulation in a filter layer (upflow direct sand filtration). This process is carried out in one reactor in which the processes of coagulation, flocculation, sedimentation and filtration run simultaneously. The resulting gel in the filter bed is accumulated not only in the intergranular space, but also on the surface creating a network structure instead of a single floc. It is caused by cohesion and adhesion forces which occur between the colloid and porous medium particles and the forces of adsorption, mainly between the sol particles and hydroxides $Al(OH)_3$ or $Fe(OH)_3$ [60].

The structures formed in the bed intensify coagulation which results in the increase of the coagulant dose. Flocculation proceeds faster in the bed compared to flocculation in separate columns and flocculation in a suspended sediment layer. Another advantage of this method is the decrease of the negative effect of low water temperatures on purification results. Water quality is the main restriction for its application. The suspended solid content together with post-coagulation suspensions should not exceed 150 g/m^3 [52, 53].

For the system of contact coagulation in a filter layer one can apply the formula suggested by Camp and Stein of the general velocity gradient (Equation 76). When there is no possibility to estimate the system geometry and immediate application of equation (76), the value of the velocity gradient can be determined from the equation of energy dissipation given by Camp [13] (Equation 16), which in a rearranged form is as follows

$$G = \sqrt{\frac{P}{\eta F \cdot H \cdot \varepsilon}} \qquad (428)$$

In the above equation

F – surface of bed intersection [m^2],
H – bed height [m],
ε – layer porosity.

Energy dissipation in a filtration bed (P) in contact coagulation can be estimated on the basis of pressure loss (h) and flow rate (Q), which are correlated in the equation:

$$P = Q(\rho_m - \rho_w)\, g\, h \qquad (429)$$

in which ρ_m and ρ are densities of the filter material and water, respectively [kg/m^3].

Substituting Equation (429) to formula (428) one obtains the formula of the mixing velocity gradient in a filtration bed [49]

$$G = \sqrt{\frac{h\left(\rho_m - \rho_w\right) g \cdot V_p}{H \cdot \varepsilon \cdot \eta}} \tag{430}$$

A known formula defining pressure loss in a filtration bed (h) with laminar flow which can be applied for the analysis of contact coagulation is the Kozena formula [49] in the form:

$$\frac{h}{H} = \frac{K\,\eta\left(1-\varepsilon\right)^2}{\rho_w\;g\;\varepsilon^3}\,s^2\;V_f \tag{431}$$

where

K – dimensionless Kozena constant,

s – ratio of grain surface to its density (in case of irregular particle $s = 6/\psi d_m$),

d_m – representative grain diameter [m],

ψ – grain sphericity.

Thus, the formula for the mixing velocity gradient in a filtration bed takes the following form [60]:

$$G = \frac{1-\varepsilon}{\varepsilon}\,\frac{V_p}{d_m}\sqrt{\frac{\rho_m - \rho_w}{\rho_w}\,K_m} \tag{432}$$

in which K_m is the modified Kozena constant

$$K_m = \frac{36\,K}{\psi^2} \tag{433}$$

For laminar flow in the velocity range: $V_f = 3 \div 12.5$ m/h and for representative grain diameters $d_m = 0.5 \cdot 10^{-3} \div 2.0 \cdot 10^{-3}$ m the Kozena constant is about 5 [23]. Assuming a sphericity of layer grains $\psi = 0.85$, the modified Kozena constant is $K_m = 249.1$.

A final form of the equation of mixing velocity gradient with laminar flow is as follows:

$$G = 15.75\,\frac{1-\varepsilon}{\varepsilon^2}\,\frac{V_p}{d_m}\sqrt{\frac{\rho_m - \rho_w}{\rho_w}} \tag{434}$$

For example, for a quartz sand layer ($\rho_m = 2{,}600$ kg/m^3) of a representative grain diameter $d_m = 0.6 \cdot 10^{-3}$ m, porosity $\varepsilon = 0.4$ and at the recommended range of flow velocity $V_f \in (3 \div 6$ m/h), the mixing velocity gradient varies from 104 s^{-1} to 207 s^{-1}. During the cycle of contact coagulation at a constant flow rate the mixing velocity gradient increases because the layer porosity decreases.

A very important parameter deciding the course of the process is the shearing stresses (τ) in the bed defined by the formula [46]:

$$\tau = \frac{d_m}{4} \cdot \rho \cdot g\left(\frac{\rho_m}{\rho_w} - 1\right)\frac{h}{H}\,\frac{\varepsilon - \delta}{\varepsilon} \tag{435}$$

in which parameter δ is defined as the degree of bed contamination.

The values of shearing stresses determined from the above equation during a filtration cycle vary depending on the type of filter material in the range [59]:

– sand bed	– $\tau = 0,23 \div 5,32\ \mathrm{Nm}^{-2}$,
– anthracite bed	– $\tau = 0,125 \div 1,95\ \mathrm{Nm}^{-2}$,
– activated carbon bed	– $\tau = 0,04 \div 0,57\ \mathrm{Nm}^{-2}$.

In beds of lower density, shearing stresses are lower; therefore, the structure of flocs in these beds is less prone to destruction and the conditions of flow stoppage are better.

Numerous research and analyses have shown [71] that exceeding the mixing velocity gradient $G = 220\ \mathrm{s}^{-1}$ causes a change in the bed working conditions and a destruction of floc structure. Shearing stresses were then equal to $1.2\ \mathrm{Nm}^{-2}$.

For the bed analyzed above, at a flow velocity $V_f = 3$ m/h, the mixing velocity gradient $G = 220\ \mathrm{s}^{-1}$ is achieved when the layer porosity decreases from the initial value $\varepsilon = 0.4$ to the value $\varepsilon = 0.297$. At the flow velocity $V_f = 6$ m/h the gradient $G = 220\ \mathrm{s}^{-1}$ is achieved when the porosity drops to the value $\varepsilon = 0.391$.

Another important parameter for design and operation of upflow direct filtration is bed run time. Bed run time can be defined on the basis of filtration Equation (128) assuming the function:

$$-\frac{\delta C}{\delta H} = \lambda C \tag{436}$$

The above function is based on the assumption that the change of the suspended solid concentration due to flow through the elementary bed layer is proportional to its initial concentration and filtration coefficient λ, which can be defined by equation [40]:

$$\lambda = \frac{6\left(1-\varepsilon\right)\Delta r}{\varepsilon\,\psi\,d_m\,H} \tag{437}$$

in which Δr – increase of grain diameter due to the accumulation of suspended solids in the bed, dependent on time.

The initial form of the filtration equation after taking into account the definition of the filtration constant is modified to the following form:

$$V_p\,\frac{6\left(1-\varepsilon\right)\Delta r}{\varepsilon\,\psi\,d_m\,H}\,C = \frac{dq}{dt} \tag{438}$$

value Δr varies from 0 at the beginning of the cycle to γ, which is equal to a part of the intergranular capillary radius.

After separating variables and integrating from $t = 0$ to $t = t_c$, where t_c is bed run time time and from $q = 0$ to $q = q_{max}$, where q_{max} is maximal bed capacity for suspended solids per unit intergranular space volume, and after taking into account the formula for the integranular capillary radius (283) one obtains

$$t_c = \frac{q_{max} \cdot \psi \cdot H}{V_f \cdot \gamma \cdot C_{ac}} \tag{439}$$

For the analyzed bed and porosity change from the value $\varepsilon = 0.4$ to $\varepsilon = 0.297$ the value of parameter γ in the equation of the length of filtration cycle is 0.32. With a porosity change from $\varepsilon = 0.4$ to $\varepsilon = 0.391$ γ is 0.031.

The concentration of suspended solids flowing into the contact filter (C_{ac}) can be determined from the equation [53]:

$$C_{ac} = C_{ss} + kD_c + 0.25C + Z \tag{440}$$

in which:

C_{ss} – suspended solids concentration in raw water [g/m^3],

k – coefficient dependent on coagulant type and the degree of its contamination (for purified aluminum sulfate k = 0.55),

D_c – coagulant dose [g/m^3],

C – color of raw water [gPt/m^3],

Z – the amount of insoluble compounds in coagulant [g/m^3].

Because contact coagulation is used for waters with no turbidity, $C_{ss} = 0$. Assuming that N = 0, Equation (440) takes the following form:

$$C_{ac} = 0.55D_c + 0.25C \tag{441}$$

The optimum dose in the case of contact coagulation is merely about 50% of the optimal dose in volumetric coagulation.

Assuming that the filtration mechanism can be analyzed by certain analogies with the process of thickening in which the flocs colliding with each other squeeze water off their structure while the hydraulics of the flow through a layer causes comprimation of sediment, it can be assumed that the initial concentration of postcoagulation sediment (C_{ac}) increases in the bed to a level similar as in the thickened sludge at the end of the cycle. This final suspended solid concentration is a measure of the suspended solid bed capacity (q_{max}).

At a determined initial (w_o) and final (w_T) the water content of sediment in the bed, the suspended solid bed capacity is defined by the formula:

$$q_{max} = C_{ac}\frac{100 - w_T}{100 - w_o} \tag{442}$$

Estimated doses of aluminum sulfate for the maximum removal of color caused by humic substances in the range 30 ÷ 120 gPt/m^3 in raw water using contact coagulation, as well as the concentration of post-coagulation sediment formed and its hydration are summarized in Table 16 [61].

Table 16. Optimum coagulant dose for various initial color values of water, post-coagulation sediment concentration and its hydration at the beginning of contact coagulation.

Raw water color	**$Al_2(SO_4)_3 \cdot 18H_2O$ dose**	**Post-coagulation sediment concentration C_{ac}**	**Post-coagulation sediment hydration w_o**
gPt/m^3	g/m^3	g/m^3	%
30	19	18	99.9982
60	27	30	99.997
90	33	41	99.9959
120	38	51	99.9949

The final post-coagulation sediment concentration (w_T) does not depend in a major way on raw water color and coagulant dose [61], but it depends on flow rate and changes from $w_T = \sim 99.91$ at $V_f = 3.0$ m/h to $w_T = \sim 99.991$ at $V_p = 6.0$ m/h.
The final hydration (water content) is inversely proportional to the coefficient γ in the equation of filtration cycle length.

9.2.1. Example Calculations

EXAMPLE 1

Water of color 30 gPt/m^3 is purified in the process of contact coagulation with a dose of aluminum sulfate $D_c = 20$ g/m^3 in the bed of a height 2.0 m, layer porosity $\varepsilon = 0.4$; representative grain diameter $d_m = 0.6 \cdot 10^{-3}$ m, grain sphericity $\psi = 0.85$ and density $\rho_m = 2{,}600$ kg/m^3.
Determine the bed run time as a linear function of flow rate. Make calculations for $V_f = 3$; 4; 5 and 6 m/h.

Defining layer porosity in the end of filtration cycle from a modified form of Equation (434):

$$\frac{\varepsilon^2}{1-\varepsilon} = \frac{15.75}{G}\frac{V_f}{d_m}\sqrt{\frac{\rho_m - \rho_w}{\rho_w}}$$

in which G is the critical mixing velocity gradient causing deterioration of floc structure $G = 220$ s^{-1}.

a) defining final bed porosity at:
   $V_f = 3.0$ m/h $= 8.33 \cdot 10^{-4}$ m/s:

$$\frac{\varepsilon_1^2}{1-\varepsilon_1}=\frac{15.75}{220}\cdot\frac{8.33\cdot10^{-4}}{6\cdot10^{-4}}\sqrt{\frac{2,600-1,000}{1,000}}=0.125$$

$$\varepsilon_1=0.297$$

b) defining final bed porosity at:
$V_f = 4.0$ m/h $= 11.1\cdot10^{-4}$ m/s:

$$\frac{\varepsilon_2^2}{1-\varepsilon_2}=\frac{15.75}{220}\cdot\frac{11.1\cdot10^{-4}}{6\cdot10^{-4}}\sqrt{1.6}=0,167$$

$$\varepsilon_2=0.334$$

c) defining final bed porosity at:
$V_f = 5.0$ m/h $= 13.89\cdot10^{-4}$ m/s:

$$\frac{\varepsilon_3^2}{1-\varepsilon_3}=\frac{15.75}{220}\cdot\frac{13.89\cdot10^{-4}}{6\cdot10^{-4}}\sqrt{1.6}=0.210$$

$$\varepsilon_3=0.365$$

d) defining final bed porosity at:
$V_f = 6.0$ m/h $= 16.67\cdot10^{-4}$ m/s:

$$\frac{\varepsilon_4^2}{1-\varepsilon_4}=\frac{15.75}{220}\cdot\frac{16.67\cdot10^{-4}}{6\cdot10^{-4}}\sqrt{1.6}=0.251$$

$$\varepsilon_4=0.391$$

Defining parameter γ of filtration cycle length equation (Equation 439):

$$\gamma=\frac{r_{k(\varepsilon)}-r_{k(\varepsilon_1)}}{r_{k(\varepsilon)}}$$

$$x=r_{k(\varepsilon)}-r_{k(\varepsilon_1)}=\frac{\varepsilon d_m}{6(1-\varepsilon)}-\frac{\varepsilon_1(d_m+2x)}{6(1-\varepsilon_1)}$$

$$x=\frac{0.4\cdot6\cdot10^{-4}}{6(1-0.4)}-\frac{\varepsilon_1(d_m+2x)}{6(1-\varepsilon_1)}$$

a) parameter γ at $V_f = 3.0$ m/h:

$$x=6.67\cdot10^{-5}-\frac{0.297(6\cdot10^{-4}+2x)}{6(1-0.297)}$$

$$x=6.67\cdot10^{-5}-4.225\cdot10^{-5}-0.14x$$

$$x=2.145\cdot10^{-5}$$

$$\gamma = \frac{2.145 \cdot 10^{-5}}{6.67 \cdot 10^{-5}} = 0.32$$

b) parameter γ at $V_f = 4.0$ m/h:

$$x = 6.67 \cdot 10^{-5} - \frac{0.334\left(6 \cdot 10^{-4} + 2x\right)}{6\left(1 - 0.334\right)}$$

$$x = 6.67 \cdot 10^{-5} - 5.015 \cdot 10^{-5} - 0.167x$$

$$x = 1.418 \cdot 10^{-5}$$

$$\gamma = \frac{1.418 \cdot 10^{-5}}{6.67 \cdot 10^{-5}} = 0.212$$

c) parameter γ at $V_f = 5.0$ m/h:

$$x = 6.67 \cdot 10^{-5} - \frac{0.365\left(6 \cdot 10^{-4} + 2x\right)}{6\left(1 - 0.365\right)}$$

$$x = 6.67 \cdot 10^{-5} - 5.748 \cdot 10^{-5} - 0.191x$$

$$x = 7.74 \cdot 10^{-6}$$

$$\gamma = \frac{7.74 \cdot 10^{-6}}{6.67 \cdot 10^{-5}} = 0.116$$

d) parameter γ at $V_f = 6.0$ m/h:

$$x = 6.67 \cdot 10^{-5} - \frac{0.391\left(6 \cdot 10^{-4} + 2x\right)}{6\left(1 - 0.391\right)}$$

$$x = 6.67 \cdot 10^{-5} - 6.42 \cdot 10^{-5} - 0.214x$$

$$x = 2.06 \cdot 10^{-6}$$

$$\gamma = \frac{2.06 \cdot 10^{-6}}{6.67 \cdot 10^{-5}} = 0.031$$

Determining the suspended solids concentration in the contact filter inflow (Equation 441):

$$C_{ac} = 0.55D_c + 0.25C = 0.55 \cdot 20 + 0.25 \cdot 30 = 18.5\ g/m^3$$

The suspended solids bed capacity with sediment hydration in the inflow $w_o = 99{,}9982\%$ and with the hydration of sediment accumulated in the bed w_T, which is dependent on flow rate and inversely proportional to parameter γ (Equation 442):

a) q_{max} at $V_f = 3.0$ m/h:
$w_T = 99.91\%$

$$q_{max} = C_{ok} \cdot \frac{100 - w_T}{100 - w_o} = 18.5 \cdot \frac{100 - 99.91}{100 - 99.9982} = 925\ g/m^3$$

b) q_{max} at $V_f = 4.0$ m/h:
$w_T = 99.94\%$

$$q_{max} = 18.5 \cdot \frac{100 - 99{,}94}{100 - 99.9982} = 612.55\ g/m^3$$

c) q_{max} at $V_f = 5.0$ m/h:
$w_T = 99.94\%$

$$q_{max} = 18.5 \cdot \frac{100 - 99.94}{100 - 99.9982} = 616.67\ g/m^3$$

d) q_{max} at $Vp = 6.0$ m/h:
$w_T = 99.9913\%$

$$q_{max} = 18.5 \cdot \frac{100 - 99.9913}{100 - 99.9982} = 96.42\ g/m^3$$

Filtration cycle time (Equation 439):

a) at $V_f = 3.0$ m/h:

$$t_c = \frac{\psi \cdot H \cdot q_{max}}{V_p \cdot \gamma \cdot C_{ac}} = \frac{0.85 \cdot 2.0 \cdot 925}{3.0 \cdot 0.32 \cdot 18.5} = 88.54\ h = \approx 3.7\ d$$

b) at $V_f = 4.0$ m/h:

$$t_c = \frac{0.85 \cdot 2.0 \cdot 612.55}{4.0 \cdot 0.212 \cdot 18.5} = 66.38\ h \approx 2.8\ d$$

c) at $V_f = 5.0$ m/h:

$$t_c = \frac{0.85 \cdot 2.0 \cdot 335.05}{5.0 \cdot 0.116 \cdot 18.5} = 53.1\ h \approx 2.2\ d$$

d) at $V_f = 6.0$ m/h:

$$t_c = \frac{0.85 \cdot 2.0 \cdot 96.42}{6.0 \cdot 0.031 \cdot 18.5} = 47.63\ h \approx 2\ d$$

9.3. Upflow Direct GAC Filtration & Adsorption

In contact filters with a sand bed, in addition to the processes of flocculation, sedimentation and filtration, there is the process of adsorption of dissolved contaminants on generated and accumulated flocs in the bed. These flocs have a relatively large specific surface and good adsorption qualities [51]. An intensification of adsorption can be achieved by replacing part of the sand layer with an adsorption layer, e.g. activated carbon [4, 5].

Modeling coagulation-adsorption processes in an activated carbon layer is based on the rules for modeling upflow direct filtration (chapter 9.2.), i.e.

- determining final bed porosity with the assumed hydrodynamics of the process and at a maximum definite mixing velocity gradient (Equation 434) in order to determine parameter γ of the filtration cycle length equation (Equation 439)
- determining the filtration cycle length as a function of initial concentration of the post-coagulation suspended solids (Equation 440), γ and ψ parameters and the layer height H (Equation 439).

Additional elements of the model are the following equations:

- efficiency of adsorption process on activated carbon as a function of medium diffusivity changing during the cycle,
- the extent of the exploitation of layer sorption capacity during one filtration cycle,
- number of filtration cycles to break through the layer.

These equations also take into account the adsorption properties of the post-coagulation sediment generated and accumulated in the bed.

To describe the adsorption efficiency for the process of contact coagulation with an adsorption bed, Fick's First Law equation of steady diffusion can be used (Equation 141). The element of the column adsorption height h and the intergranular capillary radius r_k can be converted to the form [56]:

$$\frac{d}{dt}\left(C_e - C_f\right)\pi r^2 h = -2D_m \pi r h \frac{dC}{dr} \qquad (443)$$

in which C_e and C_f are the concentration in the reactor outflow and in the boundary layer, respectively [g/m^3]

and then

$$-\frac{d}{dt}\left(C_e - C_f\right)\int_{r_a}^{r_a + r_k} \frac{r}{2} dr = D_m \int_{C_f}^{C_e} dC \qquad (444)$$

and

$$-\frac{d}{dt}\left(C_e - C_f\right)\left[\frac{\left(r_a + r_k\right)^2}{4} - \frac{r_a^2}{4}\right] = D_m\left(C_e - C_f\right) \tag{445}$$

$$-\frac{d}{dt}\left(C_e - C_f\right) = \frac{4D_m}{r_k\left(2r_a + r_k\right)}\left(C_e - C_f\right) \tag{446}$$

In the above equations, r_a is the adsorbent particle radius [m].

With the assumption that the concentration in the boundary film is constant (C_f = constant) equation (446) takes the following form:

$$\frac{dC_e}{dt} = -\frac{4D_m}{r_k\left(d_m + r_k\right)}\left(C_e - C_f\right) \tag{447}$$

d_m is a representative adsorbent particle diameter [m].

Substituting into the above equations:

$$C_e = C_o - C_a \tag{448}$$

$$\delta = \frac{C_a}{C_r} \tag{449}$$

where C_o, C_a and C_r are initial, adsorbed and equilibrium concentrations, respectively, [g/m^3], the following form of Equation (447) is achieved:

$$\frac{d}{dt}\left(C_o - \delta C_r\right) = -\frac{4D_m}{r_k\left(d_m + r_k\right)}\left(C_o - \delta C_r - C_f\right) \tag{450}$$

$$-C_r\frac{d\delta}{dt} = -C_r\frac{4D_m}{r_k\left(d_m + r_k\right)}\left(\frac{C_o}{C_r} - \delta - \frac{C_f}{C_r}\right) \tag{451}$$

Assuming that the desorption taking place is insignificant($C_f << C_r$), Equation (451) is simplified to the form:

$$\frac{d\delta}{dt} = -\frac{4D_m}{r_k\left(d_m + r_k\right)}\left(\frac{C_o}{C_r} - \delta\right) \tag{452}$$

and

$$\frac{C_r}{C_o}\frac{d\delta}{dt} = \frac{4D_m}{r_k\left(d_m + r_k\right)}\frac{C_r}{C_o}\left(\frac{C_o}{C_r} - \delta\right) \tag{453}$$

$$\frac{C_r}{C_o}\frac{d\delta}{dt} = \frac{4D_m}{r_k\left(d_m + r_k\right)}\left(1 - \frac{C_r}{C_o}\delta\right) \tag{454}$$

After separating variables and integrating:

$$\int \frac{\frac{C_r}{C_o}\, d\delta}{\left(1-\frac{C_r}{C_o}\delta\right)} = \int \frac{4D_m dt}{r_k\left(d_m + r_k\right)} \tag{455}$$

one achieves

$$-\ln\left(1-\frac{C_r}{C_o}\delta\right) = \frac{4D_m}{r_k\left(d_m + r_k\right)}\, t \tag{456}$$

$$-\ln\frac{C_e}{C_o} = \frac{4D_m}{r_k\left(d_m + r_k\right)}\, t \tag{457}$$

Defining the integranular capillary radius (r_k) with Equation (283), relation (457) becomes modified to the form:

$$t = \frac{\varepsilon\, d_m^2\left[6\left(1-\varepsilon\right)+\varepsilon\right]}{144\left(1-\varepsilon\right)^2 D_m} \ln\frac{C_e}{C_o} \tag{458}$$

The above equation allows the determination of the diffusion time required to obtain the assumed concentration of C_e in the outflow from the reactor.

The effect of adsorption (C_e/C_o) in an activated carbon layer is defined by a modified form of Equation (458) [6]:

$$\frac{C_e}{C_o} = \exp\left(-\frac{H}{V_p}\,\frac{144\left(1-\varepsilon\right)^2 D_m}{\varepsilon d_m^2\left[6\left(1-\varepsilon\right)+\varepsilon\right]}\right) \tag{459}$$

Adsorption on activated carbon in one filtration cycle of upflow direct filtration takes several steps. At the beginning of the cycle, dissolved adsorbate particles diffuse into the grains of activated carbon with the molecular diffusion coefficient (D_m) defined by the Stokes-Einstein equation (Equation 63) if the adsorbate particles are defined or at specific molecular diffusion coefficient D_{mz} (Equation 266) if the adsorbate is defined as total organic carbon. The viscosity in these equations is then the post-coagulation sediment viscosity whose concentration is determined by Equation (441).

With the increase in the suspended solid concentration in the bed, the molecular diffusion coefficient decreases because the medium average viscosity increases. As flow conditions do not change during the cycle, the time of contact with the layer is constant and the effects of adsorption on activated carbon deteriorate. Deterioration of these effects is slightly compensated for by the sorption of dissolved contaminants in the sediment retained in the layer. Thus, the concentration of adsorbate in the outflow from the column, taking into account the sorption properties of sediment at the beginning and end of the filtration cycle, is respectively

$$C_e^p = C_o^p \exp\left(-AD_h^p\right) = \left(C_o - x_{os}\, C_{ok}\right)\exp\left(-AD_{mz}^p\right) \tag{460}$$

$$C_e^k = C_o^k \exp\left(-AD_h^k\right) = \left(C_o - x_{os}\, q_{max}\right)\exp\left(-AD_{mz}^k\right) \tag{461}$$

In the above equations x_{os} is the sediment adsorption capacity [g adsorbate/g sediment], parameter A is

$$A = \frac{H}{V_p} \frac{144\left(1-\varepsilon\right)^2}{\varepsilon d_m^2 \left[6\left(1-\varepsilon\right)+\varepsilon\right]} \tag{462}$$

While, as previously mentioned:

$$D_{mz}^p = f\left(\eta_{oc}^p\right) \tag{463}$$

$$D_{mz}^k = f\left(\eta_{ok}^k\right) \tag{464}$$

The post-coagulation sediment viscosity (η_{ok}) depends on its hydration (u), water viscosity (η) and on specific sediment floc surface (S_{oc}) and can be determined from modified form of Einstein formula [85]:

$$\eta_{oc} = \eta\left[1 + 1.92 \cdot 10^{-3} \cdot S_{oc}^{1.46}\left(100 - w\right)\right] \tag{465}$$

The properties of post-coagulation sediment structure and the degree of its development depend on the composition of purified water, the dose and type of coagulant and possibly flocculant and on the performance of the flocculation process. The specific floc surface (S_{oc}) of post-coagulation sediment formed during water treatment with aluminum sulfate of water characterized by turbidity $5 \div 100$ g/m^3, color $10 \div 60$ gPt/m^3 and suspended solids concentration $0 \div 10$ g/m^3 ranges from $250 \div 260$ m^2/g [85].

With such properties of post-coagulation sediment and the initial hydration $w_o = 99.997\%$ (sediment after coagulation with aluminum sulfate of water with color 60, Table 16), sediment viscosity is

$$\eta_{oc}^p = 1.018\,\eta \tag{466}$$

With the velocity $V_f = 5$ h/h at which final hydration is $w_T = 99.97\%$ the sediment viscosity is

$$\eta_{oc}^k = 1.18\,\eta \tag{467}$$

The average value of the specific molecular diffusion coefficient (D_{mz}) for dissolved compounds present in surface water after coagulation, sedimentation and filtration, measured as TOC and sorbed on Chemviron Carbon GAC is $D_{mz} = \sim 5.9 \cdot 10^{10}$ m^2/s [1].

Thus, the estimated value of the specific molecular diffusion coefficient at the beginning of the contact coagulation cycle is

$$D_{mz}^p = \frac{5.9 \cdot 10^{-10}}{1.018} = 5.79 \cdot 10^{-10} \quad \left[\frac{m^2}{s}\right] \tag{468}$$

and at the end of the cycle:

$$D_{mz}^{k} = \frac{5.9 \cdot 10^{-10}}{1.18} = 5.0 \cdot 10^{-10} \quad \left[\frac{m^2}{s}\right] \tag{469}$$

During one filtration cycle (t_c), activated carbon per unit weight adsorbs

$$x_i = \frac{\left(C_o^p - C_e^p + C_o^k - C_e^k\right) V_f \cdot t_c}{2H\rho_a\,(1-\varepsilon)} \tag{470}$$

and

$$x_i = \frac{\left(C_o^p - C_e^p + C_o^k - C_e^k\right)\, \psi \cdot q_{max}}{2\,\rho_a\,(1-\varepsilon)\,\gamma\,C_{ac}} \tag{471}$$

The number of filtration cycles until breakthrough occurs for the activated carbon bed (N), i.e. the ratio of the maximum adsorbed quantity in a single layer per unit adsorbent weight (x) to the quantity adsorbed during one filtration cycle per unit adsorbent weight (Equation 471) is defined by the formula:

$$N = \frac{x}{x_i} = \frac{2\,x_m b\left(C_e^p + C_e^k\right)\rho_a\,(1-\varepsilon)\,\gamma\,C_{ok}}{[2 + b(C_e^p + C_e^k)]\,(C_o^p - C_e^p + C_o^k - C_e^k)\,\psi\,q_{max}} \tag{472}$$

Estimated values of x_m, b, x_{os} parameters for compounds measured by the TOC level present in surface water after coagulation with aluminum sulfate and for adsorption system with activated Chemviron Carbon are as follows: 60 gC/kg$_{GWA}$; 1,0 m^3/g; 0.1 gC/kg$_{os}$ [61, 72].

9.3.1. Example Calculations

EXAMPLE 1

Water of color 30 gPt/m^3 and dissolved organic carbon concentration DOC = 5 gC/m^3 is purified in the contact coagulation process with the dose of aluminum sulfate D_c = 20 g/m^3 m in activated carbon bed of a height H = 2.0 m, representative grain diameter $d_m = 2.0 \cdot 10^{-3}$, sphericity $\psi = 0.85$ and density of hydrated grains ρ_a = 1,900 kg/m^3.

Parameters of adsorption isotherm of Langmuir type, dissolved compounds measured by DOC concentration, determined in laboratory testing are x_m = 60 gC/kg; b = 1.0 m^3/g. The specific molecular diffusion coefficient for this type of compounds is $D_{mz} = 5.9 \cdot 10^{-10}$ m^2/s. The sorption capacity of the generated post-coagulation sediment in relation to DOC is $x_{os} = 10^{-4}$ gC/g$_{os}$. The surface of the post-coagulation sediment is S_{oc} = 250 m^2/g.

Determine the efficiency of DOC removal, bed run time and the number of cycles until the minimal achievable DOC concentration in the outflow is exceeded.

Determine the final bed porosity at the linear flow rate $V_f = 5.0$ m/h $= 1.389\cdot10^{-3}$ m/s:

$$\frac{\varepsilon_1^2}{1-\varepsilon_1} = \frac{15.75}{G}\,\frac{V_p}{d_m}\sqrt{\frac{\rho_m-\rho_w}{\rho_w}} = \frac{15.75}{220}\cdot\frac{1.389\cdot10^{-3}}{2.0\cdot10^{-3}}\sqrt{0.9} = 0.0472$$

$$\varepsilon_1 = 0.195$$

Determine the parameter γ of filtration cycle length equation:

$$\gamma = \frac{x}{r_{k(\varepsilon)}} = \frac{r_{k(\varepsilon)} - r_{k(\varepsilon_1)}}{r_{k(\varepsilon)}} = \left[\frac{\varepsilon d_m}{6(1-\varepsilon)} - \frac{\varepsilon_1\,(d_m+2x)}{6(1-\varepsilon_1)}\right]\frac{6(1-\varepsilon)}{\varepsilon\, d_m}$$

$$x = \frac{0.4\cdot2.0\cdot10^{-3}}{6(1-0.4)} - \frac{0.195\,(2.0\cdot10^{-3}+2x)}{6(1-0.195)}$$

$$x = 2.22\cdot10^{-4} - 0.875\cdot10^{-4} - 0.081\,x$$

$$x = 1.244\cdot10^{-4}$$

$$\gamma = \frac{1.244\cdot10^{-4}}{2.22\cdot10^{-4}} = 0.56$$

Determine the suspended solid concentration in the inflow to the adsorption column:

$$C_{ac} = 0.55D_c + 0.25C = 0.55\cdot20 + 0.25\cdot30 = 18.5\ \mathrm{g/m^3}$$

The suspended solid layer capacity at sediment hydration in the inflow $w_o = 99.9982\%$ and sediment hydration in the layer at the end of filtration cycle $w_T = 99.476\%$:

$$q_{max} = C_{oc}\cdot\frac{100-w_T}{100-w_o} = 18.5\cdot\frac{100-99.476}{100-99.9982} = 5{,}385.5\ \mathrm{g/m^3}$$

Bed run time:

$$t_c = \frac{\psi\cdot H\cdot q_{max}}{V_f\cdot\gamma\cdot C_{oc}} = \frac{0.85\cdot2.0\cdot5{,}385.5}{5.0\cdot0.56\cdot18.5} = 176.7\ \mathrm{h} = 7.4\ \mathrm{d}$$

Determining parameter A of adsorption efficiency (Equations 460 and 461):

$$A = \frac{H}{V_f}\cdot\frac{144\,(1-\varepsilon)^2}{\varepsilon d_m^2\,[6\,(1-\varepsilon)+\varepsilon]} = \frac{2}{5}\cdot\frac{144\,(1-0.4)^2}{(2\cdot10^{-3})^2\,[6(1-\varepsilon)+\varepsilon]} = 1{,}296{,}000$$

Determining the viscosity of the medium in which diffusion takes place at the beginning of filtration cycle (post-coagulation sediment with hydration $w = 99.9982\%$) from equation (465):

$$\eta_{oc}^{p} = \eta\,[1+1.92\cdot10^{-3}\cdot S_{oc}^{1.46}\,(100-u)] = \eta\,[1+1.92\cdot10^{-3}\cdot250^{1.46}\,(100-99.9982)]$$

$$\eta_{oc}^{p} = 1.011\eta$$

Determining viscosity of the medium in which diffusion takes place at the end of the filtration cycle (sediment with hydration w = 99.476%):

$$\eta^{p}_{oc} = \eta\,[1 + 1.92 \cdot 10^{-3} \cdot 250^{1.46}\,(100 - 99.476)] = 4.189\eta$$

Determining specific molecular diffusion coefficient at the beginning of the filtration cycle:

$$D^{p}_{mz} = \frac{D_{mz}}{1.011} = \frac{5.9 \cdot 10^{-10}}{1.011} = 5.836 \cdot 10^{-10}\ \frac{m^2}{s} \quad = 2.1009 \cdot 10^{-6}\ \frac{m^2}{h}$$

Determining specific molecular diffusion coefficient at the end of the filtration cycle:

$$D^{k}_{mz} = \frac{D_{mz}}{4.189} = \frac{5.9 \cdot 10^{-10}}{4.189} = 1.408 \cdot 10^{-10}\ \frac{m^2}{s} \quad = 0.507 \cdot 10^{-6}\ \frac{m^2}{h}$$

Determining adsorption efficiency at the beginning of the filtration cycle (Equation 460):

$$C^{p}_{e} = (C_o - x_{os}\,C_{ok})\exp\left(-AD^{p}_{mz}\right) = \left(5 - 10^{-4} \cdot 18.5\right)$$

$$\exp\left(-1{,}296{,}000 \cdot 2.1009 \cdot 10^{-6}\right) = 4.998\exp\left(-2.72\right) = 0.329\ gC/m^3$$

Determining adsorption efficiency at the end of the filtration cycle (Equation 461):

$$C^{k}_{e} = (C_o - x_{os} \cdot q_{max})\exp\left(-AD^{k}_{mz}\right) = \left(5 - 10^{-4} \cdot 5{,}385.5\right)$$

$$\exp\left(-1{,}296{,}000 \cdot 0.507 \cdot 10^{-6}\right) = 4.462\exp\left(-0.657\right) = 2.31\ gC/m^3$$

Determining the quantity adsorbed in one filtration cycle (Equation 471):

$$x_i = \frac{\left(C^{p}_{o} - C^{p}_{e} + C^{k}_{o} - C^{k}_{e}\right)\ \psi \cdot q_{max}}{2\,\rho_a\,(1-\varepsilon)\,\gamma\,C_{ok}} = \frac{(4.998 - 0.329 + 4.462 - 2.31)\ 0.85 \cdot 5{,}385.5}{2 \cdot 1{,}900\,(1 - 0.4)\,0.56 \cdot 18.5}$$

$$x_i = 1.32\,g/kg$$

Determining the number of cycles until the breakthrough of the activated carbon layer occurred, i.e. until the concentration $C_e = 2.31$ g/m^3 in the outflow from the column was exceeded (Equation 472):

$$N = \frac{2\,x_m b\left(C^{p}_{e} + C^{k}_{e}\right)\rho_a\,(1-\varepsilon)\,\gamma\,C_{ok}}{[2 + b(C^{p}_{e} + C^{k}_{e})]\,(C^{p}_{o} - C^{p}_{e} + C^{k}_{o} - C^{k}_{e})\,\psi\,q_{max}} =$$

$$= \frac{2 \cdot 60 \cdot 1\,(0.329 + 2.31) \cdot 1{,}900\,(1 - 0.4) \cdot 0.56 \cdot 18.5}{[2 + 1(0.329 + 2.31)]\,(4.998 - 0.329 + 4.462 - 2.31) \cdot 0.85 \cdot 5{,}385.5} = 26$$

Column working time until the moment of breakthrough – exceeding the concentration $C_e = 2.31$ g/m^3 in the outflow:

$$t = N \cdot t_c = 26 \cdot 7.4 = 192.4\ d$$

REFERENCES

1. Adamski W., Analiza zjawisk przenoszenia masy w układach adsorpcyjnych oczyszczania wody. Scientific works of the Department of Environmental Engineering of Wrocław University of Technology, No.61, Monografie 29. Wrocław, 1988.
2. Adamski W., Adsorption in Wastewater Treatment, Outflow and Water Treatment Journal, 24(6), 1984.
3. Adamski W., Sozański M.M., Badania modelowe procesu adsorpcji w systemach odnowy wody, Archiwum Ochrony Środowiska, 1, 1984.
4. Adamski W., Markiewicz J., Sposób oczyszczania wody powierzchniowej, zgłoszenie patentowe, No. P. 335489, dated 16.09.1999.
5. Adamski W., Markiewicz J., Cammillare T., Up-Flow Direct Filtration Through Activated Carbon Bed, Environ. Prot. Eng., 2000, Vol. 26, No 3, 53.
6. Adamski W., Markiewicz J., Price R., Formulation of a Mathematical Model for Coagulation-Adsorption Process in Up-Flow Direct Filtration Through Granular Activated Carbon Bed, Envir. Prot. Engin., 2000, Vol. 26, No 4, 101.
7. Argman Y., Kaufmann W.J., Turbulence and Floculation, Journal San. Eng. Div. ASCE 98(79), 1972.
8. Bales V., Ganho B.R., Angelino H., Determination de coefficient de transfert de materie en lit fluidise, Chem. Zwesti, 29(2), 1975
9. Benarde M.A., Kinetics and Mechanism of Bacterial Disinfection by Chlorine Dioxide, Applied Microbiology, 1967, 15(2), 257.
10. Bird R., Steward W., Lightfoot E., Transport Phenomen, John Wiley and Sons, New York, 1962.
11. Brdicka R., Podstawy chemii fizycznej, PWN, Warszawa 1970.
12. Brunauer S., Emmett P.H., Teller E., Adsorption of Gases in Multimolecular Layers, Journal Am. Chem. Society, 60, 1938.
13. Camp T.R., Stein P.C., Velocity Gradients and Internal Work in Fluid Motion, Journal Boston Society of Civil Eng., 30, 1943.
14. Carman P.C., Fluid Flow Through Granular Beds, Transactions of Institute of Chemical Engineers, 15, 1937, 150.
15. Chick H., An Investigation of the Laws of Disinfection, Journal Higiene, 8(92), 1908.
16. Chow V.T., Open Channel Hydraulics, Mc Graw-Hill, Inc. New York, 1959.
17. Chu J.C., Mass Transfer in a Fluidized Bed, Chem. Eng. Prog., 49, 1953.
18. Collins H. Selleck R., Process Kinetics of Wastewater Chlorination, Report of University of California, Berkeley, 1972.
19. Cornwell D.A., Water Quality and Treatment-Air Stripping and Aeration, A Handbook of Community Water Supplies, 4d ed., American Water Works Association, Mc Graw - Hill, Inc, New York, 1990.
20. Council Directive 98/83/EC of 3 November 1998 on the Quality of Water Intended for Human Consumption, O.I.L. 336, 5.12.1998, 32-54.

21. Dojlido J., Polskie i światowe normy jakości wody do picia, XII National Science-Technology Conference, Poznań, 1992.
22. Dubinin M.M., The Potential Theory of Adsorption of Gases and Vapors for Adsorbent with Energetically Nonuniform Surfaces, Chemical Review, 60, 1960.
23. Fair G.M., The Behavior of Chlorine as a Water Disinfectant Journal AWWA, 40(10), 1051, 1948.
24. Fair G.M., Geyer J.C., Water and Wastewater Engineering - Water Purification and Wastewater Treatment and Disposal, John Wiley and Sons, New York, 1968.
25. Ferguson J.F., McCaret P.L., Effects of Carbonate and Magnesium on Calcium Phosphate Precipitation, Environ. Sci. Tech., 58(6), 1972.
26. Ferguson J.F., Jenkins D., Eastman J., Calcium Phosphate Precipitation at Slighty Alkaline pH Values, Journal WPCF, 620(45), 1973.
27. Ferguson J.F., Mathematical Modeling for Water Pollution Control Processes - Chemical Precipitation Modeling in Sanitary Engineering, Ann Arbor Science Publishers Inc. Ann Arbor, Michigan, 1975.
28. Gard S., Chemical Inactivation of Viruses, CIBA Foundation Symposium on the Nature of Viruses, Little Brown Co., Boston, p.123, 1957.
29. Gemmel R.S., Mathematical Modeling for Water Pollution Control Processes - Modeling and Simulation of the Aggregation of Suspensions, Ann Arbor Science Publishers Inc., Ann Arbor, Michigan, 1975.
30. Glaze W.H, Water Quality and Treatment - Chemical Oxidation, A Handbook of Community Water Supplies, 4d ed. American Water Works Association, Mc Graw - Hill, Inc., New York, 1990.
31. Gluckauf E., Theory of Chromatography Part 10 - Formula for Diffusion into Sphere and Their Application to Chromatography, Trans. Faraday Society, 51(11) 1955.
32. Guidelines for Drinking-water Quality. Second edition, Volume 1, Recommendations World Health Organization, Geneva, 1993.
33. Haas Ch.N., Water Quality and Treatment - Disinfection, A Handbook of Community Water Supplies, 4d ed, American Water Works Association, Mc Graw-Hill, Inc., New York, 1990.
34. Harris H.S., Kaufmann W.J., Krine R.B., Orthokinetic Floculation in Water Purification, Journal San. Eng. Div., ASCE, 92(95) 1966.
35. Hath L.P., Fundamental Factors Governing the Streamline Flow of Water Through Sand, Journal AWWA, 11(25), 1933, p.1551.
36. Hazen A., The Filtration of Public Water Supplies, 2d ed, John Wiley and Sons, New York, 1925.
37. Hobler T., Dyfuzyjny ruch masy i absorbery, WNT, Warszawa 1976.
38. Holland F.A., Chapman F.S., Liquid Mixing and Processing in Stirred Tanks, Reinhold Publishing Corporation, New York, 1966.
39. Hom L.W., Kinetic of Chlorine Disinfection in an Ecosystem, Journal San. Eng. Div., ASCE, 2, p.183, 1973.

40. Ives K.J., New Concepts in Filtration, Part 2 Water and Water Engineering, No 8, 1961.
41. Iwasaki T., Some Notes on Sand Filtration, Journal AWWA, 10(29), p.1596, 1937.
42. Jankowska H., Świątkowski A., Choma J., Węgiel aktywny, WNT, Warszawa, 1985.
43. Keinath T.M., Wanielista M., Mathematical Modeling for Water Pollution Control Process-Modeling and Simulation of the Performance of Adsorption Contactors, Ann Arbor Science Publishers Inc., Ann Arbor Michigan, 1975.
44. Kielcew W., Podstawy techniki adsorpcyjnej, WNT, Warszawa, 1980.
45. Koch R., Procesy mechaniczne w inżynierii chemicznej, Textbook of Wrocław University of Technology, Wrocław, 1979.
46. Kowal A.L., Filtry wielowarstwowe do oczyszczania wody, Scientific works of the Deparment of Sanitary and Water Engineering of Wrocław University of Technology, Wrocław, 1972.
47. Kowal A.L., Sozański M.M., Podstawy doświadczalne systemów oczyszczania wody, Textbook of Wrocław University of Technology, Wrocław, 1977.
48. Kowal A.L., Maćkiewicz J., The Effect of Water Temperature on the Course of Alum Coagulation of Colloidal Particles in Water, Envir. Protect. Eng., 1975, vol. 1, nr 1, s.63.
49. Kowal A.L., Maćkiewicz J., Simulation of the Floculation Process in Filter Beds, Physio-chemical Methods for Water and Wastewater Treatment, Pergamon Press, Oxford, New York, 1980.
50. Kowal A.L., Maćkiewicz J., Technologiczne aspekty koagulacji w osadzie zawieszonym, conference materials, „Zagadnienia zaopatrzenia w wodę miast i wsi", PZITS, Poznań, 1983.
51. Kowal A.L., Technologia wody, Arkady, Warszawa, 1977.
52. Kowal A.L., Świderska-Bróż M., Oczyszczanie wody, PWN, Warszawa-Wrocław, 1996.
53. Kowal A.L., Maćkiewicz J., Świderska-Bróż M., Podstawy projektowe systemów oczyszczania wód, Oficyna Wydawnicza Politechniki Wrocławskiej, Wrocław 1996.
54. Langmuir I., The Adsorption of Gases on Plane Surfaces of Glass, Mica and Platinium, Journal Am. Chem. Soci., 40, 1918.
55. Lauria D.T., O`Melia Ch.R., Mathematical Modeling for Water Pollution Control Processes-Optimal Process for Iron (II) Oxidation, Ann Arbor Science Publishers Inc., Ann Arbor Michigan, 1975.
56. Letterman R.D., Quon J.N., Gemmel R.S., Film Tramsport Coefficient in Agitated Suspensions of Activated Carbon, Journal WPCF, 46(11) 1974.
57. Levenspiel O., Chemical Reaction Engineering, John Wiley and Sons, New York, 1972.
58. Maćkiewicz J., On the Importance of Velocity Gradient in the Coagulation Process, Envir. Protect. Eng., 1980, vol. 5, nr 2, s. 175.

59. Maćkiewicz J., On Forces Acting in Floculation-Filtration, Environ. Prot. Eng., vol. 10, No 2, s. 27, 1984.
60. Maćkiewicz J., Flokulacja w procesach koagulacji i filtracji wód, PWN, Warszawa 1987.
61. Markiewicz J., Modelowanie zjawisk zachodzących podczas koagulacji domieszek wody w złożu węgla aktywnego, Reports of the Department of Environment Engineering of Wrocław University of Technology, Wrocław, 2001 (unpublished work).
62. Masschelein W.J., Unit Processes in Drinking Water Treatment, Marcel Dekker Inc., New York, 1992.
63.] Miller D.E., West I.T., Pilot Plant Studies on Flock Blanket Clarification, Journal Am. Water Work Ass., 1968, vol. 60, No 2, s. 154.
64. Montgomery J.M., Water Treatment-Principles and Design, John Wiley and Sons, New York, 1985.
65. Morel F.M., Morgan J.J., A Numerical Method for Computing Equilibria in Aqueous Chemical Systems, Envir. Sci. Tech., 6(58) 1972.
66. Nawrocki J., Biłozor S., Uzdatnianie wody - procesy chemiczne i biologiczne, PWN, Warszawa-Poznań, 2000.
67. Neretnieks J., Adsorption in Finite Bath and counter-current Flow with System Having a Nonlinear Isotherm, Chem. Eng. Sci., 31, 1976.
68. O`Melia C.P., Coagulation in Water Treatment Plant, Ann Arbor Science Publishers, Ann Arbor Michigan, 1978.
69. Pankow J.F., Morgan J.J., Kinetics for the Aquatic Environment, 1, Envir. Sci. Tech., 15, p.1155, 1981.
70. Pankow J.F., Morgan J.J., Kinetics for the Aquatic Environment, 2, Envir. Sci. Tech., 15, p.1306, 1981.
71. Parker D.S., Forces Acting on Floc and Strenght of Floc, Journal Sanit. Eng. Div., vol. 108, No. 2, s. 594, 1982.
72. Perrich I.R., Activated Carbon Adsorption for Wastewater Treatment, CRC Press Inc-Boca Raton, Florida, 1981.
73. Pfeffer R., Happel J., An Analytical Study of Heat and Mass Transfer in Multiparticle Systems at Low Reynolds Numbers, AIChE Journal, 10, 1954.
74. Health Effects of Drinking Water Treatment Technologies, Lewis Publishers, 1990.
75. Roman M., Jakość wody do picia w przepisach Unii Europejskiej i w przepisach polskich, Monografia Seria: Wodociągi i Kanalizacja nr 8, Wydawnictwo PZITS, Warszawa, 2001.
76. Romankow P.G., Baszkowska N.B., Frołow W.E., Procesy wymiany masy w technologii chemicznej, WNT, Warszawa 1980.
77. Rose H.E., An Investigation of the Laws of Flow of Fluids Through Beds of Granular Materials, Proc. Institute of Mechanical Engineers, 153, p.141, 1945.
78. Roy D., Kinetics of Enteroviral Inactivation by Ozone, ASCE Journal San. Eng. Div., 107(5), p.887, 1981.

79. Roy D., Mechanism for Enteroviral Inactivation by Ozone Appl. Environ. Microbiol., 41(3), p.718, 1981.
80. Ordinance of the Minister of Health dated 4 September 2000 r. concerning the conditions of drinking water and water for domestic purposes, water in public pools and the rules for water control of Sanitary Inspection, Dziennik Ustaw RP, 2000 , no. 82, pos. 937.
81. Reynolds T.D., Unit Operation and Processes in Environmental Engineering, Brooks/Cole Engineering Division, Monterey, California 1982.
82. Selleck R., Collins H., White G.C., Kinetics of Bacterial Deactivation with Chlorine, ASCE Journal Envir. Eng. Div., 104, p.1197, 1978.
83. Snoeyink V.L., Jenkins D., Water Chemistry, John Wiley and Sons, New York, 1980.
84. Stokes R.H., The Diffusion Coefficient of Eight Uni - univalent Electrolytes in Aqueous Solution at 25^{O}C, Journal Am. Chem. Soc., 72, 1950.
85. Sozański M.M., Właściwości reologiczne uwodnionych osadów pokoagulacyjnych, Scientific works of the Department of Environmental Engineering of Wrocław University of Technology, nr 34, Seria Monografie nr 11. Wrocław 1976.
86. Stumm W., Lee G.F., Oxygenation of Ferrous Iron, Ind. Eng. Chem. 143(53) 1961.
87. Stumm W., Morgan J.J., Aquatic Chemistry, John Wiley and Sons, New York 1970.
88. Suidan M.T., Dick R.I., Mathematical Modeling for Water Pollution Control Processes – Modeling and Simulation of Clarification and Thickening, Ann Arbor Science Publishers Inc., Ann Arbor , Michigan, 1975.
89. Świderska-Bróż M., Interakcja związków humusowych z wybranymi metalami oraz jej wpływ na usuwanie badanych metali z wody, Wydawnictwa Politechniki Wrocławskiej, Wrocław, 1985.
90. Tchobanoglous G., Schroeder E.D., Water Quality, Addison-Wesley Publishing Company, Reading, Massachusetts, 1987.
91. Tchobanoglous G., Eliassen R., Filtration of Treated Sewage outflow, Journal Sanit. Eng. Div., ASCE, 96, p.243, 1970.
92. Tesarik I., Vastricil J., A Theoretical Consideration on Entrapment of Flocs in the Sludge Blanket, Wat. Res. 9(10), p.887, 1975.
93. Tesarik I., Flow in Sludge-Blanket Clarifiers, Journal of Sanit. Eng. Div. 93, p.105, 1967.
94. Van Lier W.C., Activated Carbon - a Fascinating Material-Some Thought on Activated Carbon - On the Kinetics of Adsorption on Activated Carbon from Aqueous Phase, Norit NV, Amersfoort, The Netherlands, 1983.
95. Wehner J.F., Wilhelm R.F., Boundary Conditions of Flow Reactor, Chem. Eng. Sci., 1, 1958, p.89
96. Wilke C.P., Chang P., Correlation of Diffusion Coefficient in Dilute Solution, AIChE Journal, 1(2) 1955.
97. Wroński S., Pohorecki B., Siwiński J., Przykłady obliczeń termodynamiki i kinetyki procesów inżynierii chemicznej.